

**The Development and Application of a New Approach to the
Rapid Synthesis of Polypropionate Stereotriads**

Corinne N. Foley

Submitted in partial fulfillment of the Requirement for the degree of Doctor of Philosophy in the
Graduate School of Arts and Sciences

Columbia University

2015

©2014

Corinne N. Foley

All rights reserved

Abstract

The Development and Application of a New Approach to the Rapid Synthesis of Polypropionate Stereotriads

Corinne N. Foley

The construction of polypropionate stereotriads in the synthesis of many non-aromatic polyketide natural products has typically been achieved through the “Roche ester” approach. This process starts with one of the stereocenters purchased as the Roche ester, followed by multiple redox and protecting group manipulations and only one carbon-carbon bond-forming aldol or crotylation reaction to attain the other two stereocenters of the stereotriad. Motivated by a desire for a more direct and rapid synthesis of these stereotriad constructs, we have built upon previous group methodology to develop a new approach utilizing a three step sequence of alkyne silylformylation-crotylation-Tamao oxidation. This strategy was first utilized in the synthesis of the C1-C9 fragment of the epothilones, and then this route applied to the synthesis of a C6 methyl-modified analog of epothilone B. We have also pursued the synthesis of versatile polypropionate building blocks as a way of generalizing our new approach.

Table of Contents

List of Figures.....	iii
List of Schemes	iii
List of Tables	v
Chapter 1: Introduction.....	1
1.1 Introduction	1
1.2 The Epothilones.....	2
1.2.1 Introduction: Discovery and Biological Activity	2
1.2.2 Structure-Activity Relationship (SAR) and Clinical Development.....	3
1.2.3 Retrosynthesis and Overview of Synthetic Strategies	8
1.2.4 Synthetic Approaches to the C1-C9 Fragment of the Epothilones.....	9
1.3 Leighton Group Carbonylation-Based Approach to Polyketide Synthesis	20
1.3.1 Tandem Silylformylation-Allyl(Crotyl)silylation and Strain-Release Lewis Acidity....	20
1.3.2 Tandem Silylformylation-Crotylsilylation of Alkynes.....	22
1.3.3 Extension of Methodology to Internal Alkynes for Production of Stereotriads	23
1.4 References	25
Chapter 2: Improving Selectivity and Efficiency in the Synthesis of the C1-C9 Fragment of the Epothilones.....	32
2.1 Introduction: First Generation Synthesis and the “Aprotic” Tamao Oxidation.....	32
2.2 Development of a More Selective and Streamlined Synthesis of Key Intermediate 2.10	34
2.3 Toward a More Selective Formation of the C6-C8 Stereotriad of the Epothilones.....	36
2.4 Summary/Conclusion	43
2.5 References	45
2.6 Experimental Procedures and Characterization Data	46
2.7 ¹ H and ¹³ C NMR Spectra	56
2.8 GC Traces.....	67
Chapter 3: Application of Our Fragment Synthesis for a C6 Linker Analog of Epothilone B	68
3.1 Introduction: Aims and Rationale for C6 Methyl Conjugation	68
3.2 Application of Our C1-C9 Fragment Synthesis Towards a C6 Epothilone Linker Analog ..	73
3.3 Use of Our Fragment Analog for Access to a C6 Linker Analog of Epothilone B	75

3.4 Conclusion and Outlook	77
3.5 References	79
3.6 Experimental Procedures and Characterization Data	82
3.7 ^1H and ^{13}C NMR Spectra.....	97

Chapter 4: A New Approach to the Rapid Synthesis of Polypropionate Stereotriad Building Blocks112

4.1 Introduction	112
4.2 Intermolecular Silylformylation-Crotylation of 2-Butyne.....	115
4.3 Optimization of the Standard and “Aprotic” Tamao Oxidation Conditions.....	117
4.4 Utilization of Propyne Towards the Synthesis of Aldehyde Building Blocks	119
4.5 Observed Tamao Oxidation Selectivity Trends.....	121
4.6 Demonstrated Application in Dictyostatin Analog Synthesis	123
4.7 Conclusion.....	124
4.8 References	126
4.9 Experimental Procedures and Characterization Data	128
4.10 ^1H and ^{13}C NMR Spectra.....	139
4.11 GC Traces.....	151

List of Figures

Figure 1.1 Representative Antimitotic Polyketides Containing Polypropionate Stereotriads	1
Figure 1.2 Structures of the Epothilones and Taxol	2
Figure 1.3 Structure-Activity Relationship for Epothilones	4
Figure 1.4 Selection of Epothilone Analogs Advanced to Clinical Trials.....	5
Figure 1.5 Proposed Stabilization of Anti-Felkin Transition State	13
Figure 2.1 Comparison of “Aprotic” Tamao Oxidation Substrates.....	39
Figure 3.1 Examples of Reported Epothilone Linker Strategies	69
Figure 3.2 Precedent for Tolerated C6 Methyl Extension	72
Figure 3.3 Crystal Structure of $\alpha\beta$ -Tubulin in Complex with Epothilone A	72

List of Schemes

Scheme 1.1 General Retrosynthetic Strategies	8
Scheme 1.2 Synthesis of Epothilones Using C1-C9 Fragment 1.12	9
Scheme 1.3 General Anti-Felkin Selective Aldol Approach to the C6-C8 Stereotriad	10
Scheme 1.4 Potential Transition States for Addition of (Z)-enolates to α -methyl substituted aldehydes.....	11
Scheme 1.5 Selected Aldol Reactions from Epothilone and Beneficial Effect of Acetonide Moiety	11
Scheme 1.6 Panek’s Crotylation Approach to Epothilone Stereotriad Synthesis	14
Scheme 1.7 Grieco’s Crotylation Approach to the C6-C8 Stereotriad	14
Scheme 1.8 Danishefsky’s Use of LACDAC Methodology to Construct C6-C8 Stereotriad	15
Scheme 1.9 Examples of Substrate-Based Stereocontrol in Aldol Reactions.....	16
Scheme 1.10 Oxazolidinone Auxiliary Control for the Aldol Approach to C3 Stereochemistry ..	16
Scheme 1.11 Chiral Auxiliary Control for Aldol Approach of C3 Stereochemistry	17
Scheme 1.12 Chiral Reagents and Catalysts for Aldol Stereocontrol.....	17
Scheme 1.13 Asymmetric Allylation or Prenylation for Access to C3 Stereocenter.....	18
Scheme 1.14 Derivation of C3 via Chiral Pool Synthesis (Pantonolactone)	18
Scheme 1.15 Examples of Selective Reduction to Set C3 Stereocenter	19
Scheme 1.16 Access to C3 Stereocenter via Epoxidation.....	19
Scheme 1.17 Tandem Alkene Silylformylation-Allylsilylation Reaction and Mechanism	21
Scheme 1.18 Strain-Release Lewis Acidity	22
Scheme 1.19 Tandem Alkyne Silylformylation-Crotylsilylation with Oxidative or Protodesilylative Workup.....	22
Scheme 1.20 Stereochemical Model to Explain 1,5-Anti-Diol Bias.....	23
Scheme 1.21 Tandem Silylformylation-Crotylsilylation/Tamao Oxidation for Stereotriad Formation	23
Scheme 1.22 Rationalized Model for Observed Anti Diastereoselectivity in Tautomerization	24
Scheme 2.1 Tandem Silylformylation-Crotylation with “Standard” vs “Aprotic” Tamao Oxidation.....	32

Scheme 2.2 Rationalized Models for Tautomerization Selectivity under “Standard” vs “Aprotic” Conditions	33
Scheme 2.3 Leighton Group First-Generation Route to the C1-C9 Fragment.....	33
Scheme 2.4 Approach to 2.10 via Opening of Chiral Epoxide	35
Scheme 2.5 Optimized route to 2.10	35
Scheme 2.6 Proposed Mechanism for Formation of Side Product 2.19	36
Scheme 2.7 Reagent-Based Approach to Crotylation.....	37
Scheme 2.8 Crotylation of Hindered, Electronically Deactivated Aldehydes with Leighton Group Reagent.....	37
Scheme 2.9 Application of Intermolecular Crotylation Approach	38
Scheme 2.10 Oxidative Cleavage Attempts on Substrate 2.27	38
Scheme 2.11 Precident for the Protic Tamao Oxidation of Related Substrate 2.24	39
Scheme 2.12 Representative Silanes Explored in the Three-Step Synthesis of 2.21	40
Scheme 2.13 Successful “Aprotic” Tamao Reaction of 2.21e for Proof-of-Concept	41
Scheme 2.14 Trend for Increasing Three-Step Yield with Increasing Steric Bulk on the Silane ..	42
Scheme 2.15 Optimized “Aprotic” Tamao Oxidation of 2.21g	42
Scheme 2.16 Final Step to Access C1-C9 Fragment of the Epothilones	43
Scheme 2.17 Summary of Our New Route	43
Scheme 3.1 Proposed C6 Linker Analog of Epothilone B and Disconnection Strategy.....	71
Scheme 3.2 Proposed Adaptation of Previous Synthesis for C6 Analogs	73
Scheme 3.3 Installation of C6 Linker via Alkyne 3.19	74
Scheme 3.4 “Aprotic” Tamao Oxidation to Access to 3.27	75
Scheme 3.5 Route Used to Access C6 Linker Analog of Epothilone B	75
Scheme 3.6 Conversion of Azide 3.35 into Triazole and Acetamide Derivatives.....	76
Scheme 4.1 Utility of Polypropionate Building Blocks for Natural Product Synthesis.....	112
Scheme 4.2 “Roche Ester” Approach to Stereotriad Synthesis	113
Scheme 4.3 Asymmetric Hydroformylation Approach to Stereotriad Building Blocks	113
Scheme 4.4 Proposed Carbonylation-Crotylation Approach to Stereotriad Building Blocks	114
Scheme 4.5 Optimized Conditions for the 1-Pot Silylformylation-Crotylation of 2-Butyne	117
Scheme 4.6 Standard Tamao Oxidation of 4.18	118
Scheme 4.7 Optimized Conditions for “Aprotic” Tamao Oxidation to Form 4.21 and 4.22	119
Scheme 4.8 Optimized Silylformylation-Crotylation of Propyne.....	120
Scheme 4.9 Optimized Standard Tamao Oxidation Conditions for Aldehyde Stereotriads	121
Scheme 4.10 “Aprotic” Tamao Oxidation Results	121
Scheme 4.11 Rationalized Model for Selectivity Trend Observed with Standard Tamao Oxidation Conditions	122
Scheme 4.12 Selectivity Trend for “Aprotic” Tamao Oxidation (shown for Syn, Anti Stereotriads)	123
Scheme 4.13 Application of Our Route to Access Analog of Anti, Syn Stereotriad.....	124
Scheme 4.14 Summary of the 2-Pot, 3-Step Synthesis of Stereotriad Building Blocks from 2-Butyne or Propyne.....	124
Scheme 4.15 Comparison of New Approach vs “Roche Ester” Approach.....	125

List of Tables

Table 1.1 Long-Range Effect of Aldehyde Substituents on Aldol Diastereoselectivity.....	12
Table 3.1 Preliminary Results for the Testing of C6 Linker Analogs – IC ₅₀ Values (nm)	77
Table 4.1 Optimization of the Silylformylation of 2-Butyne	116
Table 4.2 Optimization of the Standard (Protic) Tamao Oxidation Condition for 4.17	118

Chapter 1: Introduction

1.1 Introduction

Non-aromatic polyketide natural products are a pharmaceutically important class of compounds due to their often high levels of biological activity. A number of these compounds have been identified as potent antitumor agents and have thus been highly pursued for use as therapeutic agents. By binding to tubulin, the molecules disrupt microtubule dynamics, inhibiting mitosis and leading to cell death. Due to limited access to some of these important natural products or a need for innate structural modifications to improve their pharmacological properties, the use of synthetic chemistry has become paramount for the further development of a number of polyketides as therapeutic agents.

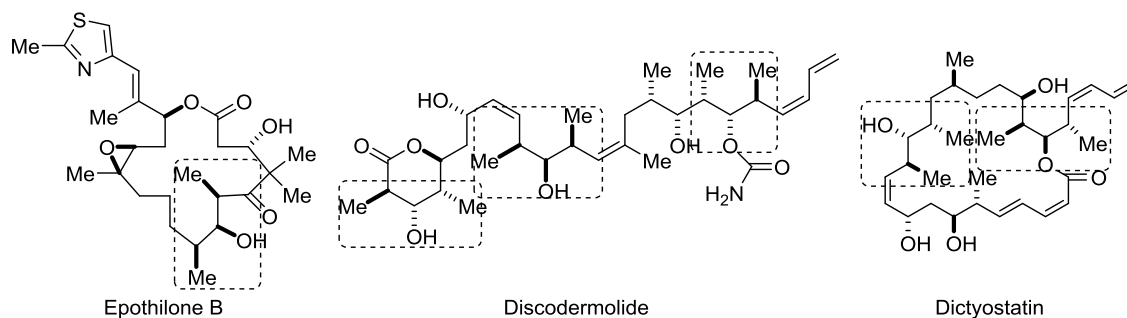


Figure 1.1 Representative Antimitotic Polyketides Containing Polypropionate Stereotriads

In the Leighton group, we are interested in developing new methodologies and strategies for highly efficient and scalable access to stereochemically complex polyketide compounds.¹⁻¹¹ One common structural motif that has been found in a variety of natural products is the polypropionate stereotriad, with alternating methyl, hydroxyl, methyl stereocenters (Figure 1.1).^{12,13} This thesis will focus broadly on the development of a new approach to the rapid synthesis of these polypropionate stereotriads. This new strategy will first be discussed in the context of the synthesis of the C1-C9 fragment of the epothilones and the utilization of this synthesis to obtain a

C6 methyl-modified analog equipped with linker functionality, followed by generalization of our approach for the synthesis of versatile polypropionate building blocks.¹⁴

1.2 The Epothilones

1.2.1 Introduction: Discovery and Biological Activity

The epothilones are a family of cytotoxic natural products that were first isolated from the myxobacterium *Sorangium cellulosum* in 1987.^{15,16} While initially of some interest for their antifungal properties, these compounds attracted much more attention from the scientific community in 1993 when they were found to exhibit potent taxane-like antitumor activity.¹⁷

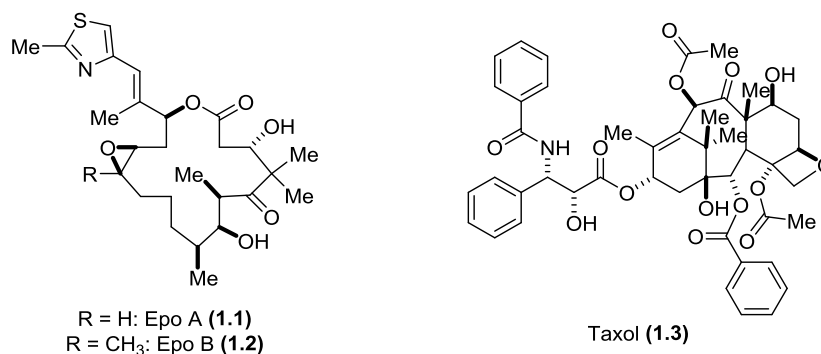


Figure 1.2 Structures of the Epothilones and Taxol

Epothilones A (Epo A, **1.1**) and B (Epo B, **1.2**), have been found to act via the same microtubule-stabilizing mechanism of action as taxol (**1.3**), the first therapeutic agent with this mechanism to obtain FDA approval (Figure 1.2). While Epo A exhibits similar activity to taxol in a number of cancer cell lines, Epo B is about tenfold more potent in the same cell lines.¹⁸ Though they act at the same microtubule binding site, the epothilones are significantly more active than taxol for inhibiting the growth of multidrug-resistant (MDR) cancer cell lines. In taxol-resistant cancer cell lines that overexpress phosphoglycoprotein 170 (P-gp), epothilones A and B are able to maintain almost full anti-proliferative activity because they are poor substrates for the P-gp efflux pump.^{17,19} Epothilones have also been shown to retain activity in cancer cell lines that have

developed taxol-resistance due to particular tubulin mutations, which is the another main mechanism of taxol-resistance.²⁰ Besides activity, the epothilones have the practical advantage of exhibiting increased solubility relative to taxol, meaning they would not require clinical formulation vehicles such as Cremophor which has been implicated for some of taxol's clinical side effects.²¹ Due to these advantages over taxol, the epothilones have become highly attractive targets for drug discovery efforts and total synthesis efforts. Over 30 total syntheses of Epo A and B have been reported, as well as extensive studies of the structure-activity relationship (SAR) of the epothilones. As a result of these efforts, a number of epothilone-derived compounds have been advanced to clinical trials as potential anticancer drugs. This thesis will give only a broad overview of these topics, as they have been extensively reviewed.^{18,22-34}

1.2.2 Structure-Activity Relationship (SAR) and Clinical Development

Due to the relative simplicity of the epothilone structure relative to taxol, thorough exploration of the structure-activity relationship of these compounds has been possible through semi-synthesis and diverted total synthesis. Most of this analog work has been undertaken by the Nicolaou²² and Danishefsky²³ groups, along with some important findings from research groups at pharmaceutical companies such as Novartis^{25,35}, Schering³⁶, and Bristol-Myers Squibb³⁷. For the purposes of discussing the SAR of these compounds, the epothilone structure can be broken into four sectors (Figure 1.3): the lactone, the densely functionalized polyketide fragment from C1-C8, the epoxide-containing fragment from C9-C14, and the heterocycle-containing side chain that extends from C15.

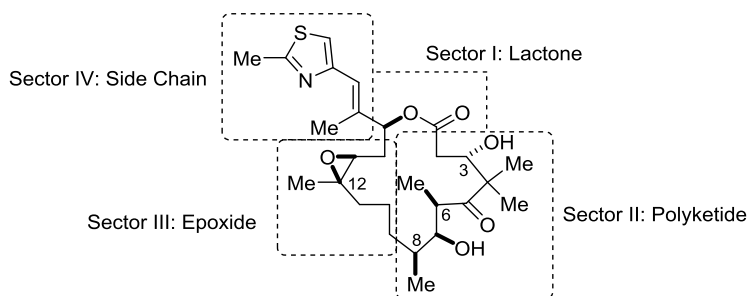


Figure 1.3 Structure-Activity Relationship for Epothilones

Some of the early work that was done in developing semi-synthetic analogs demonstrated that the lactone could be replaced by a lactam.³⁷ Though there were ultimately no stability issues found for the lactone-containing natural epothilones in human plasma, this effort by Bristol-Myers Squibb researchers was motivated by the hydrolytic instability of these compounds in rat plasma. The lactam analog, ixabepilone (**1.4**), was advanced to clinical trials and has become the only epothilone thus far to obtain FDA approval. Although approved for the treatment of breast cancer, this compound has been shown to be a better substrate for the P-gp efflux pump than the natural epothilones, so it does not exhibit the same potent activity as epothilones against many MDR cancer cell lines. The unsatisfactory activity against MDR cancers and reports of serious side effects, such as hematological toxicity and peripheral sensory neuropathy, have caused researchers to continue seeking epothilone analogs with improved therapeutic properties.

Few structural alterations have been tolerated in sector II (see figure 1.3). Replacement of the C3 hydroxyl group with a cyano group, conversion to an α,β -unsaturated lactone, or removal of C3 functionality result in analogs that retain most of the activity of the parent compound. However, biological activity is significantly reduced with most other changes to C3-C5, including inversion of C3 stereochemistry, oxidation of C3, reduction of C5, and replacement of C4 with a nitrogen.³⁰ Any changes to the stereochemistry in the C6-C8 propionate-derived stereotriad have significantly diminished the microtubule binding activity; however, it has been shown that linear extension of the C6 methyl into an allyl or propyl group is well tolerated.^{36,38} Overall, modification

of the polyketide sector has been detrimental to the activity in most cases, with the stereochemistry of the C6-C8 stereotriad being critical for cytotoxicity.

The structure of sectors III and IV have been found to be the most tolerant to structural changes, and in some cases these areas have been modified to produce analogs with increased potency or improved therapeutic properties. In sector III, it has been found that the epoxide is not vital for activity. Replacement by an alkene, cyclopropane, or aziridine (including both *cis*- and *trans*- isomers) are all tolerated changes which result in activity similar to the natural products, provided the stereochemistry is maintained. Replacement with a diol or acetonide-protected diol results in reduced activity. Given the SAR data, it has been postulated that the epoxide serves a conformational/structural role rather than acting as a hydrogen-bond acceptor or reactive electrophile.³⁰

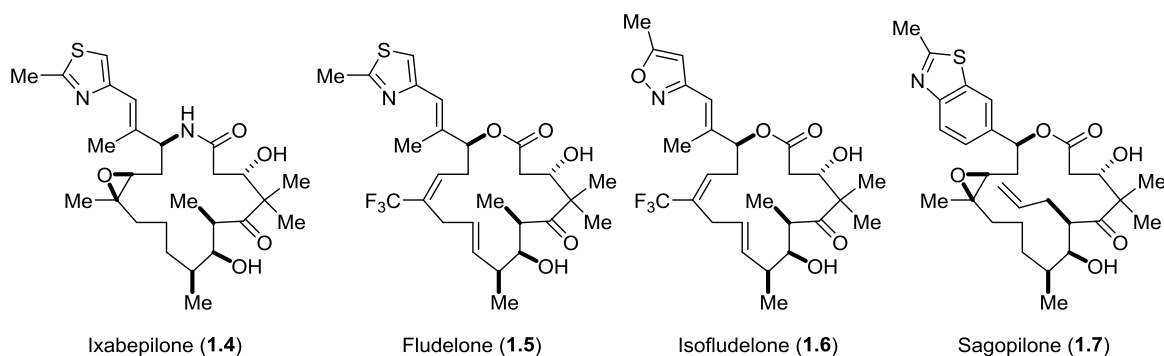


Figure 1.4 Selection of Epothilone Analogs Advanced to Clinical Trials

As indicated by the higher potency of Epo B relative to Epo A, methyl substitution of the epoxide leads to higher activity. Replacement of one hydrogen of the methyl with a fluoride, chloride, or methyl is tolerated, but larger groups decrease activity. Replacement of the methyl with a trifluoromethyl group was investigated by the Danishefsky group, and it was found to decrease toxicity and broaden the therapeutic index of analogs, ultimately leading to two promising drug candidates, fludelone (**1.5**) and isofludelone (**1.6**).^{39,40}

Other modifications of sector III, including enlarging or decreasing the size of the macrocycle and attempting to stabilize the structure by incorporating aromatic rings within the alkyl chain, caused either a decrease or a complete loss of activity. Later endeavors toward structural stabilization through installation of unsaturation in the C9-C11 portion resulted in lower activity in the case of a conjugated diene (C10-C11); however, installation of a *trans* double bond at C9-C10 to form the skipped diene resulted in increased potency relative to the natural products.

This finding has been incorporated into some of the analogs developed by the Danishefsky group which have been advanced to clinical trials.^{40,41} The most promising of these compounds is isofludelone (**1.6**), which is currently in Phase I clinical trials. The modifications made in developing this analog started with replacement of the epoxide with an alkene, which reduces activity but is thought to decrease toxicity. The next change was the installation of unsaturation at C9-C10, which improved the potency and biological stability. As mentioned previously, installation of the trifluoromethyl group helped to decrease the toxicity and broaden the therapeutic index. Finally, replacement of the thiazole ring in the side chain with an isoxazole increased the efficacy and stability. Isofludelone has been found to result in sustained tumor suppression *in vivo* for certain breast and ovarian cancer cell lines, and growth suppression of other cancer cell lines including fast-growing SK-NAS brain tumors.^{39,40}

Extensive modification of the heterocyclic side chain of sector IV has revealed that some extension of the thiazole methyl is tolerated, including substitution with hydroxyl and amino groups. Changes to the heterocycle itself are tolerated for pyrazole, tetrazole, and oxazole analogs, and pyridine analogs are tolerated when the nitrogen position is *ortho* relative to the vinyl linker. Thorough investigation by the Nicolaou group showed that rigidification of the side chain with fused biaryl moieties was tolerated for benzothiazole, benzoxazole, benzimidazole, and quinolone

groups. In fact, these analogs typically showed an increase in potency relative to the natural products, with the benzimidazole exhibiting the most pronounced effect.⁴² Independent investigation of analogs of this type by researchers at Schering AG has resulted in a compound with a benzothiazole side chain advancing to clinical trials as the first fully synthetic epothilone analog. In addition to the side chain modification, the structure of sagopilone (**1.7**) also deviates from Epo B in the substituent at C6, with an allyl group in place of the methyl found in the natural product. These changes resulted in a compound that exhibited higher potency *in vitro* than the natural products against a variety of drug-sensitive and MDR cell lines.^{38,43}

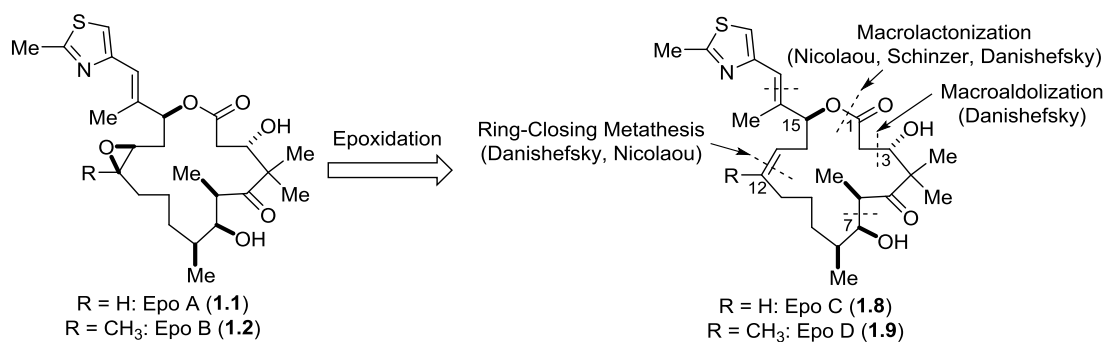
While the information presented in this section summarizes only some of the most important SAR findings, it should be clear that there have been extensive efforts from a number of research groups to amass this data. All of this accumulated information has led to the development of a number of potential drug candidates, with eight epothilone-derived compounds advancing to clinical trials, and one achieving FDA approval thus far. While the clinical development of some of these compounds has since been terminated, some of the most promising candidates are still being evaluated, namely Epo B (**1.2**), sagopilone (**1.7**), and iso-fludelone (**1.6**).

In all of this investigation, it has been revealed that the polyketide portion of the molecule (sector II) is fairly critical for potency while the other sectors are open to some modification towards obtaining optimal therapeutic properties. In fact, with the exception of **1.7**, all of the candidates that have advanced to the clinic retain the C1-C8 portion of the natural products. In the case of sagopilone, the stereochemistry is maintained and the deviation is simply a two-carbon extension of the C6 methyl group. Since this polyketide portion is the most stereochemically dense fragment of the epothilones and its synthesis most broadly useful, our group has become interested

in applying our polyketide methodology to the development of a more direct and efficient route towards the C1-C9 fragment.

1.2.3 Retrosynthesis and Overview of Synthetic Strategies

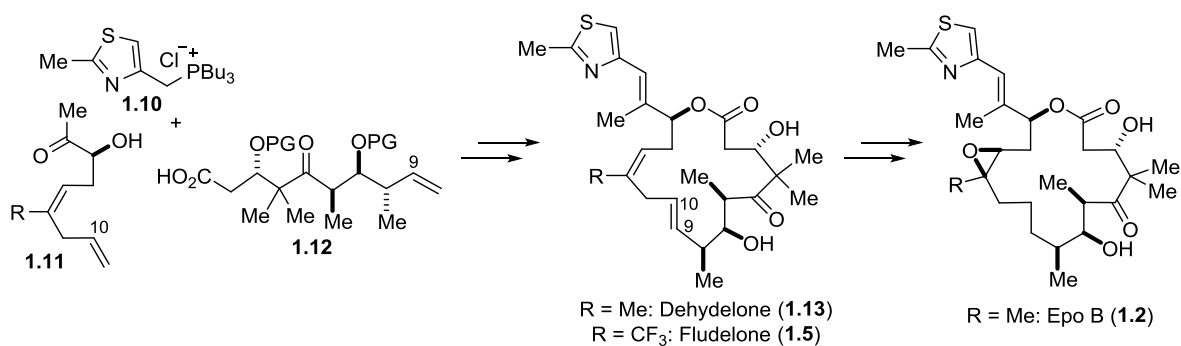
Chemists quickly began their efforts towards the synthesis of these compounds once the absolute stereochemistry of natural epothilones Epo A and B had been determined via X-ray structural analysis and reported in 1996.¹⁵ There have now been over 30 complete and formal syntheses of these natural products reported, with most going through epoxidation of the Epo C (1.8) or Epo D (1.9) precursor to obtain Epo A or Epo B (Scheme 1.1). Most of the later syntheses also depend on the same disconnection strategies and key fragments that were utilized in the initially reported syntheses. The first synthesis of Epo A was reported by the Danishefsky group in 1996,⁴⁴ followed within months by the Nicolaou⁴⁵ and Shinzer⁴⁶ groups. Scheme 1.1 shows popular disconnection strategies in building the epothilone structures, with the most common ring-closing strategies indicated more specifically. Macrolactonization via the Yamaguchi protocol⁴⁷ has become perhaps the most favored ring-closing method, due to selectivity issues with the ring-closing metathesis of C12-C13 and the macroaldolization route for C2-C3 bond construction. Other methods of connecting the fragments include Suzuki coupling at C11-C12, and aldol condensation at C6-C7.



Scheme 1.1 General Retrosynthetic Strategies

Since the related work in this thesis will be focused on the C1-C9 polyketide fragment, only approaches to that portion of the molecule will be described in more detail. It should be noted, however, that the efforts in total synthesis for the epothilones have resulted in a number of advances; in particular, the first application of ring-closing metathesis to complex substrates, the development of many stereoselective approaches to (*Z*)-trisubstituted olefins, the finding that the Yamaguchi macrolactonization is robust and useful, and the ability to use dimethyldioxirane (DMDO) for stereo- and regioselective epoxidation.

Another point to note, for the purposes of this thesis, is the development of a ring-closing metathesis strategy for the formation of a C9-C10 olefin,⁴⁸ which has been shown to be a positive structural modification in a number of analogs such as dehydellone (**1.13**) and fludelone (**1.5**) (Scheme 1.2).⁴⁰ It has also been demonstrated that selective hydrogenation of this newly formed double bond can be achieved to access the natural products.⁴⁹ Thus, an efficient synthesis of a C1-C9 fragment **1.12** would provide versatile access to the natural epothilones as well as a variety of important analogs.



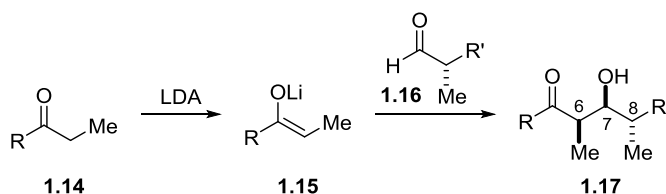
Scheme 1.2 Synthesis of Epothilones Using C1-C9 Fragment **1.12**

1.2.4 Synthetic Approaches to the C1-C9 Fragment of the Epothilones

While the fragment containing the C1-C8 polyketide sector may differ depending on the overall synthetic strategy, there are two key challenges in assembling these fragments: the construction of the C6-C8 stereotriad and control of the stereochemistry at C3.

C6-C8 Stereotriad

Most reported approaches to the C6-C8 stereotriad utilize a C6-C7 bond-forming reaction to set those two stereocenters. This is most often achieved through an aldol addition of an ethyl ketone **1.14** with an α -chiral aldehyde **1.16**. Other approaches that have been reported include crotylation and Danishefsky's Lewis acid catalyzed diene aldehyde cyclocondensation (LACDAC) methodology.

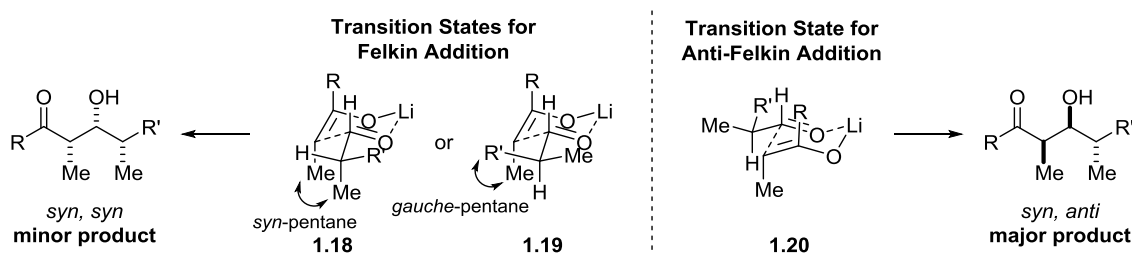


Scheme 1.3 General Anti-Felkin Selective Aldol Approach to the C6-C8 Stereotriad

As mentioned, the strategy that has been used the vast majority of the time to construct the stereotriad has been an aldol addition. In particular, an anti-Felkin selective aldol between a (*Z*)-enolate **1.15** and an α -chiral aldehyde **1.16** is required to achieve the required *syn-anti* stereochemistry of the desired product **1.17** (Scheme 1.3). Precedent for aldol selectivity would suggest that the bulky *geminal*-dimethyl group that is present as part of the R group of ketone **1.14** would favor the (*Z*)-enolate, and thus a reaction that proceeds *via* a chairlike Zimmerman-Traxler transition state would lead to formation of the desired C6-C7 *syn* stereochemistry.

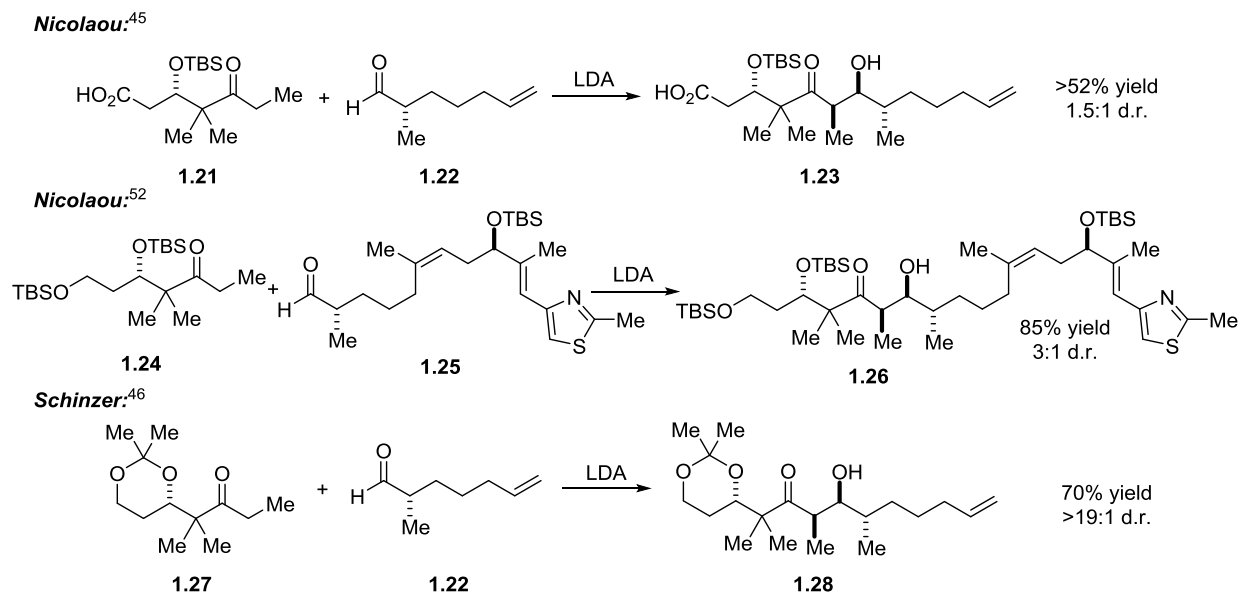
The selectivity for the stereochemistry of the new C6 and C7 stereocenters relative to the existing C8 stereocenter must also be considered. A preference for anti-Felkin selectivity has been noted previously in reactions of (*Z*)-enolates and (*Z*)-crotylboronates^{50,51} due to the unfavorable *syn*-pentane interaction of the α -methyl (see **1.18**) or *gauche*-pentane interaction of the larger α -substituent (see **1.19**) from the aldehyde with the enolate methyl substituent that would result with Felkin selectivity. Reaction with the opposite face of the aldehyde would minimize steric

interactions and result in the lowest energy transition state **1.20**, favoring the anti-Felkin product with relative *anti* relationship as the major product (Scheme 1.4).



Scheme 1.4 Potential Transition States for Addition of (*Z*)-enolates to α -methyl substituted aldehydes

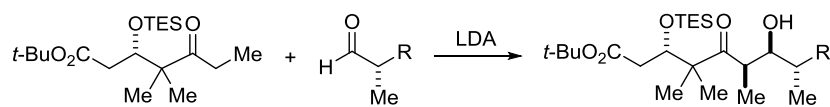
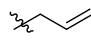
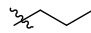
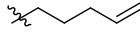
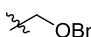
The described effect has been known to be useful in reliably predicting the major product for this type of aldol condensation, however, the selectivity is often not very good. This seemed to be the case for the substrates used in a number of the early epothilone syntheses, with the diastereoselectivities reported ranging from only 1.5:1 to 3:1 in favor of the desired anti-Felkin product **1.17** relative to the *syn, syn* Felkin product (representative examples are presented in Scheme 1.5).^{28,45,52} In all cases, the (*Z*)-enolate was favored, giving the *syn* relative stereochemistry for the newly formed C6 and C7 stereocenters, as expected.



Scheme 1.5 Selected Aldol Reactions from Epothilone and Beneficial Effect of Acetonide Moiety

As additional syntheses were reported, it became clear that the selectivity in this aldol reaction was highly dependent on the particular substrates used, with higher selectivities induced from longer-range substrate interactions. Schinzer and colleagues found that by utilizing a ketone substrate **1.27** containing an acetonide moiety, they could obtain the desired anti-Felkin product in 70% yield with >19:1 d.r.⁴⁶ Although various proposals have suggested a chelation effect between the lithium cation and the acetonide moiety,^{53,54} it is unclear which specific transition-state interactions are responsible for the high selectivity observed with an acetonide at C3 compared to other substrates containing a protected alcohol at C3.

Table 1.1 Long-Range Effect of Aldehyde Substituents on Aldol Diastereoselectivity

		
Entry	R ≡	<u>anti:syn</u> diastereoselectivity
1		5.5:1
2		1.3:1
3		2.0:1
4		4.0:1

Investigations by the Danishefsky group found that other long-range effects, this time from substituents on the aldehyde, are also at play in the diastereoselectivity of these aldol reactions.^{23,55} In a screening exercise of various aldehyde substituents, it was found that unsaturation in the aldehyde side chain helped improve the diastereoselectivity relative to a substrate without unsaturation (Table 1.1, entries 1 and 2). In comparing entries 1 and 3, it can be seen that this effect is also dependent on the position of the unsaturation. It has been speculated that this enhancement in anti-Felkin selectivity is a result of a non-bonded interaction between the unsaturated moiety and either the aldehyde carbonyl⁵⁵ or lithium cation^{56,57} that stabilizes the anti-Felkin transition

state (Figure 1.5). It should be noted that aldehydes derived from the Roche ester also exhibited higher selectivity favoring the anti-Felkin product as expected⁵¹ (Table 1.1, entry 4).

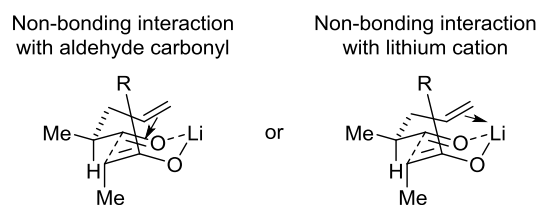
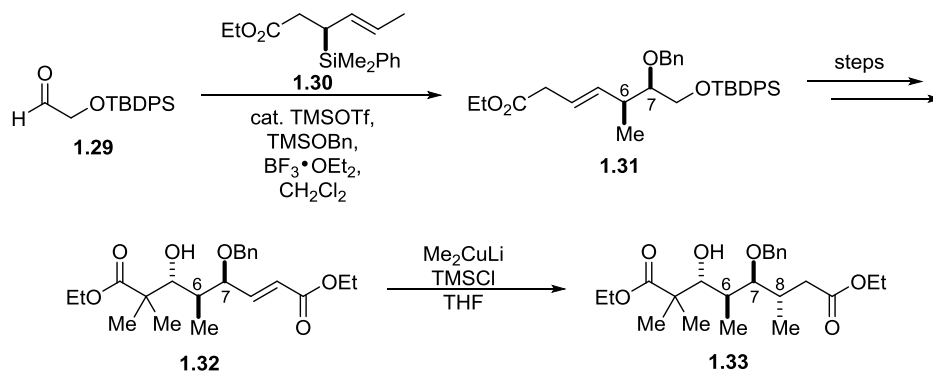


Figure 1.5 Proposed Stabilization of Anti-Felkin Transition State

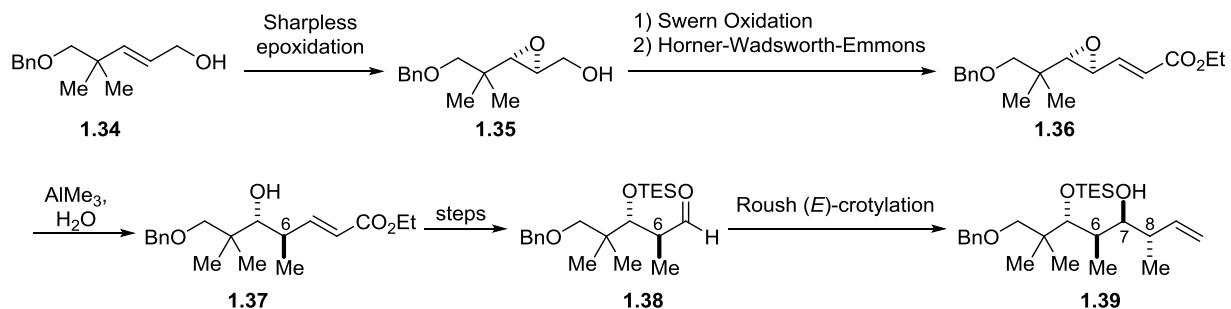
Thus far, this discussion has focused on how the C6 and C7 stereocenters can be set, but it is also important to note the origin of the C8 stereocenter. In the vast majority of cases in which an aldol reaction is used to form the C6-C8 stereotriad, the α -chiral aldehyde has either been derived from a chiral pool, typically as the Roche ester, or has been set via enolate alkylation utilizing chiral auxiliary methodology. While either of these strategies can provide reliable access to the desired intermediate, they are not particularly direct syntheses of these chiral α -methyl aldehydes because they typically involve a number of oxidation state adjustments, removal of chiral auxiliaries, and/or protecting group manipulations. We believe that this is a general problem in stereotriad synthesis, and that we might be able to find a more efficient way of accessing the third stereocenter of the stereotriad.

Although an anti-Felkin selective aldol reaction has been the most widely used approach to form the C6-C8 stereotriad, there are a few examples of other approaches in the literature. Panek has reported the use of his group's methodology for the TMSOTf-catalyzed crotylation of α -silyloxyaldehyde **1.29** with crotylsilane **1.30** to set the C6 and C7 stereocenters in 83% yield and 15:1 d.r. (Scheme 1.6). Following additional steps, lithium dimethylcuprate addition to enoate **1.32** gave the desired C8 stereocenter in >10:1 d.r.^{58,59}



Scheme 1.6 Panek's Crotylation Approach to Epothilone Stereotriad Synthesis

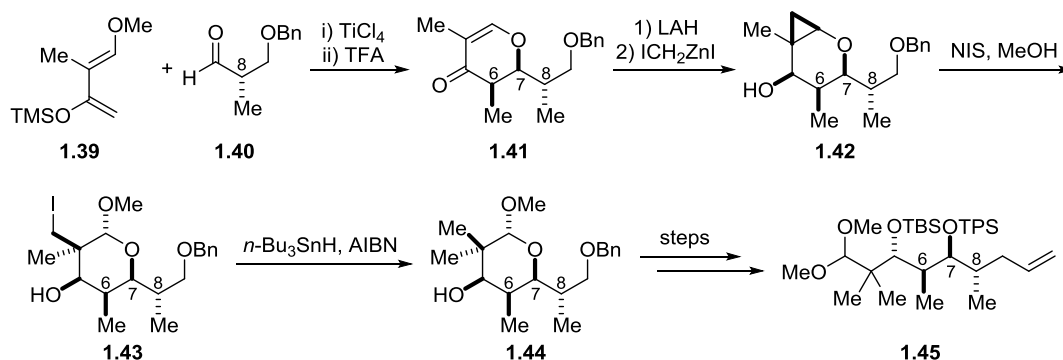
Another crotylation approach to the C6-C8 stereotriad was reported by Grieco (Scheme 1.7).⁶⁰ In this synthesis, formation of a chiral epoxide via Sharpless epoxidation of **1.34** enabled later installation of the chiral C6 methyl through a stereospecific epoxide opening of **1.36** using trimethylaluminum to give **1.37**. After accessing aldehyde **1.38**, Roush asymmetric (*E*)-crotylation was able to install the desired C7 and C8 stereocenters to produce **1.39** as a single diastereomer in 94% yield.



Scheme 1.7 Grieco's Crotylation Approach to the C6-C8 Stereotriad

Danishefsky's Lewis acid catalyzed diene aldehyde cyclocondensation (LACDAC) approach towards the C6-C8 stereotriad was used in the group's first reported synthesis of epothilones.^{44,61} This method utilizes chiral α -methyl aldehyde **1.40** derived from the Roche ester in a chelation-controlled hetero-Diels-Alder reaction with Danishefsky's diene **1.39** to access dihydropyranone **1.41** as essentially one stereoisomer with all three stereocenters of the stereotriad in place (Scheme 1.8). 1,2-Reduction of the carbonyl and a directed Simmons-Smith reaction

provided cyclopropane **1.42**. Regioselective opening of this strained ring with NIS in methanol, followed by deiodination gave **1.44**, containing the desired *geminal*-dimethyl moiety. Subsequent steps opened the ring and provided the elaborated C3-C11 linear fragment **1.45**.

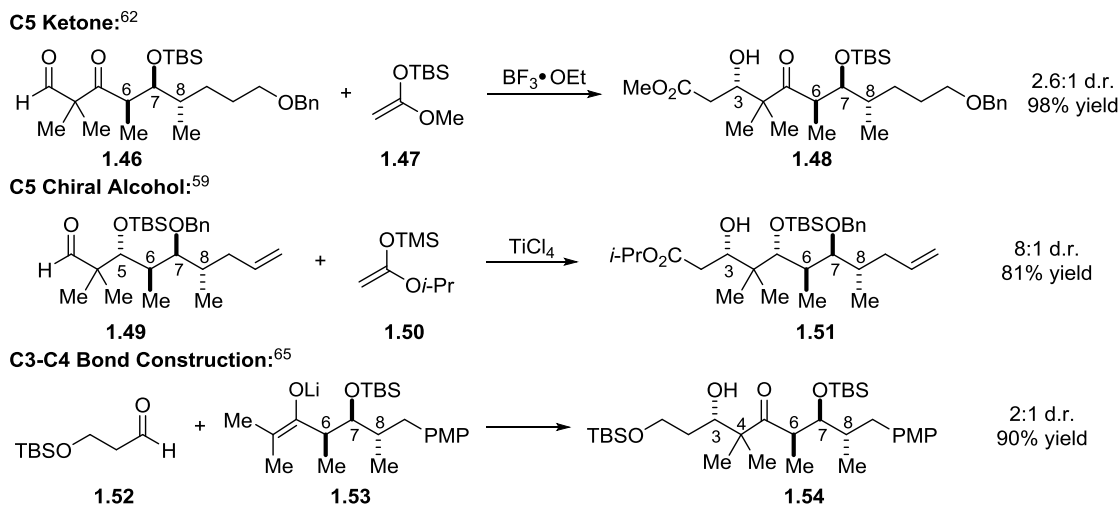


Scheme 1.8 Danishefsky's Use of LACDAC Methodology to Construct C6-C8 Stereotriad

Installation of C3 Stereochemistry

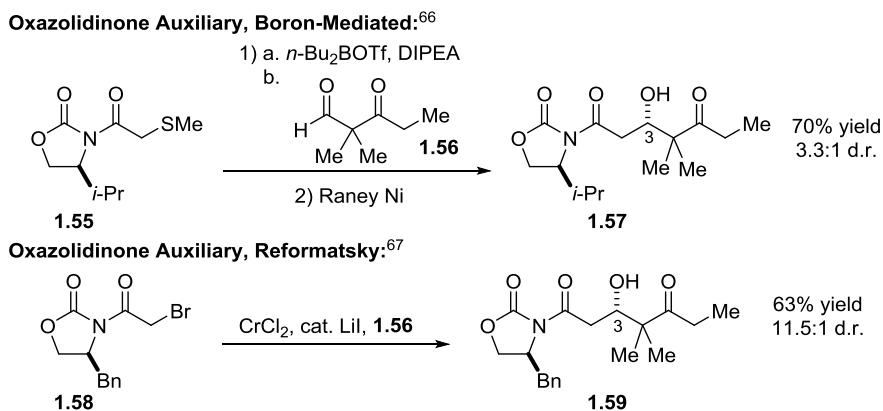
The problem of setting the C3 stereocenter has been approached by a variety of strategies. Stereoselective aldol condensations have been the most widely used, however the C3 stereocenter has also been derived from the chiral pool or established through stereoselective allylation, reduction, or epoxidation.

Aldol-based approaches to the C3 stereochemistry can be divided into three different categories: substrate-based induction, chiral auxiliary, and chiral reagent/catalyst control. For substrate-based control (Scheme 1.9), aldol reactions that rely on the stereochemistry of the C6-C8 stereotriad (with the C5 ketone as it is in the natural product) have been shown to favor the desired 3(*S*) configuration with only approximately 2.5:1 d.r.^{62,63} Approaches that utilize a C5 chiral alcohol have been shown to increase selectivity in some cases,^{60,64} with the highest selectivity of 8:1 d.r. reported by Panek using a TiCl₄-mediated Mukaiyama aldol reaction between **1.49** and **1.50**.⁵⁹ Sinha's alternative strategy to construct the C3-C4 bond instead of the C2-C3 bond was able to achieve only modest selectivity.⁶⁵



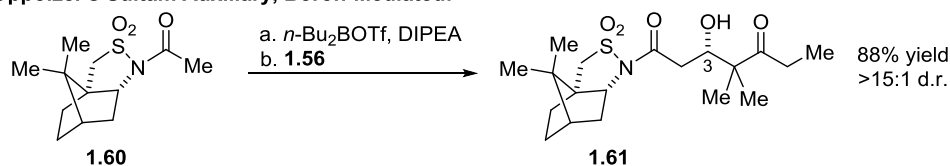
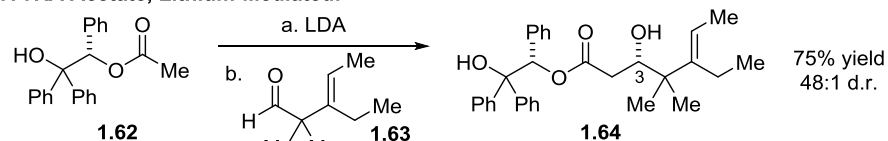
Scheme 1.9 Examples of Substrate-Based Stereocontrol in Aldol Reactions

Chiral auxiliary control has also been used in aldol-based approaches to the formation of the C3 stereocenter (Scheme 1.10). Avery's approach, using the Evans oxazolidinone auxiliary, was able to achieve only a modest selectivity of 3:1 for the formation of **1.57**.⁶⁶ However, Wessjohann showed that a similar auxiliary could be used in a chromium-mediated, Reformatsky-type reaction to access **1.59** in 11.5:1 d.r.⁶⁷

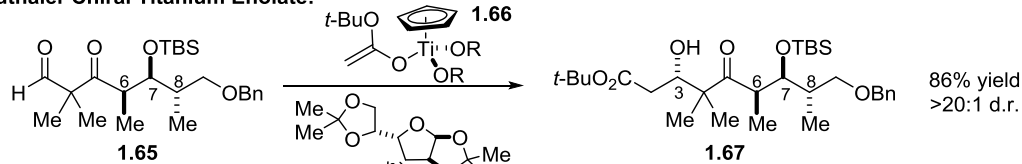
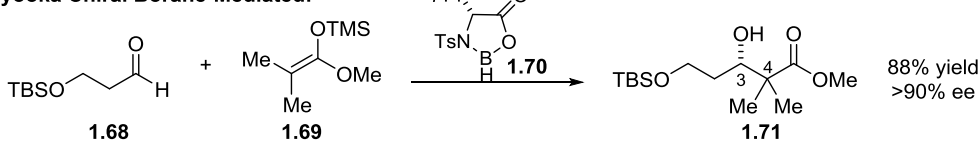
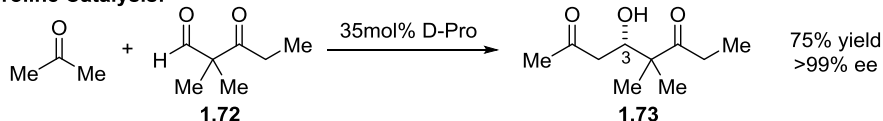


Scheme 1.10 Oxazolidinone Auxiliary Control for the Aldol Approach to C3 Stereochemistry

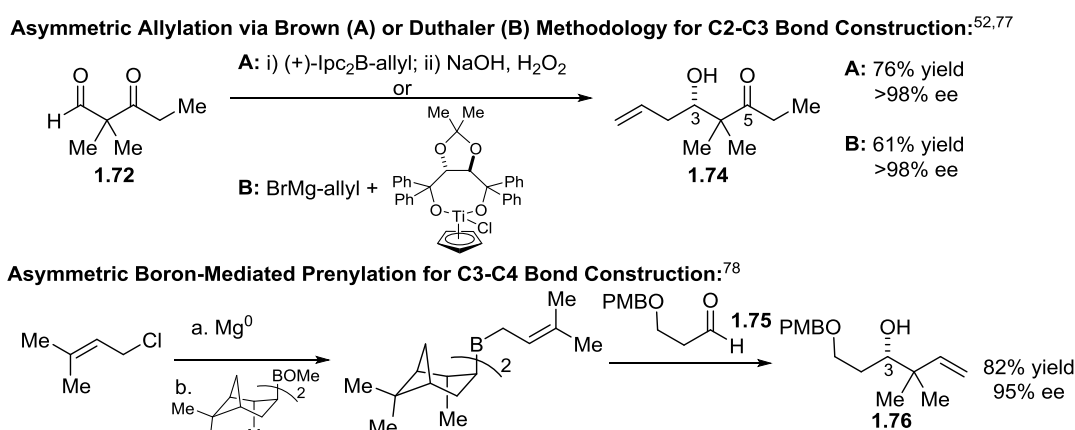
De Brabander reported the use of Oppolzer's sultam auxiliary for a highly diastereoselective boron-mediated aldol reaction to set the C3 stereocenter (Scheme 1.11).⁶⁸ Another highly selective approach by Schinzer utilized HYTRA acetate **1.62**⁶⁹ as the enolate partner in a lithium-mediated aldol.⁷⁰

Oppolzer's Sultam Auxiliary, Boron-Mediated:⁶⁸**HYTRA Acetate, Lithium-Mediated:**⁷⁰**Scheme 1.11** Chiral Auxiliary Control for Aldol Approach of C3 Stereochemistry

Stereinduction of aldol reactions through the use of chiral reagents or catalysts has also been reported for generation of the epothilone C3 stereocenter (Scheme 1.12). Using Duthaler's chiral titanium enolate methodology,⁷¹ Danishefsky was able to access **1.67** from the C3-C9 fragment **1.65** in >20:1.⁷² Another use of chiral reagents, this time with Kiyooka's chiral borane **1.70**,⁷³ has been reported by both Mulzer and Ley to construct the bond between C3-C4 via an enantioselective Mukaiyama aldol reaction, with >90% ee at C3.^{74,75} An organocatalysis approach utilizing D-proline has been used by Avery and co-workers for the aldol reaction of acetone with aldehyde **1.72** to form **1.73** in >99% ee.⁷⁶

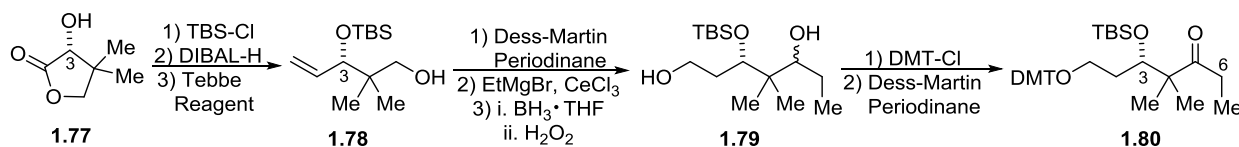
Duthaler Chiral Titanium Enolate:⁷²**Kiyooka Chiral Borane-Mediated:**^{74,75}**D-Proline Catalysis:**⁷⁶**Scheme 1.12** Chiral Reagents and Catalysts for Aldol Stereocontrol

Asymmetric allylation has also been frequently reported as an approach to setting the C3 stereochemistry (Scheme 1.13). Nicolaou's first synthesis utilized this approach for the construction of the bond between C2 and C3. In this case, Brown allylation provided **1.74** in excellent enantioselectivity.⁵² Muzter accomplished the same transformation with the same enantioselectivity using Duthaler's allylation methodology.⁷⁷ These routes have both been used in subsequent total syntheses. Construction of the bond between C3 and C4 has also been achieved with high enantioselectivity by Ramachandran through asymmetric prenylation.⁷⁸



Scheme 1.13 Asymmetric Allylation or Prenylation for Access to C3 Stereocenter

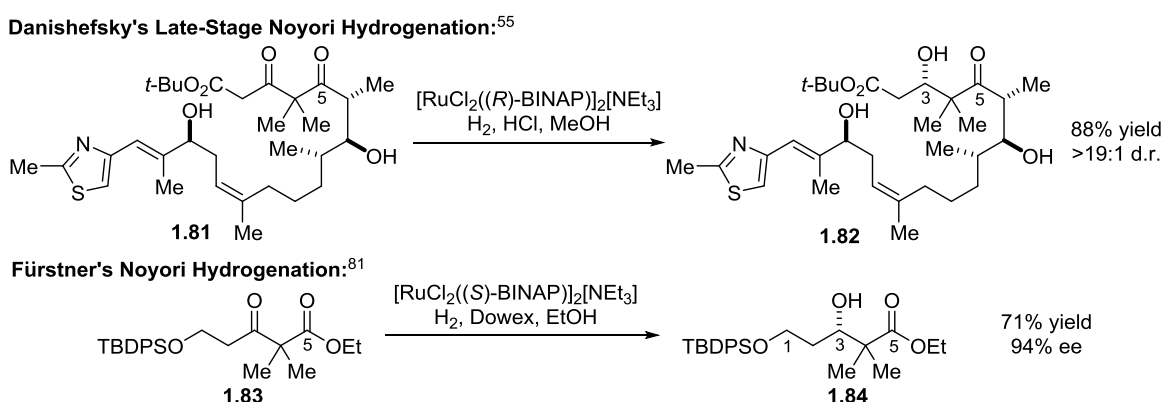
Utilizing a chiral pool, Thomas reported an approach in which epothilone C3 stereochemistry is derived from (*R*)-pantolactone **1.77** (Scheme 1.14). The C1-C6 fragment can be obtained in eight steps by this route.⁷⁹ Researchers at Schering AG utilized a similar route in their synthesis of sagopilone (**1.7**) and other C6 analogs.^{43,80}



Scheme 1.14 Derivation of C3 via Chiral Pool Synthesis (Pantolactone)

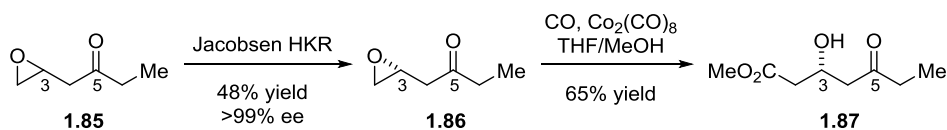
Asymmetric reduction of a ketone is an approach that is less frequently used to access the C3 stereochemistry. Cases utilizing Noyori's chiral catalyst for reduction of a β -ketoester have shown high levels of selectivity (Scheme 1.15). Danishefsky first reported that a Noyori

hydrogenation at a late-stage in his second-generation synthesis was high yielding and proceeded in excellent diastereoselectivity (>19:1 d.r.). Their studies towards implementing the reduction revealed that the terminal double bond in the substrate was susceptible to competitive reduction, but that the C5 ketone was not. In fact, the additional carbonyl group at C5 seemed to be important for high levels of selectivity with this substrate, at least in comparison to a substrate containing an acetate-protected alcohol at C5.⁵⁵ Fürstner later reported an application of a highly enantioselective Noyori hydrogenation on substrate **1.83** that was closer to the beginning of the route and did not have an additional β -carbonyl group.⁸¹



Scheme 1.15 Examples of Selective Reduction to Set C3 Stereocenter

Recently, Liu has reported a highly enantioselective route to the C1-C6 fragment **1.87** using a Jacobsen hydrolytic kinetic resolution of epoxide **1.85** followed by cobalt-catalyzed carbonylation of chiral epoxide **1.86** (Scheme 1.16).⁸²



Scheme 1.16 Access to C3 Stereocenter via Epoxidation

Overall, it should be noted that while a number of the examples that have been described are able to install the C3 stereocenter with high levels of selectivity, there are often additional oxidation state adjustments and/or protecting group manipulations required in order to either

access the desired substrate or to convert the product into a useful form for the next productive step (i.e. carbon-carbon bond construction or for selectively accessing a stereocenter). In evaluating the construction of the entire C1-C9 fragment, including the incorporation of the C6-C8 stereotriad, there is still a need for a more efficient overall synthesis. It is our aim to address this need through the use of a carbonylation-based approach previously developed by our group.

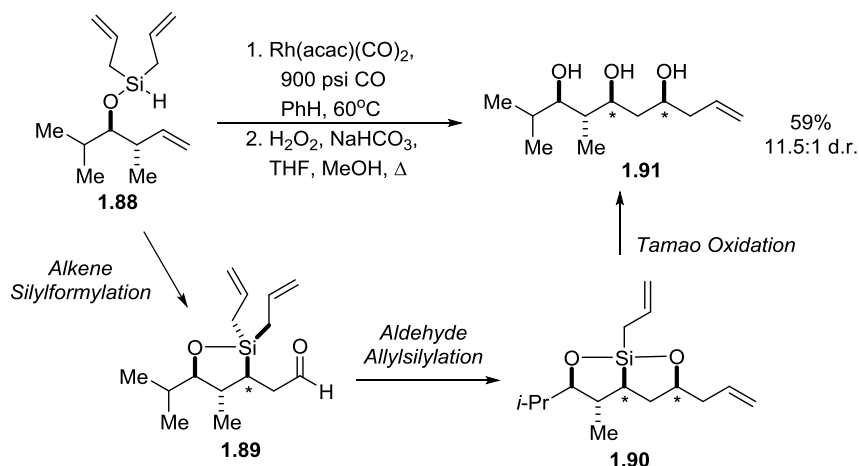
1.3 Leighton Group Carbonylation-Based Approach to Polyketide Synthesis

The Leighton group has had a long standing interest in developing alternative strategies for rapid access to polyketide motifs. A strategy utilizing carbonylation was appealing since it could provide more direct access to aldehyde functionality without the extra protecting group manipulations and oxidation state adjustments necessary in other approaches. A tandem silylformylation-allyl(crotyl)silylation approach was developed, first with homoallylic alcohol substrates to form skipped polyol arrays⁸³ and then extended to homopropargylic alcohol substrates for access to β,β' -dihydroxyketones.^{84,85} Most recently, this methodology has been utilized for the formation of polypropionate stereotriads.

1.3.1 Tandem Silylformylation-Allyl(Crotyl)silylation and Strain-Release Lewis Acidity

The Leighton group tandem silylformylation-allylsilylation chemistry was first described for homoallylic alcohols (Scheme 1.17). In this approach, the rhodium-catalyzed intramolecular alkene silylformylation of diallylsilyl ether **1.88** provides aldehyde **1.89**, which undergoes a spontaneous and diastereoselective intramolecular aldehyde allylsilylation to form **1.90**. Oxidative cleavage of the carbon-silicon bond using Tamao oxidation conditions yields skipped triol **1.91** with the formation of two new stereocenters in 11.5:1 d.r. The mechanism of the silylformylation is believed to occur via a similar mechanism as alkene hydrosilylation. After the silicon-hydrogen bond undergoes oxidative addition to the rhodium species, the coordination of the alkene and 1,2-

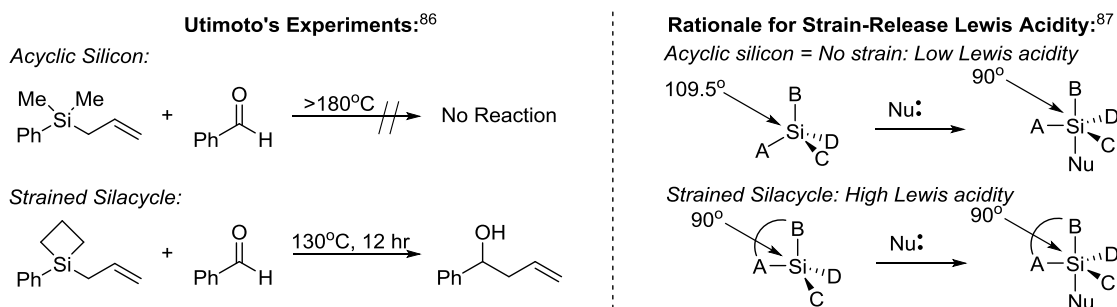
insertion would provide the same intermediate species as in hydrosilylation. However, the migratory insertion of a molecule of carbon monoxide that is coordinated to the metal, followed by reductive elimination would give the aldehyde product **1.89** and regenerate the rhodium catalyst.



Scheme 1.17 Tandem Alkene Silylformylation-Allylsilylation Reaction and Mechanism

The key to this tandem reaction is strain-release Lewis acidity of the silicon that results in the spontaneous allylsilylation of aldehyde **1.89**. While an acyclic silicon species exhibits relatively low Lewis acidity, it has been found that a silane that is incorporated into a four-membered ring has much higher Lewis acid acidity. Utimoto previously reported this effect in the allylation of benzaldehyde using acyclic versus strained allylsilanes (Scheme 1.18).⁸⁶ Denmark has proposed that this property originates from the angle strain at silicon, since the C-Si-C bond angle has been compressed from the ideal tetrahedral bond angle of 109.5° to approximately 79°. With the coordination of a nucleophile, the silicon can rehybridize to a trigonal bipyramidal species, where the compressed angle can be better accommodated by spanning one apical and one equatorial position, for which the ideal bond angle is 90°. ⁸⁷ This concept of strain-release Lewis acidity also applies to five-membered silacycles such as **1.89** because the approximate C-Si-O bond angle is 95°. The coordination of the aldehyde oxygen to the Lewis acidic silicon would

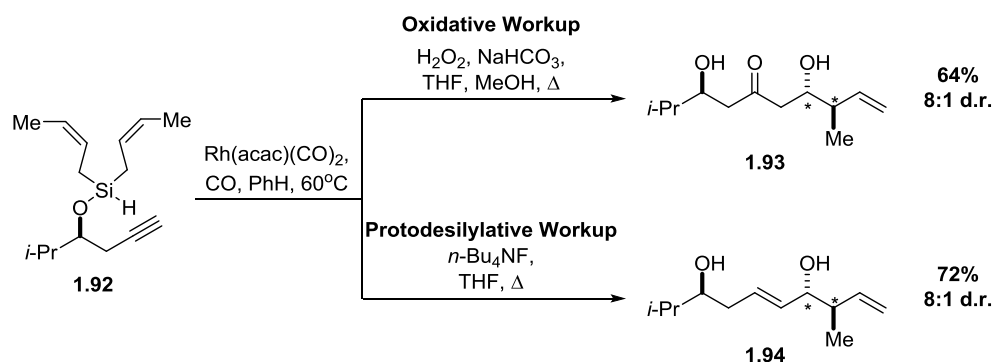
relieve the angle strain by allowing the silicon atom to rehybridize as described, and it would also activate the aldehyde and allyl group for transfer.



Scheme 1.18 Strain-Release Lewis Acidity

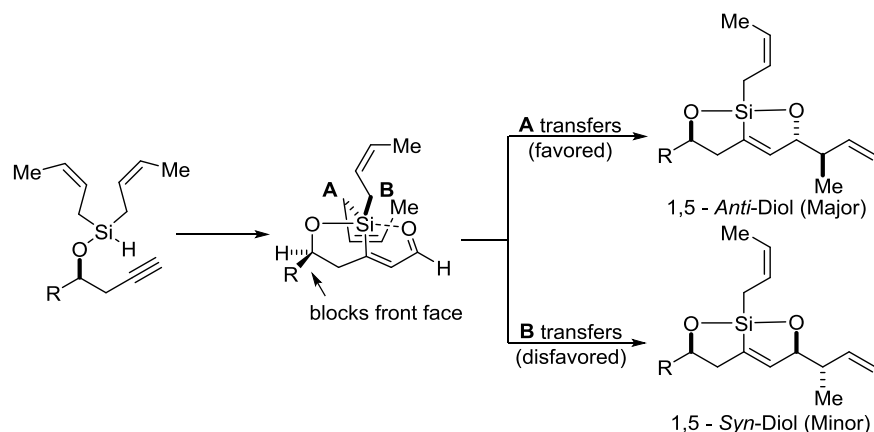
1.3.2 Tandem Silylformylation-Crotylsilylation of Alkynes

The silylformylation-crotylsilylation methodology has been further extended to alkyne substrates (Scheme 1.19).^{84,85} Homopropargylic di(*cis*-crotyl)silyl ethers such as **1.92** undergo the same tandem reaction; however, after oxidative cleavage in the Tamao oxidation, the transient enol intermediate undergoes tautomerization to provide a ketone-containing 1,5-*anti*-diol product **1.93**. A protodesilylative workup is also possible, to give the corresponding alkene product **1.94**.



Scheme 1.19 Tandem Alkyne Silylformylation-Crotylsilylation with Oxidative or Protodesilylative Workup

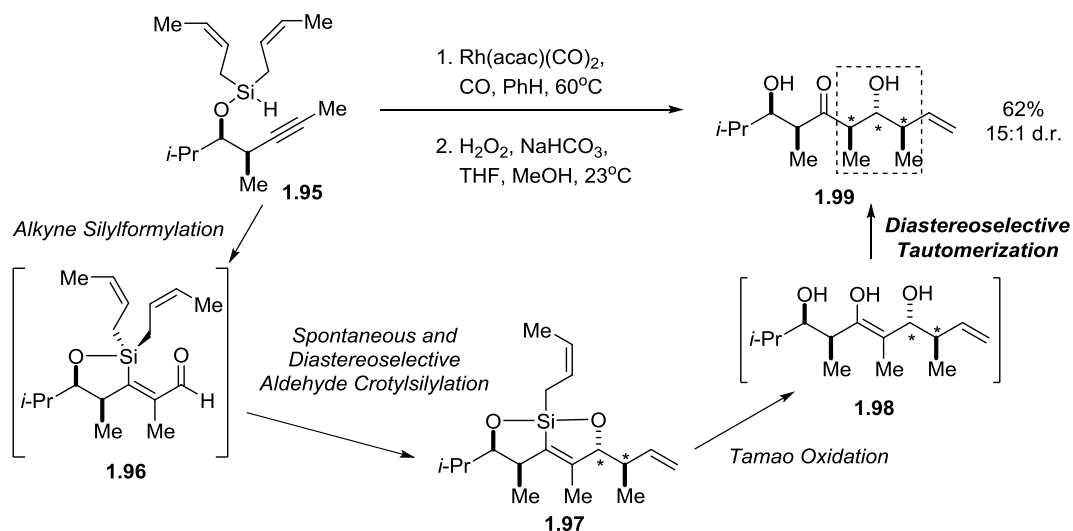
The observed diastereoselectivity favoring the 1,5-*anti*-diol has been attributed to the relative rates at which the diastereotopic crotyl groups transfer due to the steric interactions associated with the R group (Scheme 1.20). The level of selectivity for these transformations varies based on the substituents at the homo-propargylic and propargylic positions.⁸⁵



Scheme 1.20 Stereochemical Model to Explain 1,5-*Anti*-Diol Bias

1.3.3 Extension of Methodology to Internal Alkynes for Production of Stereotriads

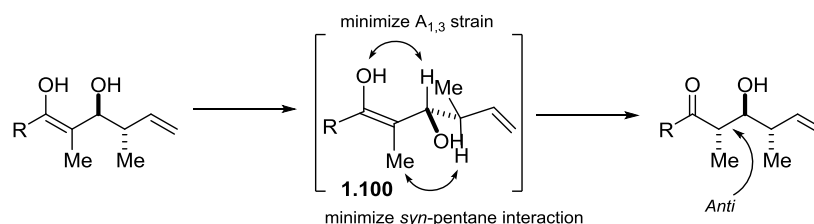
Substrates containing internal alkynes are also amenable to the tandem silylformylation-crotylsilylation methodology (Scheme 1.21).⁴ The tandem reaction followed by a Tamao oxidation resulted in the stereoselective formation of **1.99** in 15:1 d.r. Since the initial product of oxidative cleavage is a substituted enol **1.98**, diastereoselective tautomerization must occur stereoselectively in order to obtain diastereomerically enriched stereotriad product **1.99**.



Scheme 1.21 Tandem Silylformylation-Crotylsilylation/Tamao Oxidation for Stereotriad Formation

The observed *anti* relationship that is favored for this new methyl-bearing stereocenter relative to the vicinal hydroxyl group has been proposed to result from the enol conformation **1.100**

that results from minimization of steric interactions in a polar, protic environment (Scheme 1.22). In this model, the crotyl group can effectively block the back face of the enol, leaving the front face open for delivery of a proton.



Scheme 1.22 Rationalized Model for Observed *Anti* Diastereoselectivity in Tautomerization

This methodology has provided a new approach to the synthesis of polypropionate stereotriads, which has thus far been utilized in a step-economical synthesis of zincophorin methyl ester.⁷ The application of this particular approach to the C1-C9 fragment of the epothilones will be described further in the following chapter.

1.4 References

- (1) Zacuto, M. J.; O'Malley, S. J.; Leighton, J. L. Tandem Silylformylation-Allyl(Crotyl)silylation: A New Approach to Polyketide Synthesis. *Tetrahedron* **2003**, *59*, 8889–8900.
- (2) Zacuto, M. J.; Leighton, J. L. Divergent Synthesis of Complex Polyketide-Like Macrolides From A Simple Polyol Fragment. *Org. Lett.* **2005**, *7*, 5525–5527.
- (3) Park, P. K.; O'Malley, S. J.; Schmidt, D. R.; Leighton, J. L. Total Synthesis of Dolabelide D. *J. Am. Chem. Soc.* **2006**, *128*, 2796–2797.
- (4) Spletstoser, J. T.; Zacuto, M. J.; Leighton, J. L. Tandem Silylformylation-Crotylsilylation/Tamao Oxidation of Internal Alkynes: A Remarkable Example of Generating Complexity from Simplicity. *Org. Lett.* **2008**, *10*, 5593–5596.
- (5) Chalifoux, W. A.; Reznik, S. K.; Leighton, J. L. Direct and Highly Regioselective and Enantioselective Allylation of Beta-Diketones. *Nature* **2012**, *487*, 86–89.
- (6) Kim, H.; Ho, S.; Leighton, J. L. A More Comprehensive and Highly Practical Solution to Enantioselective Aldehyde Crotylation. *J. Am. Chem. Soc.* **2011**, *133*, 6517–6520.
- (7) Harrison, T. J.; Ho, S.; Leighton, J. L. Toward More “Ideal” Polyketide Natural Product Synthesis: A Step-Economical Synthesis of Zincophorin Methyl Ester. *J. Am. Chem. Soc.* **2011**, *133*, 7308–7311.
- (8) Reznik, S. K.; Leighton, J. L. Toward a More Step-Economical and Scalable Synthesis of Spongistatin 1 to Facilitate Cancer Drug Development Efforts. *Chem. Sci.* **2013**, *4*, 1497.
- (9) Reznik, S. K.; Marcus, B. S.; Leighton, J. L. Complex Fragment Coupling by Crotylation: A Powerful Tool for Polyketide Natural Product Synthesis. *Chem. Sci.* **2012**, *3*, 3326–3330.
- (10) Suen, L. M.; Steigerwald, M. L.; Leighton, J. L. A New and More Powerfully Activating Diamine for Practical and Scalable Enantioselective Aldehyde Crotylsilylation Reactions. *Chem. Sci.* **2013**, *4*, 2413.
- (11) Ho, S.; Bucher, C.; Leighton, J. L. A Highly Step-Economical Synthesis of Dictyostatin. *Angew. Chem. Int. Ed.* **2013**, *52*, 6757–6761.
- (12) Li, J.; Menche, D. Direct Methods for Stereoselective Polypropionate Synthesis: A Survey. *Synthesis* **2009**, *2009*, 2293–2315.
- (13) Koskinen, A. M. P.; Karisalmi, K. Polyketide Stereotetrads in Natural Products. *Chem. Soc. Rev.* **2005**, *34*, 677–690.

- (14) Foley, C. N.; Leighton, J. L. Beyond the Roche Ester: A New Approach to Polypropionate Stereotriad Synthesis. *Org. Lett.* **2014**, *16*, 1180–1183.
- (15) Höfle, G.; Bedorf, N.; Steinmetz, H.; Schomburg, D.; Gerth, K.; Reichenbach, H. Epothilone A and B--Novel 16-Membered Macrolides with Cytotoxic Activity: Isolation, Crystal Structure, and Conformation in Solution. *Angew. Chem. Int. Ed.* **1996**, *35*, 1567–1569.
- (16) Gerth, K.; Bedorf, N.; Höfle, G.; Irschik, H.; Reichenbach, H. Epothilons A and B: Antifungal and Cytotoxic Compounds from *Sorangium Cellulosum* (Myxobacteria). Production, Physico-Chemical and Biological Properties. *J. Antibiot.* **1996**, *49*, 560–563.
- (17) Bollag, D.; McQueney, P.; Zhu, J.; Hensens, O.; Koupal, L.; Liesch, J.; Goetz, M.; Lazarides, E.; Woods, C. M. Epothilones, a New Class of Microtubule-Stabilizing Agents with a Taxol-like Mechanism of Action. *Cancer Res.* **1995**, *55*, 2325–2333.
- (18) Altmann, K.-H.; Pfeiffer, B.; Arseniyadis, S.; Pratt, B. A.; Nicolaou, K. C. The Chemistry and Biology of Epothilones--The Wheel Keeps Turning. *ChemMedChem* **2007**, *2*, 396–423.
- (19) Altmann, K. H.; Wartmann, M.; O'Reilly, T. Epothilones and Related Structures--A New Class of Microtubule Inhibitors with Potent in Vivo Antitumor Activity. *Biochim. Biophys. Acta* **2000**, *1470*, M79–M91.
- (20) Giannakakou, P.; Sackett, D. L.; Kang, Y.-K.; Zhan, Z.; Buters, J. T. M.; Fojo, T.; Poruchynsky, M. S. Paclitaxel-Resistant Human Ovarian Cancer Cells Have Mutant Beta-Tubulins That Exhibit Impaired Paclitaxel-Driven Polymerization. *J. Biol. Chem.* **1997**, *272*, 17118–17125.
- (21) Rowinsky, E. K. The Development and Clinical Utility of the Taxane Class of Antimicrotubule Chemotherapy Agents. *Annu. Rev. Med.* **1997**, *48*, 353–374.
- (22) Nicolaou, K. C.; Roschangar, F.; Vourloumis, D. Chemical Biology of Epothilones. *Angew. Chem. Int. Ed.* **1998**, *37*, 2014–2045.
- (23) Harris, C.; Danishefsky, S. Complex Target-Oriented Synthesis in the Drug Discovery Process: A Case History in the dEpoB Series. *J. Org. Chem.* **1999**, 8434–8456.
- (24) Nicolaou, K. C.; Ritzén, A.; Namoto, K. Recent Developments in the Chemistry, Biology and Medicine of the Epothilones. *Chem. Commun.* **2001**, 1523–1535.
- (25) Altmann, K.; Bold, G.; Caravatti, G.; End, N.; Florsheimer, A.; Guagnano, V.; Reilly, T. O.; Wartmann, M. Epothilones and Their Analogs--Potential New Weapons in the Fight Against Cancer. *Chimia* **2000**, *54*, 612–621.
- (26) Altmann, K.-H. The Merger of Natural Product Synthesis and Medicinal Chemistry: On the Chemistry and Chemical Biology of Epothilones. *Org. Biomol. Chem.* **2004**, *2*, 2137–2152.

- (27) Watkins, E. B.; Chittiboyina, A. G.; Avery, M. A. Recent Developments in the Syntheses of the Epothilones and Related Analogues. *European J. Org. Chem.* **2006**, 2006, 4071–4084.
- (28) Mulzer, J.; Altmann, K.-H.; Höfle, G.; Müller, R.; Prantz, K. Epothilones – A Fascinating Family of Microtubule Stabilizing Antitumor Agents. *C. R. Chim.* **2008**, 11, 1336–1368.
- (29) Luduvico, I.; Hyaric, M.; De Almeida, M.; Da Silva, A. Synthetic Methodologies for the Preparation of Epothilones and Analogs. *Mini. Rev. Org. Chem.* **2006**, 3, 49–75.
- (30) Altmann, K.-H.; Memmert, K. Epothilones as Lead Structures for New Anticancer Drugs--Pharmacology, Fermentation, and Structure-Activity-Relationships. *Prog. Drug Res.* **2008**, 66, 273, 275–334.
- (31) Nicolaou, K.; Vourloumis, D. Designed Epothilones: Combinatorial Synthesis, Tubulin Assembly Properties, and Cytotoxic Action against Taxol-Resistant Tumor Cells. *Angew. Chem. Int. Ed.* **1997**, 36, 2097–2103.
- (32) Cheng, K. L.; Bradley, T.; Budman, D. R. Novel Microtubule-Targeting Agents - The Epothilones. *Biologics* **2008**, 2, 789–811.
- (33) Krause, W.; Klar, U. Differences and Similarities of Epothilones. *Curr. Cancer Ther. Rev.* **2011**, 7, 10–36.
- (34) Mulzer, J.; Prantz, K. Total Synthesis of Epothilones A-F. In *The Epothilones: An Outstanding Family of Anti-Tumor Agents. From Soil to the Clinic*; Altmann, K.-H.; Hofle, G.; Muller, R.; Mulzer, J.; Prantz, K., Eds.; Springer Vienna, 2009; Vol. 90, pp. 55–133.
- (35) Altmann, K.; Blommers, M. J. J.; Caravatti, G.; Flörsheimer, A.; Nicolaou, K. C.; Reilly, T. O.; Schmidt, A.; Schinzer, D.; Wartmann, M. Synthetic and Semisynthetic Analogs of Epothilones: Chemistry and Biological Activity. In *ACS Symposium Series Vol. 796*; Ojima, I.; Vite, G. D.; Altmann, K.-H., Eds.; American Chemical Society, 2001; pp. 112–130.
- (36) Klar, U.; Skuballa, W.; Buchmann, B.; Schwede, W.; Bunte, T.; Hoffmann, J.; Lichtner, R. B. Synthesis and Biological Activity of Epothilones Syntheses of Epothilone B and D Analogs. In *ACS Symposium Series Vol. 796*; Ojima, I.; Vite, G. D.; Altmann, K.-H., Eds.; American Chemical Society, 2001; pp. 131–147.
- (37) Vite, G. D.; Borzilleri, R. M.; Kim, S.; Regueiro-ren, A.; Humphreys, W. G.; Lee, F. Y. F. Highly Efficient Semisynthesis of Biologically Active Epothilone Derivatives. In *ACS Symposium Series Vol. 796*; Ojima, I.; Vite, G. D.; Altmann, K.-H., Eds.; American Chemical Society, 2001; pp. 97–111.
- (38) Klar, U.; Buchmann, B.; Schwede, W.; Skuballa, W.; Hoffmann, J.; Lichtner, R. B. Total Synthesis and Antitumor Activity of ZK-EPO: The First Fully Synthetic Epothilone in Clinical Development. *Angew. Chem. Int. Ed.* **2006**, 45, 7942–7948.

- (39) Wilson, R. M.; Danishefsky, S. J. On the Reach of Chemical Synthesis: Creation of a Mini-Pipeline from an Academic Laboratory. *Angew. Chem. Int. Ed.* **2010**, *49*, 6032–6056.
- (40) Chou, T.-C.; Zhang, X.; Zhong, Z.-Y.; Li, Y.; Feng, L.; Eng, S.; Myles, D. R.; Johnson, R.; Wu, N.; Yin, Y. I.; Wilson, R. M.; Danishefsky, S. J. Therapeutic Effect against Human Xenograft Tumors in Nude Mice by the Third Generation Microtubule Stabilizing Epothilones. *Proc. Natl. Acad. Sci. U. S. A.* **2008**, *105*, 13157–13162.
- (41) Rivkin, A.; Chou, T.-C.; Danishefsky, S. J. On the Remarkable Antitumor Properties of Fludelone: How We Got There. *Angew. Chem. Int. Ed. Engl.* **2005**, *44*, 2838–2850.
- (42) Nicolaou, K. C.; Pratt, B. A.; Arseniyadis, S.; Wartmann, M.; O'Brate, A.; Giannakakou, P. Molecular Design and Chemical Synthesis of a Highly Potent Epothilone. *ChemMedChem* **2006**, *1*, 41–44.
- (43) Klar, U.; Platzek, J. Asymmetric Total Synthesis of the Epothilone Sagopilone—From Research to Development. *Synlett* **2012**, *23*, 1291–1299.
- (44) Balog, A.; Meng, D.; Kamenecka, T.; Bertinato, P.; Su, D.-S.; Sorensen, E. J.; Danishefsky, S. J. Total Synthesis of (-)-Epothilone A. *Angew. Chem. Int. Ed.* **1996**, *35*, 2801–2803.
- (45) Yang, Z.; He, Y.; Vourloumis, D.; Vallberg, H.; Nicolaou, K. C. Total Synthesis of Epothilone A: The Olefin Metathesis Approach. *Angew. Chem. Int. Ed.* **1997**, *36*, 166–168.
- (46) Schinzer, D.; Limberg, A.; Bauer, A.; Bohm, O. M.; Cordes, M. Total Synthesis of (-)-Epothilone A. *Angew. Chem. Int. Ed.* **1997**, *36*, 523–524.
- (47) Inanaga, J.; Hirata, K.; Saeki, H.; Katsuki, T.; Yamaguchi, M. A Rapid Esterification by Means of Mixed Anhydride and Its Application to Large-Ring Lactonization. *Bull. Chem. Soc. Jpn.* **1979**, *52*, 1989–1993.
- (48) Sun, J.; Sinha, S. C. Stereoselective Total Synthesis of Epothilones by the Metathesis Approach Involving C9-C10 Bond Formation. *Angew. Chem. Int. Ed.* **2002**, *41*, 1381–1383.
- (49) Rivkin, A.; Yoshimura, F.; Gabarda, A. E.; Chou, T.-C.; Dong, H.; Tong, W. P.; Danishefsky, S. J. Complex Target-Oriented Total Synthesis in the Drug Discovery Process: The Discovery of a Highly Promising Family of Second Generation Epothilones. *J. Am. Chem. Soc.* **2003**, *125*, 2899–2901.
- (50) Heathcock, C. H. 1.6 - The Aldol Reaction: Group I and Group II Enolates. In *Comprehensive Organic Synthesis; Volume 2: Addition to C-X π bonds, Part 2*; Trost, B. M.; Fleming, I., Eds.; Pergamon Press: Oxford, 1991; pp. 133–179.
- (51) Roush, W. R. Concerning the Diastereofacial Selectivity of the Aldol Reactions of α -Methyl Chiral Aldehydes and Lithium and Boron Propionate Enolates. *J. Org. Chem.* **1991**, *56*, 4151–4157.

- (52) Nicolaou, K. C.; Ninkovic, S.; Sarabia, F.; Vourloumis, D.; He, Y.; Vallberg, H.; Finlay, M. R. V.; Yang, Z.; Dri, V.; Jolla, L.; April, R. V. Total Syntheses of Epothilones A and B via a Macrolactonization-Based Strategy. *1997*, *119*, 7974–7991.
- (53) White, J.; Carter, R. Total Synthesis of Epothilone B, Epothilone D, and Cis-and Trans-9, 10-Dehydroepothilone D. *J. Am. Chem. Soc.* **2001**, *123*, 5407–5413.
- (54) Wu, Z.; Zhang, F.; Danishefsky, S. J. Subtle Variations in the Long-Range Transmission of Stereochemical Information: Matched and Mismatched Aldol Reactions. *Angew. Chem. Int. Ed.* **2000**, *39*, 4505–4508.
- (55) Harris, C.; Kuduk, S.; Balog, A.; Savin, K.; Glunz, P. W.; Danishefsky, S. J. New Chemical Synthesis of the Promising Cancer Chemotherapeutic Agent 12, 13-Desoxyepothilone B: Discovery of a Surprising Long-Range Effect on the Diastereoselectivity of an Aldol Condensation. *J. Am. Chem. Soc.* **1999**, *121*, 7050–7062.
- (56) Posner, G. H.; Lentz, C. M. A Directing Effect of Neighboring Aromatic Groups on the Regiochemistry of Formation and on the Stereochemistry of Alkylation and Bromination of Ketone Lithium Enolates. *J. Am. Chem. Soc.* **1979**, *101*, 934–946.
- (57) Ghera, E.; Kleiman, V.; Hassner, A. Remote Asymmetric Induction in Michael Additions of Allylic Sulfones. *J. Org. Chem.* **1999**, *64*, 8–9.
- (58) Zhu, B.; Panek, J. S. Total Synthesis of Epothilone A. *Org. Lett.* **2000**, *2*, 2575–2578.
- (59) Zhu, B.; Panek, J. S. Methodology Based on Chiral Silanes in the Synthesis of Polypropionate-Derived Natural Products - Total Synthesis of Epothilone A. *European J. Org. Chem.* **2001**, 1701–1714.
- (60) May, S. A.; Grieco, P. A. Total Synthesis of (-)-Epothilone B. *Chem. Commun.* **1998**, 1597–1598.
- (61) Bertinato, P.; Sorensen, E. J.; Meng, D.; Danishefsky, S. J. Studies toward a Synthesis of Epothilone A: Stereocontrolled Assembly of the Acyl Region and Models for Macrocyclization. *J. Org. Chem.* **1996**, *61*, 8000–8001.
- (62) Broadrup, R. L.; Sundar, H. M.; Swindell, C. S. Total Synthesis of 12,13-Desoxyepothilone B (Epothilone D). *Bioorg. Chem.* **2005**, *33*, 116–133.
- (63) Ermolenko, M. S.; Potier, P. Synthesis of Epothilones B and D from D-Glucose. *Tetrahedron Lett.* **2002**, *43*, 2895–2898.
- (64) Meng, D.; Su, D.; Balog, A.; Bertinato, P.; Sorensen, E. J.; Danishefsky, S. J.; Zheng, Y.; Chou, T.; He, L.; Horwitz, S. B. Remote Effects in Macrolide Formation through Ring-Forming Olefin Metathesis: An Application to the Synthesis of Fully Active Epothilone Congeners. *J. Am. Chem. Soc.* **1997**, *119*, 2733–2734.

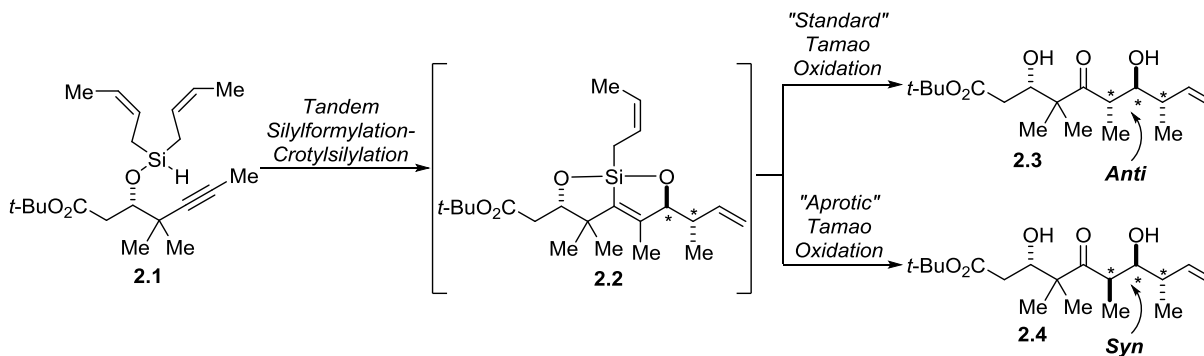
- (65) Sinha, S. C.; Barbas, C. F.; Lerner, R. A. The Antibody Catalysis Route to the Total Synthesis of Epothilones. *Proc. Natl. Acad. Sci. U. S. A.* **1998**, *95*, 14603–14608.
- (66) Valluri, M.; Hindupur, R. M.; Bijoy, P.; Labadie, G.; Jung, J.-C.; Avery, M. A. Total Synthesis of Epothilone B. *Org. Lett.* **2001**, *3*, 3607–3609.
- (67) Scheid, G.; Ruijter, E.; Konarzycka-Bessler, M.; Bornscheuer, U. T.; Wessjohann, L. A. Synthesis and Resolution of a Key Building Block for Epothilones: A Comparison of Asymmetric Synthesis, Chemical and Enzymatic Resolution. *Tetrahedron: Asymmetry* **2004**, *15*, 2861–2869.
- (68) De Brabander, J.; Rosset, S.; Bernardinelli, G. Towards a Synthesis of Epothilone A: Rapid Assembly of the C1-C6 and C7-C12 Fragments. *Synlett* **1997**, 824–826.
- (69) Braun, M.; Waldmuller, D. Simple Three-Step Synthesis of (R)- and (S)-4-Amino-3-Hydroxybutanoic Acid (GABOB) by Stereoselective Aldol Addition. *Synthesis* **1989**, 856–858.
- (70) Schinzer, D.; Bauer, A.; Böhm, O. M.; Limberg, A.; Cordes, M. Total Synthesis of (-)-Epothilone A. *Chem. Eur. J.* **1999**, *5*, 2483–2491.
- (71) Duthaler, R. O.; Herold, P.; Lottenbach, W.; Oertle, K.; Riediker, M. Enantioselective Aldol Reaction of Tert-Butyl Acetate Using Titanium-Carbohydrate Complexes. *Angew. Chem. Int. Ed.* **1989**, *28*, 495–497.
- (72) Rivkin, A.; Yoshimura, F.; Gabarda, A. E.; Cho, Y. S.; Chou, T.-C.; Dong, H.; Danishefsky, S. J. Discovery of (E)-9,10-Dehydroepothilones through Chemical Synthesis: On the Emergence of 26-Trifluoro-(E)-9,10-Dehydro-12,13-Desoxyepothilone B as a Promising Anticancer Drug Candidate. *J. Am. Chem. Soc.* **2004**, *126*, 10913–10922.
- (73) Kiyooka, S.; Kaneko, Y.; Komura, M.; Matsuo, H.; Nakano, M. Enantioselective Chiral Borane-Mediated Aldol Reactions of Silyl Ketene Acetals with Aldehydes. Novel Effect of the Trialkylsilyl Group of the Silyl Ketene Acetal on the Reaction Course. *J. Org. Chem.* **1991**, *56*, 2276–2278.
- (74) Mulzer, J.; Mantoulidis, A.; Öhler, E. Easy Access to the Epothilone Family- Synthesis of Epothilone B. *Tetrahedron Lett.* **1998**, *39*, 8633–8636.
- (75) Storer, R. I.; Takemoto, T.; Jackson, P. S.; Ley, S. V. A Total Synthesis of Epothilones Using Solid-Supported Reagents and Scavengers. *Angew. Chem. Int. Ed.* **2003**, *42*, 2521–2525.
- (76) Zheng, Y.; Avery, M. A. Asymmetric Aldol Reactions Using Catalytic D(+)-Proline: A New, Economic and Practical Approach to a Commonly Employed C1–C6 Keto-Acid Synthon of the Epothilones. *Tetrahedron* **2004**, *60*, 2091–2095.

- (77) Martin, H. J.; Pojarliev, P.; Kählig, H.; Mulzer, J. The 12,13-Diol Cyclization Approach for a Truly Stereocontrolled Total Synthesis of Epothilone B and the Synthesis of a Conformationally Restrained Analogue. *Chem. Eur. J.* **2001**, 7, 2261–2271.
- (78) Ramachandran, P. V.; Prabhudas, B.; Chandra, J. S.; Reddy, M. V. R.; Brown, H. C. Preparative-Scale Synthesis of Both Antipodes of B- Γ , γ -Dimethylallyldiisopinocampheylborane: Application for the Synthesis of C1–C6 Subunit of Epothilone. *Tetrahedron Lett.* **2004**, 45, 1011–1013.
- (79) Martin, N.; Thomas, E. J. Total Syntheses of Epothilones B and D: Applications of Allylstannanes in Organic Synthesis. *Tetrahedron Lett.* **2001**, 42, 8373–8377.
- (80) Klar, U.; Röhr, B.; Kuczynski, F.; Schwede, W.; Berger, M.; Skuballa, W.; Buchmann, B. Efficient Chiral Pool Synthesis of the C1–C6 Fragment of Epothilones. *Synthesis* **2005**, 301–305.
- (81) Fürstner, A.; Mathes, C.; Lehmann, C. W. Alkyne Metathesis: Development of a Novel Molybdenum-Based Catalyst System and Its Application to the Total Synthesis of Epothilone A and C. *Chem. Eur. J.* **2001**, 7, 5299–5317.
- (82) Liu, Z.-Y.; Chen, Z.-C.; Yu, C.-Z.; Wang, R.-F.; Zhang, R.-Z.; Huang, C.-S.; Yan, Z.; Cao, D.-R.; Sun, J.-B.; Li, G. Total Synthesis of Epothilone A through Stereospecific Epoxidation of the P-Methoxybenzyl Ether of Epothilone C. *Chem. Eur. J.* **2002**, 8, 3747–3756.
- (83) Zacuto, M.; Leighton, J. Tandem Intramolecular Silylformylation-Allylsilylation. *J. Am. Chem. Soc.* **2000**, 122, 8587–8588.
- (84) O'Malley, S. J.; Leighton, J. L. Tandem Intramolecular Alkyne Silylformylation-Allylsilylation: A Case of Remote 1,5-Asymmetric Induction. *Angew. Chem. Int. Ed.* **2001**, 40, 2915–2917.
- (85) Zacuto, M. J.; O'Malley, S. J.; Leighton, J. L. Tandem Intramolecular Silylformylation-Crotylsilylation: Highly Efficient Synthesis of Polyketide Fragments. *J. Am. Chem. Soc.* **2002**, 124, 7890–7891.
- (86) Matsumoto, K.; Oshima, K.; Utimoto, K. Noncatalyzed Stereoselective Allylation of Carbonyl Compounds with Allylsilacyclobutanes. *J. Org. Chem.* **1994**, 59, 7152–7155.
- (87) Denmark, S. E.; Jacobs, R. T.; Dai-Ho, G.; Wilson, S. Synthesis, Structure, and Reactivity of an Organogermanium Lewis Acid. *Organometallics* **1990**, 9, 3015–3019.

Chapter 2: Improving Selectivity and Efficiency in the Synthesis of the C1-C9 Fragment of the Epothilones

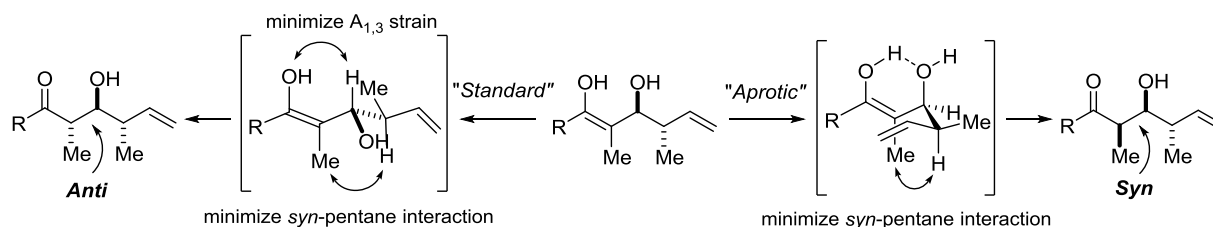
2.1 Introduction: First Generation Synthesis and the “Aprotic” Tamao Oxidation

As mentioned in the previous chapter, the Leighton group has been interested in applying our tandem silylformylation-crotylsilylation/Tamao oxidation methodology towards the development of a new highly efficient synthesis of the critical C1-C9 fragment of the epothilones. Our group’s first-generation synthesis implemented and further built on this strategy with the critical development of alternate Tamao oxidation conditions to allow access to the required *syn,anti* stereochemistry of the C6-C8 stereotriad **2.4**.¹ Since the previously utilized “standard” Tamao oxidation conditions impart *anti* selectivity in the tautomerization event (as in **2.3**), a new set of conditions for the Tamao oxidation were developed which promote a *syn*-selective tautomerization following the oxidative cleavage of the C-Si bond (Scheme 2.1).



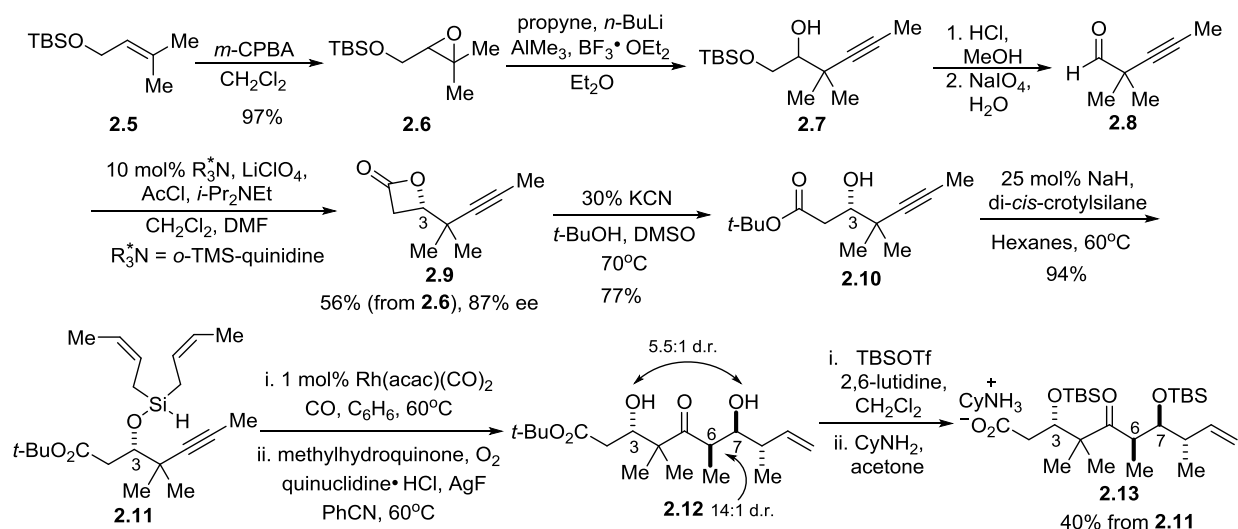
Scheme 2.1 Tandem Silylformylation-Crotylation with “Standard” vs “Aprotic” Tamao Oxidation

When considering how the intrinsic selectivity of this tautomerization event could be reversed, it was hypothesized that a favorable conformational change in the intermediate enol might be caused by the use of “aprotic” conditions that would promote intramolecular hydrogen bonding. A conformational model invoking this hydrogen bonding effect seems to predict that instead of the back face being blocked by the crotyl group, now the front face would be blocked, leaving the back face open to protonation to give the *syn* product (Scheme 2.2).



Scheme 2.2 Rationalized Models for Tautomerization Selectivity under "Standard" vs "Aprotic" Conditions

Utilizing the *in situ* generation of dry hydrogen peroxide from a hydroquinone under atmospheric pressure of oxygen, as previously reported by Tamao,² conditions that provided the desired *syn* product **2.4** in 14:1 d.r. at the C6 stereocenter were ultimately found. The development of this switch in selectivity, which has enabled access to the desired *syn*, *anti*-stereochemistry of the stereotriad, was a vital step towards achieving a highly efficient synthesis of the targeted epothilone fragment. However, we believed that there were a few problems remaining in the overall synthesis of this fragment that could be improved upon.



Scheme 2.3 Leighton Group First-Generation Route to the C1-C9 Fragment

In the first generation route (Scheme 2.3), synthesis of the key β -hydroxyester intermediate **2.10** was achieved in 6 steps with 42% overall yield and 87% ee. This was accomplished starting with the racemic epoxidation of **2.5**, followed by regioselective epoxide opening with an *in situ* formed propynyl aluminate reagent,³ and then TBS deprotection and oxidative cleavage to access

aldehyde **2.8**. The C3 stereocenter was set via an enantioselective ketene cycloaddition,⁴ followed by alcoholysis of β -lactone **2.9** to provide **2.10**. While this strategy provided a reliable route to access the desired intermediate, we thought that a more step-economical route to **2.10** could be developed, perhaps with enhanced enantioselectivity in setting the C3 stereocenter.

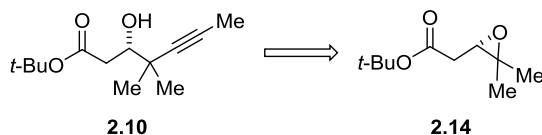
Addressing the rest of the synthesis, the overall approach of the tandem silylformylation-crotylsilylation/“aprotic” Tamao oxidation of **2.11** was successful for the rapid construction of the C6-C8 stereotriad, with excellent diastereoselectivity for the newly developed “aprotic” Tamao oxidation. However, the diastereoselectivity of the crotylation reaction was only 5.5:1 favoring the 1,5-*anti*-diol. As mentioned in the previous chapter, in using this tandem silylformylation-crotylsilylation approach, the level of selectivity in the crotylation is substrate dependent and directly influenced by the substituents around the homopropargylic alcohol. Unfortunately, the substrate that was required in this synthesis did not exhibit the excellent levels of diastereoselectivity that have been found with some of the previously studied substrates. We thought that this diastereoselectivity could be improved through the modification of our approach.

Thus, in our approach to a second-generation synthesis of this fragment, we had two goals: first, we hoped to streamline our synthesis for the formation of intermediate **2.10**, and second, we hoped to improve the diastereoselectivity of the crotylation step.

2.2 Development of a More Selective and Streamlined Synthesis of Key Intermediate **2.10**

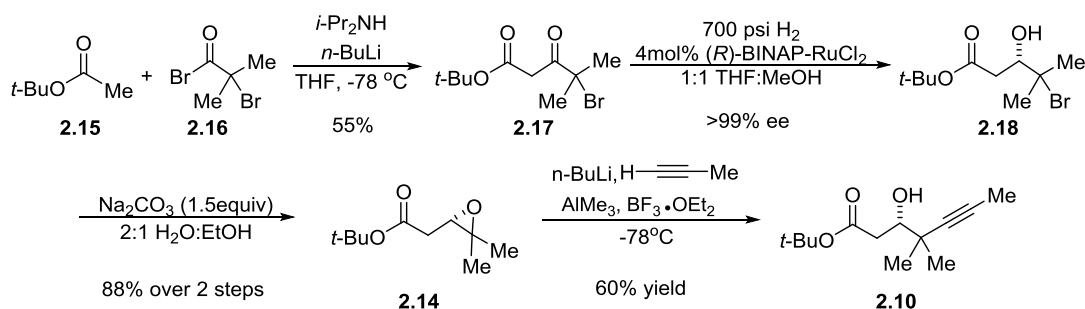
In considering how we could access **2.10** more directly, we thought that we could utilize the same regioselective epoxide-opening approach as above to install the alkyne moiety, but instead use a chiral epoxide with the ester already in place such as **2.14** (Scheme 2.4). Unfortunately, previous attempts for enantioselective epoxidation of the corresponding trisubstituted alkene were only able to afford **2.14** in 78% ee at best, via the Shi epoxidation

protocol.⁵ Although this level of enantioselectivity could be acceptable given the more direct route, it would also require the “unnatural” enantiomer of the Shi catalyst, which is more difficult to access.



Scheme 2.4 Approach to **2.10** via Opening of Chiral Epoxide

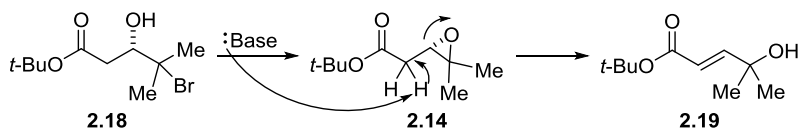
Thinking about other ways to form the chiral epoxide aside from epoxidation of a trisubstituted olefin, we considered that **2.14** could be formed from a *vicinal*-halohydrin, with the hydroxyl group stereocenter already established. This strategy ultimately found success with the Noyori asymmetric hydrogenation of β -ketoester **2.17** providing *vicinal*-bromohydrin **2.18** in excellent enantioselectivity (>99% ee). After filtration of the ruthenium catalyst, treatment of **2.18** with sodium carbonate in a mixture of water and ethanol provided chiral epoxide **2.14** in 88% yield over two steps. The regioselective epoxide opening gave desired intermediate **2.10** in 60% yield (Scheme 2.5).



Scheme 2.5 Optimized route to **2.10**

During the optimization of this new route, we ran into some difficulties with the epoxide-forming step. While the base-promoted cyclization of a bromohydrin is a well-precedented method for epoxide formation,^{6–9} we found that our epoxide product **2.14** was susceptible to isomerization, forming allylic alcohol **2.19** under these conditions (Scheme 2.6). This was the case even in the

absence of a strong base, presumably due to the favorable deprotonation of the β -position (α to ester) to form the conjugated ester. We found that weaker bases such as sodium bicarbonate resulted in significantly slower conversion to epoxide **2.14**, so a balance in the strength of the base had to be found to promote fast conversion to **2.14** without significant production of **2.19**. Ultimately, we found that the conditions given above were able to provide our desired epoxide **2.14** cleanly in about ten minutes, with **2.19** beginning to form only with extended reaction times.

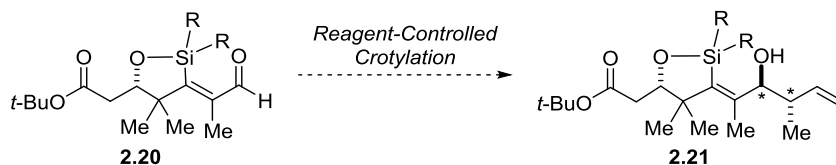


Scheme 2.6 Proposed Mechanism for Formation of Side Product **2.19**

In comparison to the previous route (Scheme 2.3), our new synthesis of **2.10** is more efficient (4 steps vs 6 steps) and provides higher enantioselectivity in the formation of the C3 stereocenter (>99% ee vs 87% ee). In addition, we were able to demonstrate that this route is amenable to multi-gram synthesis, producing 6.5 grams of **2.10** with one pass through the sequence.

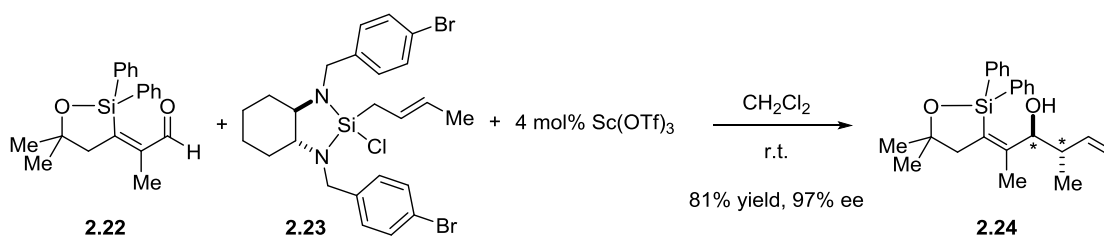
2.3 Toward a More Selective Formation of the C6-C8 Stereotriad of the Epothilones

With an efficient route in place to form **2.10**, we also sought to improve the selectivity of the crotylation step. As mentioned, the previous intramolecular approach had only provided 5.5:1 d.r. relative to the existing C3 stereocenter for the crotylation event (Scheme 2.3). Since the 1,5-*anti*-diol bias of the crotyl group transfer is substrate-dependent, we thought that the use of an external crotylation reagent in an intermolecular approach could provide an opportunity for improvement because selectivity would be induced by the reagent instead of the substrate.



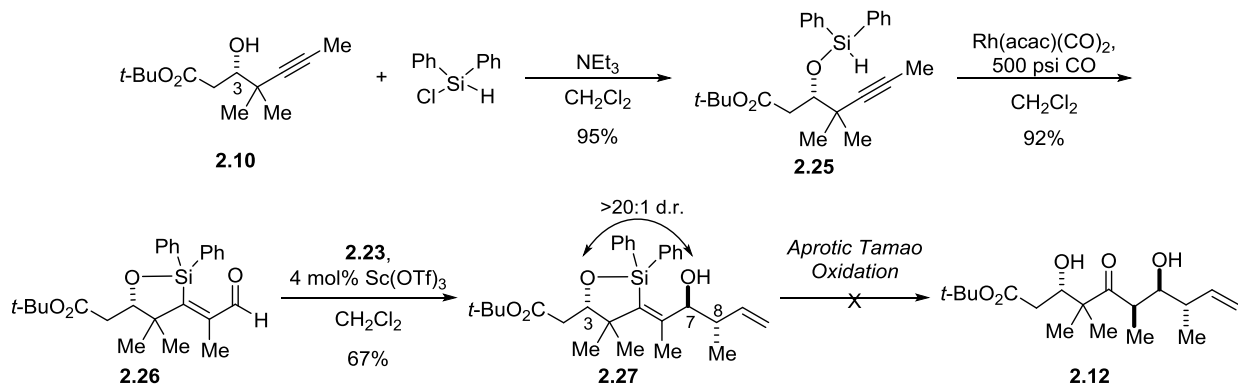
Scheme 2.7 Reagent-Based Approach to Crotylation

In an intermolecular reagent-based approach, the crotylation of a sterically hindered and electronically deactivated aldehyde **2.20** would be required (Scheme 2.7). Fortunately, around that time, another member of the Leighton group had found that the reactivity of our diamine-based crotylation reagents **2.23** could be significantly enhanced in the presence of catalytic scandium(III) triflate.¹⁰ With this breakthrough, the highly efficient and enantioselective crotylation of sterically hindered and electronically deactivated aldehydes such as **2.22** was now possible (Scheme 2.8). With this close precedent, we were optimistic that our new approach could be easily implemented to afford a high level of diastereoselectivity for the crotylation.

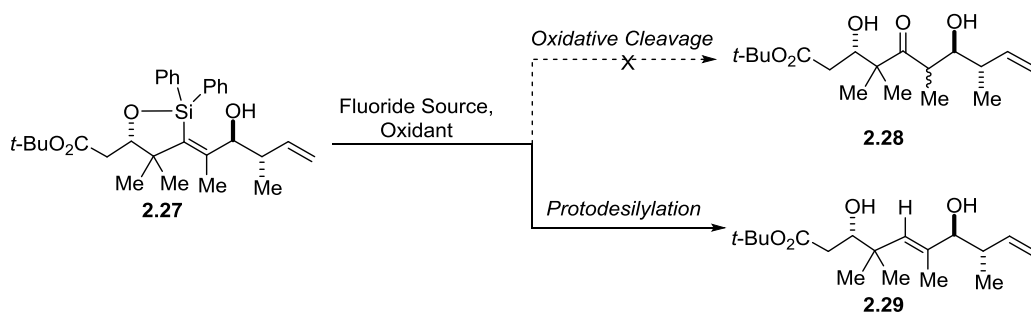


Scheme 2.8 Precedent for Crotylation of Hindered, Electronically Deactivated Aldehydes

To put our new approach into practice, we began with silylation of our β -hydroxyester intermediate **2.10** with diphenylchlorosilane, followed by rhodium-catalyzed silylformylation to form aldehyde **2.26**. Crotylation of **2.26** with (*R,R*)-*trans*-reagent **2.23** afforded **2.27** in 58% overall yield for the three steps with >20:1 d.r. (Scheme 2.9). While these steps proceeded smoothly and with excellent selectivity induced by the crotylation reagent, attempts to apply the previously developed “aprotic” Tamao oxidation conditions to our new substrate **2.27** failed to produce the desired ketone **2.12**, providing only unreacted starting material.



Applying the “standard” Tamao oxidation conditions provided only very minimal product under forcing conditions, with the mass balance consisting of mostly starting material with some protodesilylation product **2.29** and other unidentified side products. Additional attempts for the oxidative cleavage of substrate **2.27** utilizing conditions that varied the fluoride source and oxidant typically resulted in unreacted starting material or **2.29** under some of the harsher conditions (Scheme 2.10).



In considering the source of our difficulties with the oxidative cleavage of **2.27**, we hypothesized that the presence of the free hydroxyl group at C7 may be impeding the addition of the fluoride ion and/or hydrogen peroxide necessary for the Tamao mechanism because of its ability to coordinate to silicon. Bearing in mind the strain-release Lewis acidic properties of silicon constrained in a five-membered oxasilacycle, it would be expected that the addition of a nucleophile to a tetrahedral silicon such as **2.27** would be highly favored to relieve strain through

rehydridization into a trigonal bipyramidal species. In the case of the previous substrate **2.2** (which has an additional strained ring containing the silicon), this Lewis acidity should promote the addition by a fluoride ion, which would activate the substrate for the addition of the hydrogen peroxide. In our new substrate **2.27**, the intramolecular coordination of the C7 hydroxyl group to the silicon may be favored over addition by fluoride, thereby occupying a coordination site on the silicon and thus inhibiting the necessary addition by both fluoride and hydrogen peroxide (Figure 2.1).

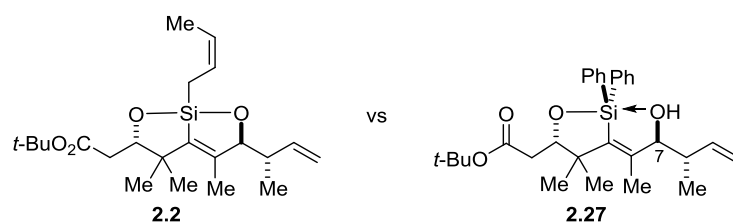
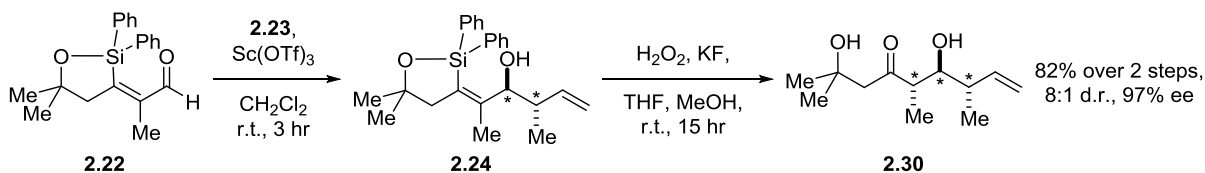


Figure 2.1 Comparison of “Aprotic” Tamao Oxidation Substrates

The observation that other diphenylsilacycle substrates such as **2.24** have been shown to undergo facile oxidative cleavage using the standard (protic) conditions (Scheme 2.11) seems to contradict our proposed inhibition effect from intramolecular coordination of the hydroxyl group to the silicon. However, since protic conditions would invoke intermolecular hydrogen-bonding interactions with the solvent, use of these conditions would be expected to decrease the coordination effect described above. Since it was observed that the standard (protic) Tamao conditions were not very effective for substrate **2.27**, it is likely that there may also be a steric effect at play with this substrate due to the *geminal*-dimethyl moiety close to the silicon.

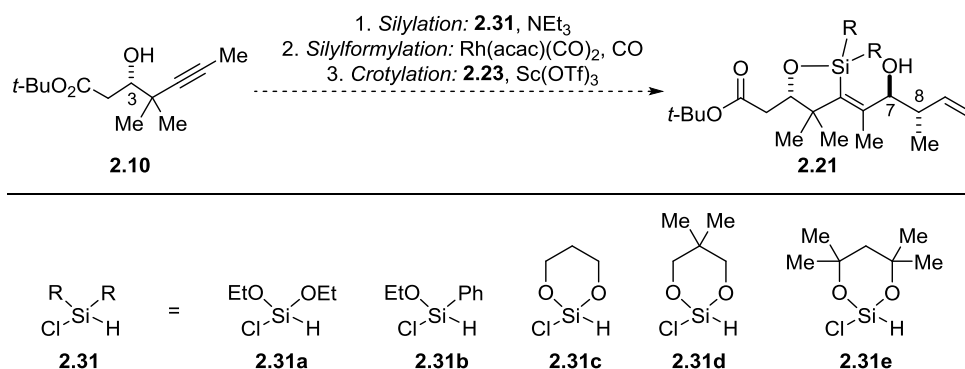


Scheme 2.11 Precident for the Protic Tamao Oxidation of Related Substrate **2.24**

At this point, we decided that in order for this new intermolecular crotylation approach to work in our synthesis, we would need to find a way to activate our Tamao oxidation substrate towards oxidative cleavage. We imagined that the utilization of a silane that had at least one fluoride-labile group could allow for its initial displacement by a fluoride group under the Tamao oxidation conditions so that the substrate would be more activated for attack by the hydrogen peroxide oxidant.

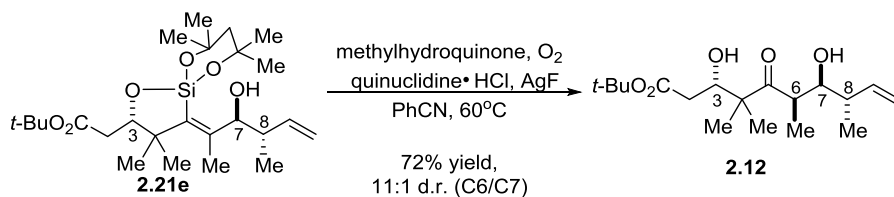
In our initial efforts to utilize a more “activated” silane, we examined a variety of alkoxy-substituted chlorosilanes (Scheme 2.12). Unfortunately, we encountered problems using silanes such as **2.31a,b** due to difficulties in the synthesis or isolation of the silane itself. Furthermore, the crotylation product **2.21** from silanes **2.31a,b** were unstable and could not be isolated in reasonable yields over the three steps from **2.10**, presumably due to hydrolysis.

It became clear that we would need to find a compromise between the stability of the silane group and the reactivity of the silane under oxidative cleavage conditions. We imagined that the use of a diol-based silane might be able to achieve this desired balance. By linking the two alkoxy substituents, the silane could potentially be more activated toward fluoride attack and replacement relative to our previous diphenyl substrate **2.27**, while at the same time decreasing the hydrolytic lability of these alkoxy substituents.



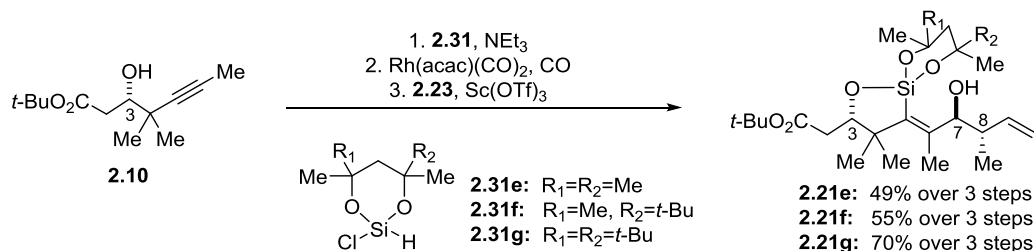
Scheme 2.12 Representative Silanes Explored in the Three-Step Synthesis of **2.21**

While efficient synthesis and isolation of the diol-based silanes **2.31c,d** still proved problematic, we were able to isolate **2.31e** in a reasonable 68% yield and proceed with the silylation-silylformylation-crotylation sequence to provide the corresponding intermediate **2.21e** in 49% yield over 3 steps from **2.10**. With a seeming solution to the stability issues in the synthesis of **2.21**, we were finally able to test our hypothesis with regards to the “aprotic” Tamao oxidation problem. In applying the previously developed “aprotic” Tamao oxidation conditions, we found that we could obtain **2.12** in 72% yield and 11:1 d.r. (Scheme 2.13).



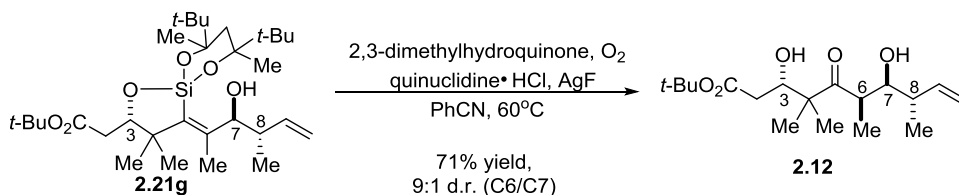
Scheme 2.13 Successful “Aprotic” Tamao Reaction of **2.21e** for Proof-of-Concept

This finding established the proof-of-concept, but there was still room to improve upon the yield of the isolated crotylation product **2.21**. Since the increased steric bulk near the Si-O bond could play a significant role in the increased hydrolytic stability of these compounds, we hypothesized that increasing the steric bulk even more could further enhance the stabilizing effect and increase the yield. Indeed, replacing first one (for silane **2.31f**) and then two (for silane **2.31g**) of the methyl groups on the diol with a *tert*-butyl group seemed to exhibit a trend for increasing yield of the crotylation product (Scheme 2.14). It was also the case that these diol-based silanes were synthesized more cleanly and efficiently (93% yield for multiple grams of **2.31g**) and were easier to handle. The increased steric bulk in silane **2.31g** seemed to induce some hindrance in the rate for each step of the sequence, however, did not extend reaction times by an appreciable extent.



Scheme 2.14 Trend for Increasing Three-Step Yield with Increasing Steric Bulk on the Silane

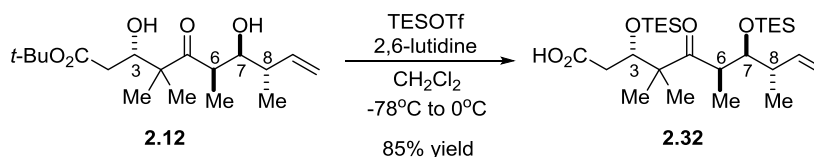
Slight optimization of the “aprotic” Tamao oxidation conditions was achieved through the exchange of the previously used 2-methylhydroquinone for 2,3-dimethylhydroquinone. The basis for this optimization comes from Tamao’s original report² for the hydroquinone/dioxygen system. This work indicated that the rate of the oxidative cleavage reaction was related to the concentration of active oxidant present, and that the rate of hydrogen peroxide generation had a correlation to the substitution of the hydroquinone. With increasing substitution from hydroquinone to 2-methylhydroquinone to 2,3-dimethylhydroquinone, the rate was increased. Thus, when we found that the “aprotic” Tamao reaction with **2.21g** was stalling as it approached completion, we made the exchange to 2,3-dimethylhydroquinone with the hopes that the effect of an increased concentration of active oxidant would help drive the reaction to completion. This seemed to be the case, with fully optimized conditions providing **2.12** in 71% yield and 9:1 d.r. (Scheme 2.15).



Scheme 2.15 Optimized “Aprotic” Tamao Oxidation of **2.21g**

Overall, our new intermolecular crotylation approach has achieved the rapid generation of **2.12** from **2.10** in 50% overall yield over four steps with high levels of selectivity in setting the three new stereocenters. The final one-pot di-TES-protection and *tert*-butyl ester hydrolysis of **2.12** provided the C1-C9 fragment of the epothilones **2.32** in 85% yield (Scheme 2.16). The entire

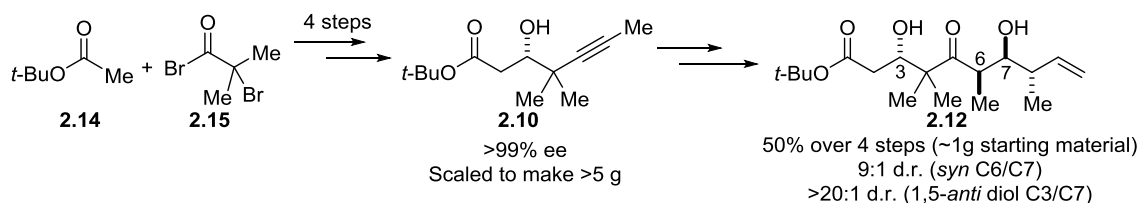
sequence has been performed on a gram scale starting from β -ketoester **2.10**, and it is possible that even larger scales could ultimately be used to provide efficient access to useful amounts of an epothilone or analog.



Scheme 2.16 Final Step to Access C1-C9 Fragment of the Epothilones

2.4 Summary/Conclusion

In our new route to the C1-C9 fragment of the epothilones, we have been able to address both of the goals that we had at the outset of this project. First, we have developed a more direct and streamlined route to the key intermediate **2.10** with excellent selectivity. Our new route is able to access **2.10** in just four steps and utilizes an enantioselective Noyori hydrogenation to set the C3 stereocenter in >99% enantioselectivity, compared to our previous route which required 6 steps and set the C3 stereocenter in 87% ee. From this intermediate **2.10**, we can now obtain **2.12** in 50% over 4 steps. With regards to our second goal of increasing the selectivity of the crotylation step, we now achieve >20:1 d.r. for the 1,5-*anti*-diol (C3/C7) utilizing our crotylation reagent **2.23** in the presence of catalytic scandium triflate, as compared to the previous 5.5:1 d.r. obtained from the intramolecular tandem silylformylation-crotylsilylation approach.



Scheme 2.17 Summary of Our New Route

Along the way to our new route, we encountered the unexpected setback of the unreactive intermediate **2.27**. By finding a way to balance the stability of the intermediates and reactivity

under the oxidative cleavage conditions through the use of the diol-based silane **2.31g**, we have been able to circumvent this problem.

Comparing our synthesis to other reported syntheses of this important polyketide fragment of the epothilones, ours has been able to leverage two external sources of chiral induction to set the four stereocenters with high levels of selectivity while most other syntheses require three external sources of chiral induction for the four stereocenters. Of the reported cases that have been able to leverage existing stereochemistry to set other stereocenters, most are through the aldol reaction to join (and set) the C6 and C7 stereocenters via anti-Felkin selectivity induced by the existing C8 stereocenter. This strategy typically does not provide high levels of selectivity, except for very specific substrates which are not generally obtained through the most direct routes.

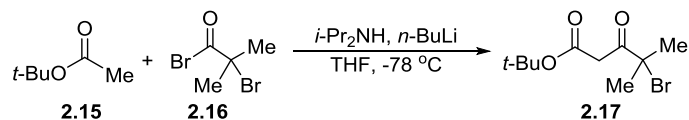
Since our new synthesis is direct, scalable, and highly selective, it has potential use towards the efficient preparation of an epothilone natural product or analog. As an example of its utility, this synthesis has provided a way for us to explore the installation of linker functionality in a C6 methyl analog, which will be discussed in the following chapter.

2.5 References

- (1) Harrison, T. J.; Rabbat, P. M. A.; Leighton, J. L. An “Aprotic” Tamao Oxidation/Syn-Selective Tautomerization Reaction for the Efficient Synthesis of the C1-C9 Fragment of Fludelone. *Org. Lett.* **2012**, *14*, 4890–4893.
- (2) Tamao, K.; Hayashi, T.; Ito, Y. An Efficient Oxidative Cleavage of Carbon-Silicon Bonds by a Dioxxygen/Hydroquinone System. *Tetrahedron Lett.* **1989**, *30*, 6533–6536.
- (3) Zhao, H.; Engers, D. W.; Morales, C. L.; Pagenkopf, B. L. Reactions of Alanes and Aluminates with Tri-Substituted Epoxides. Development of a Stereospecific Alkynylation at the More Hindered Carbon. *Tetrahedron* **2007**, *63*, 8774–8780.
- (4) Zhu, C.; Shen, X.; Nelson, S. G. Cinchona Alkaloid-Lewis Acid Catalyst Systems For Enantioselective Ketene-Aldehyde Cycloadditions. *J. Am. Chem. Soc.* **2004**, *126*, 5352–5253.
- (5) Harrison, T. *Unpublished results*.
- (6) Honda, Y.; Kataoka, Y.; Unno, M.; Tsuchihashi, G. Syn-Epoxidation of Chiral (Z)-2-Methyl-3-Alkenal Acetal via Stereo-Selective Bromohydrin Formation. *Chem. Lett.* **1987**, 2133–2134.
- (7) Barr, A.; Boyd, D. R.; Sharma, N. D.; Evans, T. A.; Malone, J. F.; Mehta, V. D. Resolution of Prenyl Bromohydrin Esters and Derivatives: Synthesis of the Quinoline Alkaloid (+)-(R)- and (-)-(S)-Lunacridine. *Tetrahedron* **1994**, *50*, 11219–11234.
- (8) Viola, F.; Balliano, G.; Milla, P.; Cattell, L.; Rocco, F.; Ceruti, M. Stereospecific Syntheses of Trans-Vinyldioxidosqualene and Beta-Hydroxysulfide Derivatives, as Potent and Time-Dependent 2,3-Oxidosqualene Cyclase Inhibitors. *Bioorg. Med. Chem.* **2000**, *8*, 223–232.
- (9) Raghavan, S.; Kumar, V. V. Stereoselective Synthesis of the C1–C8 Subunit of Peloruside A. *Tetrahedron* **2013**, *69*, 4835–4844.
- (10) Kim, H.; Ho, S.; Leighton, J. L. A More Comprehensive and Highly Practical Solution to Enantioselective Aldehyde Crotylation. *J. Am. Chem. Soc.* **2011**, *133*, 6517–6520.

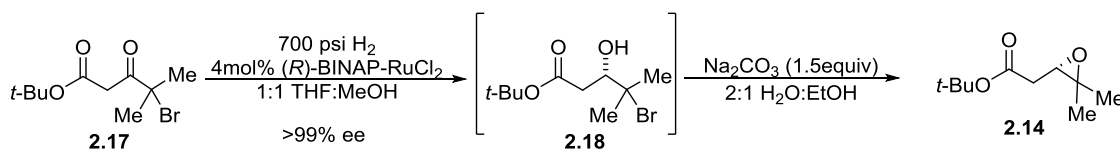
2.6 Experimental Procedures and Characterization Data

General Information. All reactions were carried out under an atmosphere of nitrogen in flame-dried glassware with magnetic stirring unless otherwise indicated. Degassed solvents were purified by passage through an activated alumina column. Thin-layer chromatography (TLC) was carried out on glass-backed silica gel XHL TLC plates (250 μm) from Sorbent Technologies; visualization by UV light, *p*-anisaldehyde stain, phosphomolybdic acid stain, or potassium permanganate (KMnO_4) stain. Gas chromatographic analyses were performed on a Hewlett-Packard 6890 Series Gas Chromatograph equipped with a capillary split-splitless inlet and flame ionization detector with electronic pneumatics control using a Supelco β -Dex 325 (30 m x 0.25 mm) capillary GLC column. ^1H NMR spectra were recorded on a Bruker DPX-400 (400 MHz) or a Bruker Avance III 500 (500 MHz) spectrometer and are reported in ppm from CDCl_3 internal standard (7.26 ppm). Data are reported as follows: (bs= broad singlet, s = singlet, d = doublet, t = triplet, q = quartet, quin = quintet, sep = septet, m = multiplet, dd = doublet of doublets, ddd = doublet of doublet of doublets; coupling constant(s) in Hz; integration). Proton decoupled ^{13}C NMR spectra were recorded on a Bruker Avance III 500 (125 MHz) spectrometer and are reported in ppm from CDCl_3 internal standard (77.16 ppm). Infrared spectra were recorded on a Perkin-Elmer Spectrum Two (Diamond ATR) IR spectrometer. Optical rotations were recorded on a Jasco DIP-1000 digital polarimeter.



To a cooled (0°C) solution of diisopropylamine (4.9 mL, 34.7 mmol) in Et_2O (100 mL) was added $n\text{-BuLi}$ (13.3 mL, 2.5M in hexanes, 33.1 mmol). After 30 minutes, the reaction was cooled to -78°C and *tert*-butyl acetate **2.15** (4.2 mL, 31.6 mmol) was added. After 45 minutes, α -

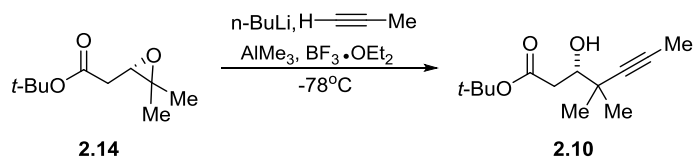
bromoisobutyl bromide **2.16** (4.7 mL, 37.9 mmol) was added. After 90 minutes, the reaction was quenched with saturated aqueous NH_4Cl (75 mL). The reaction was diluted with Et_2O (50 mL) and the layers were separated. The aqueous layer was extracted with Et_2O (3 x 50 mL), then the combined organics were dried over MgSO_4 , filtered, and concentrated. The crude residue was purified via silica gel chromatography (5% EtOAc /hexanes) to provide **2.17** (4.64 g, 55% yield) as a clear, colorless oil. ^1H NMR (500 MHz, CDCl_3) δ 3.77 (s, 2H), 1.88 (s, 6H), 1.46 (s, 9H); ^{13}C NMR (125 MHz, CDCl_3) δ 198.3, 166.5, 82.2, 63.9, 44.6, 29.4, 28.0; IR (neat): ν (cm^{-1}) 2979, 2933, 1738, 1713, 1369, 1322, 1257, 1147, 1107, 1056, 956.



A glass liner for a 300 mL capacity Parr bomb apparatus was charged with a solution of **2.17** (14.13 g, 53.3 mmol) in 1:1 THF:MeOH (100 mL). (R) -BINAP- RuCl_2 (1.69g, 2.13 mmol) was added then the Parr bomb was assembled and pressurized to 700 psi H_2 . After 7 hours at room temperature the bomb was carefully vented. The solution was concentrated, then the residue diluted with pentane and filtered through Celite. The filtrate was concentrated to provide **2.18** as a white solid, which was used directly in the next step. For characterization purposes, a pure sample of product was obtained via silica gel chromatography (10% EtOAc /hexanes, *p*-anisaldehyde stain). ^1H NMR (500 MHz, CDCl_3) δ 3.88 (ddd, J = 10.0, 4.7, 2.5 Hz, 1H), 3.15 (d, J = 4.8 Hz, 1H), 2.72 (dd, J = 16.1, 2.5 Hz, 1H), 2.47 (dd, J = 16.1, 10.0 Hz, 1H), 1.78 (s, 3H), 1.75 (s, 3H), 1.48 (s, 9H); ^{13}C NMR (125 MHz, CDCl_3) δ 172.0, 81.7, 75.7, 70.3, 39.0, 30.5, 30.2, 28.2; IR (neat): ν (cm^{-1}) 3452, 2978, 2932, 1733, 1708, 1367, 1149, 1110, 851; $[\alpha]^{21}_{\text{D}}$ -32.9 (*c* 1.7, CHCl_3).

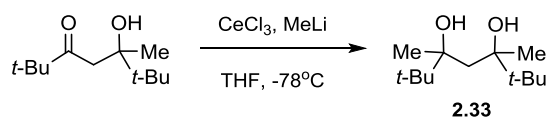
Chiral GC analysis of **2.10** (Supelco β -dex 325, Isothermal 120°C, 1 mL/min) revealed that **2.18** was produced in >99% enantiomeric excess (ee).

The concentrated **2.18** was dissolved in EtOH (175 mL) and deionized water (350 mL). Na_2CO_3 (8.46 g, 80.0 mmol) was added and the reaction carefully monitored by TLC (α,β -unsaturated ester side product **2.19** can form under these conditions with longer reaction times). Within 5-10 minutes the starting material was consumed, then reaction was diluted with pentane (200 mL). The layers were separated and the aqueous layer was extracted with pentane (3 x 150 mL). The combined organics were dried over Na_2SO_4 , filtered, and concentrated to provide **2.14** (8.72 g, 88% yield over 2 steps) as a clear colorless oil. ^1H NMR (500 MHz, CDCl_3) δ 3.07 (dd, J = 6.3, 6.3 Hz, 1H), 2.57 (dd, J = 16.5, 6.3 Hz, 1H), 2.43 (dd, J = 16.5, 6.3 Hz, 1H), 1.47 (s, 9H), 1.35 (s, 3H), 1.28 (s, 3H); ^{13}C NMR (125 MHz, CDCl_3) δ 170.0, 81.1, 59.6, 58.0, 36.1, 28.1, 24.6, 18.9; IR (neat): ν (cm^{-1}) 2979, 2931, 1729, 1368, 1341, 1253, 1154, 1122, 846; LRMS (APCI+) calcd $\text{C}_{10}\text{H}_{19}\text{O}_3$ $[\text{M}+\text{H}]^+$: 187.13, found 187.16; $[\alpha]^{21}_{\text{D}} +7.3$ (c 1.5, CHCl_3).



To a cooled (-78°C) solution of propyne (approx. 27 mL, 470 mmol, condensed into a cooled (-78°C) graduated cylinder) in Et_2O (160 mL) was added $n\text{-BuLi}$ (41.2 mL, 2.5 M in hexane, 103.0 mmol) dropwise. After 20 minutes, the reaction was warmed to 0°C and AlMe_3 (49.2 mL, 2 M in toluene, 98.3 mmol) was added dropwise. The reaction was warmed to room temperature and stirred for 20 minutes. The reaction was again cooled to -78°C and **2.14** (8.72 g, 46.8 mmol) was added as a solution in Et_2O (40 mL), followed by $\text{BF}_3\cdot\text{OEt}_2$ (8.2 mL, 65.5 mmol). After 45 minutes, the reaction was slowly quenched with MeOH (50 mL). The mixture was stirred for 10 minutes at -78°C then poured into 800 mL of saturated aqueous NaHCO_3 solution of pH 10.

After stirring for about 45 minutes, the layers were separated and the aqueous layer extracted with Et₂O (3 x 150 mL). The combined organics were washed with brine, dried over MgSO₄, filtered, and concentrated. The crude material was purified by silica gel chromatography (10% EtOAc/hexanes, *p*-anisaldehyde stain) to provide **2.10** as a clear, yellow oil (6.30 g, 60% yield).¹ ¹H NMR (500 MHz, CDCl₃) δ 3.77 (ddd, *J* = 10.4, 4.6, 2.3 Hz, 1H), 2.94 (d, *J* = 4.6 Hz, 1H), 2.66 (dd, *J* = 16.1, 2.4 Hz, 1H), 2.44 (dd, *J* = 16.1, 10.4 Hz, 1H), 1.83 (s, 3H), 1.50 (s, 9H), 1.23 (s, 3H), 1.20 (s, 3H); ¹³C NMR (125 MHz, CDCl₃) δ 172.7, 83.4, 81.1, 77.7, 74.5, 38.7, 36.1, 28.1, 26.2, 24.9, 3.6; IR (neat): ν (cm⁻¹) 3480, 2976, 2925, 1718, 1368, 1304, 1153, 1080, 1040, 954; [α]_D²⁰ -43.9 (*c* 1.6, CHCl₃).



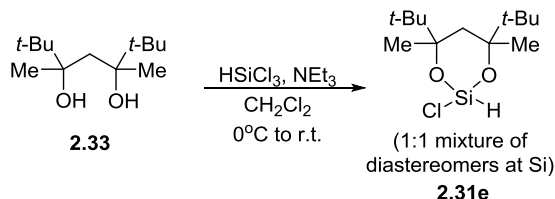
A suspension of dried CeCl₃ (31.11 g, 126 mmol) in THF (450 mL) was stirred at 40°C (oil bath, external temperature) for 2 hours.^{2,3} The suspension was cooled to -78°C then MeLi (78.8 mL, 1.6 M in Et₂O, 126 mmol) was slowly added. After 2 hours, 5-hydroxy-2,2,5,6,6-pentamethylheptan-3-one (6.32 g, 31.6 mmol) was added via cannula as a solution in THF (250 mL). After 1 hour, the reaction was quenched with 10% aqueous acetic acid. After stirring for about 1 hour, the reaction was diluted with Et₂O (200 mL). The layers were separated and the aqueous layer extracted with Et₂O (3 x 150 mL). The combined organics were washed with brine, dried over MgSO₄, filtered, and concentrated. The crude material was purified by silica gel chromatography (10% EtOAc/hexanes, PMA stain) to provide one diastereomer of **2.33** as a white

¹ Full characterization has been reported: Harrison, T. J.; Rabbatt, P. M. A.; Leighton, J. L. *Org. Lett.* **2012**, *14*, 4890-4893.

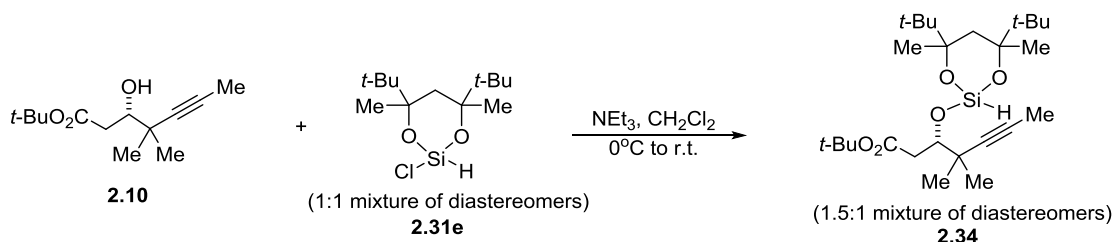
² Cerium chloride activation: Conlon, D. A.; Kumke, D.; Moeder, C.; Hardiman, M.; Hutson, G.; Sailer, L. *Adv. Synth. Catal.* **2004**, *346*, 1307-1315.

³ Precedent for diol synthesis: Bartoli, G.; Bosco, M.; Van Beek, J.; Sambri, L. *Tet. Lett.* **1996**, *37*, 2293-2296.

solid (5.60 g, 82% yield). ^1H NMR (500 MHz, CDCl_3) δ 2.64 (s, 2H), 1.63 (s, 2H), 1.32 (s, 6H), 0.94 (s, 18H); ^{13}C NMR (125 MHz, CDCl_3) δ 77.4, 38.9, 37.7, 25.7, 25.1; IR (neat): ν (cm^{-1}) 3341, 2974, 2124, 1636, 1468, 1372, 538.

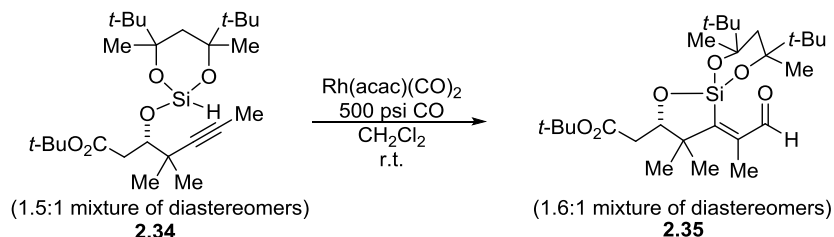


To a cooled (0°C) solution of dried diol **2.33** (2.49 g, 11.5 mmol) in CH_2Cl_2 (115 mL) in a vigorously dried multi-neck flask was slowly added trichlorosilane (1.28 g, 12.7 mmol) (Caution! Evolution of HCl gas), followed by Et_3N (4.01 mL, 28.8 mmol) dropwise. After one hour (reaction allowed to warm to room temperature), the solvent (and excess trichlorosilane and Et_3N) was removed *in vacuo* under inert conditions. Et_2O was added and the suspension stirred for thirty minutes. The salts were filtered using an inert frit and the filtrate was concentrated to yield **2.31g** (2.98 g, 93% yield) as a viscous, yellow oil. Analysis by ^1H NMR spectroscopy showed **2.31g** to be a clean 1:1 mixture of diastereomers at silicon. ^1H NMR (500 MHz, CDCl_3) δ 5.21 (s, 1H), 1.82 (s, 1H), 1.81 (s, 1H), 1.44 (s, 3H), 1.41 (s, 3H), 0.95 (s, 9H), 0.94 (s, 9H); ^{13}C NMR (125 MHz, CDCl_3) δ 82.1, 81.6, 39.3, 39.3, 38.7, 26.8, 25.8, 24.8; IR (neat): ν (cm^{-1}) 2957, 2914, 2877, 2225, 1475, 1396, 1376, 1364, 1150, 1012, 971, 886, 855, 546.



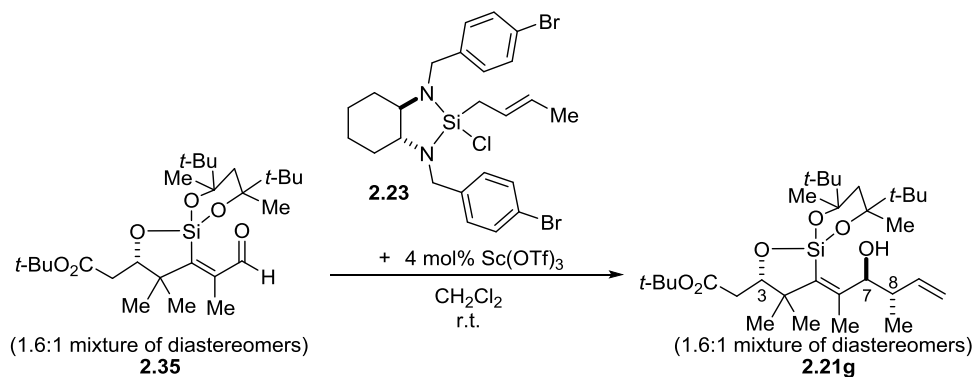
To a cooled (0°C) solution of silane **2.31g** (1.05 g, 3.76 mmol) in CH_2Cl_2 (20 mL) was added β -ketoester **2.10** (707 mg, 3.13 mmol) as a solution in CH_2Cl_2 (10 mL), followed by NEt_3

(0.65 mL, 4.70 mmol). The reaction was warmed to room temperature over one hour. After five hours, ^1H NMR analysis was used to determine the conversion of the reaction mixture. Additional silane was added if starting material remained. Once complete, the reaction was concentrated and the residue filtered through an oven-dried frit with Et_2O . The filtrate was concentrated to provide intermediate **2.34** as a 1.5:1 mixture of diastereomers, which was used directly in the next step. Since this intermediate is difficult to purify due to hydrolytic sensitivity, and both diastereomers useful for our purposes, characterization reflects the mixture we obtained. Observed spectra: ^1H NMR (500 MHz, CDCl_3) δ 4.52 (s, 1H), 4.19 (d, $J = 9.2$ Hz, 1H), 2.82 (d, $J = 15.9$ Hz, 1H), 2.46 (dd, $J = 15.2, 10.0$ Hz, 1H), 1.80 (s, 3H), 1.75 (s, 2H), 1.51 (s, 9H), 1.37 (s, 3H), 1.36 (s, 3H), 1.25 (s, 3H), 1.15 (s, 3H), 0.95 (s, 18H). ^{13}C NMR (125 MHz, CDCl_3) δ 171.0, 171.0, 84.5, 84.5, 80.4, 80.3, 79.9, 79.7, 79.5, 79.2, 76.1, 75.9, 40.3, 40.0, 39.1, 39.0, 38.9, 38.9, 38.3, 38.2, 36.1, 28.2, 28.2, 27.0, 27.0, 27.0, 26.9, 25.7, 25.6, 24.8, 24.7, 24.7, 23.5, 23.1, 3.5, 3.4; LRMS (FAB+) calcd $\text{C}_{26}\text{H}_{49}\text{O}_5\text{Si}$ $[\text{M}+\text{H}]^+$: 469.33, found 469.35.



A glass liner for a Parr bomb was charged with the crude **2.34** (from previous reaction) as a solution in CH_2Cl_2 (7.8 mL). The bomb was assembled and pressurized with CO to approximately 500 psi and then vented. This procedure was repeated two more times, then the bomb was pressurized again to 500 psi and stirred for about fifteen minutes. The bomb was carefully vented and opened, then $\text{Rh}(\text{acac})(\text{CO})_2$ (0.125 mmol, 32 mg) was added. The bomb was reassembled and pressurized to 500 psi with CO then stirred at ambient temperature. After 16

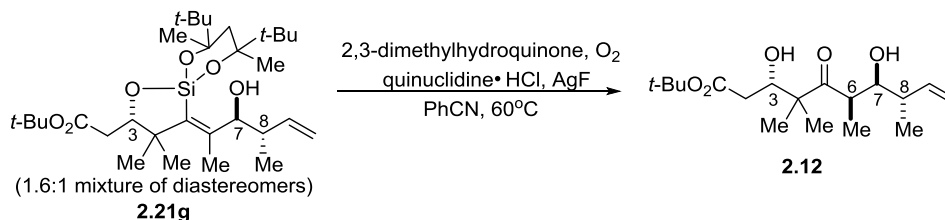
hours, the bomb was carefully vented and opened. ^1H NMR analysis indicated complete consumption of starting material and clean formation of product **2.35** as a 1.6:1 mixture of diastereomers. This reaction solution was used directly in the following crotylation reaction. Observed spectra of the diastereomeric mixture were as follows: ^1H NMR (500 MHz, CDCl_3) δ 10.09 (s, 1H), 10.05 (s, 1H), 4.17 (dd, $J = 10.4, 3.2$ Hz, 1H), 4.09 (dd, $J = 9.9, 2.7$ Hz, 1H), 2.53 – 2.41 (m, 2H), 2.42 – 2.29 (m, 2H), 2.16 (m, 1H), 2.00 (s, 3H), 1.99 (s, 2H), 1.83 (m, 3H), 1.50 (m, 2H), 1.48 (m, 16H), 1.45 (s, 3H), 1.42 (s, 3H), 1.35 – 1.26 (m, 16H), 1.11 (s, 3H), 0.98 (s, 7H), 0.99 – 0.92 (m, 37H). ^{13}C NMR (125 MHz, CDCl_3) δ 195.5, 195.3, 171.2, 170.7, 165.2, 163.2, 148.1, 147.4, 81.2, 81.1, 80.7, 80.6, 80.5, 80.1, 80.0, 78.2, 48.0, 47.2, 41.6, 39.6, 39.5, 39.3, 39.2, 38.4, 37.9, 28.1, 27.9, 27.7, 26.9, 26.8, 26.2, 24.9, 24.9, 24.1, 23.7, 22.3, 20.1, 14.1, 11.9, 11.9. LRMS (FAB+) calcd $\text{C}_{27}\text{H}_{49}\text{O}_6\text{Si}$ $[\text{M}+\text{H}]^+$: 497.32, found 497.35.



To a solution of the reaction mixture from aldehyde **2.35** formation in CH_2Cl_2 (31 mL) was added (R,R)-*trans*-crotylsilane reagent **2.23** (2.32 g, 4.07 mmol) and $\text{Sc}(\text{OTf})_3$ (154 mg, 0.313 mmol).⁴ After 20 hours at room temperature, the reaction was cooled to 0°C and tetrabutylammonium fluoride (TBAF) trihydrate (0.99 g, 3.13 mmol) was added portion-wise over 20 minutes. After about 3 hours, the reaction was concentrated and the residue purified via silica

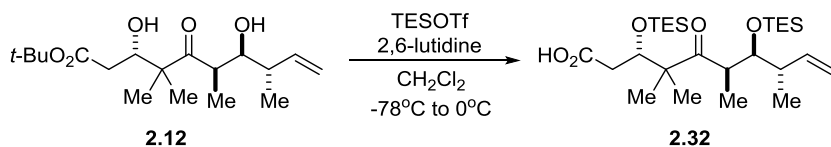
⁴ Kim, H.; Ho, S.; Leighton, J. L.; *J. Am. Chem. Soc.* **2011**, *133*, 6517-6520.

gel chromatography (10% EtOAc/hexanes) to afford **2.21g** (1.21 g, 70% over 3 steps) as a viscous yellow oil. **2.21g** was a 1.5:1 mixture of diastereomers at silicon, with the crotylation providing >20:1 d.r for the installation of C7/C8 relative to the existing stereocenter at C3. ^1H NMR (500 MHz, CDCl_3) δ 5.81 – 5.62 (m, 2H), 4.95 (s, 2H), 4.93 – 4.90 (m, 2H), 4.18 – 4.05 (m, 4H), 2.92 (s, 2H), 2.56 – 2.43 (m, 4H), 2.28 (dd, J = 10.5, 3.6 Hz, 1H), 2.25 (dd, J = 10.5, 3.8 Hz, 1H), 1.86 (s, 3H), 1.85 (s, 3H), 1.79 (s, 2H), 1.78 (s, 1H), 1.44 (s, 9H), 1.44 (s, 12H), 1.42 (s, 3H), 1.41 (s, 6H), 1.27 (s, 4H), 1.25 (s, 2H), 1.22 (s, 2H), 1.19 (s, 3H), 1.17 (d, J = 4.9 Hz, 3H), 1.16 (d, J = 4.9 Hz, 3H), 1.00 – 0.92 (m, 36H); ^{13}C NMR (125 MHz, CDCl_3) δ 173.5, 173.4, 158.4, 158.1, 139.2, 139.1, 134.2, 134.1, 114.8, 114.8, 83.4, 83.2, 80.8, 80.7, 80.5, 80.2, 80.1, 79.9, 73.8, 73.8, 41.7, 41.6, 41.6, 41.4, 40.0, 39.9, 39.6, 39.5, 38.5, 38.4, 38.1, 37.8, 28.6, 28.4, 28.3, 28.3, 28.1, 27.8, 26.5, 26.4, 25.3, 25.2, 25.2, 24.5, 24.4, 18.4, 18.3, 17.8, 17.6; IR (neat): ν (cm^{-1}) 3497, 2972, 2929, 2875, 1713, 1472, 1452, 1367, 1151, 1026; LRMS (FAB+) calcd $\text{C}_{31}\text{H}_{57}\text{O}_6\text{Si}$ $[\text{M}+\text{H}]^+$: 553.38, found 553.40.



To a solution of 2,3-dimethylhydroquinone (694 mg, 5.03 mmol), quinuclidine hydrochloride (801 mg, 5.43 mmol), and silver fluoride (816 mg, 6.43 mmol) in benzonitrile (10 mL) was added **2.21g** (1.11 g, 2.01 mmol) as a solution in benzonitrile (10 mL). The solution was purged with O_2 then the reaction was heated to 60°C (oil bath, external temperature) and stirred under a balloon of O_2 . After 16 hours, the reaction was cooled to room temperature and diluted with CHCl_3 (20 mL). The solution was filtered through Celite, then washed with distilled water. The aqueous layer was extracted with CHCl_3 (3 x 20 mL). The combined organics were washed

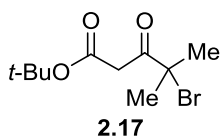
with brine, dried over MgSO₄, filtered, and concentrated. Most of the benzonitrile was removed by distillation under reduced pressure. The residue was purified via silica gel chromatography (stepwise: 5% EtOAc/hexanes to 10% EtOAc/hexanes to 15% EtOAc/hexanes) to provide **2.12** (470 mg, 71%) as a red oil with 9:1 diastereomeric ratio (d.r.) with respect to the newly formed stereocenter at C6. ¹H NMR (400 MHz, CDCl₃) δ 5.90 (ddd, *J* = 17.4, 10.4, 7.6 Hz, 1H), 5.15 – 5.04 (m, 2H), 4.20 (ddd, *J* = 10.2, 3.2, 2.6 Hz, 1H), 3.53 (ddd, *J* = 8.0, 2.2, 2.0 Hz, 1H), 3.36 (d, *J* = 3.4 Hz, 1H), 3.25 (qd, *J* = 6.9, 2.4 Hz, 1H), 3.16 (d, *J* = 2.0 Hz, 1H), 2.39 (dd, *J* = 16.3, 2.5 Hz, 1H), 2.34 – 2.25 (m, 2H), 1.47 (s, 9H), 1.20 (s, 3H), 1.13 (s, 3H), 1.11 (d, *J* = 6.9 Hz, 3H), 1.00 (d, *J* = 6.9 Hz, 3H); ¹³C NMR (125 MHz, CDCl₃) δ 221.5, 172.7, 141.3, 115.0, 81.8, 74.7, 72.7, 52.1, 41.8, 40.8, 37.5, 28.3, 21.5, 19.1, 16.8, 10.8; [α]_D²¹ -50.4 (*c* 1.15, CHCl₃). **Stereochemical Proof:** ¹H and ¹³C NMR spectra and sign of optical rotation for **2.12** match the previously published compound, for which stereochemical proof of correct epothilone stereochemistry was established.¹



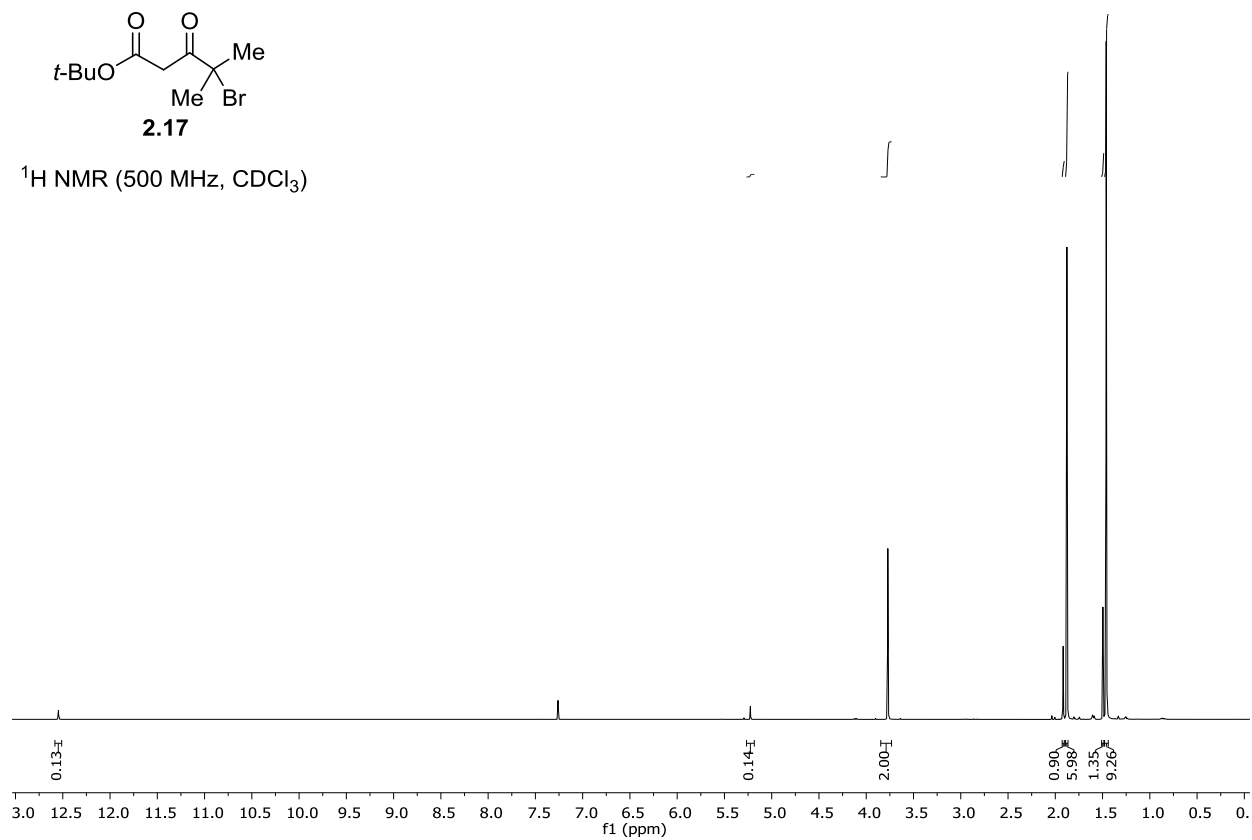
To a cooled (-78°C) solution of **2.12** (170 mg, 0.517 mmol) in CH₂Cl₂ (5.2 mL) was added 2,6-lutidine (0.48 mL, 4.14 mmol). TESOTf (0.35 mL, 1.55 mmol) was then added dropwise. After 30 minutes, a second portion of TESOTf (0.35 mL, 1.55 mmol) was added and the cold bath was removed, allowing the reaction to warm to ambient temperature. After 3 hours, the reaction was cooled to 0°C and quenched with saturated aqueous NaHCO₃. After stirring for thirty minutes, the layers were separated and the aqueous layer was extracted with CH₂Cl₂ (2 x 5 mL). The combined organics were concentrated then the residue was diluted with Et₂O. This was washed quickly and carefully with 0.25 M aqueous HCl (TLC monitoring of ether layer is necessary to separate layers before silyl group deprotection). The organic layer was washed with brine, dried over Na₂SO₄,

filtered, and concentrated. Purification via silica gel chromatography (15% EtOAc/hexanes) provided **2.32** (220 mg, 85% yield) as a light yellow oil. ^1H NMR (500 MHz, CDCl_3) δ 10.02 (bs, 1H), 5.92 (ddd, $J = 17.9, 10.5, 8.0$ Hz, 1H), 5.06 (dd, $J = 10.6, 1.4$ Hz, 1H), 5.00 (dd, $J = 17.5, 2.8$ Hz, 1H), 4.39 (dd, $J = 7.1, 3.1$ Hz, 1H), 3.88 (dd, $J = 7.9, 1.8$ Hz, 1H), 3.03 (dq, $J = 14.2, 7.0$ Hz, 1H), 2.51 (dd, $J = 16.4, 3.1$ Hz, 1H), 2.33 (dd, $J = 16.4, 7.1$ Hz, 1H), 2.10 – 2.02 (m, 1H), 1.21 (s, 3H), 1.11 (s, 3H), 1.06 (d, $J = 5.5$ Hz, 3H), 1.04 (d, $J = 5.5$ Hz, 3H), 1.01 – 0.92 (m, 18H), 0.69 – 0.61 (m, 12H); ^{13}C NMR (125 MHz, CDCl_3) δ 218.6, 175.7, 139.8, 115.5, 77.2, 73.6, 53.3, 46.3, 43.0, 39.4, 23.9, 19.2, 18.9, 15.2, 7.1, 6.9, 5.5, 5.1; IR (neat): ν (cm^{-1}) 2955, 2913, 2877, 1710, 1458, 1416, 1100, 1004, 988, 733; LRMS (APCI+) calcd $\text{C}_{14}\text{H}_{23}\text{O}_3$ $[\text{M}+\text{Na}]^+$: 523.33, found 523.17; $[\alpha]^{22}_{\text{D}} -22.0$ (c 0.29, CHCl_3).

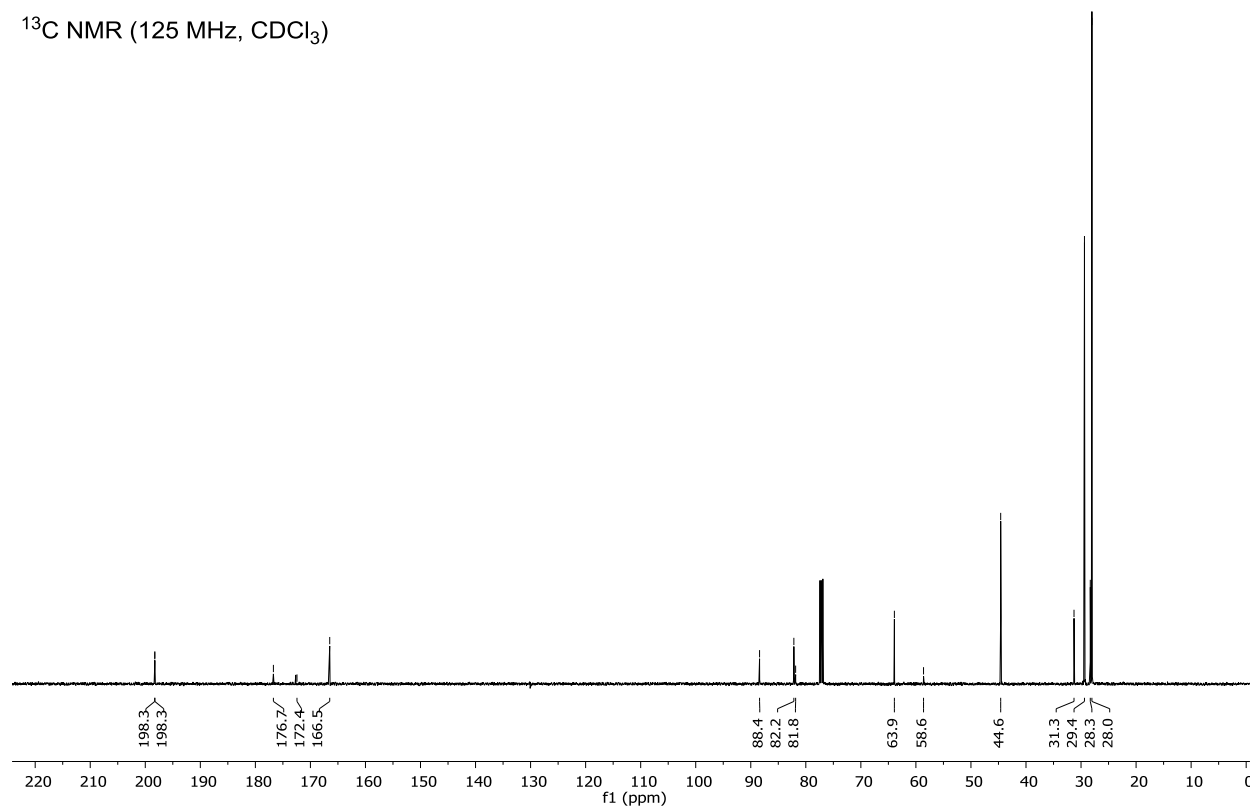
2.7 ^1H and ^{13}C NMR Spectra

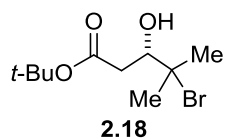


^1H NMR (500 MHz, CDCl_3)

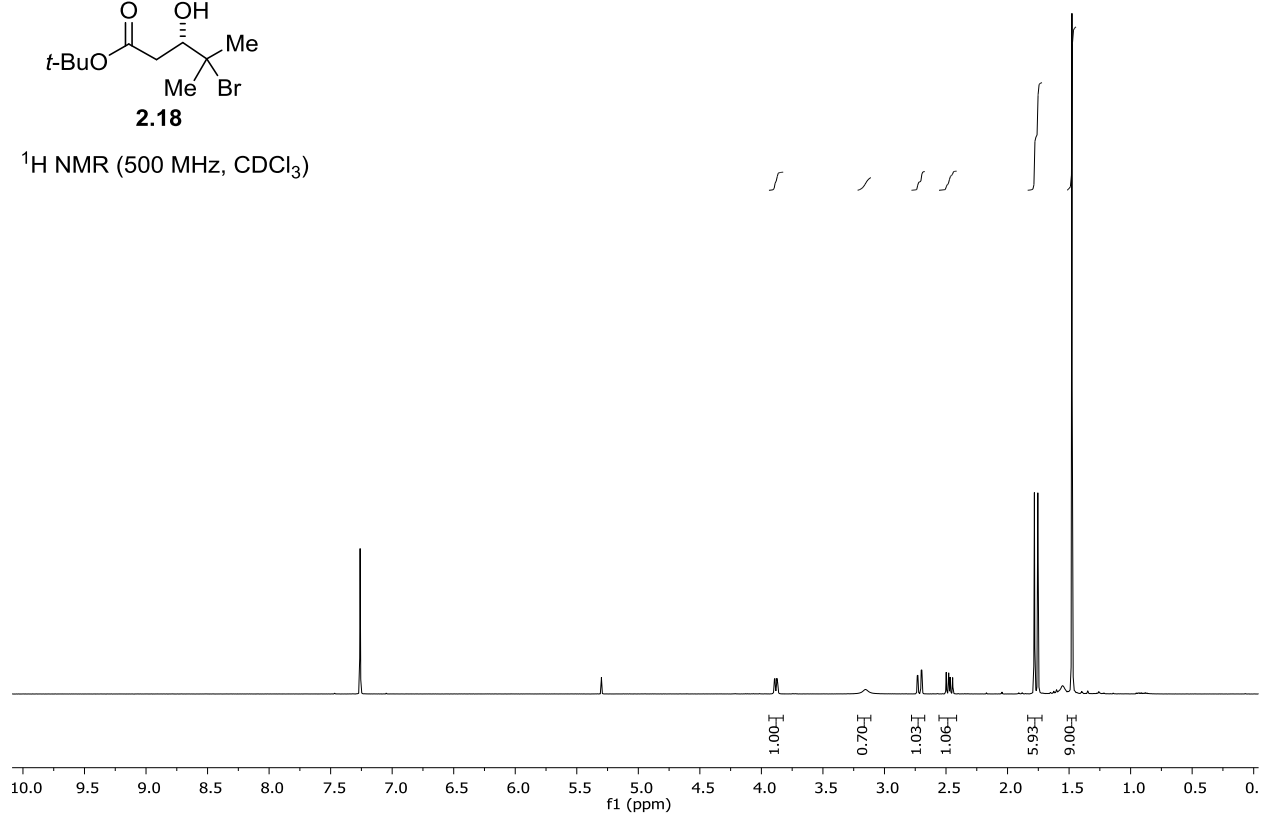


^{13}C NMR (125 MHz, CDCl_3)

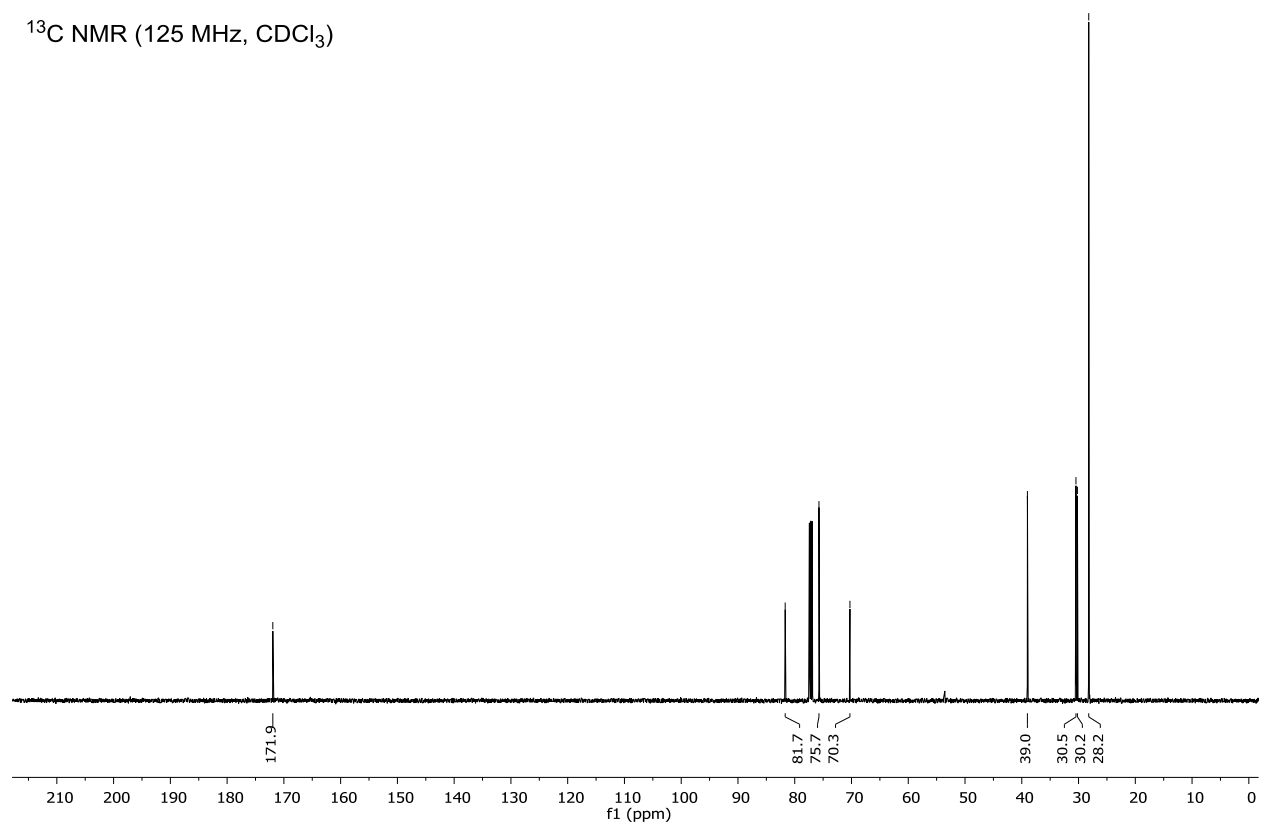


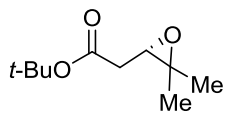


^1H NMR (500 MHz, CDCl_3)



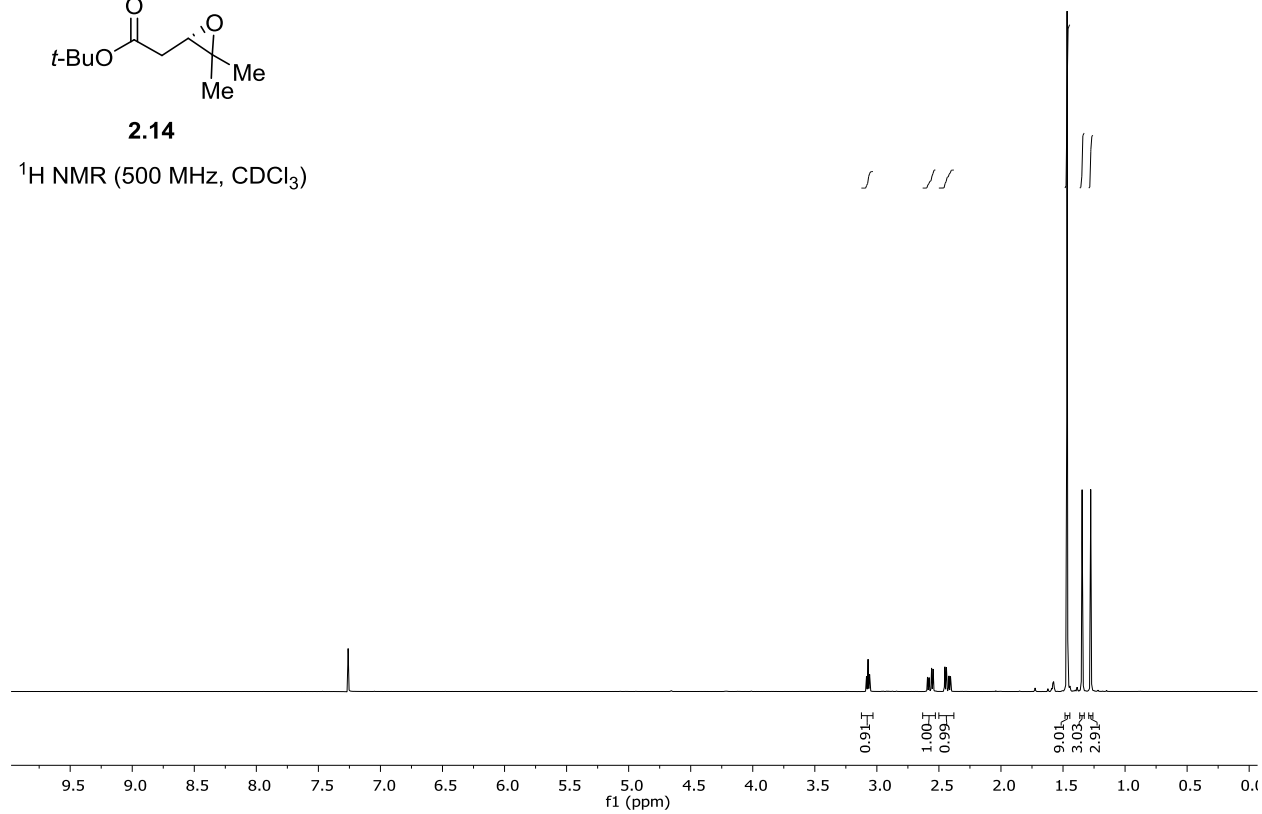
^{13}C NMR (125 MHz, CDCl_3)



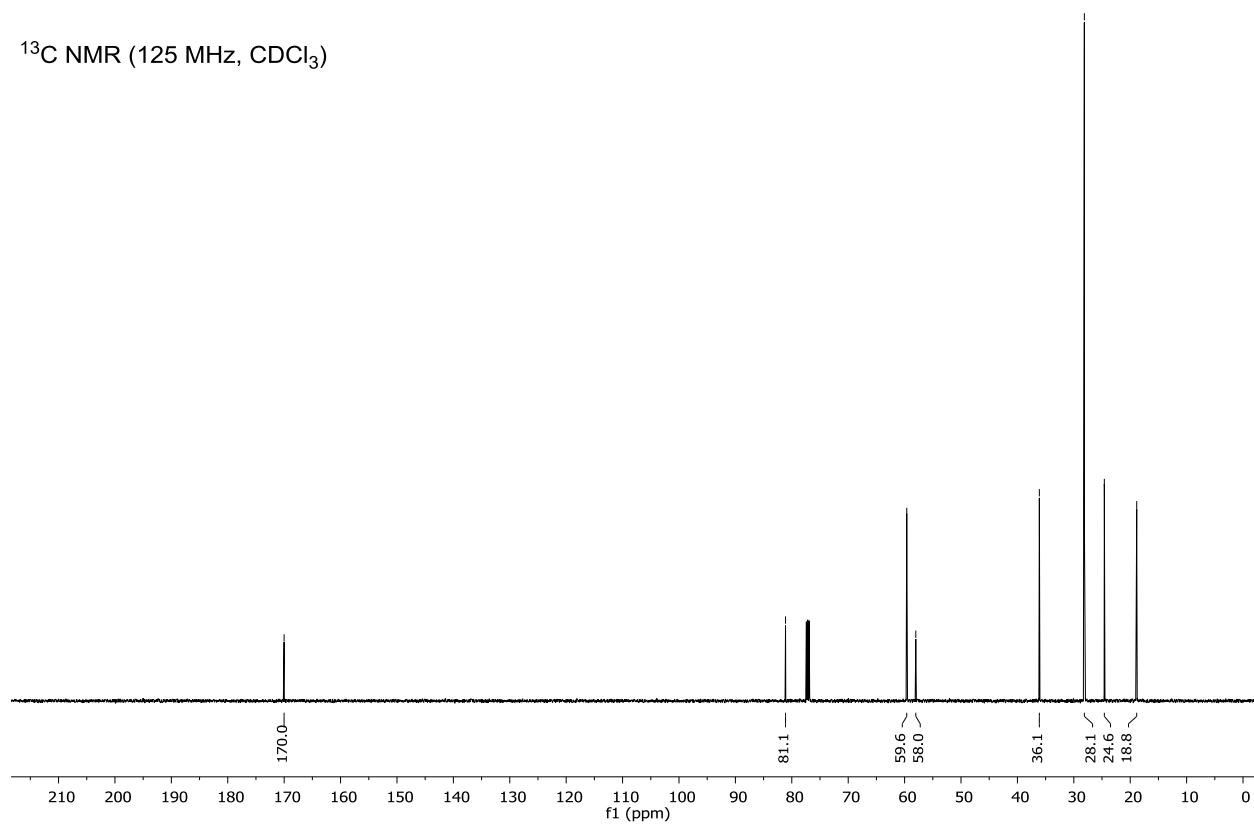


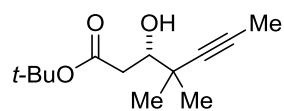
2.14

^1H NMR (500 MHz, CDCl_3)



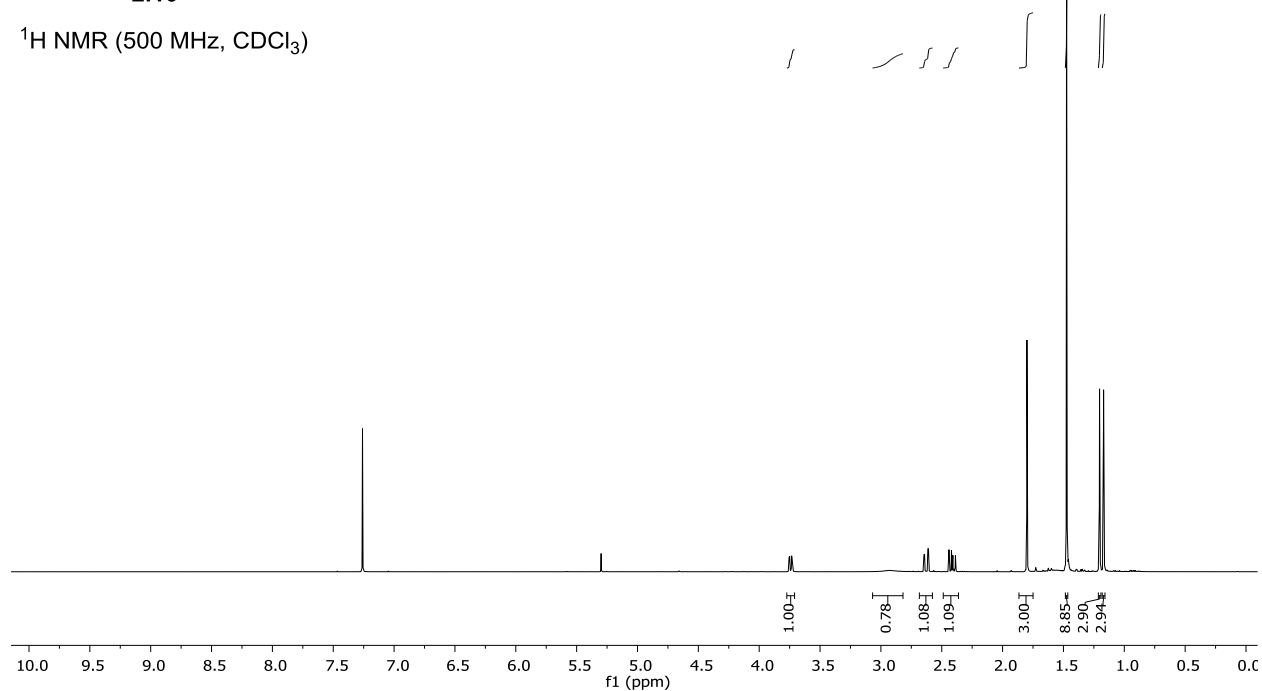
^{13}C NMR (125 MHz, CDCl_3)



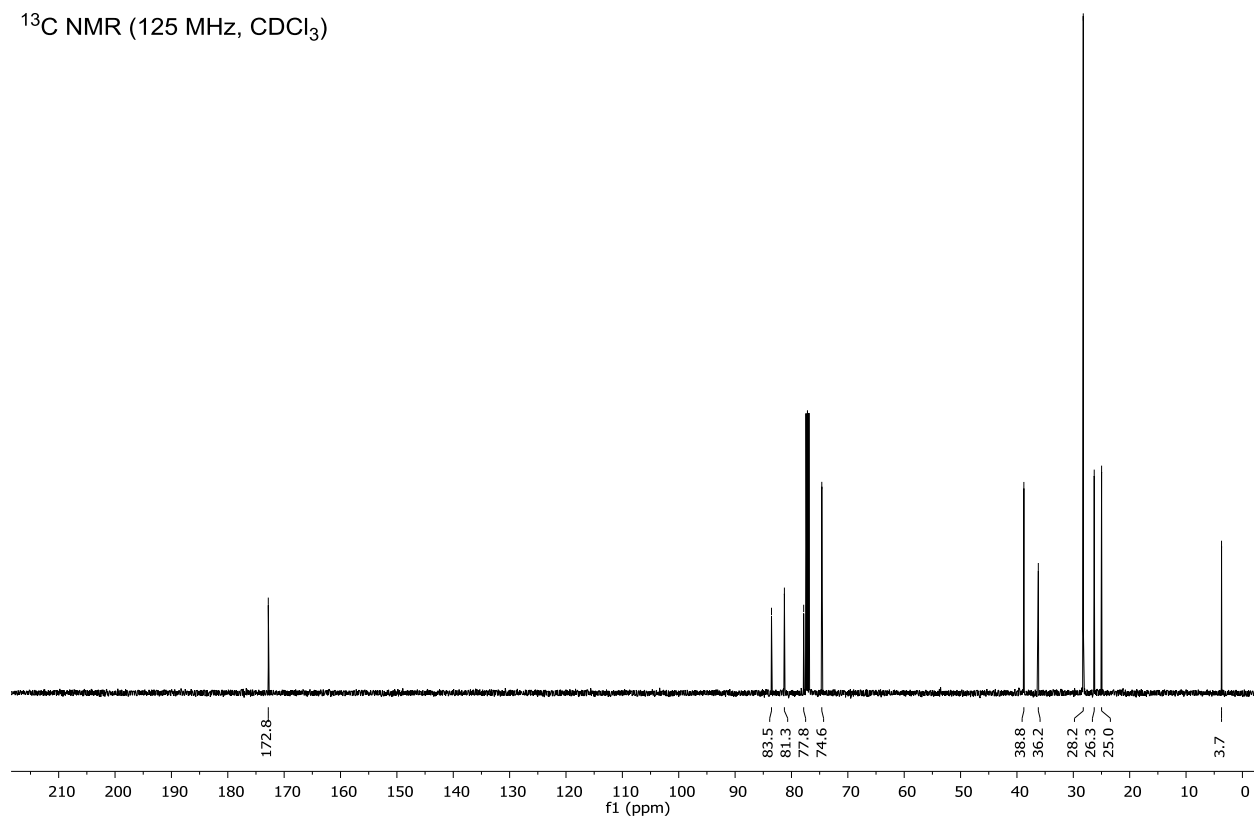


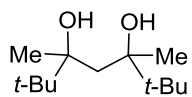
2.10

¹H NMR (500 MHz, CDCl₃)



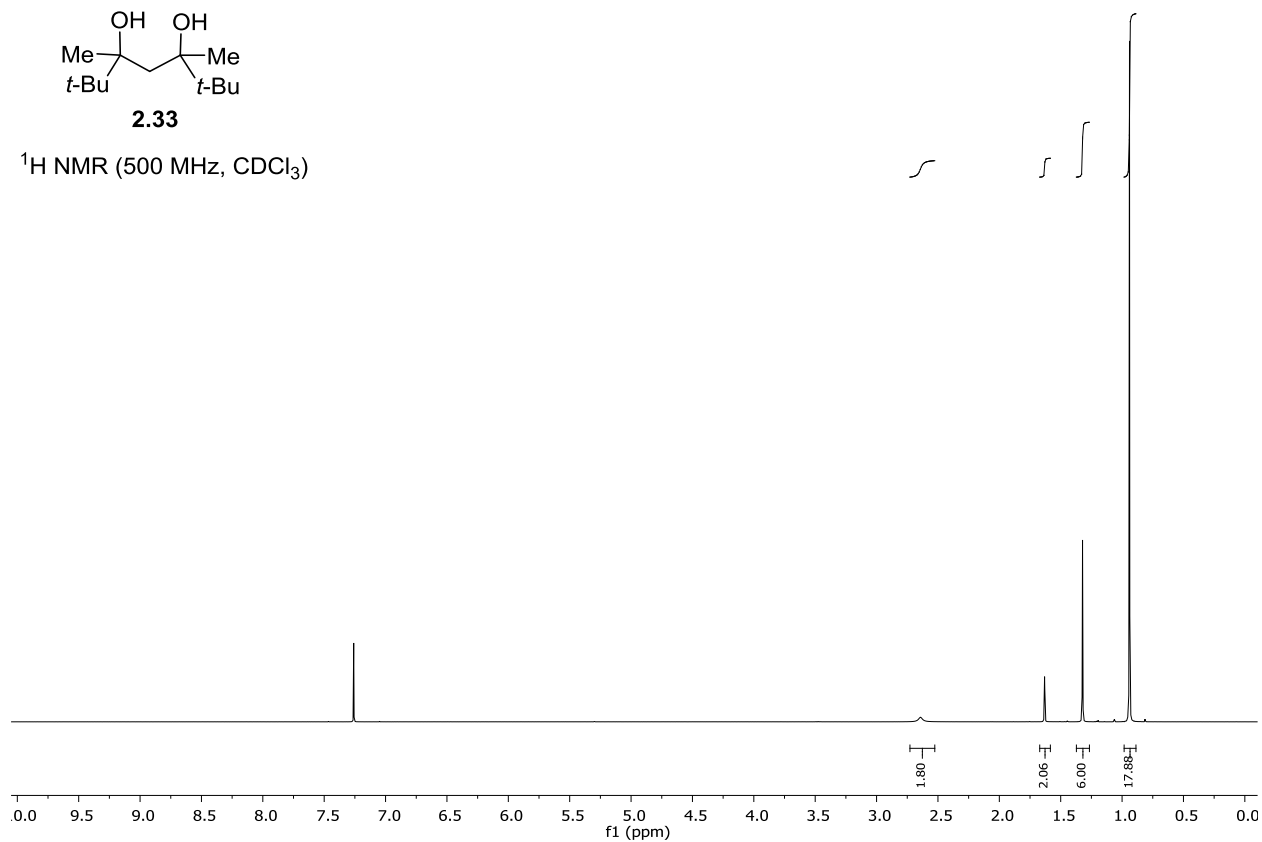
¹³C NMR (125 MHz, CDCl₃)



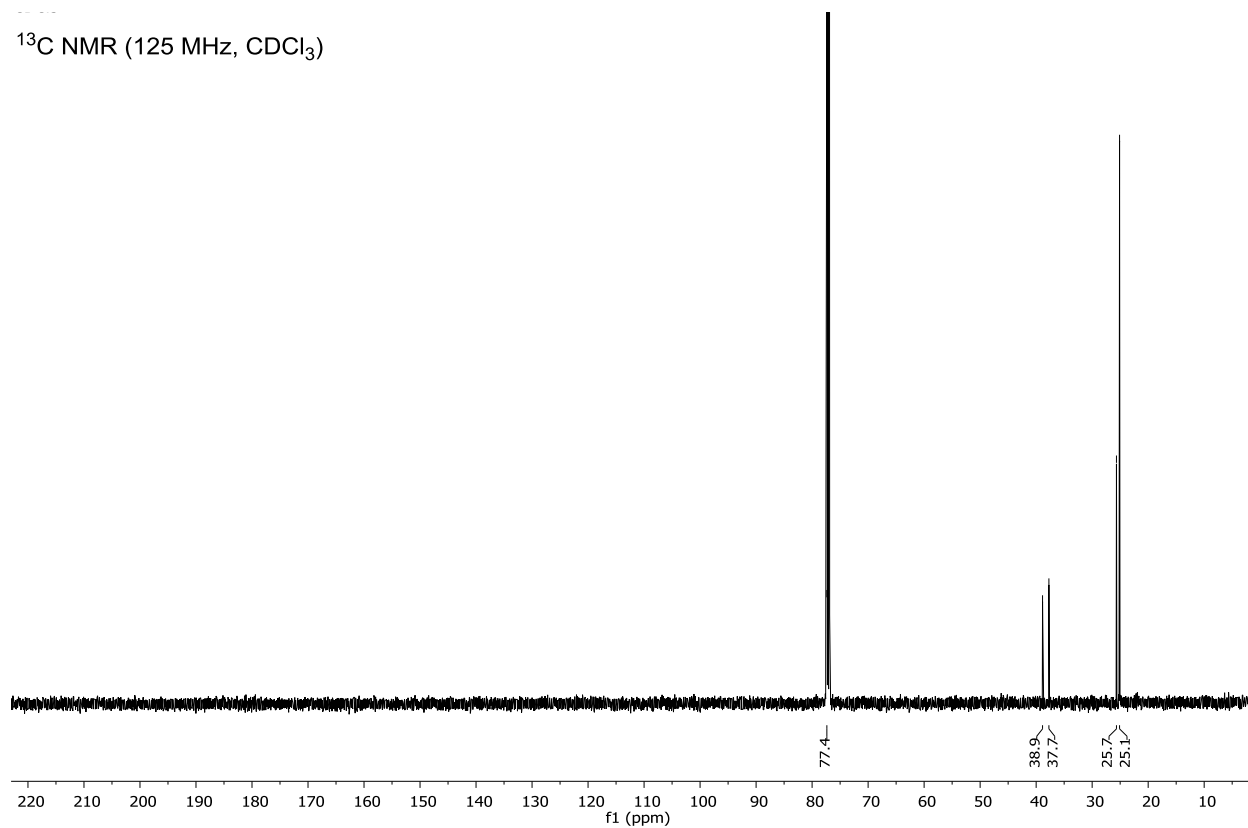


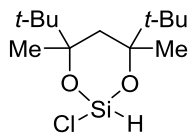
2.33

^1H NMR (500 MHz, CDCl_3)



^{13}C NMR (125 MHz, CDCl_3)

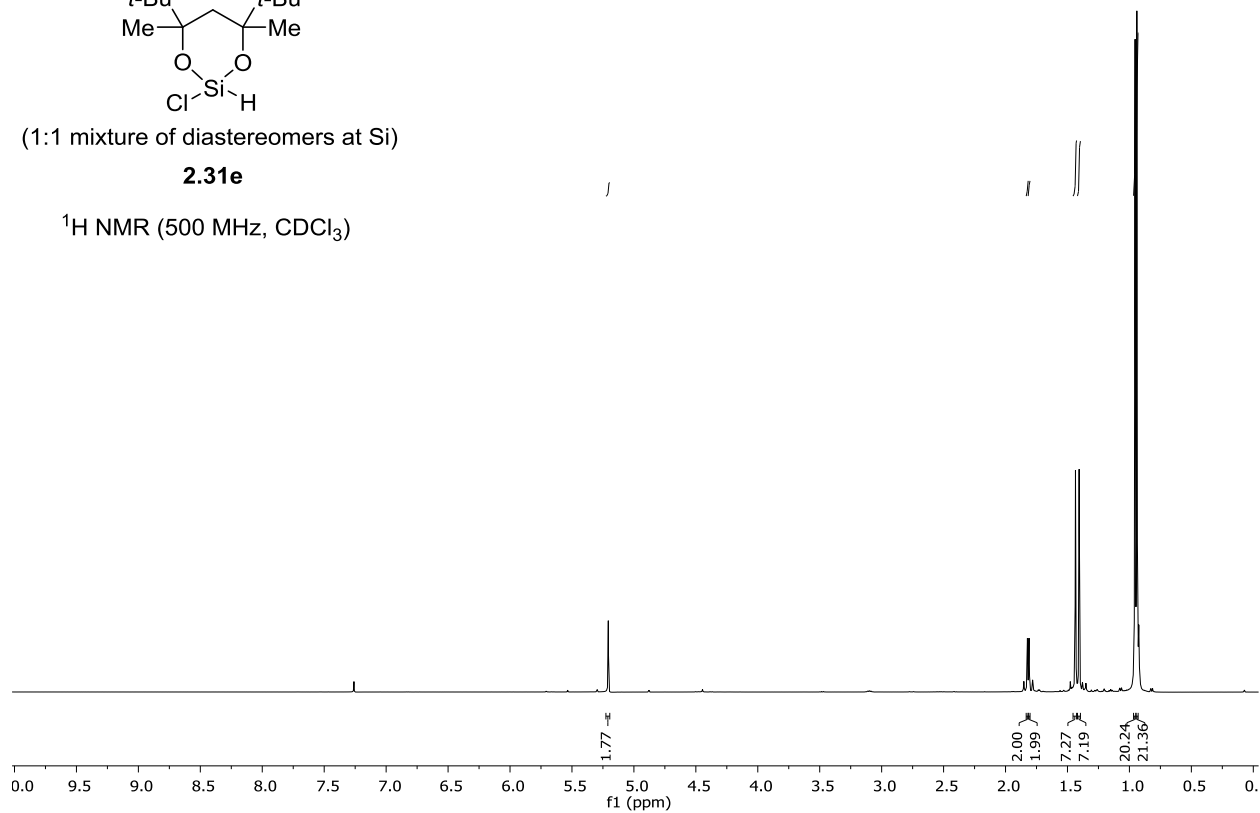




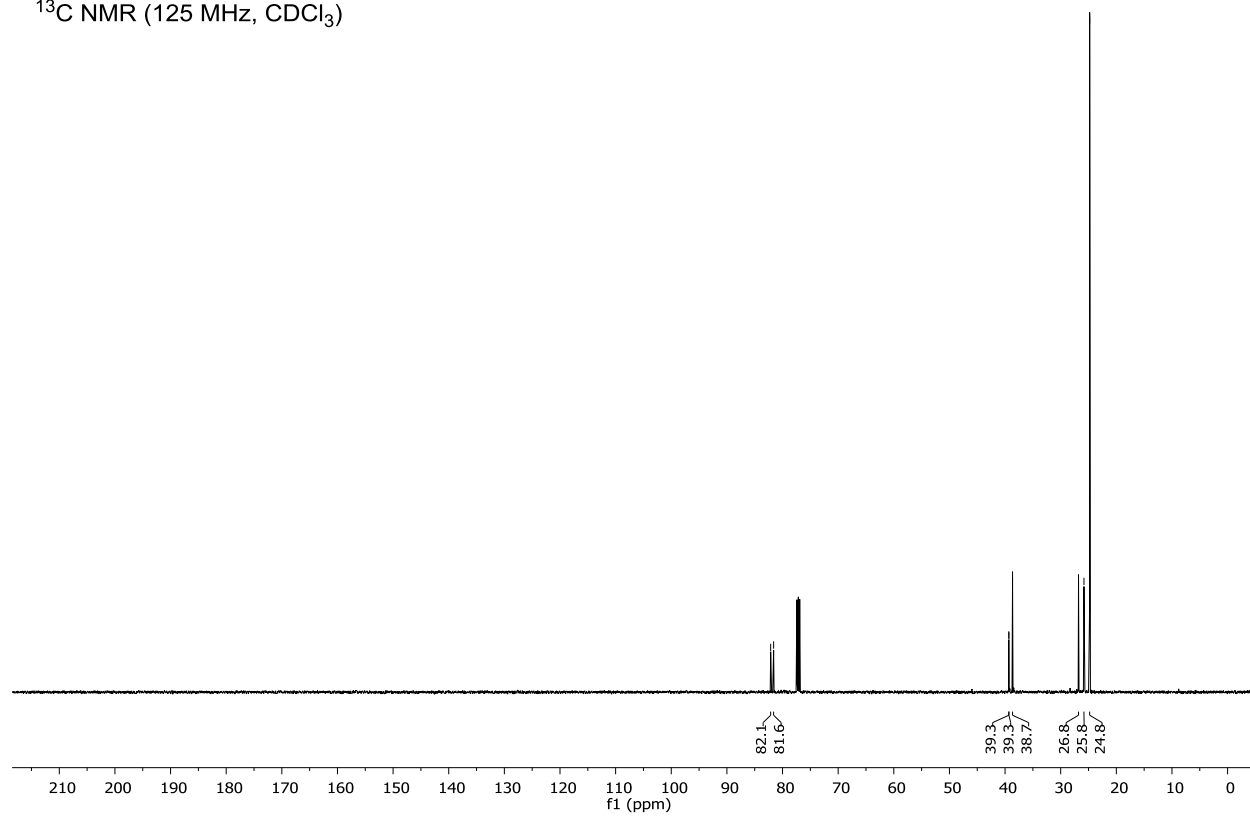
(1:1 mixture of diastereomers at Si)

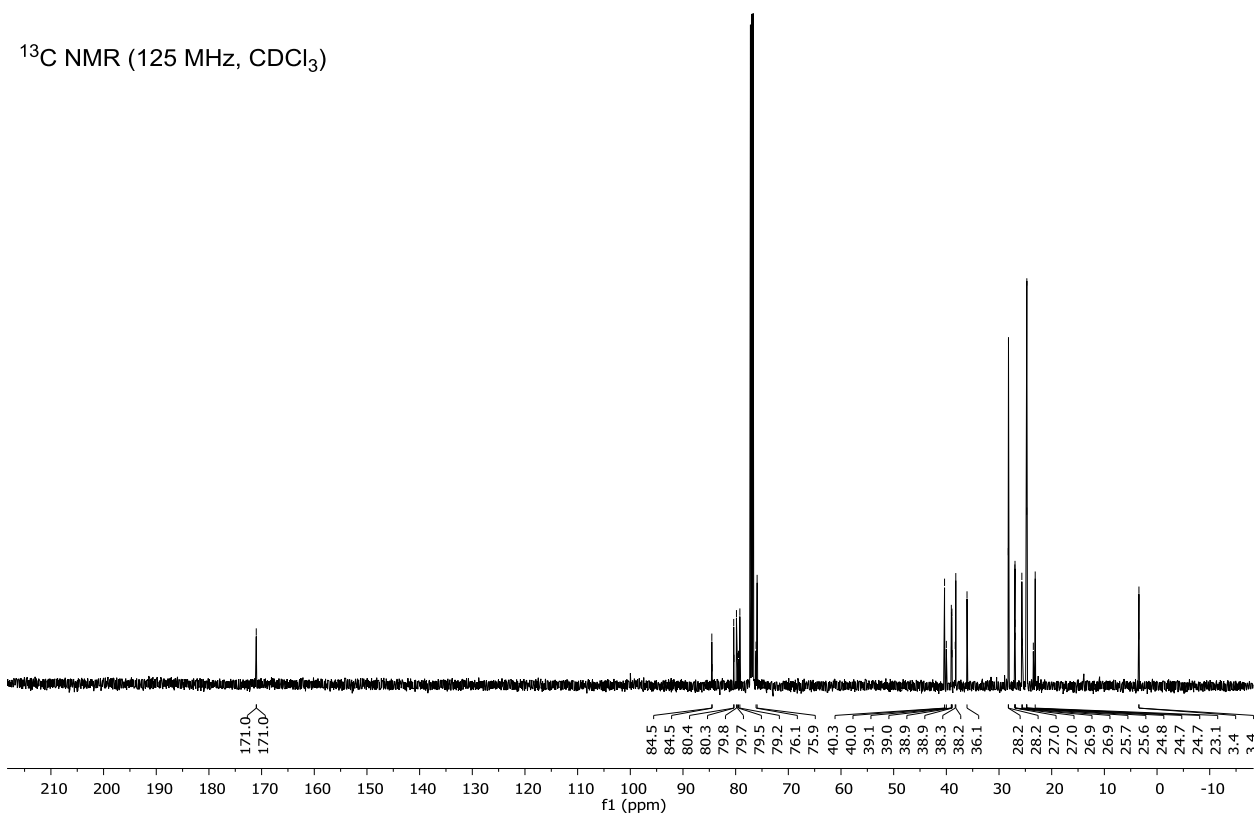
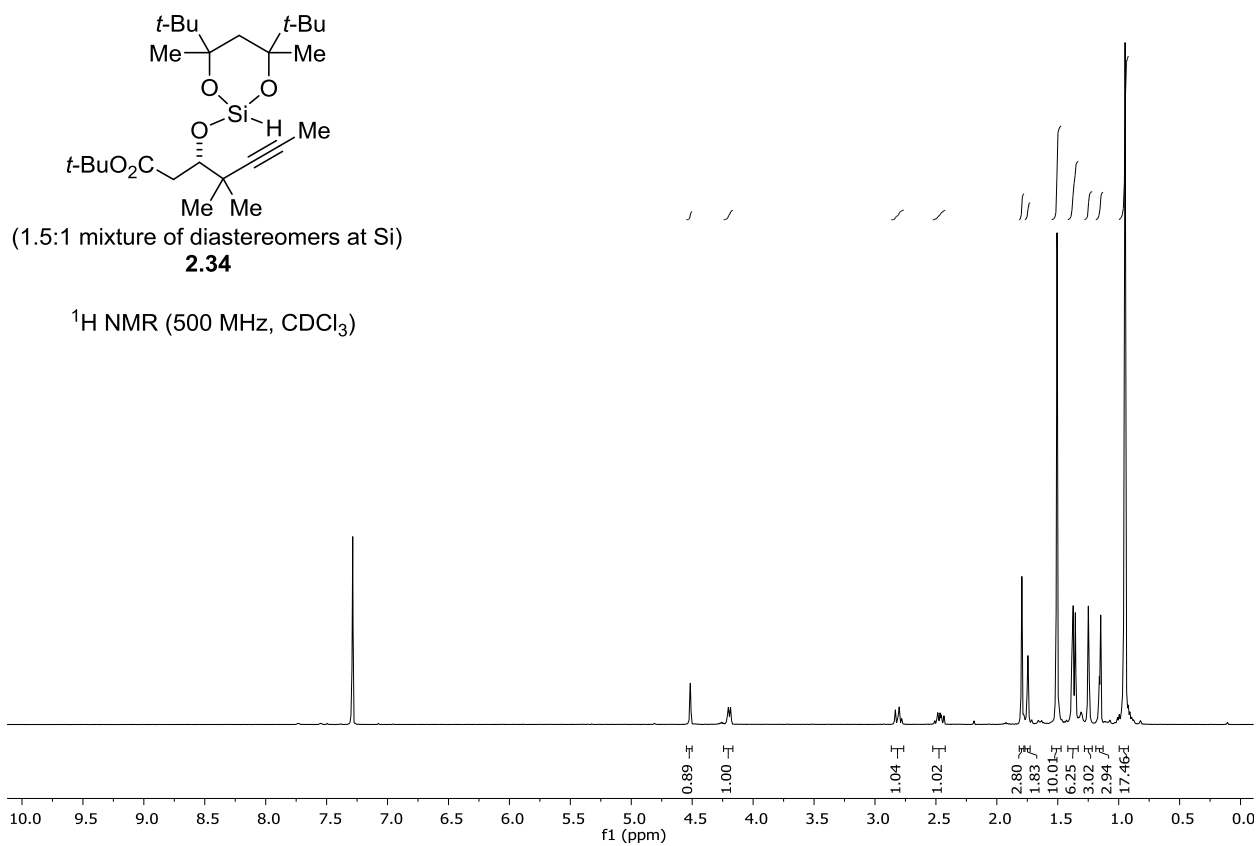
2.31e

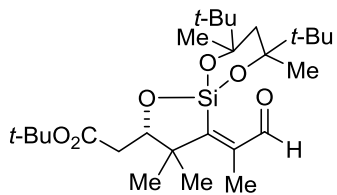
^1H NMR (500 MHz, CDCl_3)



^{13}C NMR (125 MHz, CDCl_3)

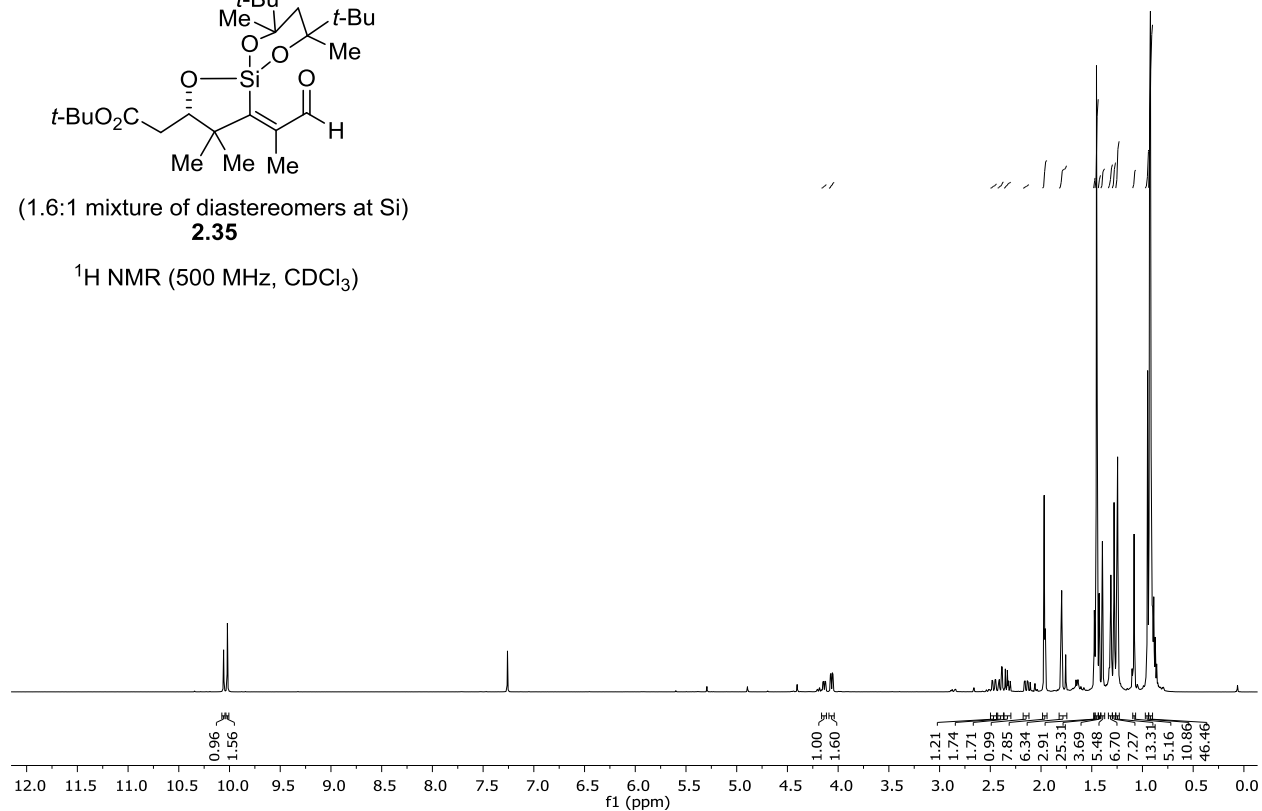




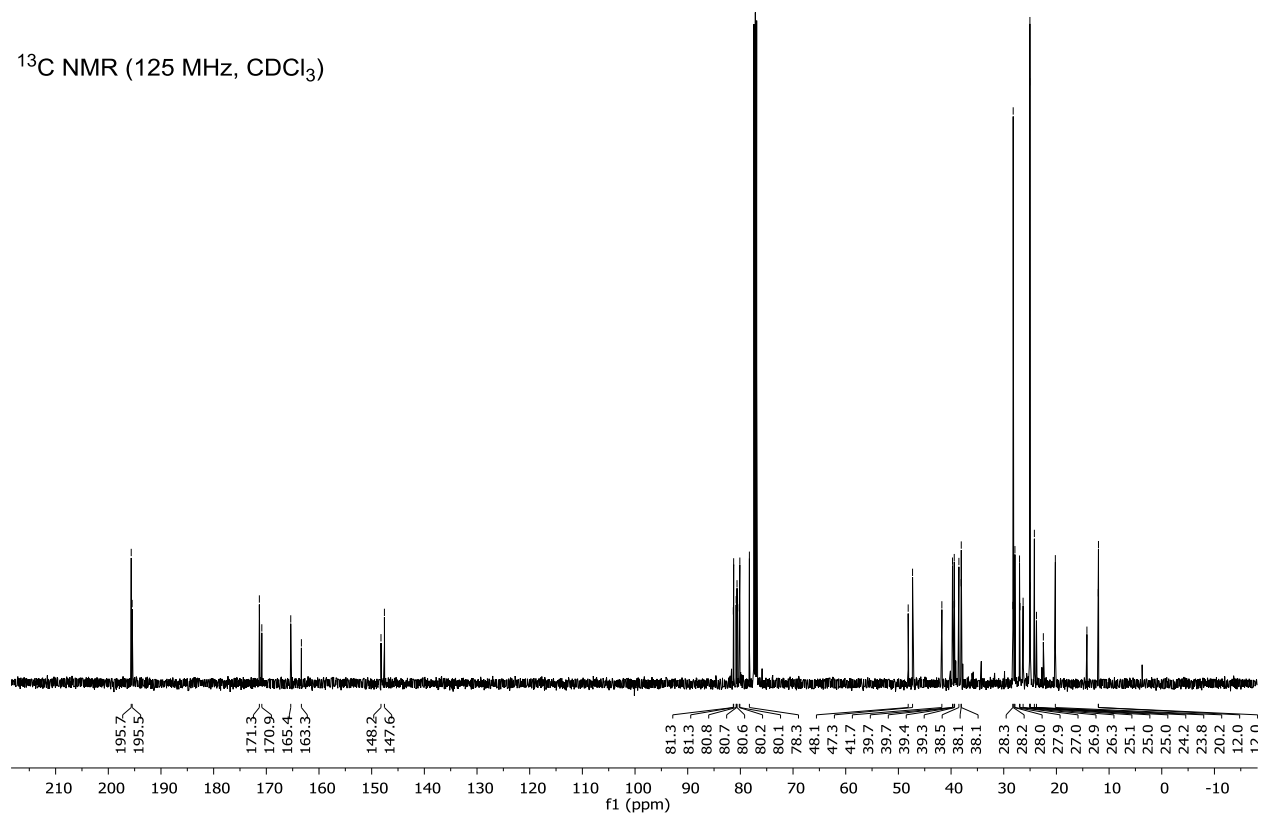


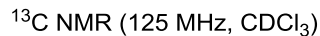
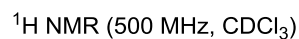
(1.6:1 mixture of diastereomers at Si)
2.35

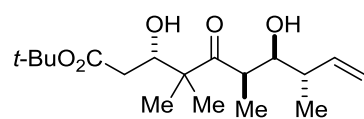
^1H NMR (500 MHz, CDCl_3)



^{13}C NMR (125 MHz, CDCl_3)

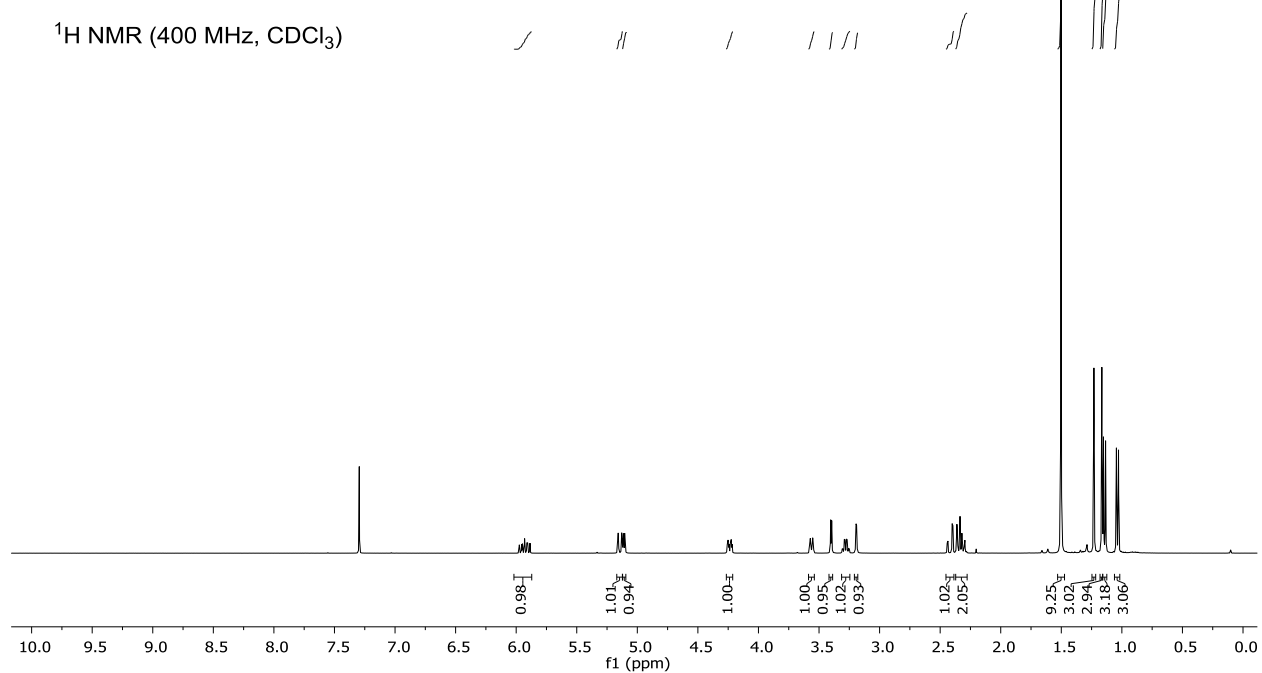




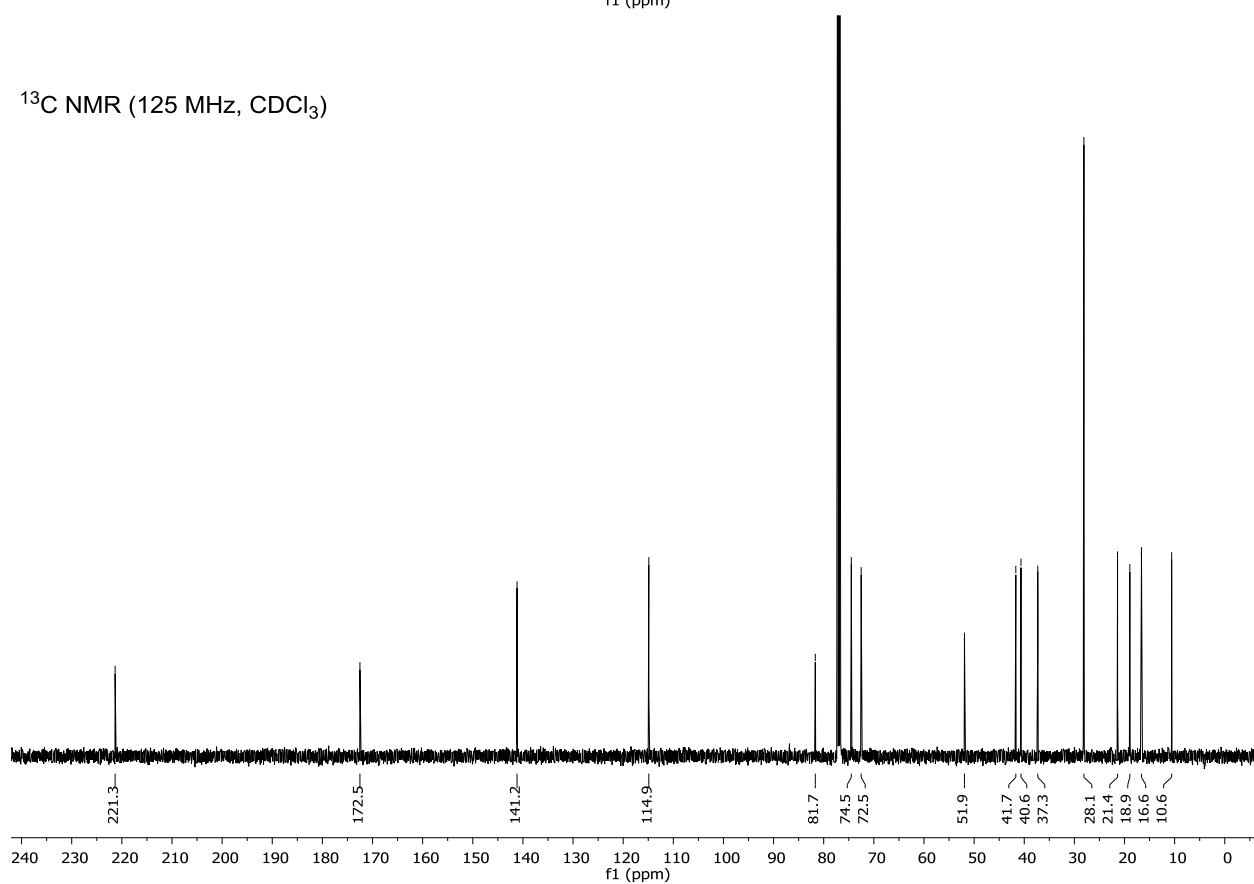


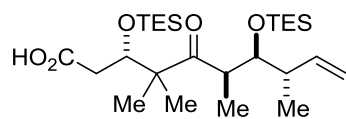
2.12

^1H NMR (400 MHz, CDCl_3)



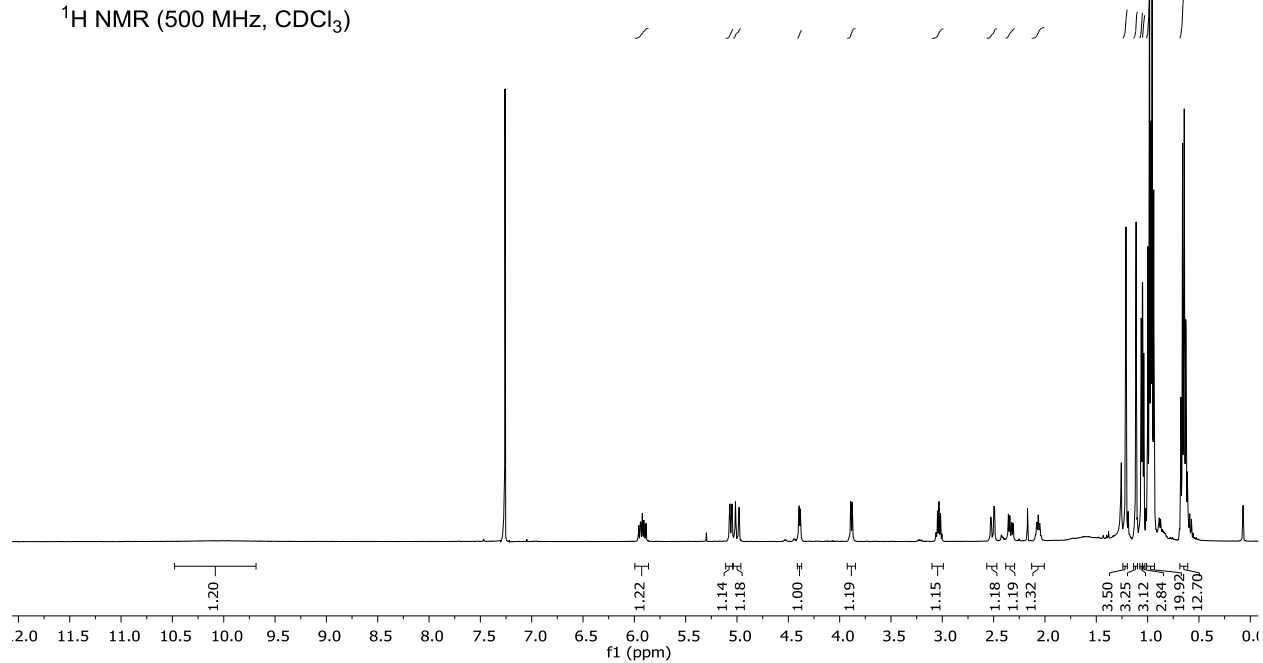
^{13}C NMR (125 MHz, CDCl_3)



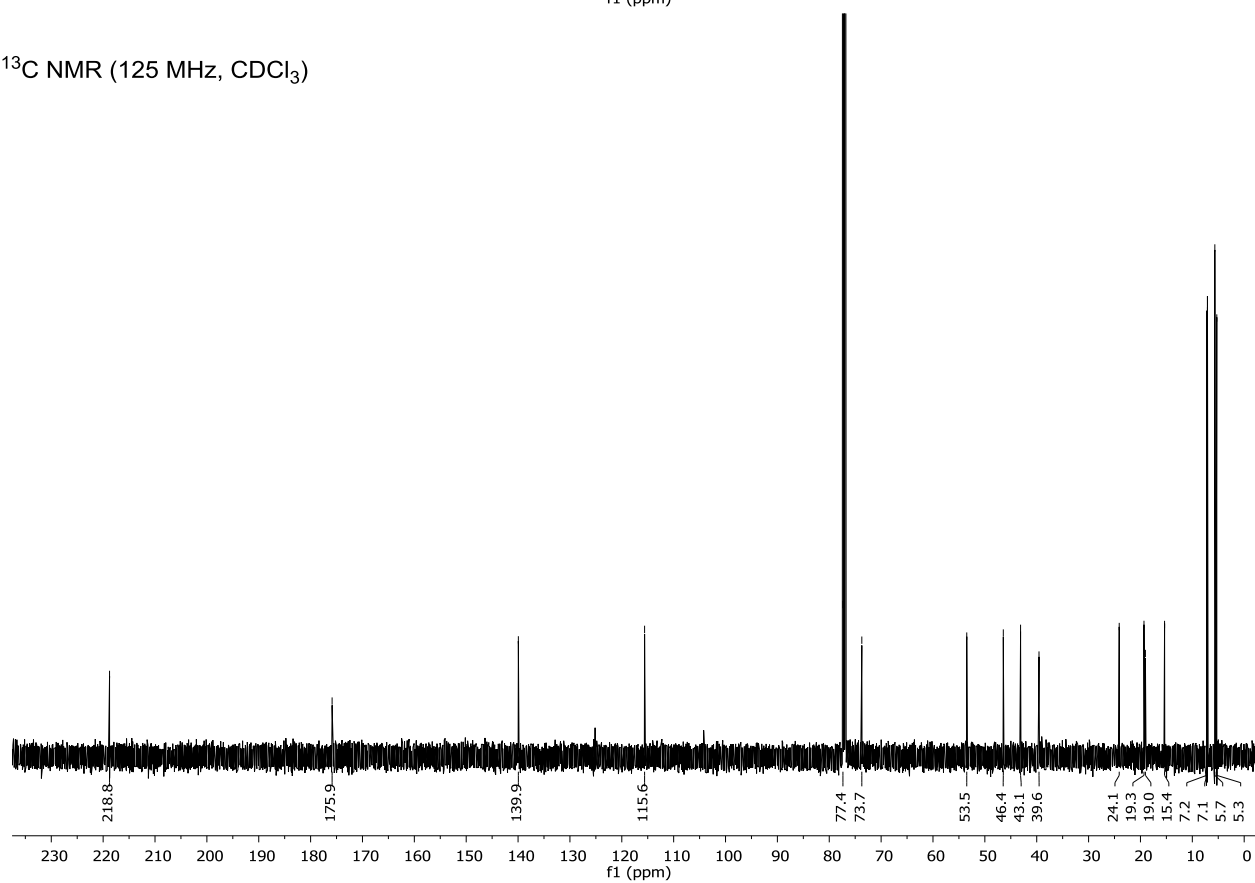


2.32

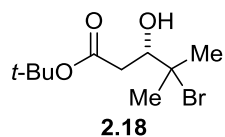
¹H NMR (500 MHz, CDCl₃)



¹³C NMR (125 MHz, CDCl₃)

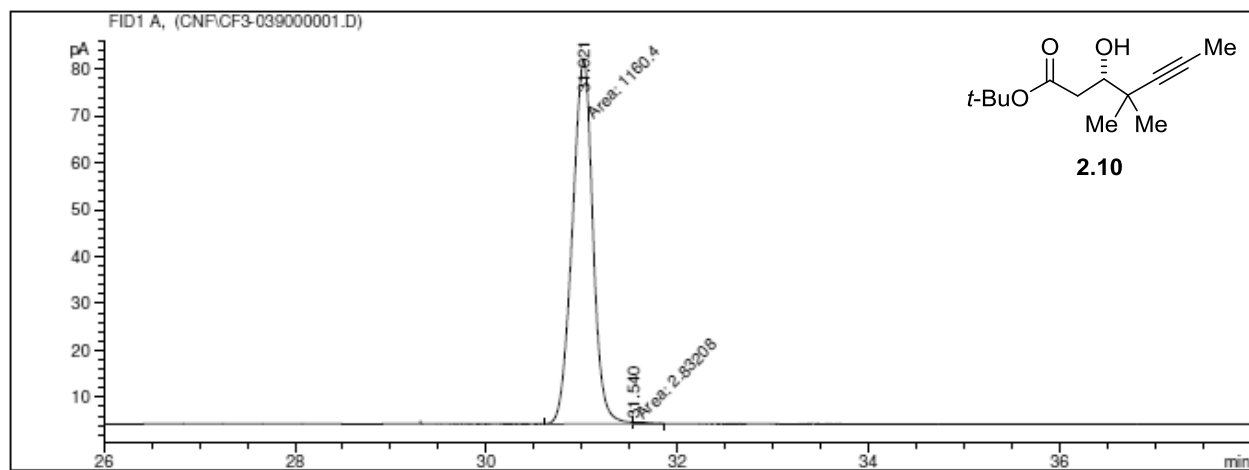
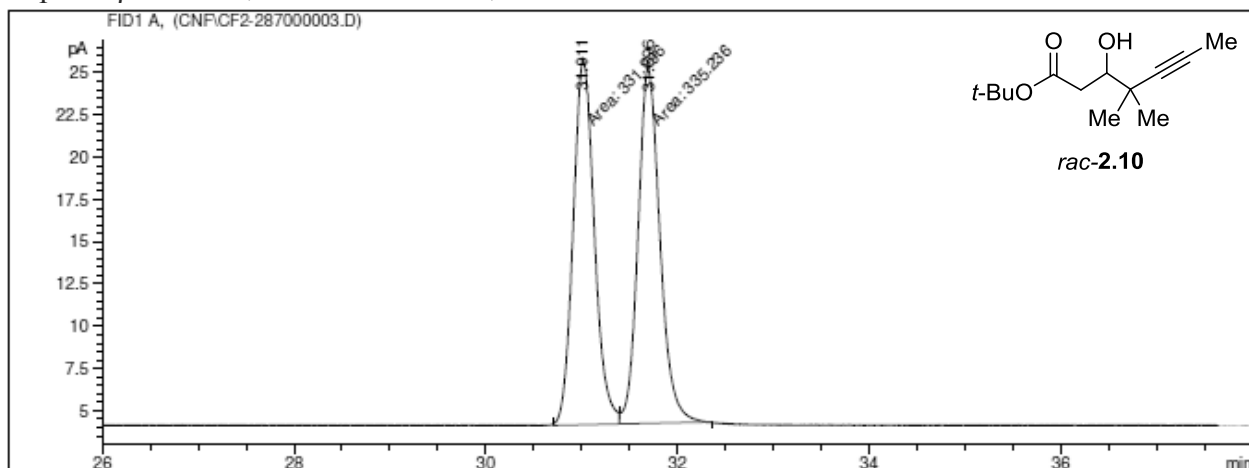


2.8 GC Traces



Chiral GC analysis of **2.10** (product after opening of epoxide **2.14**) revealed that **2.18** was produced in >99% enantiomeric excess (ee).

Supelco β -dex 325, Isothermal 100°C, 1 mL/min



Chapter 3: Application of Our Fragment Synthesis for a C6 Linker Analog of Epothilone B

3.1 Introduction: Aims and Rationale for C6 Methyl Conjugation

Despite potent antiproliferative and cytotoxic activity against a variety of cancer cell lines, epothilones have not yet achieved their full potential as chemotherapeutic agents due to their intrinsic lack of selectivity in acting against malignant versus normal cells. Since these compounds act by binding to tubulin to disrupt microtubule dynamics and thus arrest cells during cell division, the increased rate of proliferation of many cancer cells can impart enough selectivity for some clinical value; however, simultaneous action against healthy tissues often leads to significant side effects. The most problematic of these adverse effects include hematological toxicity, peripheral sensory neuropathy, and a variety of gastrointestinal complications.¹

A strategy that could reduce these side effects is the targeted delivery of a drug molecule via conjugation to a tumor-targeting moiety.² Antibody-drug conjugates (ADCs) have become a popular way to approach targeting efforts, with many currently in clinical trials.^{3,4} Two ADCs have recently been approved by the FDA, both for cancer chemotherapy.⁵ Other groups such as receptor-binding proteins, folates, and nanoparticles have also been used for this type of targeting strategy.^{6,7} The development of bioorthogonal reactions has provided a useful way to selectively assemble these systems once the components (targeting moiety and drug molecule) are obtained, without disturbing the other functionality that is present.⁸

In approaching the conjugation of a drug molecule, the two main points to be considered are the location of the linker and how it will be installed. Addressing the first point, the most important concern is that the linker must be tolerated such that there is not significant loss of binding affinity or potency. In order to do that, the extension must be pointing away from the

binding pocket of its receptor. Since it is impossible to know whether an unexplored linker position will be useful without making the compounds and testing it, the second concern of how the linker will be installed is very important as well. If a promising linker position is difficult to access, it may not be pursued.

Considering ways to install a covalent linker to a drug molecule in the non-aromatic polyketide class, the simplest approach is often through the acylation of a hydroxyl group present in the parent molecule. Concerns for potential ester hydrolysis *in vivo* make this type of covalent attachment less desirable to implement than an alternative approach that would ensure that the linker could not be cleaved unintentionally. In addition, the modification of an alcohol moiety may disrupt important hydrogen bonding interactions with the binding site. In the case of the epothilones, both of the hydroxyl groups (at C3 and C7) appear to be important for binding due to hydrogen-bonding interactions with β -tubulin. The high resolution crystal structure of Epo A bound to tubulin that has been reported shows that the C3 OH has a hydrogen-bonding interaction with the side chain nitrogen of the Gln²⁸¹ residue and the C7 OH has a hydrogen-bonding interaction with the side chain oxygen of the Asp²²⁶ residue.⁹

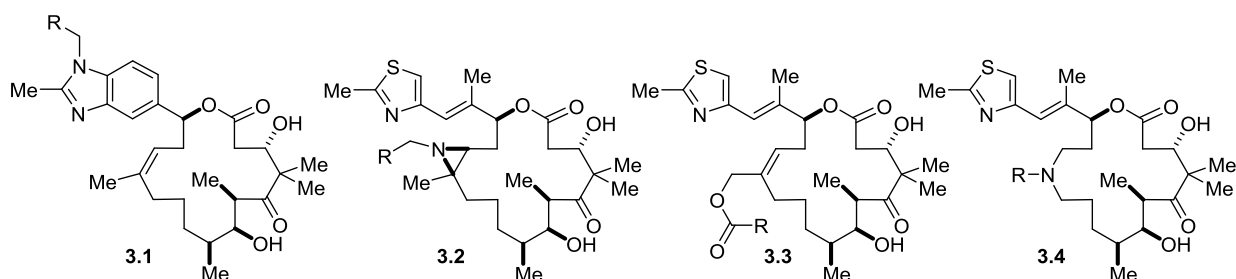


Figure 3.1 Examples of Reported Epothilone Linker Strategies

Other ways of attaching a molecule to a linker require more direct structural modification, potentially through the installation of a new functional group or the modification of an existing group in the parent compound. Reports of epothilone analog exploration towards bioconjugation, whether for targeted delivery or for labeling studies, have focused primarily on modification of

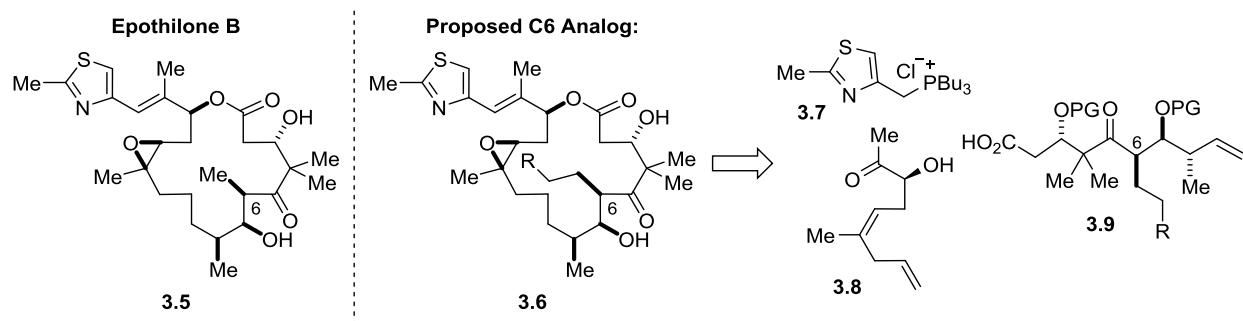
either the heterocyclic side chain, such as in **3.1**,⁶ or the epoxide region, such as in **3.2**,¹⁰ **3.3**,^{11,12} and **3.4**¹³ (Figure 3.1). The only epothilone conjugate that has had reported success and advanced to clinical trials is epofolate, which is comprised of an aziridine-based analog **3.2** linked to folic acid.⁶ However, these trials have since been terminated due to instability issues.

Although there have been some reports of C-H activation methods used for conjugation,^{14,15} the modification of unactivated C-H bonds has been largely unexplored. A strategy that would require a less obtrusive structural change to the parent molecule would be the linear extension of one of the existing methyl groups within the molecule. This type of modification would replace the methyl with a longer chain that has functionality at the end to allow covalent coupling of the completed drug molecule to a longer linker. Modification to a solvent-exposed methyl group should, in principle, have minimal steric and electronic perturbation of the conformation relative to the parent compound such that coordination to the binding site would be as efficient and thus the compound should maintain its activity. To our knowledge, there are only two reported examples of this approach being used. The first example is a C16 methyl modification explored in Schreiber's discodermolide studies, which ultimately did not prove useful due to lack of activity.¹⁶ The second example is a C6 modification of a methyl substituent into an allyl group in epothilones B and D for the purpose of tritium radiolabeling studies, as investigated by researchers at Schering AG.¹⁷ This modification and the subsequent labelled products maintained activity, but only represent a two-carbon extension of the methyl group so does not demonstrate whether conjugation with a longer linker is possible.

Our group has recently become interested in methyl modification as a general conjugation strategy to explore polyketide linker analogs. Since such a deep-seated modification requires a full synthesis for each analog, we are most interested in pursuing this strategy with molecules for which

we have developed highly efficient syntheses that would allow rapid access to analogs. Exploration towards methyl conjugation of dictyostatin is currently under way, utilizing our group's recently reported synthesis.¹⁸

Upon completion of our highly stereoselective synthesis of the C1-C9 fragment of the epothilones, we became interested in applying it towards the investigation of C6 methyl conjugation analogs **3.6** of the natural product epothilone B **3.5**. Since the overall synthesis of the epothilones is modular and our synthesis of the C1-C9 fragment is highly efficient, the installation and study of products containing various linker chains at the C6 position within a reasonable timeframe is feasible, given a stockpile of the other two epothilone components **3.7** and **3.8**. Although we decided to use the natural product epothilone B for this study, a fragment **3.9** could easily be used in the future towards the synthesis of C6 linker analogs for many of the other synthetic epothilones by varying the other components **3.7** and **3.8**.



Scheme 3.1 Proposed C6 Linker Analog of Epothilone B and Disconnection Strategy

The rationale behind our interest in targeting modification of the C6 methyl is twofold. First, although the stereochemistry of the C6-C8 stereotriad cannot be modified, there has been precedent for the extension of the C6 methyl to a longer group by the researchers at Schering AG, as mentioned previously. The SAR data they reported for the C6 ethyl analog of epothilone B **3.11** has shown at least a four-fold enhancement in potency relative to the parent compound across a variety of cancer cell lines, while more limited data for the related C6 allyl (**3.12**) and propyl (**3.13**)

analogs have indicated only slightly reduced activity in multi-drug resistant cell lines relative to epothilone B **3.5**.¹⁷ These studies are related to the more familiar example of C6 modification represented by the exchange of this methyl for an allyl group in sagopilone **3.10**, a compound currently in clinical trials.^{19,20}

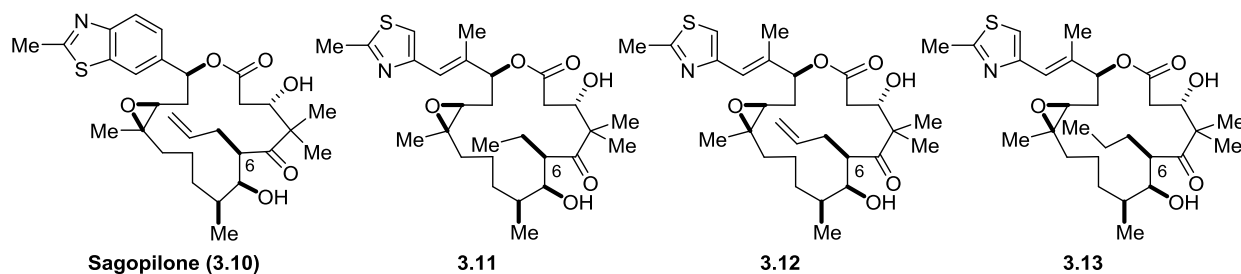


Figure 3.2 Precedent for Tolerated C6 Methyl Extension

Second, the high resolution crystal structure of $\alpha\beta$ -tubulin in complex with epothilone A that was just reported in 2013 indicates that the C6 methyl is solvent exposed (Figure 3.3).⁹ The choice of a solvent-exposed position is vital if we want to be able to extend a much longer chain from our linker without altering the binding affinity. Since this information was consistent with the previously described precedent of C6 methyl extension, it provided more motivation for targeting conjugation of the C6 methyl.

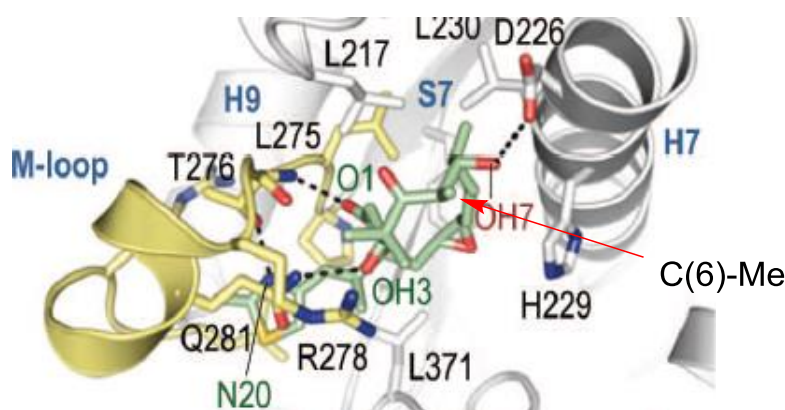


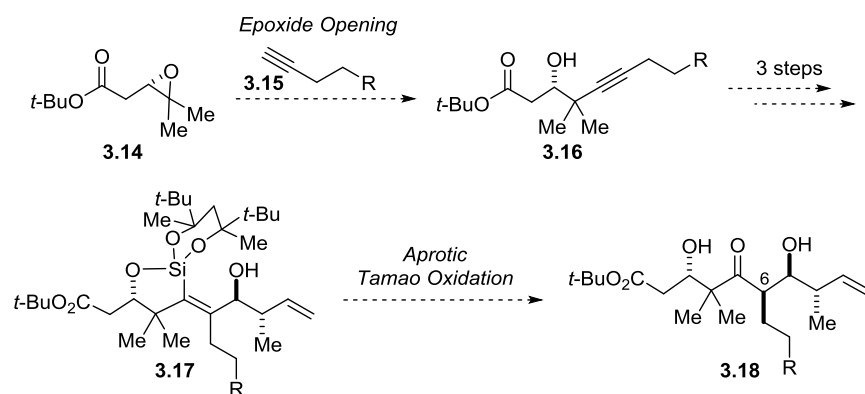
Figure 3.3 Crystal Structure of $\alpha\beta$ -Tubulin in Complex with Epithilone A (C6 Indicated with Arrow)

With our new route in place for access to the C1-C9 fragment and some precedent for our intended C6 modification, we were hopeful that we would be able to obtain our desired analog. If

biological testing shows that our analogs can maintain potency, then applications utilizing a linker at this position can be further pursued.

3.2 Application of Our C1-C9 Fragment Synthesis Towards a C6 Epothilone Linker Analog

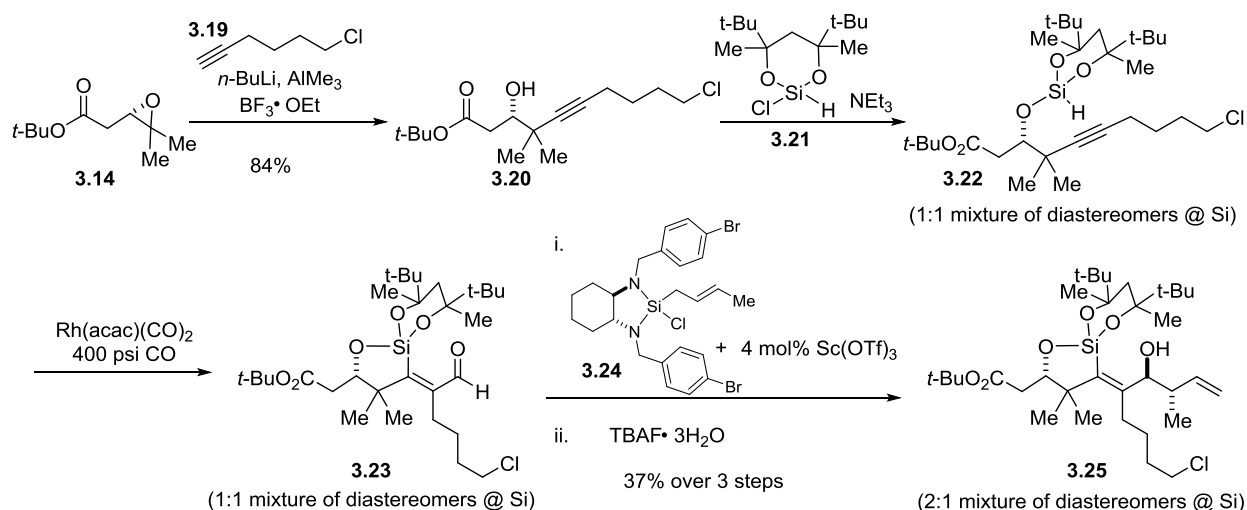
In applying our previously described synthesis to access C6 methyl derivatives of the C1-C9 epothilone fragment, the linker group could be installed by utilizing the corresponding terminal alkyne **3.15** in place of propyne for the epoxide opening step (Scheme 3.2). The required stereochemistry for this C6 position would be set using the “aprotic” Tamao oxidation conditions. Since these *syn*-selective conditions had not been applied for use outside of the previously described work towards the epothilone fragment in chapter 2, we did not know if the methyl group substitution would affect the selectivity of this reaction.



Scheme 3.2 Proposed Adaptation of Previous Synthesis for C6 Analogs

In choosing a linker group to install, we decided to target a carbon chain with a terminal chloride, which could later be converted to an azide. Since we were not confident that an azide would be tolerated under all of the conditions necessary to access an epothilone B analog, we planned to install it as one of the final steps. With an azide at the end of our linker, we should be able to evaluate the potential use of either a click reaction^{21,22} or traceless Staudinger ligation²³ for covalent attachment to a longer tether.

Putting this approach into practice, we found that the epoxide-opening step proceeded smoothly using chloroalkyne **3.19** to afford **3.20** in 84% yield. Silylation with chlorosilane **3.21** followed by rhodium-catalyzed silylformylation provided **3.23**, as expected. However, crotylation with reagent **3.24** exhibited decreased rate and selectivity, providing a 3.5:1 mixture of desired 1,5-*anti*-diols with 1,5-*syn*-diol. After removing the undesired 1,5-*syn*-diol product by chromatography, **3.25** was isolated in 37% yield over 3 steps from **3.20** in a 2:1 mixture of diastereomers at silicon.

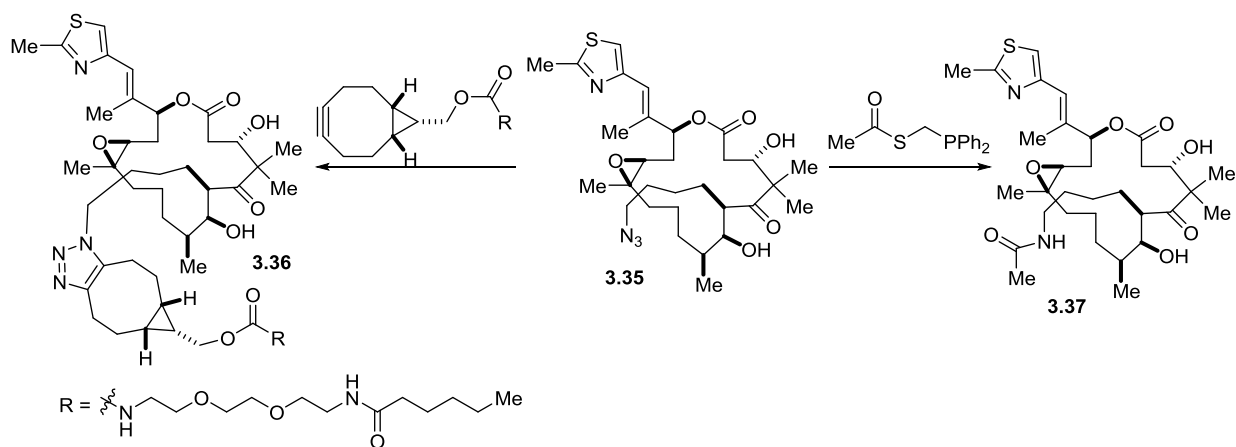


Scheme 3.3 Installation of C6 Linker via Alkyne **3.19**

Although the crotylation selectivity has been eroded, we were still able to access the required “aprotic” Tamao oxidation substrate **3.25** via this route, so we could continue with our analog exploration. If our C6 methyl analogs prove useful, this route can be revisited to examine the use of silanes other than **3.21**. In particular, since the increased steric hindrance from the substitution at the C6 methyl may help stabilize the intermediates relative to original system, it may be possible to reduce the bulkiness of silane **3.21** to a silane with methyl substituents in place of the *tert*-butyl groups.

epothilone B via our C1-C9 fragment.^{24–27} Following the double TES protection and the *tert*-butyl ester cleavage of **3.27**, fragment **3.28** was used directly for the esterification of fragment **3.8**. Ring-closing metathesis of **3.29** using Grubbs second generation catalyst provided **3.30** in 66% yield. The thiazole-containing side chain was installed via Wittig olefination of **3.30** using the phosphonium ylide derived from **3.7** to complete the construction of the epothilone skeleton. Silyl group deprotection followed by selective diimide reduction of the C9-C10 disubstituted olefin provided **3.33**. We chose this point to install the azide, forming **3.34** in excellent yield. This was followed by diastereoselective epoxidation using dimethyldioxirane to access our desired C6 linker analog of epothilone B **3.35**.

After obtaining our azide-containing analog **3.35**, we were able to access both a triazole derivative **3.36** and an acetamide derivative **3.37**, through a strain-released click reaction²¹ and traceless Staudinger ligation,²³ respectively (Scheme 3.6). All three of these compounds were submitted for biological testing against a variety of cancer cell lines.



Scheme 3.6 Conversion of Azide **3.35** into Triazole and Acetamide Derivatives

Table 3.1 shows the preliminary results that our collaborators have determined thus far for compounds **3.35**, **3.36**, and **3.37**, along with some reference compounds, across four different cell lines. From this data, it appears that our linker analogs have not lost activity through extension of

the methyl group or through incorporation of the amide or triazole functionalities at the end of the butyl linker. Although repeat experiments are still underway for future publication, the consistency of potency across different cancer cell lines indicates that the qualitative result (that the analogs maintain potency compared to the parent compounds) is reliable, and thus our C6 linker strategy is viable and can be further developed.

Table 3.1 Preliminary Results for the Testing of C6 Linker Analogs – IC₅₀ Value (nm)

Compound	PC3 (Prostate)	MCF7 (Breast)	H522 (Lung)	OVCAR8 (Ovarian)
Taxol	(6)	(<0.13)	2.6	1.9
Ixabepilone	4	(2)	2.5	3.3
Epo A	7	(7)	5.5	6
3.35	(2.1)	(<0.65)	(0.4)	(1)
3.36	2.3	(<0.65)	0.5	7
3.37	(1)	(0.65)	(0.6)	(2.2)

Notes: These are preliminary results, with further testing underway (Dan Sackett, NIH)

Numbers in () represent one data point and numbers without () represent two data points

3.4 Conclusion and Outlook

Through application of our previously described synthesis of the C1-C9 fragment of the epothilones, we have been able to install a linker at the C6 position through a methyl modification strategy. Although we have utilized the natural product epothilone B as a basis to assess the viability of this linker position and strategy, our modified C1-C9 fragment would not be limited to this use. Since the vast majority of natural and synthetic epothilones do not contain any structural modification within the C1-C9 portions of the molecule,^{28,29} our linker-equipped C1-C9 fragment could be utilized in the synthesis of linker analogs of a variety of other known and promising epothilones. In fact, the route that we have used to access the final product (Scheme 3.6) proceeds through intermediates which are themselves C6 analogs of known potent compounds, such as **3.32**²⁶ and **3.33** (epothilone D).

Given our positive results in the biological testing of our compounds, we believe that we now have a viable linker strategy with which we can move forward to explore potential targeting applications.

3.5 References

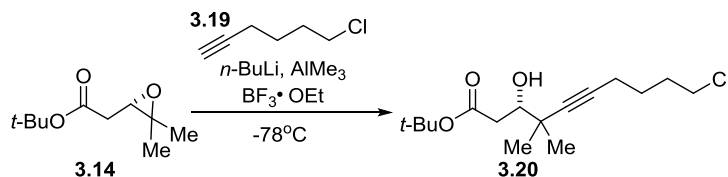
- (1) Krause, W.; Klar, U. Differences and Similarities of Epothilones. *Curr. Cancer Ther. Rev.* **2011**, *7*, 10–36.
- (2) Chari, R. V. J. Targeted Cancer Therapy: Conferring Specificity to Cytotoxic Drugs. *Acc. Chem. Res.* **2007**, *41*, 98–107.
- (3) Firer, M. A.; Gellerman, G. Targeted Drug Delivery for Cancer Therapy: The Other Side of Antibodies. *J. Hematol. Oncol.* **2012**, *5*, 70–85.
- (4) Ducry, L.; Stump, B. Antibody-Drug Conjugates: Linking Cytotoxic Payloads to Monoclonal Antibodies. *Bioconjug. Chem.* **2010**, *21*, 5–13.
- (5) Sliwkowski, M. X.; Mellam, I. Antibody Therapeutics in Cancer. *Science* **2013**, *341*, 1192–1198.
- (6) Vlahov, I. R.; Vite, G. D.; Kleindl, P. J.; Wang, Y.; Santhapuram, H. K. R.; You, F.; Howard, S. J.; Kim, S.-H.; Lee, F. F. Y.; Leamon, C. P. Regioselective Synthesis of Folate Receptor-Targeted Agents Derived from Epothilone Analogs and Folic Acid. *Bioorg. Med. Chem. Lett.* **2010**, *20*, 4578–4581.
- (7) Rana, S.; Yeh, Y.; Rotello, V. M. Engineering the Nanoparticle-Protein Interface: Applications and Possibilities. *Curr. Opin. Chem. Biol.* **2010**, *14*, 828–834.
- (8) Sletten, E. M.; Bertozzi, C. R. Bioorthogonal Chemistry: Fishing for Selectivity in a Sea of Functionality. *Angew. Chem. Int. Ed.* **2009**, *48*, 6974–6998.
- (9) Prota, A. E.; Bargsten, K.; Zurwerra, D.; Field, J. J.; Díaz, J. F.; Altmann, K.-H.; Steinmetz, M. O. Molecular Mechanism of Action of Microtubule-Stabilizing Anticancer Agents. *Science* **2013**, *339*, 587–590.
- (10) Vlahov, I. R.; Vite, G. D.; Kleindl, P. J.; Wang, Y.; Santhapuram, H. K. R.; You, F.; Howard, S. J.; Kim, S.-H.; Lee, F. F. Y.; Leamon, C. P. Regioselective Synthesis of Folate Receptor-Targeted Agents Derived from Epothilone Analogs and Folic Acid. *Bioorg. Med. Chem. Lett.* **2010**, *20*, 4578–4581.
- (11) Ganesh, T.; Schilling, J. K.; Palakodety, R. K.; Ravindra, R.; Shanker, N.; Bane, S.; Kingston, D. G. . Synthesis and Biological Evaluation of Fluorescently Labeled Epothilone Analogs for Tubulin Binding Studies. *Tetrahedron* **2003**, *59*, 9979–9984.
- (12) Reiff, E. A.; Nair, S. K.; Henri, J. T.; Greiner, J. F.; Reddy, B. S.; Chakrasali, R.; David, S. A.; Chiu, T.-L.; Amin, E. A.; Himes, R. H.; Vander Velde, D. G.; Georg, G. I. Total Synthesis and Evaluation of C26-Hydroxyepothilone D Derivatives for Photoaffinity Labeling of Beta-Tubulin. *J. Org. Chem.* **2010**, *75*, 86–94.

- (13) Gertsch, J.; Feyen, F.; Bützberger, A.; Gerber, B.; Pfeiffer, B.; Altmann, K.-H. Making Epothilones Fluoresce: Design, Synthesis, and Biological Characterization of a Fluorescent N12-Aza-Epothilone (Azathilone). *Chembiochem* **2009**, *10*, 2513–2521.
- (14) Li, J.; Cisar, J. S.; Zhou, C.-Y.; Vera, B.; Williams, H.; Rodriguez, A. D.; Cravatt, B. F.; Romo, D. Simultaneous Structure-Activity Studies and Arming of Natural Products by C-H Amination Reveal Cellular Targets of Eupalmerin Acetate. *Nat. Chem.* **2013**, *5*, 510–517.
- (15) Zhou, Q.; Gui, J.; Pan, C.-M.; Albone, E.; Cheng, X.; Suh, E. M.; Grasso, L.; Ishihara, Y.; Baran, P. S. Bioconjugation by Native Chemical Tagging of C-H Bonds. *J. Am. Chem. Soc.* **2013**, *135*, 12994–12997.
- (16) Hung, D. T.; Nerenberg, J. B.; Schreiber, S. L. Syntheses of Discodermolides Useful for Investigating Microtubule Binding and Stabilization. *J. Am. Chem. Soc.* **1996**, *118*, 11054–11080.
- (17) Klar, U.; Skuballa, W.; Buchmann, B.; Schwede, W.; Bunte, T.; Hoffmann, J.; Lichtner, R. B. Synthesis and Biological Activity of Epothilones Syntheses of Epothilone B and D Analogs. In *ACS Symposium Series Vol. 796*; Ojima, I.; Vite, G. D.; Altmann, K.-H., Eds.; American Chemical Society, 2001; pp. 131–147.
- (18) Ho, S.; Bucher, C.; Leighton, J. L. A Highly Step-Economical Synthesis of Dictyostatin. *Angew. Chem. Int. Ed.* **2013**, *52*, 6757–6761.
- (19) Klar, U.; Buchmann, B.; Schwede, W.; Skuballa, W.; Hoffmann, J.; Lichtner, R. B. Total Synthesis and Antitumor Activity of ZK-EPO: The First Fully Synthetic Epothilone in Clinical Development. *Angew. Chem. Int. Ed.* **2006**, *45*, 7942–7948.
- (20) Klar, U.; Platzek, J. Asymmetric Total Synthesis of the Epothilone Sagopilone—From Research to Development. *Synlett* **2012**, *23*, 1291–1299.
- (21) Dommerholt, J.; Schmidt, S.; Temming, R.; Hendriks, L. J. A.; Rutjes, F. P. J. T.; van Hest, J. C. M.; Lefeber, D. J.; Friedl, P.; van Delft, F. L. Readily Accessible Bicyclononynes for Bioorthogonal Labeling and Dhree-Dimensional Imaging of Living Cells. *Angew. Chem. Int. Ed.* **2010**, *49*, 9422–9425.
- (22) Hein, J. E.; Fokin, V. V. Copper-Catalyzed Azide-Alkyne Cycloaddition (CuAAC) and Beyond: New Reactivity of Copper(I) Acetylides. *Chem. Soc. Rev.* **2010**, *39*, 1302–1315.
- (23) Soellner, M. B.; Nilsson, B. L.; Raines, R. T. Reaction Mechanism and Kinetics of the Traceless Staudinger Ligation. *J. Am. Chem. Soc.* **2006**, *128*, 8820–8828.
- (24) Rivkin, A.; Biswas, K.; Chou, T.-C.; Danishefsky, S. J. On the Introduction of a Trifluoromethyl Substituent in the Epothilone Setting: Chemical Issues Related to Ring

- Forming Olefin Metathesis and Earliest Biological Findings. *Org. Lett.* **2002**, *4*, 4081–4084.
- (25) Rivkin, A.; Yoshimura, F.; Gabarda, A. E.; Cho, Y. S.; Chou, T.-C.; Dong, H.; Danishefsky, S. J. Discovery of (E)-9,10-Dehydroepothilones through Chemical Synthesis: On the Emergence of 26-Trifluoro-(E)-9,10-Dehydro-12,13-Desoxyepothilone B as a Promising Anticancer Drug Candidate. *J. Am. Chem. Soc.* **2004**, *126*, 10913–10922.
- (26) Rivkin, A.; Yoshimura, F.; Gabarda, A. E.; Chou, T.-C.; Dong, H.; Tong, W. P.; Danishefsky, S. J. Complex Target-Oriented Total Synthesis in the Drug Discovery Process: The Discovery of a Highly Promising Family of Second Generation Epothilones. *J. Am. Chem. Soc.* **2003**, *125*, 2899–2901.
- (27) Stachel, S. J.; Danishefsky, S. J. Chemo- and Stereoselective Epoxidation of 12,13-Desoxyepothilone B Using 2,2'-Dimethyldioxirane. *Tetrahedron Lett.* **2001**, *42*, 6785–6787.
- (28) Rivkin, A.; Chou, T.-C.; Danishefsky, S. J. On the Remarkable Antitumor Properties of Fludelone: How We Got There. *Angew. Chem. Int. Ed. Engl.* **2005**, *44*, 2838–2850.
- (29) Chou, T.-C.; Zhang, X.; Zhong, Z.-Y.; Li, Y.; Feng, L.; Eng, S.; Myles, D. R.; Johnson, R.; Wu, N.; Yin, Y. I.; Wilson, R. M.; Danishefsky, S. J. Therapeutic Effect against Human Xenograft Tumors in Nude Mice by the Third Generation Microtubule Stabilizing Epothilones. *Proc. Natl. Acad. Sci. U. S. A.* **2008**, *105*, 13157–13162.

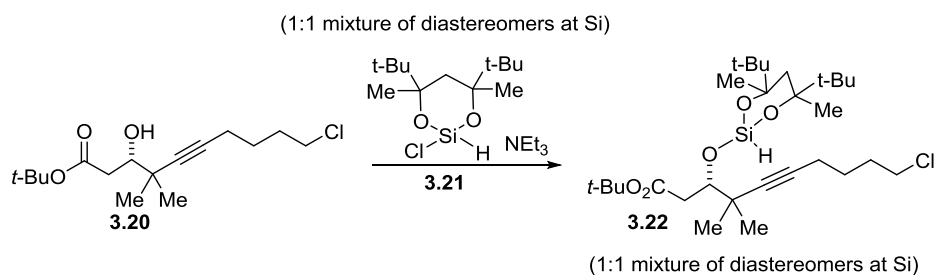
3.6 Experimental Procedures and Characterization Data

General Information. All reactions were carried out under an atmosphere of nitrogen in flame-dried glassware with magnetic stirring unless otherwise indicated. Degassed solvents were purified by passage through an activated alumina column. Thin-layer chromatography (TLC) was carried out on glass-backed silica gel XHL TLC plates (250 μm) from Sorbent Technologies; visualization by UV light, *p*-anisaldehyde stain, phosphomolybdic acid stain, or potassium permanganate (KMnO_4) stain. Gas chromatographic analyses were performed on a Hewlett-Packard 6890 Series Gas Chromatograph equipped with a capillary split-splitless inlet and flame ionization detector with electronic pneumatics control using a Supelco β -Dex 325 (30 m x 0.25 mm) capillary GLC column. ^1H NMR spectra were recorded on a Bruker DPX-400 (400 MHz) or a Bruker Avance III 500 (500 MHz) spectrometer and are reported in ppm from CDCl_3 internal standard (7.26 ppm). Data are reported as follows: (bs= broad singlet, s = singlet, d = doublet, t = triplet, q = quartet, quin = quintet, sep = septet, m = multiplet, dd = doublet of doublets, ddd = doublet of doublet of doublets; coupling constant(s) in Hz; integration). Proton decoupled ^{13}C NMR spectra were recorded on a Bruker Avance III 500 (125 MHz) spectrometer and are reported in ppm from CDCl_3 internal standard (77.16 ppm). Infrared spectra were recorded on a Perkin-Elmer Spectrum Two (Diamond ATR) IR spectrometer. Optical rotations were recorded on a Jasco DIP-1000 digital polarimeter.



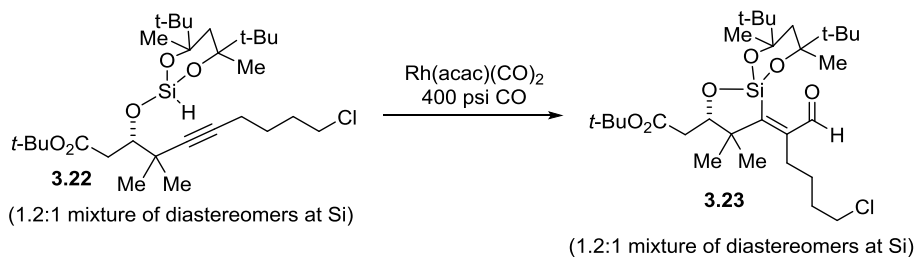
To a cooled (0°C) solution of **3.19** (2.3 mL, 19.1 mmol) in Et_2O (60 mL) was added $n\text{-BuLi}$ (7.6 mL, 2.5 M in hexane, 19.1 mmol) dropwise. After 5 minutes, AlMe_3 (9.1 mL, 2 M in

toluene, 18.3 mmol) was added dropwise. The reaction was warmed to room temperature and stirred for 15 minutes. The reaction was then cooled to -78°C and **3.14** (1.62 g, 8.70 mmol) was added as a solution in Et₂O (15 mL), followed by BF₃•OEt₂ (2.2 mL, 17.4 mmol). After 45 minutes, the reaction was slowly quenched with MeOH (20 mL). The mixture was stirred for 10 minutes then poured into 30 mL of saturated aqueous NaHCO₃ solution of pH 10. After stirring for about 45 minutes, the layers were separated and the aqueous layer extracted with Et₂O (3 x 60 mL). The combined organics were washed with brine, dried over MgSO₄, filtered, and concentrated. The crude material was purified by silica gel chromatography (8% EtOAc/hexanes, *p*-anisaldehyde stain) to provide **3.20** as a clear, yellow oil (2.20 g, 84% yield). ¹H NMR (500 MHz, CDCl₃) δ 3.75 (ddd, *J* = 10.4, 4.5, 2.3 Hz, 1H), 3.56 (t, *J* = 6.6 Hz, 2H), 2.91 (d, *J* = 4.5 Hz, 1H), 2.62 (dd, *J* = 16.0, 2.4 Hz, 1H), 2.39 (dd, *J* = 16.0, 10.4 Hz, 1H), 2.21 (t, *J* = 7.0 Hz, 2H), 1.92 – 1.82 (m, 2H), 1.69 – 1.60 (m, 2H), 1.47 (s, 9H), 1.20 (s, 3H), 1.18 (s, 3H); ¹³C NMR (125 MHz, CDCl₃) δ 172.8, 85.4, 81.6, 81.3, 74.6, 44.7, 38.8, 36.3, 31.8, 28.3, 26.4, 26.3, 24.9, 18.2; IR (film): 3494, 2974, 2934, 2868, 1712, 1455, 1392, 1367, 1302, 1254, 1151, 1079, 1041, 950, 762, 651 cm⁻¹; LRMS (FAB+) calcd C₁₆H₂₈ClO₃ [M+H]⁺: 303.16, found 303.29; [α]_D²⁰ -28.7 (*c* 1.20, CHCl₃).



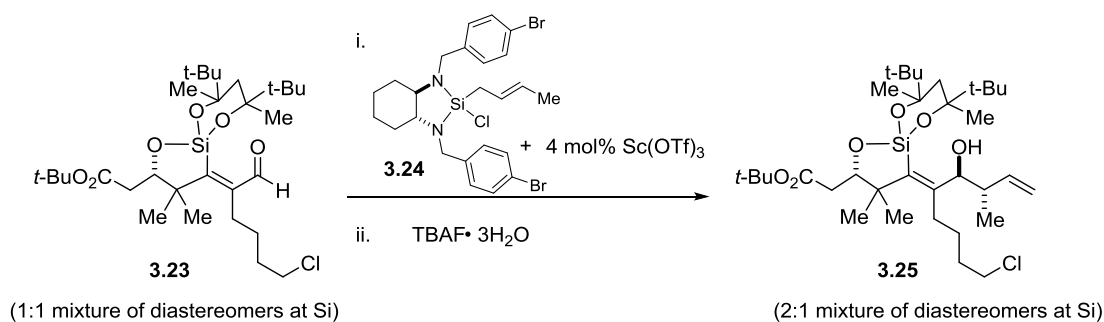
To a cooled (0°C) solution of silane **3.21** (817 mg, 2.93 mmol) in CH₂Cl₂ (28 mL) was added β -ketoester **3.20** (845 mg, 2.79 mmol) as a solution in CH₂Cl₂ (10 mL), followed by NEt₃ (0.58 mL, 4.19 mmol). The reaction was warmed to room temperature after 30 minutes. ¹H NMR analysis was used to determine the conversion of the reaction mixture. Additional silane was added

if starting material remained. Once complete, the reaction was concentrated and the residue filtered with Et₂O through an oven-dried frit. The filtrate was concentrated to provide intermediate **3.22** as a 1:1 mixture of diastereomers, which was used directly in the next step. Since this intermediate is difficult to purify due to hydrolytic sensitivity, and both diastereomers useful for our purposes, characterization reflects the mixture we obtained. Observed spectra: ¹H NMR (500 MHz, CDCl₃) δ 4.47 (m, 2H), 4.13 (m, 2H), 3.55 (t, *J* = 6.6 Hz, 4H), 2.76 (m, 2H), 2.44 (m, 2H), 2.19 (t, *J* = 6.9 Hz, 4H), 1.92 – 1.81 (m, 4H), 1.69 (m, 4H), 1.67 – 1.57 (m, 4H), 1.47 (m, 18H), 1.37 – 1.28 (m, 12H), 1.21 (m, 6H), 1.12 (m, 6H), 0.94 – 0.87 (m, 36H); ¹³C NMR (125 MHz, CDCl₃) δ 171.2, 171.2, 86.3, 86.2, 81.2, 81.1, 80.7, 80.6, 80.0, 79.8, 79.6, 79.3, 77.4, 76.1, 75.9, 44.8, 40.5, 40.1, 39.2, 39.2, 39.1, 39.0, 38.3, 38.2, 36.2, 36.1, 31.7, 31.6, 28.4, 28.3, 27.3, 27.1, 27.1, 26.2, 25.8, 25.7, 24.9, 24.9, 24.9, 23.7, 23.4, 18.2, 18.2.



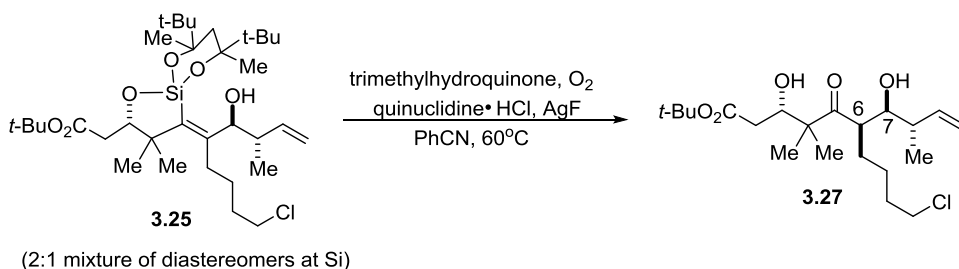
A glass liner for a Parr bomb was charged with the crude **3.22** (from previous reaction) as a solution in CH₂Cl₂ (5.6 mL). The bomb was assembled and pressurized with CO to approximately 500 psi and then vented. This procedure was repeated two more times, then the bomb was pressurized again to 500 psi and stirred for about fifteen minutes. The bomb was carefully vented and opened, then Rh(acac)(CO)₂ (0.223 mmol, 58 mg) was added. The bomb was reassembled and pressurized to 500 psi with CO then stirred at ambient temperature. After 24 hours, the bomb was carefully vented and opened. ¹H NMR analysis indicated complete consumption of starting material and clean formation of product **3.23** as a 1.2:1 mixture of

diastereomers. This reaction solution was used directly in the following crotylation reaction. Observed spectra of the diastereomeric mixture were as follows: ^1H NMR (500 MHz, CDCl_3) δ 10.09 (s, 1H), 10.04 (s, 1H), 4.16 (dd, $J = 10.3, 3.4$ Hz, 1H), 4.10 (dd, $J = 10.0, 2.8$ Hz, 1H), 3.57 (m, 4H), 2.59 – 2.40 (m, 6H), 2.35 (dd, $J = 14.4, 10.0$ Hz, 1H), 2.15 (dd, $J = 14.6, 10.4$ Hz, 1H), 1.93 – 1.80 (m, 8H), 1.48 (m, 18H), 1.46 (s, 3H), 1.43 (s, 3H), 1.38 (s, 3H), 1.35 (s, 3H), 1.32 (s, 3H), 1.27 (m, 6H), 1.14 (s, 3H), 0.98 (s, 9H), 0.97 – 0.93 (m, 28H); ^{13}C NMR (125 MHz, CDCl_3) δ 195.8, 195.6, 171.1, 170.6, 165.1, 163.1, 152.3, 151.6, 81.3, 81.2, 80.7, 80.6, 80.5, 80.1, 80.0, 78.2, 48.2, 47.3, 44.6, 41.7, 39.6, 39.5, 39.3, 39.2, 38.5, 37.9, 37.9, 33.0, 32.9, 28.1, 27.9, 27.8, 27.5, 27.0, 26.9, 26.7, 26.6, 25.8, 25.6, 24.9, 24.9, 24.9, 24.5, 23.8, 21.3.



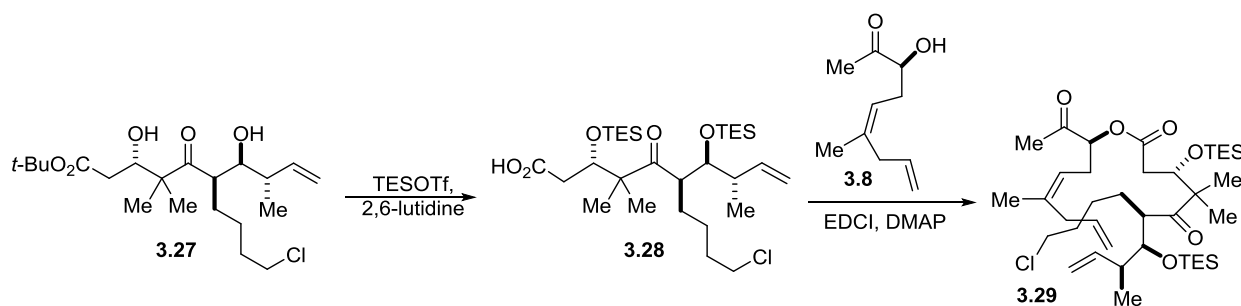
To a solution of the reaction mixture from aldehyde **3.23** formation in CH_2Cl_2 (28 mL) was added (*R,R*)-*trans*-crotylsilane diamine reagent **3.24** (2.38 g, 4.19 mmol) and $\text{Sc}(\text{OTf})_3$ (138 mg, 0.279 mmol). After 24 hours at room temperature, additional $\text{Sc}(\text{OTf})_3$ and reagent were added. After another 16 hours, the reaction was still incomplete as judged by ^1H NMR. The solution was then cooled to 0°C and tetrabutylammonium fluoride (TBAF) trihydrate (879 mg, 2.79 mmol) was added portion-wise over 20 minutes. After about 3 hours, the reaction was concentrated and the residue purified via silica gel chromatography (5% EtOAc/hexanes) to afford **3.25** (658 mg, 37% over 3 steps) as a viscous yellow oil. **3.25** was a 2:1 mixture of diastereomers at silicon. (Another diastereomer that was formed in equal amount with the minor from unselective crotylation of one of the aldehyde diastereomers was removed via the silica gel chromatography.) ^1H NMR (400

MHz, CDCl₃) δ 5.76 (m, 3H), 5.06 – 4.89 (m, 6H), 4.39 (d, J = 2.3 Hz, 2H), 4.34 (d, J = 2.3 Hz, 1H), 4.19 – 4.11 (m, 3H), 3.58 (m, 6H), 2.99 (d, J = 3.4 Hz, 1H), 2.95 (d, J = 3.1 Hz, 2H), 2.83 (m, 3H), 2.52 (m, 6H), 2.30 (m, 3H), 1.99 (m, 3H), 1.82 (m, 12H), 1.76 – 1.61 (m, 5H), 1.57 – 1.48 (m, 4H), 1.47 (m, 34H), 1.44 (m, 13H), 1.34 – 1.25 (m, 17H), 1.26 – 1.17 (m, 13H), 1.00 – 0.97 (m, 57H); ¹³C NMR (125 MHz, CDCl₃) δ 173.3, 173.1, 162.2, 138.9, 138.8, 134.6, 114.9, 114.8, 80.7, 80.6, 80.4, 80.1, 79.9, 79.9, 79.7, 74.2, 74.1, 44.7, 41.8, 41.4, 41.3, 39.9, 39.8, 39.5, 39.4, 38.7, 38.4, 38.3, 37.9, 37.6, 32.8, 32.7, 31.6, 29.8, 28.4, 28.2, 28.1, 28.1, 27.9, 27.7, 27.1, 26.4, 26.1, 25.9, 25.5, 25.2, 25.1, 25.1, 25.0, 24.7, 24.4, 22.7, 18.3, 18.2, 14.1.



To a solution of trimethylhydroquinone (515 mg, 3.39 mmol), quinuclidine hydrochloride (450 mg, 3.05 mmol), and silver fluoride (459 mg, 3.62 mmol) in benzonitrile (5.0 mL) was added **3.25** (711 mg, 1.13 mmol) as a solution in benzonitrile (6.3 mL). The solution was purged with O₂ then the reaction was heated to 60°C (oil bath, external temperature) and stirred overnight under a balloon of O₂. After 22 hours, the reaction was cooled to room temperature and diluted with CHCl₃ (15 mL). The solution was filtered through Celite, then washed with distilled water. The aqueous layer was extracted with CHCl₃ (3 x 15 mL). The combined organics were washed with brine, dried over MgSO₄, filtered, and concentrated. The residue was purified via silica gel chromatography (stepwise: 10% EtOAc/hexanes, 30% EtOAc/hexanes) to provide **3.27** (345 mg, 75%) as a brown oil with >18:1 diastereomeric ratio (d.r.) with respect to the newly formed stereocenter at C6. ¹H NMR (300 MHz, CDCl₃) δ 5.87 (ddd, J = 17.8, 10.4, 7.7 Hz, 1H), 5.12 (dd,

$J = 8.4, 1.5$ Hz, 1H), 5.09 – 5.05 (m, 1H), 4.24 (dt, $J = 10.0, 3.2$ Hz, 1H), 3.61 (dt, $J = 8.1, 2.6$ Hz, 1H), 3.53 (td, $J = 6.6, 3.4$ Hz, 2H), 3.36 (d, $J = 3.5$ Hz, 1H), 3.23 (dt, $J = 8.8, 3.2$ Hz, 1H), 2.54 (d, $J = 2.6$ Hz, 1H), 2.40 (dd, $J = 16.1, 2.9$ Hz, 1H), 2.31 (dd, $J = 16.2, 9.7$ Hz, 2H), 1.89 – 1.71 (m, 3H), 1.47 (s, 9H), 1.43 – 1.29 (m, 2H), 1.23 (s, 3H), 1.10 (s, 3H), 1.03 (d, $J = 6.8$ Hz, 3H); ^{13}C NMR (125 MHz, CDCl_3) δ 219.7, 172.5, 141.2, 115.4, 81.8, 73.7, 72.9, 52.0, 48.4, 44.8, 41.3, 37.4, 33.00, 28.2, 25.5, 24.7, 22.2, 19.2, 16.9; IR (film): 3494, 2971, 2932, 2872, 1706, 1457, 1392, 1368, 1303, 1253, 1221, 1153, 1033, 997, 915, 765, 727, 650 cm^{-1} ; LRMS (FAB+) calcd $\text{C}_{21}\text{H}_{37}\text{ClO}_5\text{Na}$ $[\text{M}+\text{Na}]^+$: 427.22, found 427.5; $[\alpha]_D^{20}$ -46.7 (c 0.45, CHCl_3).



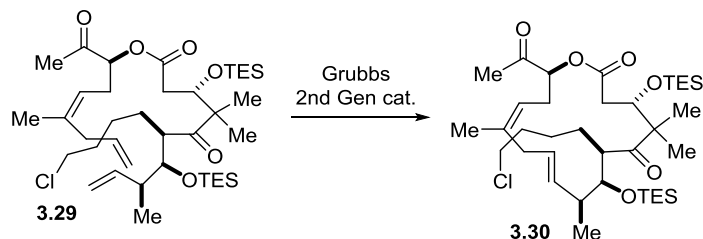
To a cooled (-78°C) solution of **3.27** (345 mg, 0.852 mmol) in CH_2Cl_2 (8.8 mL) was added 2,6-lutidine (0.61 mL, 5.27 mmol). TESOTf (0.40 mL, 1.76 mmol) was then added dropwise. After 30 minutes, a second portion of TESOTf (0.40 mL, 1.76 mmol) was added and the cold bath was removed, allowing the reaction to warm to room temperature. After 2 hours, the reaction was diluted with Et_2O (80 mL), washed with 5% aqueous KHSO_4 (2 x 10 mL) then brine (15 mL), and then dried over Na_2SO_4 and concentrated. The residue was dissolved in aqueous THF (15 mL, 6:1 THF/ H_2O) and treated with saturated aqueous NaHCO_3 (2 mL). After stirring at room temperature for 20 minutes, the mixture was diluted with Et_2O (20 mL) and acidified with 5% aqueous KHSO_4 (10 mL). The layers were separated then the aqueous layer extracted with Et_2O (2 x 15 mL). The combined organic layers were washed with brine, dried over Na_2SO_4 , filtered, and concentrated to provide **3.28** as a mixture with TESO H . The crude product was used directly in the next step. For

characterization purpose, purification via silica gel chromatography (15% EtOAc/hexanes, pH 7 buffered silica gel) provided **3.28** as a light yellow oil.¹ ¹H NMR (500 MHz, CDCl₃) δ 10.73 (bs, 1H), 5.94 – 5.79 (m, 1H), 5.11 – 4.98 (m, 2H), 4.32 (dd, *J* = 7.4, 2.9 Hz, 1H), 3.86 (dd, *J* = 5.3, 3.3 Hz, 1H), 3.50 (t, *J* = 6.6 Hz, 2H), 3.03 – 3.00 (m, 1H), 2.60 (dd, *J* = 16.6, 2.9 Hz, 1H), 2.33 (dd, *J* = 16.6, 7.3 Hz, 1H), 2.20 – 2.13 (m, 1H), 1.76 – 1.59 (m, 3H), 1.51 – 1.45 (m, 1H), 1.39 – 1.28 (m, 2H), 1.21 (s, 3H), 1.12 (s, 3H), 1.05 (s, 3H), 0.98 – 0.94 (m, 18H), 0.71 – 0.52 (m, 12H). ¹³C NMR (125 MHz, CDCl₃) δ 216.6, 177.0, 140.2, 115.5, 75.8, 74.3, 53.3, 51.6, 45.0, 44.3, 39.6, 33.2, 27.0, 25.4, 24.2, 19.5, 18.7, 7.3, 7.1, 5.6, 5.3; IR (film): 2955, 2877, 2916, 1709, 1692, 1458, 1416, 1302, 1238, 1093, 1003, 914, 731 cm⁻¹; LRMS (FAB+) calcd C₂₇H₅₇ClO₅Si₂ [M+H]⁺: 577.34, found 577.95; [α]_D²⁴ -22.6 (*c* 1.43, CHCl₃).

To a cooled (0°C) solution of dried **3.8** (207 mg, 1.23 mmol) in CH₂Cl₂ (5.0 mL) was added solid DMAP (172 mg, 1.41 mmol) and EDCI (270 mg, 1.41 mmol). After stirring for 15 minutes, the crude **3.28** (azeotroped 3x with benzene) was added slowly as a solution in CH₂Cl₂ (7.6 mL). After 5 minutes, the cooling bath was removed and the reaction was allowed to warm to ambient temperature. After 4 hours, the reaction mixture was filtered directly through a plug of silica gel (10% EtOAc/hexanes). Purification via silica gel chromatography (2.5% EtOAc/hexanes) provided **3.29** (453 mg, 73% over 2 steps). ¹H NMR (500 MHz, CDCl₃) δ 5.86 (ddd, *J* = 17.2, 10.6, 8.1 Hz, 1H), 5.83 – 5.64 (m, 1H), 5.19 (t, *J* = 7.2 Hz, 1H), 5.07 – 4.99 (m, 4H), 4.97 (t, *J* = 6.2 Hz, 1H), 4.28 (dd, *J* = 7.3, 2.8 Hz, 1H), 3.84 (dd, *J* = 4.9, 3.5 Hz, 1H), 3.50 (t, *J* = 6.6 Hz, 2H), 3.04 – 3.01 (m, 1H), 2.80 – 2.73 (m, 2H), 2.70 (dd, *J* = 17.2, 2.9 Hz, 1H), 2.48 (t, *J* = 6.8 Hz, 2H), 2.39 (dd, *J* = 17.2, 7.4 Hz, 1H), 2.21 – 2.15 (m, 1H), 2.13 (s, 3H), 1.76 – 1.62 (m, 6H), 1.50 – 1.46 (m, 1H), 1.34 (d, *J* = 8.0 Hz, 2H), 1.24 (s, 4H), 1.10 (s, 3H), 1.04 (d, *J* = 7.0 Hz, 3H), 0.98 – 0.92

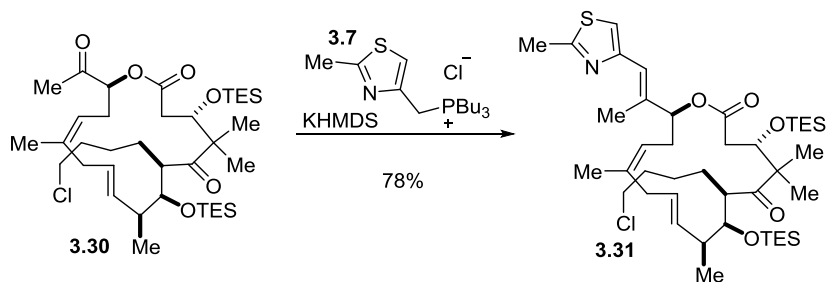
¹ Procedures for the synthesis of compounds **3.29** – **3.33** adapted from: Rivkin, A.; Yoshimura, F.; Gabarda, A. E.; Chou, T.-C.; Dong, H.; Tong, W. P.; Danishefsky, S. J. *J. Am. Chem. Soc.* **2003**, *125*, 2899-2901.

(m, 18H), 0.61 (q, $J = 8.2$ Hz, 12H); ^{13}C NMR (125 MHz, CDCl_3) δ 216.1, 205.3, 172.1, 140.3, 137.4, 135.4, 119.0, 115.8, 115.4, 78.8, 75.8, 74.7, 53.0, 51.8, 45.0, 44.4, 39.5, 36.5, 33.3, 29.2, 26.8, 26.6, 25.4, 24.0, 23.7, 20.4, 18.6, 7.3, 7.2, 5.6, 5.2; IR (film): 2955, 2877, 2911, 1731, 1693, 1638, 1458, 1416, 1379, 1295, 1238, 1161, 1092, 1003, 913, 728 cm^{-1} ; HRMS (FAB+) calcd $\text{C}_{39}\text{H}_{70}\text{ClO}_6\text{Si}_2$ $[\text{M}-\text{H}]^+$: 725.45, found 725.4413; $[\alpha]^{24}_{\text{D}} -24.5$ (c 0.84, CHCl_3).



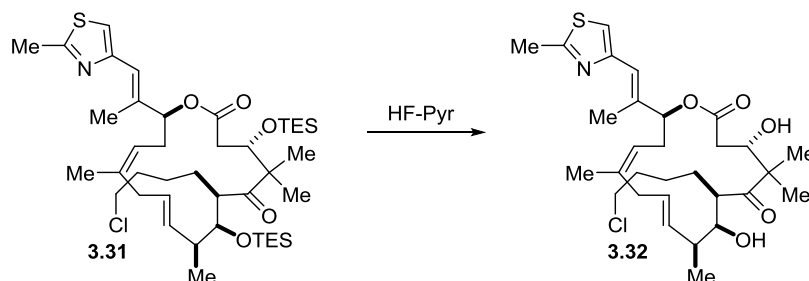
To a refluxing solution of **3.29** (93 mg, 0.128 mmol) in toluene (250 mL) was added a solution of Grubbs second generation catalyst (16 mg, 0.0192 mmol) in toluene (10 mL). After 30 minutes, the solution was cooled to 0°C and then filtered through a plug of silica gel (hexanes then CH_2Cl_2). The combined filtrate was concentrated then the residue purified via silica gel chromatography (7.5% EtOAc/hexanes) to provide **3.30** (60 mg, 66%) as a 10:1 mixture with an unidentified but related impurity. Further chromatography provided pure product for characterization. ^1H NMR (400 MHz, CDCl_3) δ 5.58 (dd, $J = 15.8, 8.1$ Hz, 1H), 5.34 (t, $J = 5.9$ Hz, 1H), 5.19 (t, $J = 8.0$ Hz, 1H), 4.96 (dd, $J = 9.2, 2.4$ Hz, 1H), 4.17 (dd, $J = 9.7, 2.5$ Hz, 1H), 4.10 (d, $J = 9.7$ Hz, 1H), 3.61 – 3.42 (m, 2H), 3.17 – 3.04 (m, 1H), 3.03 – 2.89 (m, 2H), 2.72 (dd, $J = 15.4, 2.6$ Hz, 1H), 2.62 – 2.52 (m, 1H), 2.52 – 2.43 (m, 1H), 2.38 (dd, $J = 14.5, 7.5$ Hz, 1H), 2.29 (p, $J = 7.1$ Hz, 1H), 2.21 (s, 3H), 1.78 – 1.67 (m, 3H), 1.66 (s, 3H), 1.54 – 1.38 (m, 2H), 1.27 – 1.19 (m, 1H), 1.17 (s, 3H), 1.11 (s, 3H), 1.05 (d, $J = 7.1$ Hz, 3H), 1.00 (t, $J = 7.9$ Hz, 9H), 0.91 (t, $J = 7.9$ Hz, 9H), 0.67 (q, $J = 7.9$ Hz, 6H), 0.57 (q, $J = 8.1$ Hz, 6H); ^{13}C NMR (125 MHz, CDCl_3) δ 213.9, 204.8, 171.4, 140.3, 132.6, 129.7, 118.6, 79.2, 77.0, 75.8, 54.0, 53.7, 44.8, 41.0, 40.3, 34.9, 33.1, 29.1, 28.3, 26.6, 23.8, 23.7, 23.6, 23.5, 21.4, 7.3, 7.1, 5.8, 5.4. IR (film): 2955, 2877,

2911, 1744, 1730, 1692, 1459, 1415, 1380, 1357, 1305, 1239, 1158, 1102, 1007, 855, 728 cm^{-1} ;
LRMS (FAB+) calcd $\text{C}_{37}\text{H}_{68}\text{ClO}_6\text{Si}_2$ $[\text{M}+\text{H}]^+$: 699.42, found 699.46; $[\alpha]^{22}_{\text{D}} -10.0$ (c 0.71, CHCl_3).



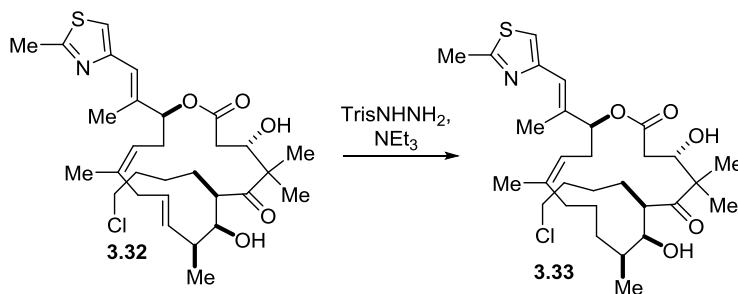
To a cooled (0°C) solution of Wittig reagent **3.7** (180 mg, 0.515 mmol) in THF (4.6 mL) was added KHMDS (1.03 mL, 0.515 mmol). The mixture was stirred for 30 minutes, then cooled to -78°C . To the solution was added **3.30** (60 mg, 0.0858 mmol) as a solution in THF (4.0 mL), and the resulting mixture allowed to warm to about -20°C over the course of 1.5 hour. The reaction was quenched with sat. aq. NH_4Cl (8 mL) and extracted with EtOAc (3 x 15 mL). The combined organic layers were dried over Na_2SO_4 and concentrated. The residue was purified via silica gel chromatography (4% EtOAc/hexanes) to afford **3.31** (53 mg, 78%) as a 14:1 mixture with the Z-isomer. Pure compound was obtained through further silica gel chromatography for characterization purposes. ^1H NMR (400 MHz, CDCl_3) δ 6.96 (s, 1H), 6.56 (s, 1H), 5.66 (dd, $J = 15.7, 8.1$ Hz, 1H), 5.40 – 5.28 (m, 2H), 5.22 (dd, $J = 10.0, 5.7$ Hz, 1H), 4.31 (dd, $J = 9.5, 1.8$ Hz, 1H), 4.11 (d, $J = 9.7$ Hz, 1H), 3.56 – 3.40 (m, 2H), 3.15 (dd, $J = 14.5, 6.8$ Hz, 1H), 3.00 (dt, $J = 9.6, 4.0$ Hz, 1H), 2.71 (s, 3H), 2.71 – 2.62 (m, 2H), 2.47 (dd, $J = 14.6, 2.1$ Hz, 1H), 2.41 (dd, $J = 14.6, 5.7$ Hz, 1H), 2.24 – 2.13 (m, 2H), 2.13 (d, $J = 1.3$ Hz, 3H), 1.90 – 1.78 (m, 1H), 1.75 – 1.61 (m, 5H), 1.54 – 1.37 (m, 2H), 1.22 – 1.12 (m, 1H), 1.11 (s, 3H), 1.07 (d, $J = 7.1$ Hz, 3H), 1.04 (s, 3H), 1.01 (t, $J = 7.9$ Hz, 9H), 0.88 (t, $J = 7.9$ Hz, 9H), 0.68 (q, $J = 8.0$ Hz, 6H), 0.56 (qd, $J = 8.3, 7.9, 1.7$ Hz, 6H); ^{13}C NMR (125 MHz, CDCl_3) δ 214.9, 170.7, 164.7, 152.7, 138.1, 138.1, 132.0, 129.6, 120.9, 120.4, 116.3, 79.3, 76.3, 74.8, 53.9, 53.8, 44.8, 41.2, 41.1, 35.4, 33.3, 33.2, 28.1,

24.5, 23.7, 23.5, 21.9, 21.7, 19.4, 15.1, 7.4, 7.1, 5.9, 5.5; IR (film): 2956, 2877, 2911, 1739, 1690, 1459, 1414, 1379, 1240, 1181, 1100, 1031, 1009, 971, 731 cm^{-1} ; LRMS (FAB+) calcd $\text{C}_{42}\text{H}_{73}\text{ClNO}_5\text{SSi}_2$ $[\text{M}+\text{H}]^+$: 794.44, found 794.5; $[\alpha]^{21}_{\text{D}} -11.5$ (c 0.66, CHCl_3).

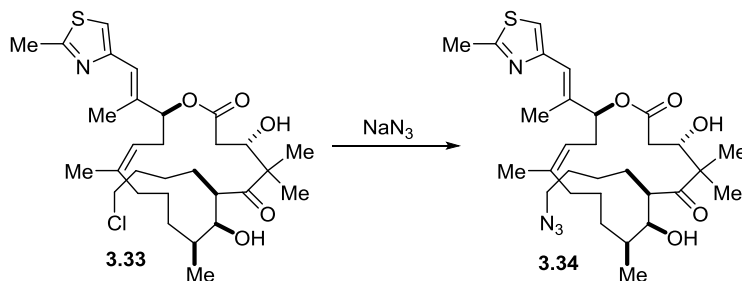


To a cooled (0°C) solution of **3.31** (42 mg, 0.0528 mmol) in THF (1.1 mL) in a plastic tube was added HF·pyridine (0.24 mL). After addition, the reaction was warmed to ambient temperature and stirred for 3 hours. The reaction was cooled to 0°C and TMSOMe (2.5 mL) was added dropwise. After the addition, the reaction was warmed to ambient temperature and stirred for 15 minutes. The reaction was concentrated and dried under high vacuum, then the residue purified by silica gel chromatography (10% EtOAc/DCM) to provide **3.32** (26 mg, 87%). ^1H NMR (400 MHz, CDCl_3) δ 6.97 (s, 1H), 6.54 (s, 1H), 5.58 (ddd, $J = 15.7, 7.6, 5.0$ Hz, 1H), 5.47 (dd, $J = 15.7, 7.3$ Hz, 1H), 5.33 (dd, $J = 9.0, 2.9$ Hz, 1H), 5.12 (dd, $J = 9.2, 5.3$ Hz, 1H), 4.29 (dt, $J = 8.2, 3.6$ Hz, 1H), 3.77 – 3.67 (m, 1H), 3.51 (td, $J = 6.6, 4.1$ Hz, 2H), 3.36 – 3.24 (m, 1H), 3.21 (d, $J = 4.8$ Hz, 1H), 2.94 (dd, $J = 14.8, 7.6$ Hz, 1H), 2.70 (s, 3H), 2.68 – 2.56 (m, 2H), 2.53 (dd, $J = 20.7, 4.1$ Hz, 1H), 2.48 – 2.40 (m, 2H), 2.42 – 2.30 (m, 2H), 2.08 (s, 2H), 1.95 – 1.85 (m, 1H), 1.80 – 1.67 (m, 5H), 1.55 – 1.37 (m, 1H), 1.39 – 1.26 (m, 6H), 1.09 (d, $J = 6.9$ Hz, 3H), 1.01 (s, 3H); ^{13}C NMR (125 MHz, CDCl_3) δ 217.3, 170.8, 165.1, 152.3, 138.0, 137.8, 131.3, 129.9, 120.5, 119.7, 116.2, 78.4, 75.5, 72.7, 53.0, 51.1, 44.8, 39.3, 39.2, 35.3, 32.9, 32.3, 28.0, 24.6, 23.9, 21.6, 20.6, 19.4, 19.3, 15.9; IR (film): 3460, 2964, 2930, 2871, 1730, 1687, 1506, 1446, 1377, 1293, 1252,

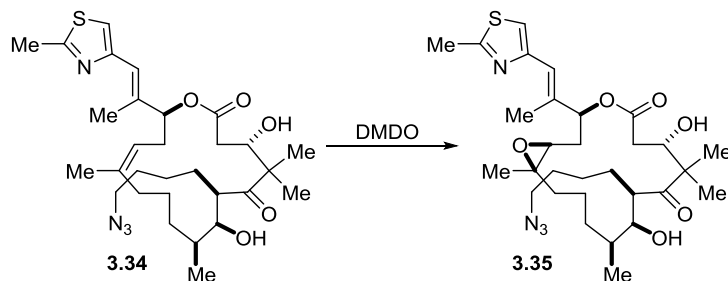
1187, 1155, 1044, 977, 755 cm^{-1} ; LRMS (FAB+) calcd $\text{C}_{30}\text{H}_{45}\text{ClNO}_5\text{S}$ $[\text{M}+\text{H}]^+$: 566.26, found 566.32; $[\alpha]^{22}_{\text{D}} -82.4$ (c 0.75, CHCl_3).



To a solution of **3.32** (26 mg, 0.0459 mmol) and TrisNHNH_2 (548 mg, 1.84 mmol) in $\text{ClCH}_2\text{CH}_2\text{Cl}$ (13 mL) at 50°C (external temp, oil bath) was added NEt_3 (0.26 mL, 1.84 mmol). After 8 hours, the reaction was cooled to ambient temperature and diluted with EtOAc, then filtered through a plug of silica gel. The filtrate was concentrated, then the residue purified via silica gel chromatography (30% EtOAc/hexanes) to provide **3.33** (25 mg, 96%). ^1H NMR (500 MHz, CDCl_3) δ 6.95 (s, 1H), 6.56 (s, 1H), 5.23 (dd, $J = 10.3, 2.1$ Hz, 1H), 5.12 (dd, $J = 10.0, 4.6$ Hz, 1H), 4.25 (d, $J = 10.6$ Hz, 1H), 3.77 – 3.68 (m, 1H), 3.58 – 3.42 (m, 3H), 3.29 (dt, $J = 7.9, 4.1$ Hz, 1H), 2.70 (s, 3H), 2.68 – 2.60 (m, 1H), 2.57 (d, $J = 3.7$ Hz, 1H), 2.48 (dd, $J = 14.8, 10.4$ Hz, 1H), 2.39 (dd, $J = 14.8, 2.8$ Hz, 1H), 2.33 – 2.27 (m, 1H), 2.27 – 2.21 (m, 1H), 2.07 (s, 3H), 1.91 – 1.70 (m, 6H), 1.69 (s, 3H), 1.66 – 1.56 (m, 1H), 1.48 – 1.37 (m, 3H), 1.33 (s, 3H), 1.29 – 1.21 (m, 2H), 1.08 (s, 3H), 1.04 (d, $J = 7.0$ Hz, 3H); ^{13}C NMR (125 MHz, CDCl_3) δ 219.2, 170.7, 165.2, 152.2, 139.6, 139.2, 120.4, 119.5, 115.9, 79.4, 74.4, 72.6, 53.5, 48.9, 44.8, 39.6, 36.2, 33.0, 32.8, 32.3, 30.7, 27.0, 25.1, 25.0, 23.8, 22.1, 19.7, 19.3, 17.1, 15.9; IR (film): 3474, 2960, 2932, 2871, 1731, 1686, 1507, 1464, 1446, 1377, 1337, 1291, 1252, 1187, 1151, 1072, 1029, 981, 755 cm^{-1} ; LRMS (FAB+) calcd $\text{C}_{30}\text{H}_{47}\text{ClNO}_5\text{S}$ $[\text{M}+\text{H}]^+$: 568.28, found 568.34; $[\alpha]^{23}_{\text{D}} -55.0$ (c 0.70, CHCl_3).

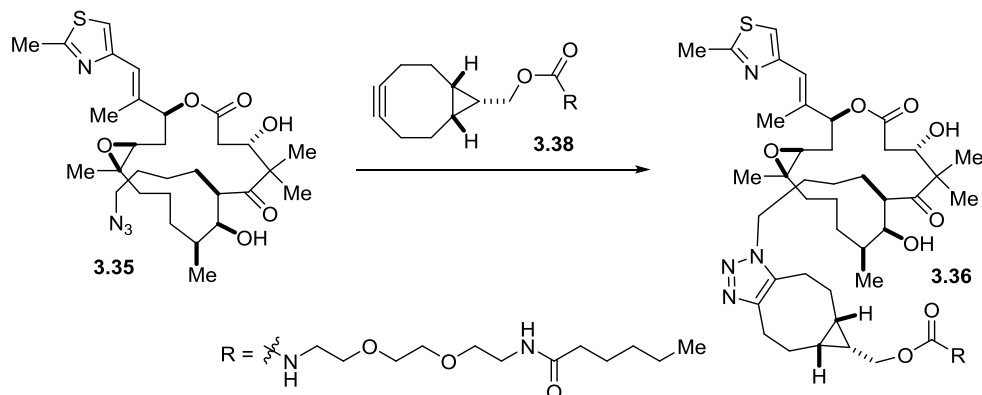


To a solution of **3.33** (25 mg, 0.044 mmol) in DMF (0.5 mL) was added NaN_3 (3.4 mg, 0.0523 mmol). The reaction was heated to 60°C (external temp, oil bath) and stirred overnight. After 24 hours, the reaction was cooled to ambient temperature, then diluted with EtOAc and deionized water. The layers were separated and the aqueous layer extracted with EtOAc (3 x 5 mL). The combined organic layers were dried over Na_2SO_4 and concentrated. The residue was purified via silica gel chromatography to provide **3.34** (25 mg, 99%). ^1H NMR (400 MHz, CDCl_3) δ 6.95 (s, 1H), 6.56 (s, 0H), 5.22 (d, $J = 9.8$ Hz, 1H), 5.11 (dd, $J = 10.0, 4.8$ Hz, 1H), 4.31 – 4.23 (m, 1H), 3.75 – 3.65 (m, 2H), 3.59 (d, $J = 5.6$ Hz, 1H), 3.32 – 3.23 (m, 3H), 2.69 (s, 3H), 2.67 – 2.61 (m, 1H), 2.62 – 2.56 (m, 2H), 2.48 (dd, $J = 14.8, 10.4$ Hz, 1H), 2.38 (dd, $J = 14.8, 2.9$ Hz, 1H), 2.33 – 2.26 (m, 1H), 2.28 – 2.18 (m, 2H), 2.06 (d, $J = 1.3$ Hz, 3H), 1.88 – 1.71 (m, 4H), 1.69 (s, 2H), 1.67 – 1.59 (m, 3H), 1.58 – 1.51 (m, 1H), 1.37 – 1.28 (m, 6H), 1.07 (s, 3H), 1.04 (d, $J = 7.0$ Hz, 3H); ^{13}C NMR (125 MHz, CDCl_3) δ 219.1, 170.7, 165.1, 152.2, 139.6, 139.2, 120.4, 119.5, 115.9, 79.3, 74.4, 72.5, 53.4, 51.3, 48.9, 39.6, 36.2, 32.8, 32.3, 30.7, 29.5, 27.3, 25.0, 23.7, 22.0, 19.7, 19.2, 17.1, 15.9; IR (film): 3464, 2955, 2927, 2854, 2096, 1733, 1685, 1463, 1378, 1289, 1261, 1184, 1148, 1075, 1029, 803 cm^{-1} ; LRMS (FAB+) calcd $\text{C}_{30}\text{H}_{47}\text{N}_4\text{O}_5\text{S}$ $[\text{M}+\text{H}]^+$: 575.32, found 575.40; $[\alpha]^{21}_{\text{D}} -51.0$ (c 0.68, CHCl_3).



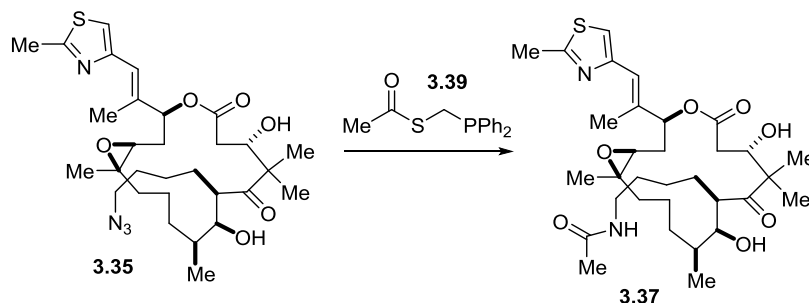
To a cooled (-78°C) solution of **3.34** (25 mg, 0.0433 mmol) in CH_2Cl_2 (2.2 mL) was added a cooled (-78°C) solution of DMDO (1.5 mL, 0.130 mmol, 0.086 M in acetone) via cannula. After the addition was complete, the solution was warmed to -50°C and stirred for 2 hours. Additional DMDO solution was added since there was starting material remaining. After another 2 hours the reaction seemed to have stalled, so dimethyl sulfide was added to quench any remaining DMDO, then the solution concentrated. The residue was purified via silica gel chromatography (pH 7 buffered silica gel, 40% EtOAc/hexanes) to provide **3.35** (14.5 mg, 59%).² ^1H NMR (400 MHz, CDCl_3) δ 6.97 (s, 1H), 6.55 (s, 1H), 5.46 (t, $J = 5.0$ Hz, 1H), 4.61 (d, $J = 5.7$ Hz, 1H), 4.27 (ddd, $J = 10.2, 5.5, 2.5$ Hz, 1H), 3.63 (q, $J = 5.3$ Hz, 1H), 3.44 (dt, $J = 8.3, 3.9$ Hz, 1H), 3.26 (td, $J = 6.7, 4.1$ Hz, 2H), 2.87 (d, $J = 5.8$ Hz, 1H), 2.80 (t, $J = 6.2$ Hz, 1H), 2.70 (s, 3H), 2.56 (dd, $J = 14.3, 10.3$ Hz, 1H), 2.41 (dd, $J = 14.3, 2.6$ Hz, 1H), 2.10 (d, $J = 1.3$ Hz, 3H), 2.02 (t, $J = 5.7$ Hz, 2H), 1.92 – 1.77 (m, 1H), 1.78 – 1.69 (m, 2H), 1.64 – 1.50 (m, 4H), 1.53 – 1.41 (m, 1H), 1.37 (s, 3H), 1.33 – 1.22 (m, 9H), 1.03 (s, 3H), 0.99 (d, $J = 6.9$ Hz, 3H); ^{13}C NMR (125 MHz, CDCl_3) δ 220.0, 170.7, 165.2, 152.1, 137.0, 119.4, 116.4, 76.7, 75.5, 73.5, 61.4, 61.0, 53.2, 51.3, 50.4, 39.0, 34.8, 32.2, 31.7, 30.1, 29.4, 28.3, 25.2, 22.3, 21.2, 21.1, 20.5, 19.3, 17.5, 16.2; IR (film): 3446, 2960, 2926, 2859, 2095, 1735, 1685, 1504, 1463, 1379, 1345, 1289, 1259, 1183, 1144, 1050, 1025, 978, 803, 735 cm^{-1} ; LRMS (FAB+) calcd $\text{C}_{30}\text{H}_{47}\text{N}_4\text{O}_6\text{S}$ $[\text{M}+\text{H}]^+$: 591.31, found 591.45; $[\alpha]^{23}_{\text{D}} -71.6$ (c 0.53, CHCl_3).

² Synthesis adapted from: Stachel, S. J.; Danishefsky, S. J. *Tetrahedron Lett.* **2001**, 42, 6785-6787.



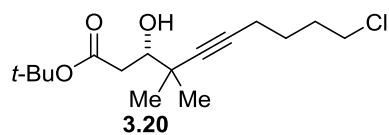
To **3.35** (2.4 mg, 0.00406 mmol) was added **3.38** (1.7 mg, 0.00406 mmol) as a solution in a 1:2 mixture of $\text{CD}_3\text{CN}:\text{D}_2\text{O}$ (0.5 mL). This was left to stir overnight at ambient temperature, then the next day loaded directly onto a plug of silica gel and filtered (EtOAc then acetone). The filtrate was concentrated, then the residue purified via silica gel chromatography (4% MeOH/ CH_2Cl_2) to provide **3.36** (4.0 mg, 97%). ^1H NMR (500 MHz, CDCl_3) δ 6.97 (s, 1H), 6.56 (s, 1H), 5.95 (s, 1H), 5.46 (dd, $J = 6.5, 3.5$ Hz, 1H), 5.18 (s, 1H), 4.42 (s, 1H), 4.28 – 4.18 (m, 3H), 4.16 (d, $J = 8.0$ Hz, 2H), 3.69 – 3.54 (m, 9H), 3.46 (q, $J = 5.3$ Hz, 2H), 3.43 – 3.33 (m, 5H), 3.17 – 3.05 (m, 3H), 2.93 – 2.83 (m, 2H), 2.81 (t, $J = 6.2$ Hz, 1H), 2.70 (s, 3H), 2.69 – 2.61 (m, 1H), 2.55 (dd, $J = 14.3, 10.1$ Hz, 1H), 2.41 (dd, $J = 14.4, 2.9$ Hz, 1H), 2.27 – 2.19 (m, 1H), 2.17 (t, $J = 7.6$ Hz, 2H), 2.10 (d, $J = 1.2$ Hz, 3H), 2.06 – 1.97 (m, 2H), 1.96 – 1.84 (m, 1H), 1.85 – 1.75 (m, 1H), 1.79 – 1.69 (m, 1H), 1.68 – 1.61 (m, 2H), 1.60 – 1.47 (m, 6H), 1.47 – 1.35 (m, 1H), 1.37 – 1.28 (m, 7H), 1.27 (s, 4H), 1.26 – 1.15 (m, 3H), 1.03 – 0.97 (m, 5H), 0.89 (t, $J = 6.9$ Hz, 4H); ^{13}C NMR (125 MHz, CDCl_3) δ 219.5, 170.7, 165.2, 156.8, 152.1, 145.0, 144.9, 137.0, 132.8, 119.6, 116.4, 76.7, 75.0, 73.5, 70.4, 70.4, 70.2, 70.2, 62.8, 61.4, 61.2, 53.1, 53.1, 50.3, 47.4, 41.0, 39.3, 39.1, 36.9, 35.0, 32.1, 31.9, 31.6, 30.3, 29.9, 27.7, 26.1, 25.6, 24.0, 23.2, 22.8, 22.6, 22.5, 22.3, 21.6, 21.1, 20.5, 20.2, 19.6, 19.3, 17.9, 17.7, 16.1, 14.1; IR (film): 3341, 2956, 2930, 2869, 1713, 1696, 1649, 1549, 1535,

1466, 1379, 1253, 1143, 1100, 1048, 1024, 753 cm^{-1} ; LRMS (FAB+) calcd $\text{C}_{53}\text{H}_{85}\text{N}_6\text{O}_{11}\text{S}$ $[\text{M}+\text{H}]^+$: 1013.59, found 1013.79; $[\alpha]^{22}_{\text{D}} -31.9$ (c 0.44, CHCl_3).

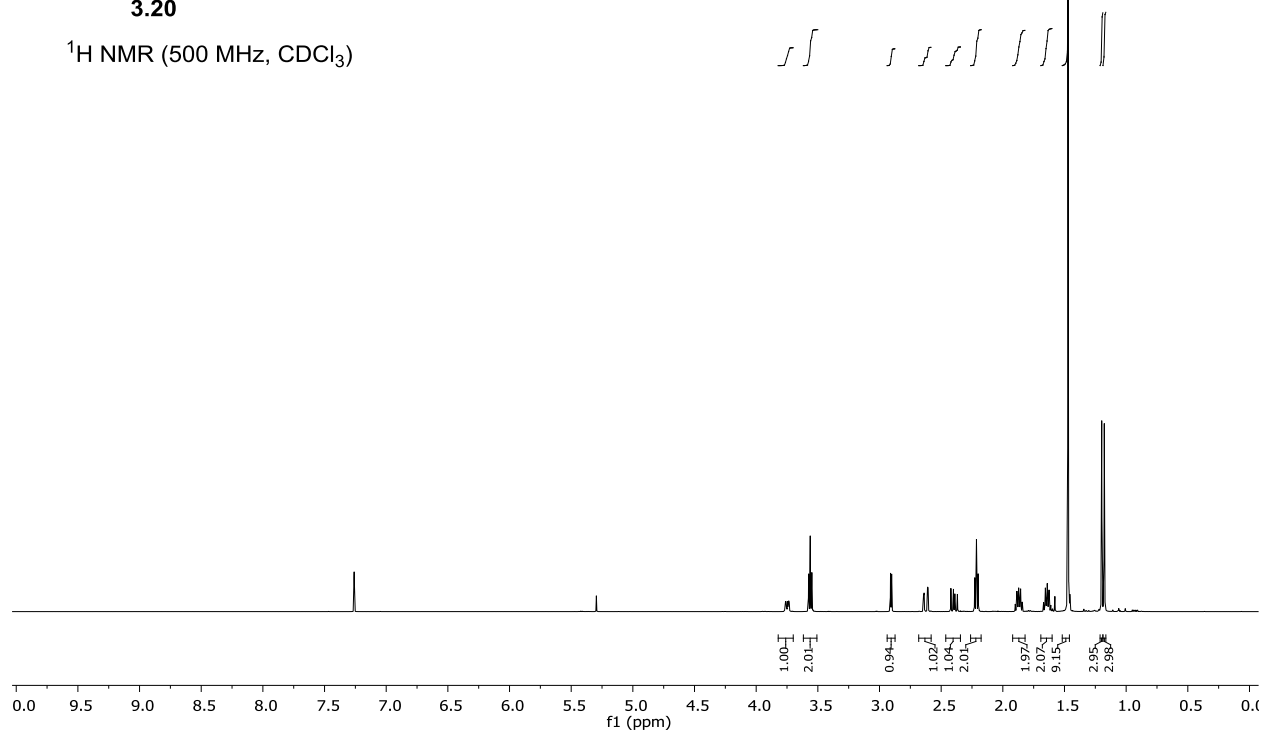


To **3.35** (5.6 mg, 0.00948 mmol) was added phosphinothioester **3.39** (75 mg, 0.260 mmol) as a solution in 1:1 THF: D_2O (2 mL). The reaction was allowed to stir overnight at ambient temperature. Most of the starting material transformed into an unidentified side product, but a small amount of **3.37** (0.7 mg, 11% yield) was isolated from silica gel chromatography (5% MeOH/ CH_2Cl_2). ^1H NMR (400 MHz, CHCl_3) δ 6.97 (s, 1H), 6.56 (s, 1H), 5.53 – 5.39 (m, 2H), 4.51 (d, J = 5.9 Hz, 1H), 4.29 – 4.19 (m, 1H), 3.72 – 3.60 (m, 1H), 3.42 (dt, J = 8.3, 4.3 Hz, 1H), 3.33 – 3.12 (m, 2H), 3.01 (d, J = 5.7 Hz, 1H), 2.81 (t, J = 6.2 Hz, 1H), 2.70 (s, 3H), 2.56 (dd, J = 14.4, 10.1 Hz, 1H), 2.42 (dd, J = 14.4, 2.9 Hz, 1H), 2.10 (d, J = 1.3 Hz, 3H), 2.06 – 1.97 (m, 1H), 1.97 (s, 3H), 1.94 – 1.79 (m, 1H), 1.74 – 1.63 (m, 1H), 1.54 – 1.37 (m, 10H), 1.35 (s, 3H), 1.31 – 1.17 (m, 8H), 1.03 (s, 3H), 0.99 (d, J = 6.8 Hz, 3H); LRMS (APCI+) calcd $\text{C}_{32}\text{H}_{51}\text{N}_2\text{O}_7\text{S}$ $[\text{M}+\text{H}]^+$: 607.33, found 606.86.

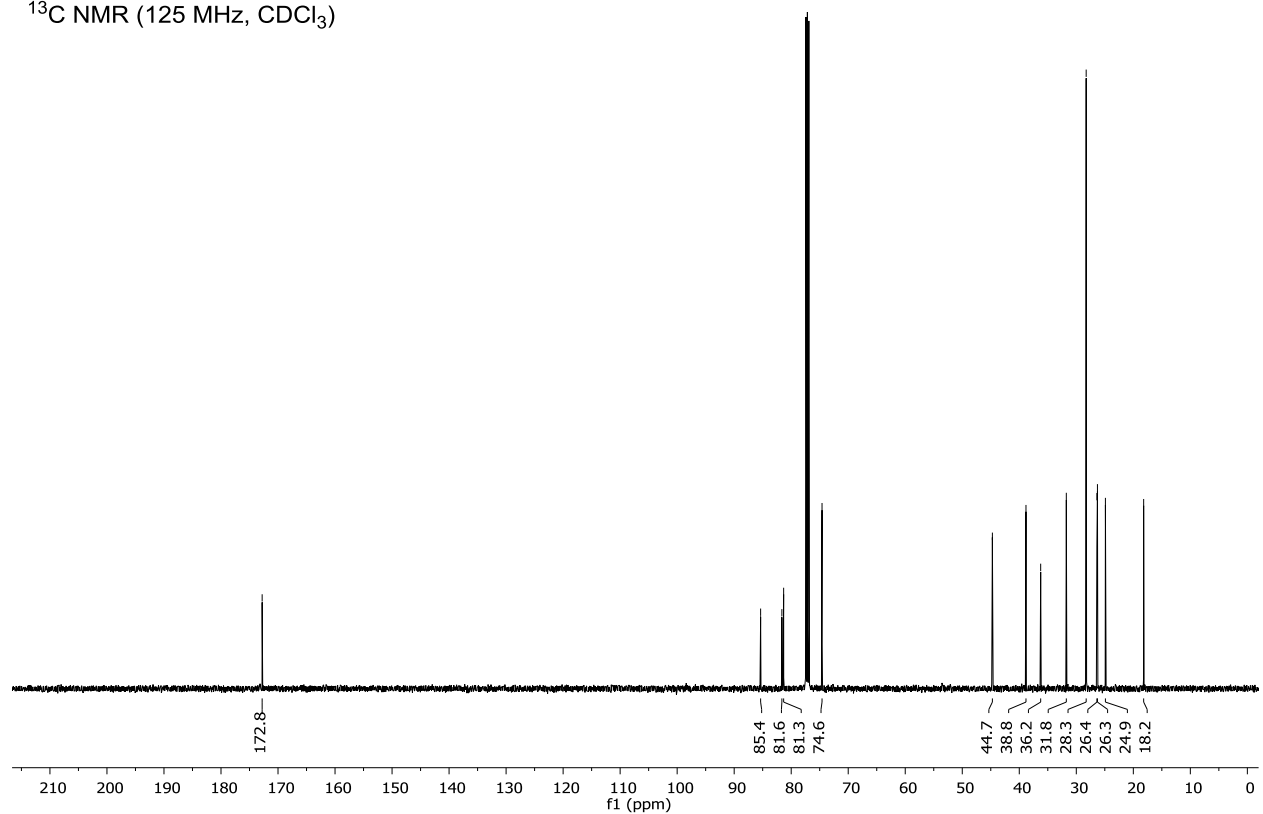
3.7 ^1H and ^{13}C NMR Spectra

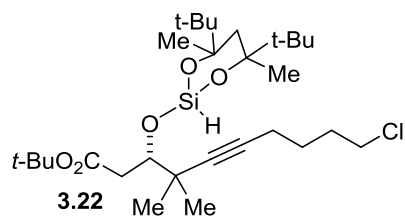


^1H NMR (500 MHz, CDCl_3)



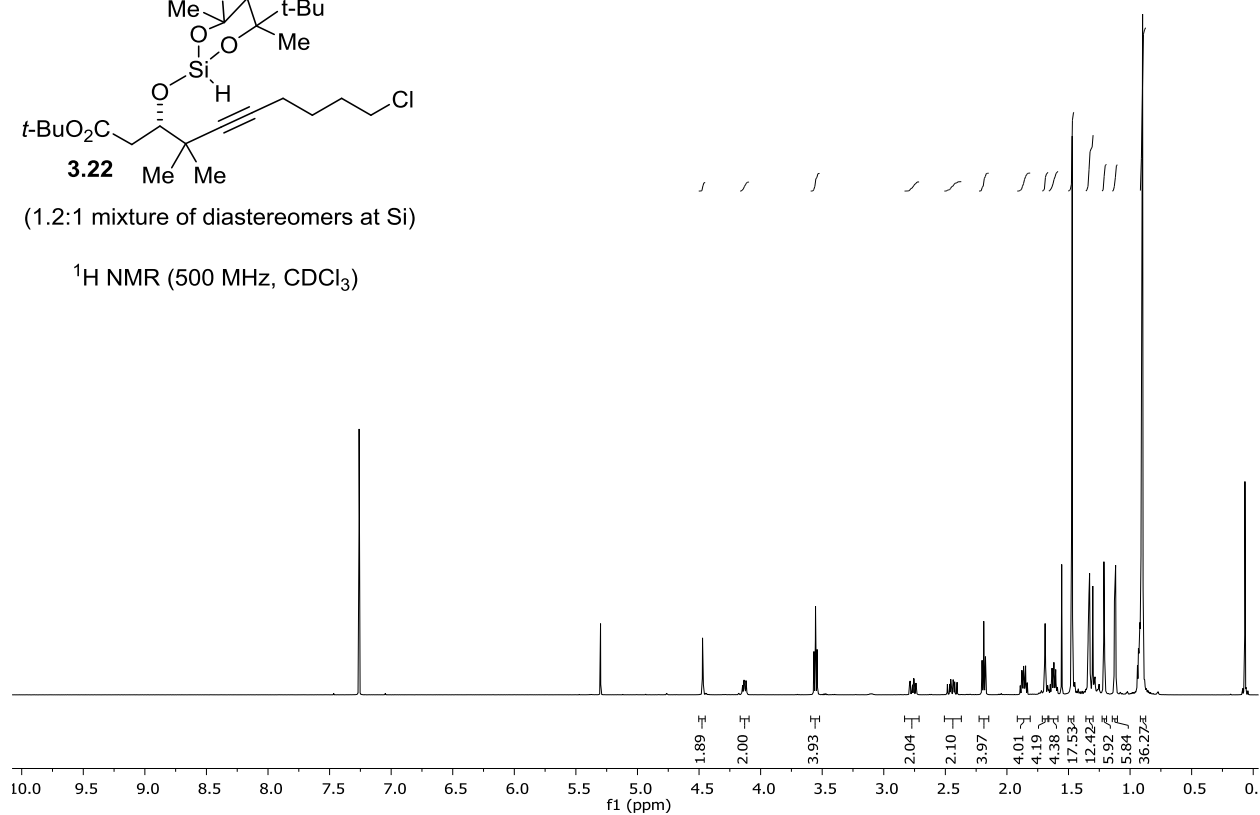
^{13}C NMR (125 MHz, CDCl_3)



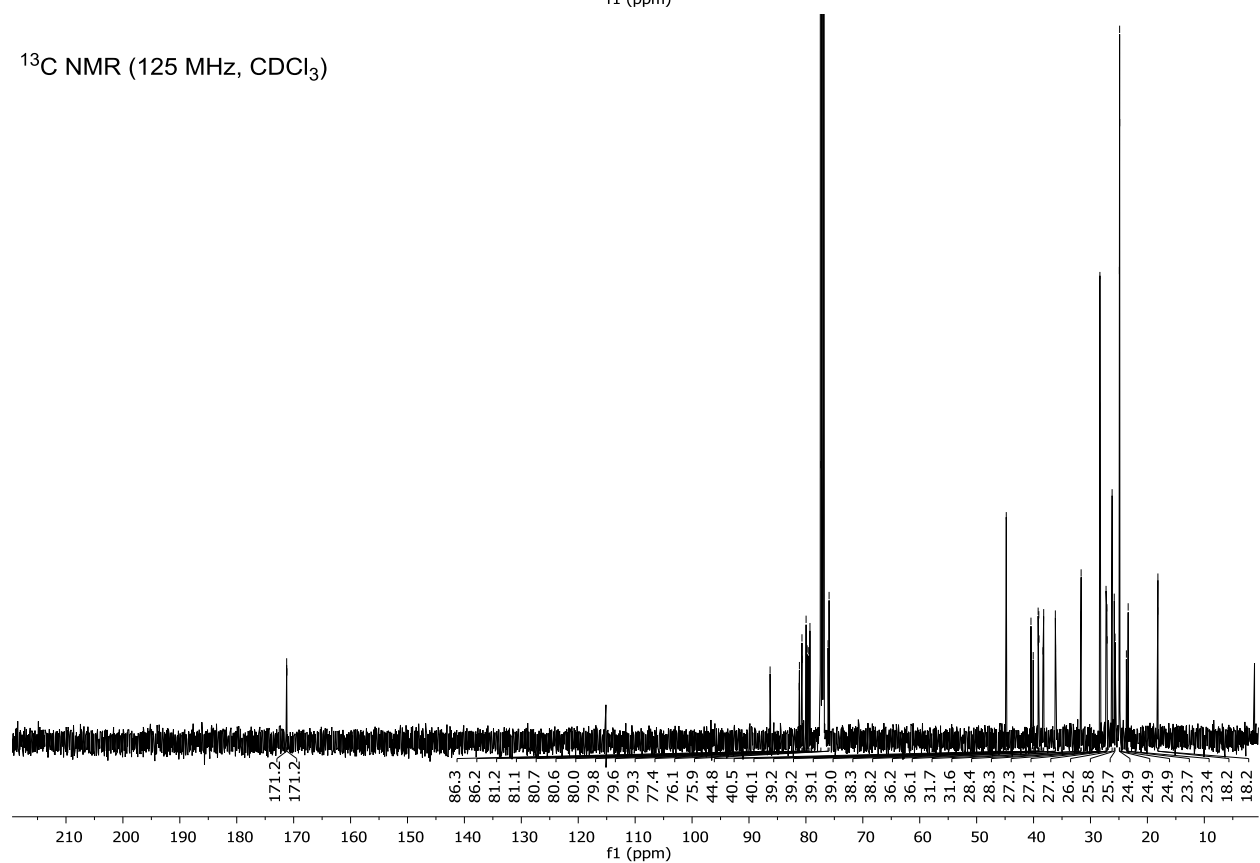


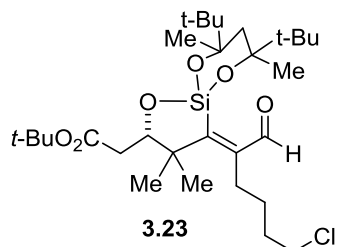
(1.2:1 mixture of diastereomers at Si)

^1H NMR (500 MHz, CDCl_3)



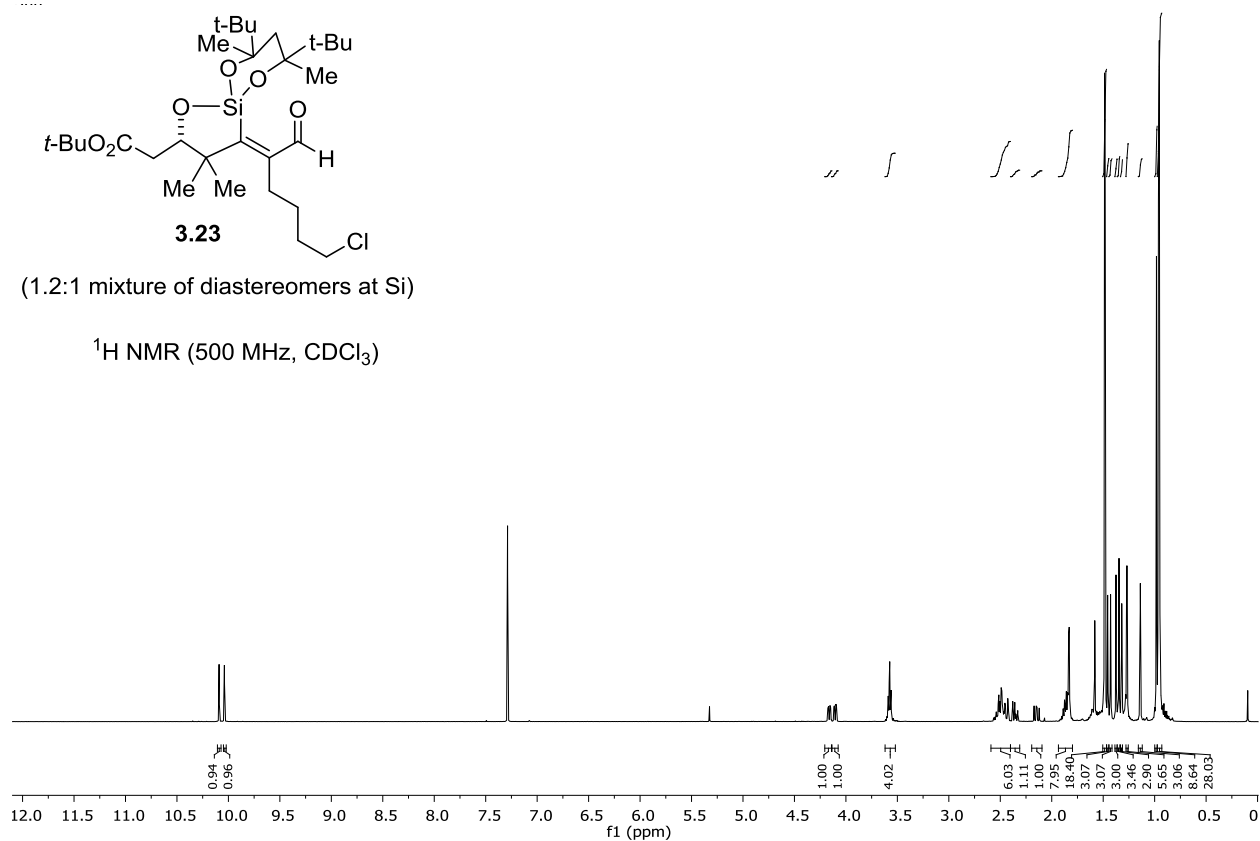
^{13}C NMR (125 MHz, CDCl_3)



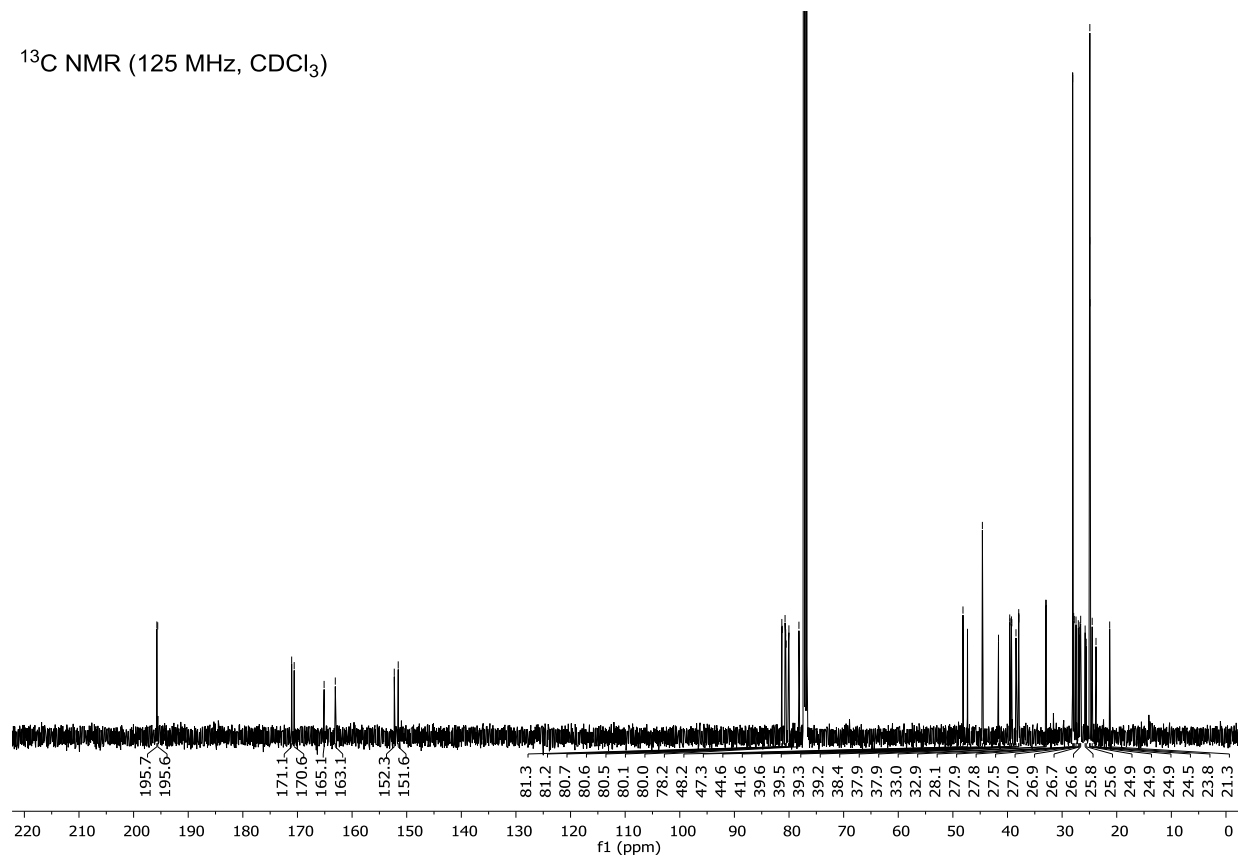


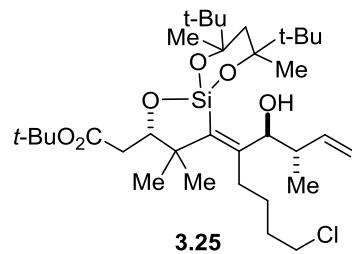
(1.2:1 mixture of diastereomers at Si)

^1H NMR (500 MHz, CDCl_3)



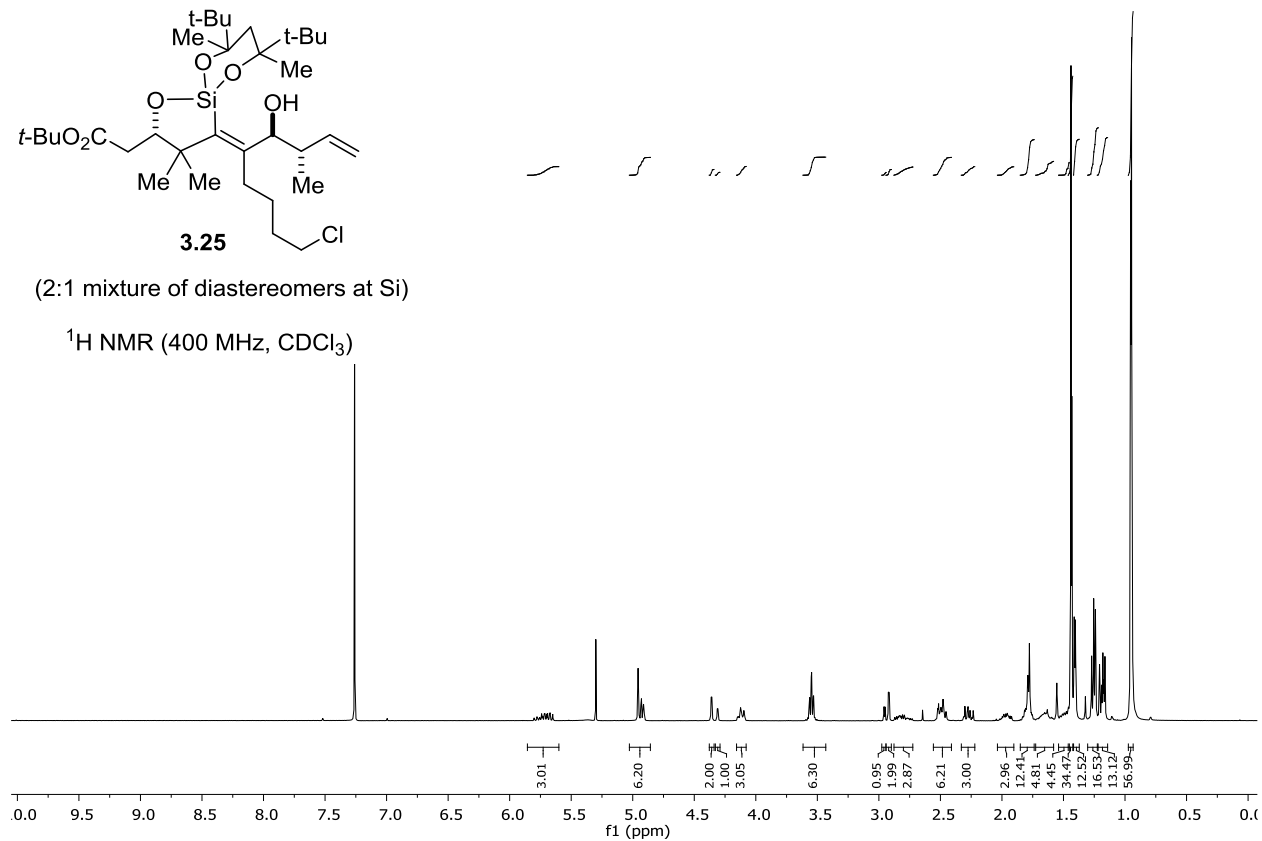
^{13}C NMR (125 MHz, CDCl_3)



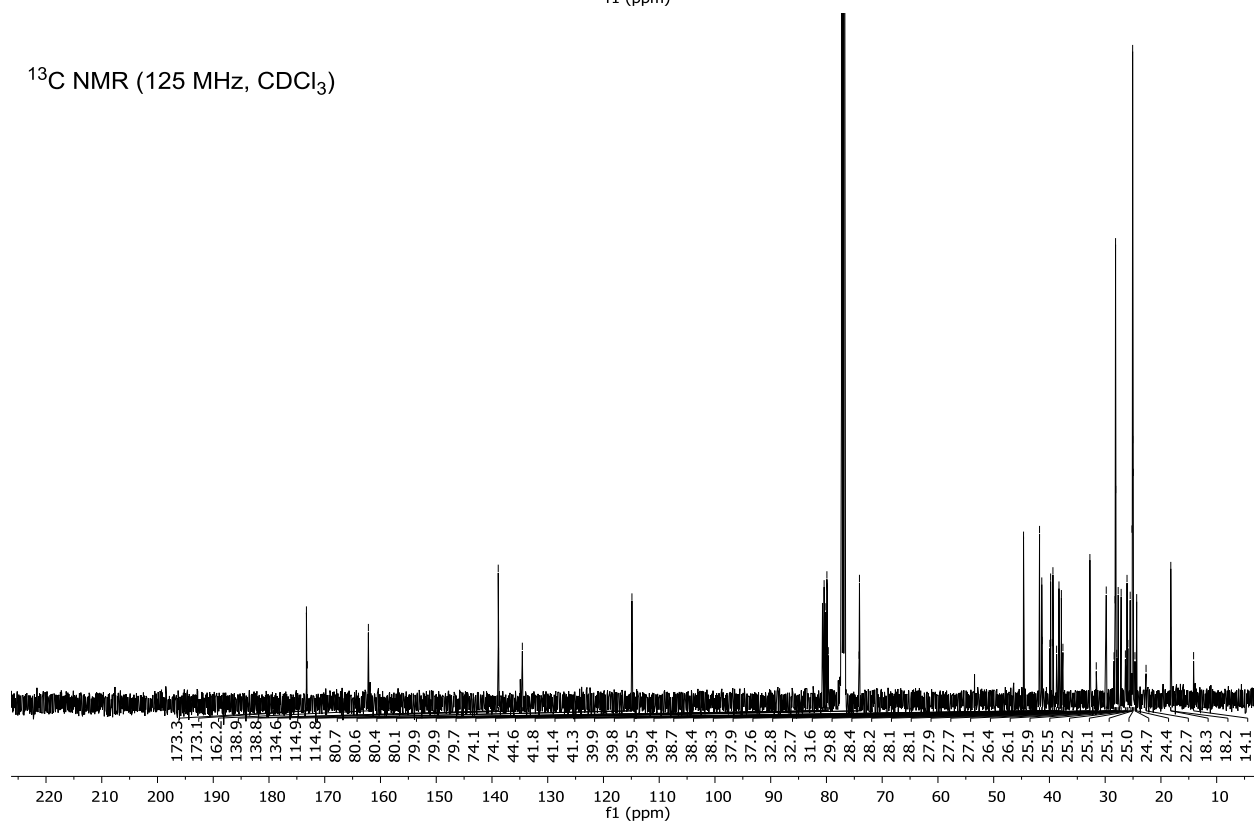


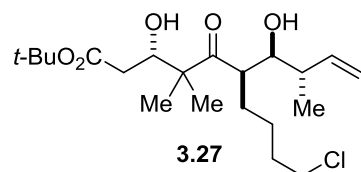
(2:1 mixture of diastereomers at Si)

^1H NMR (400 MHz, CDCl_3)

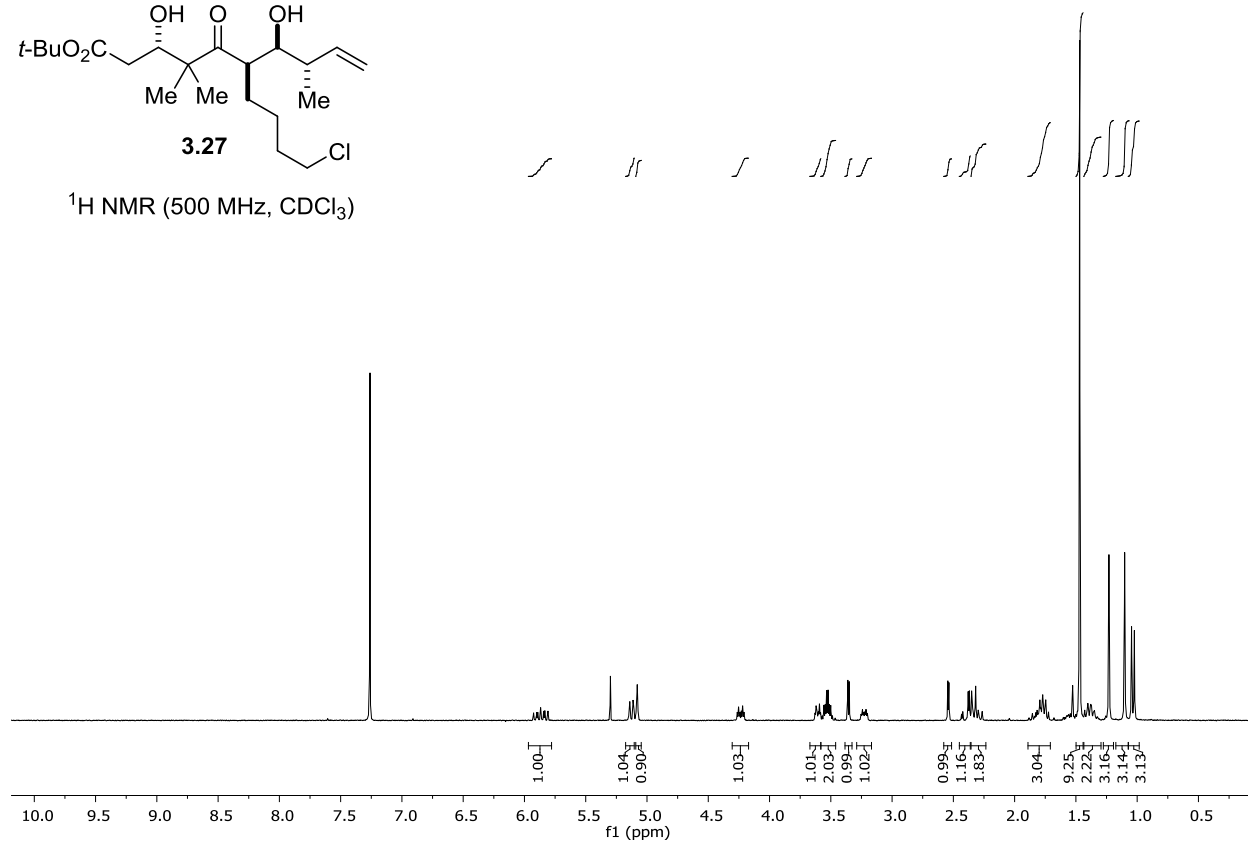


^{13}C NMR (125 MHz, CDCl_3)

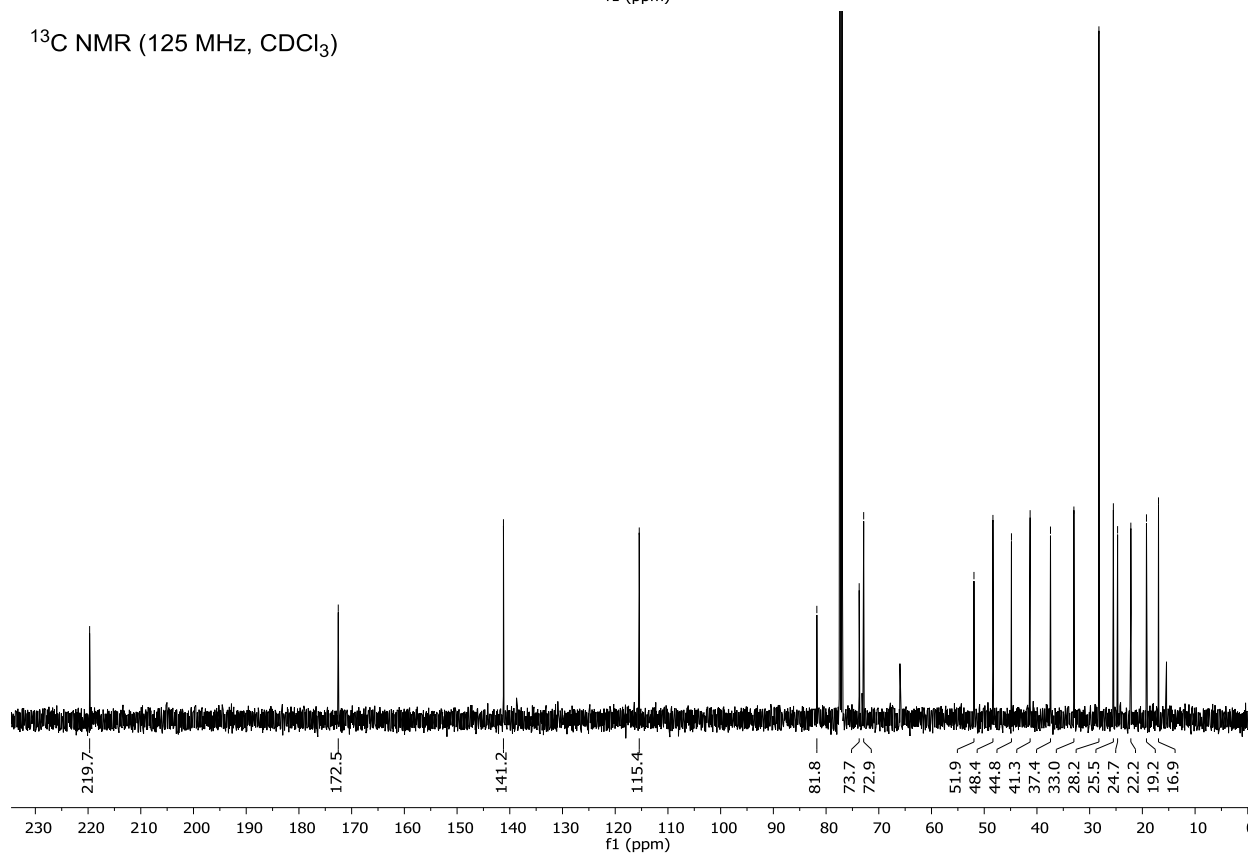


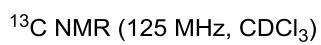
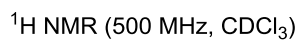


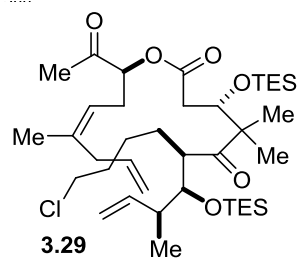
^1H NMR (500 MHz, CDCl_3)



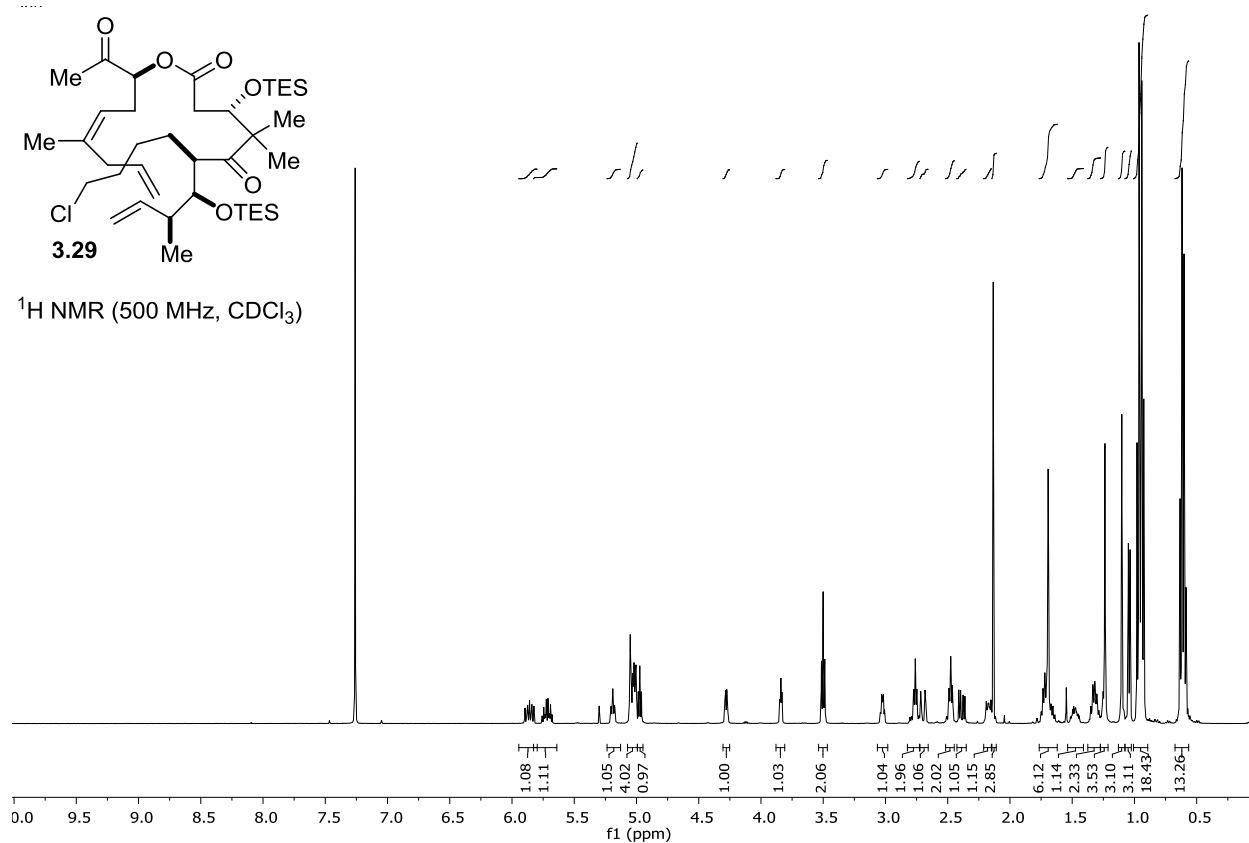
^{13}C NMR (125 MHz, CDCl_3)



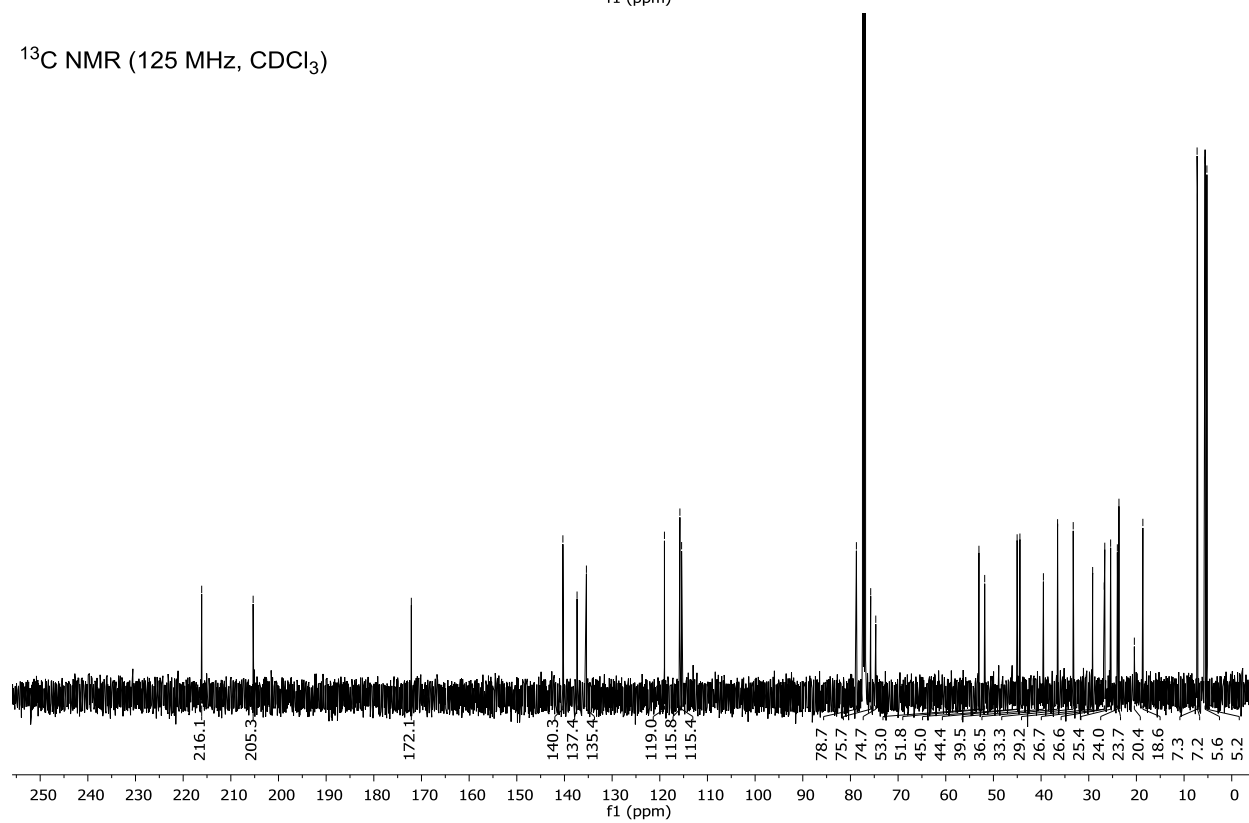


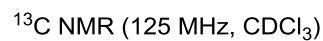
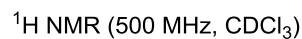


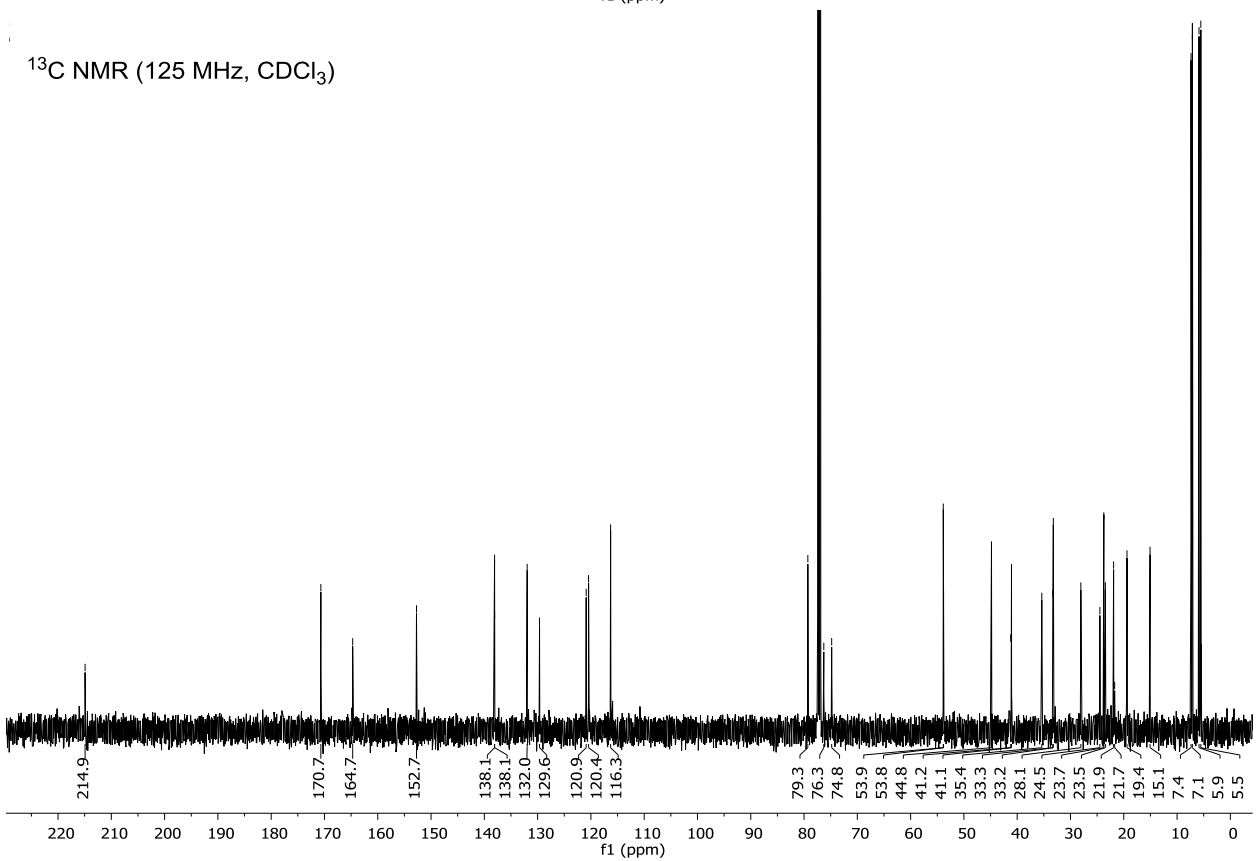
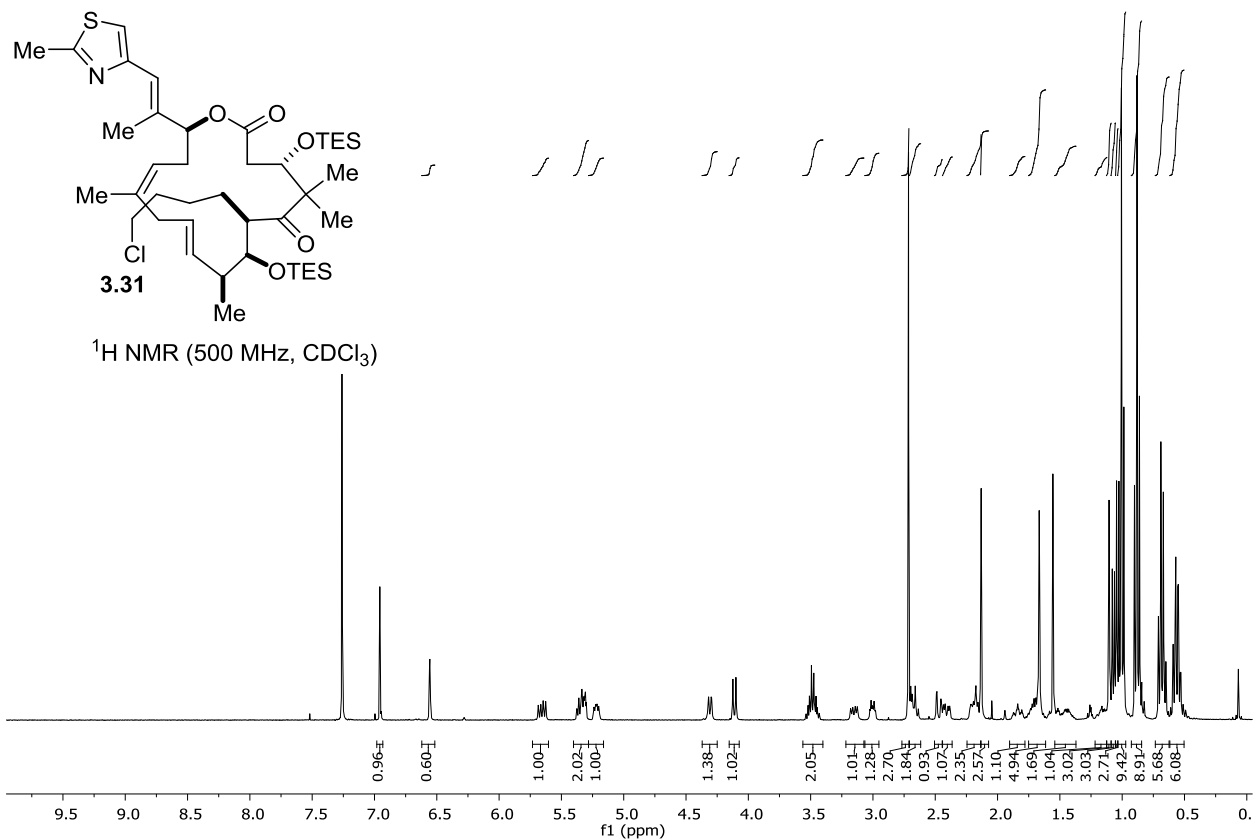
^1H NMR (500 MHz, CDCl_3)

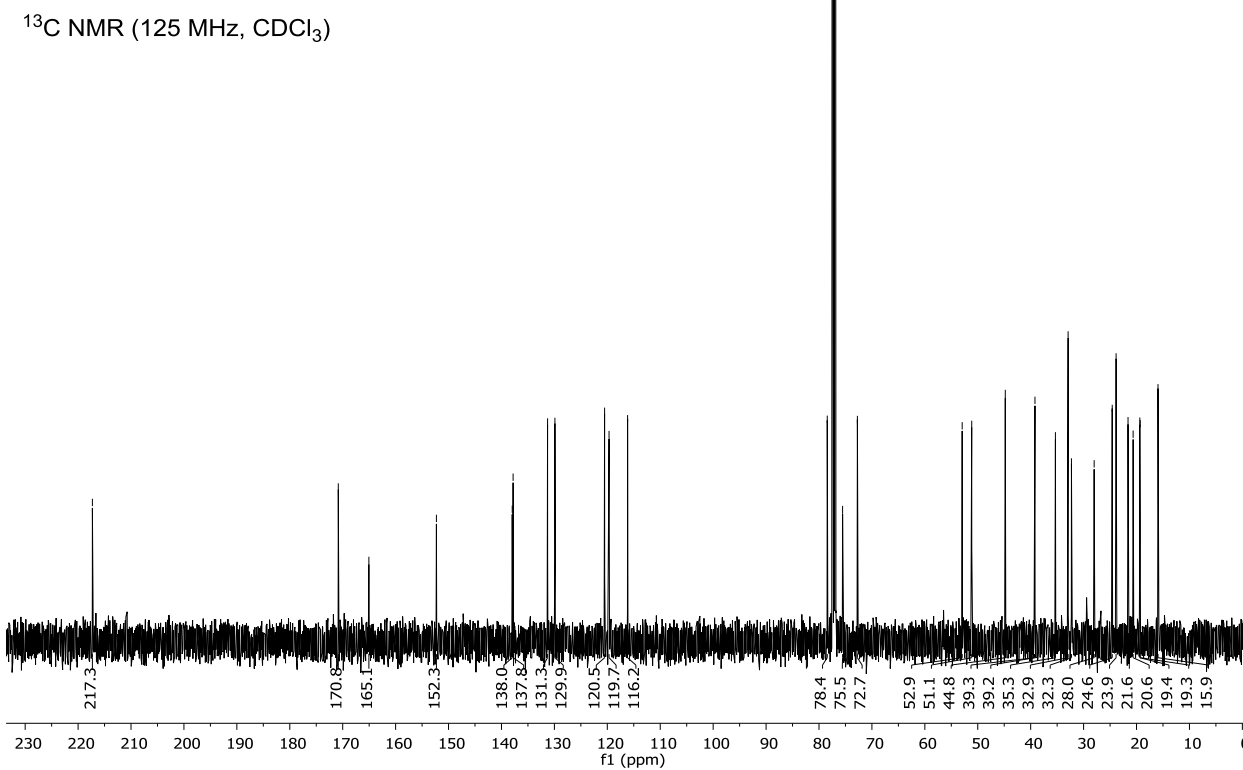
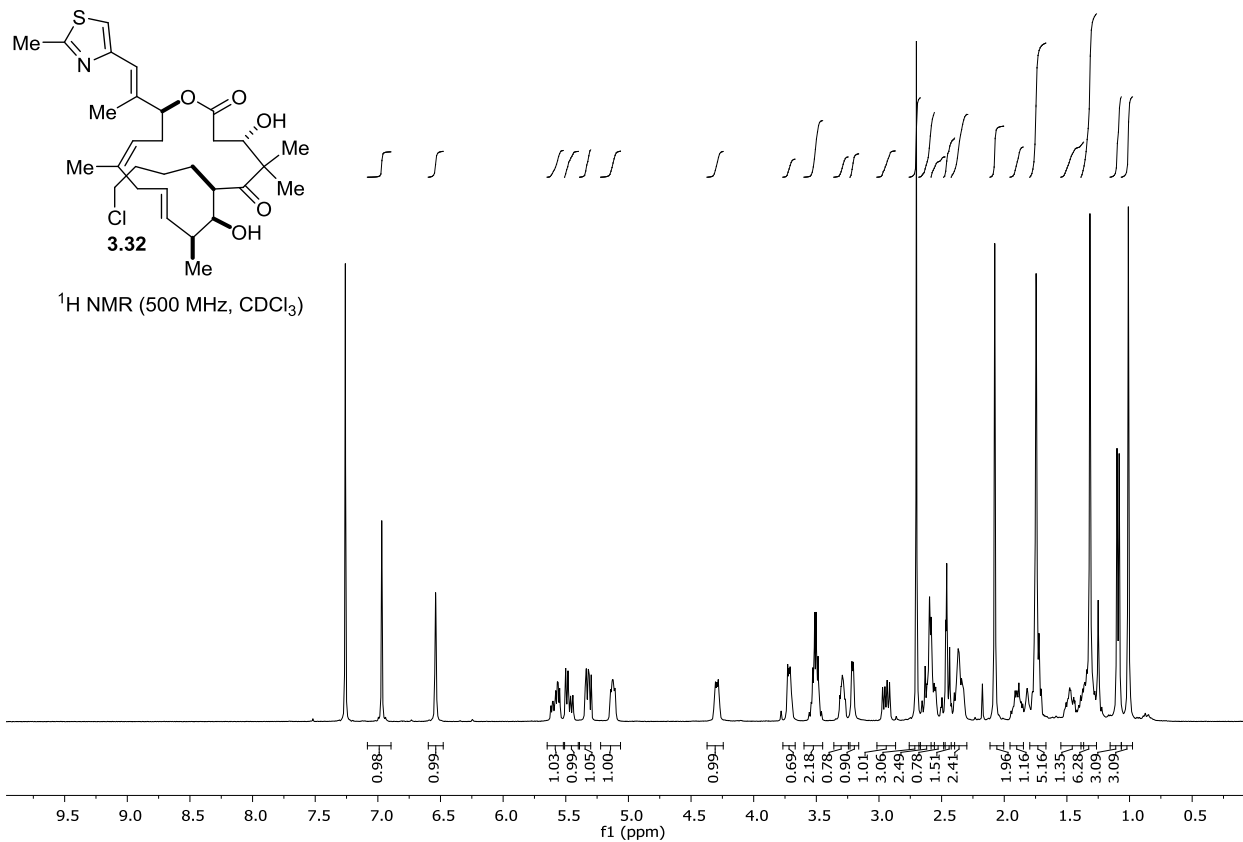


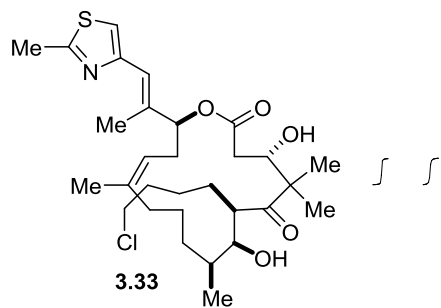
^{13}C NMR (125 MHz, CDCl_3)



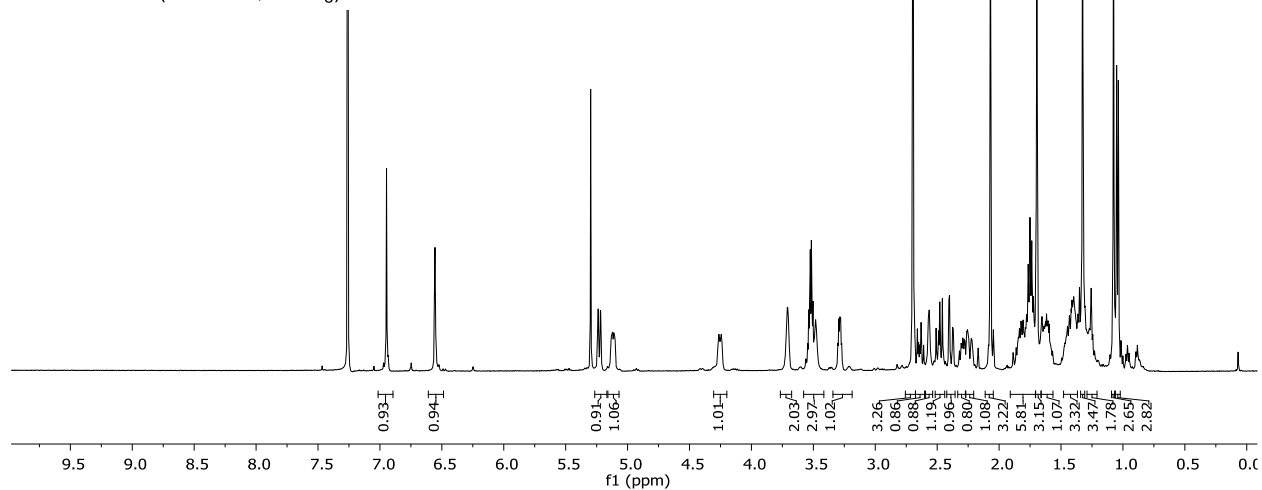




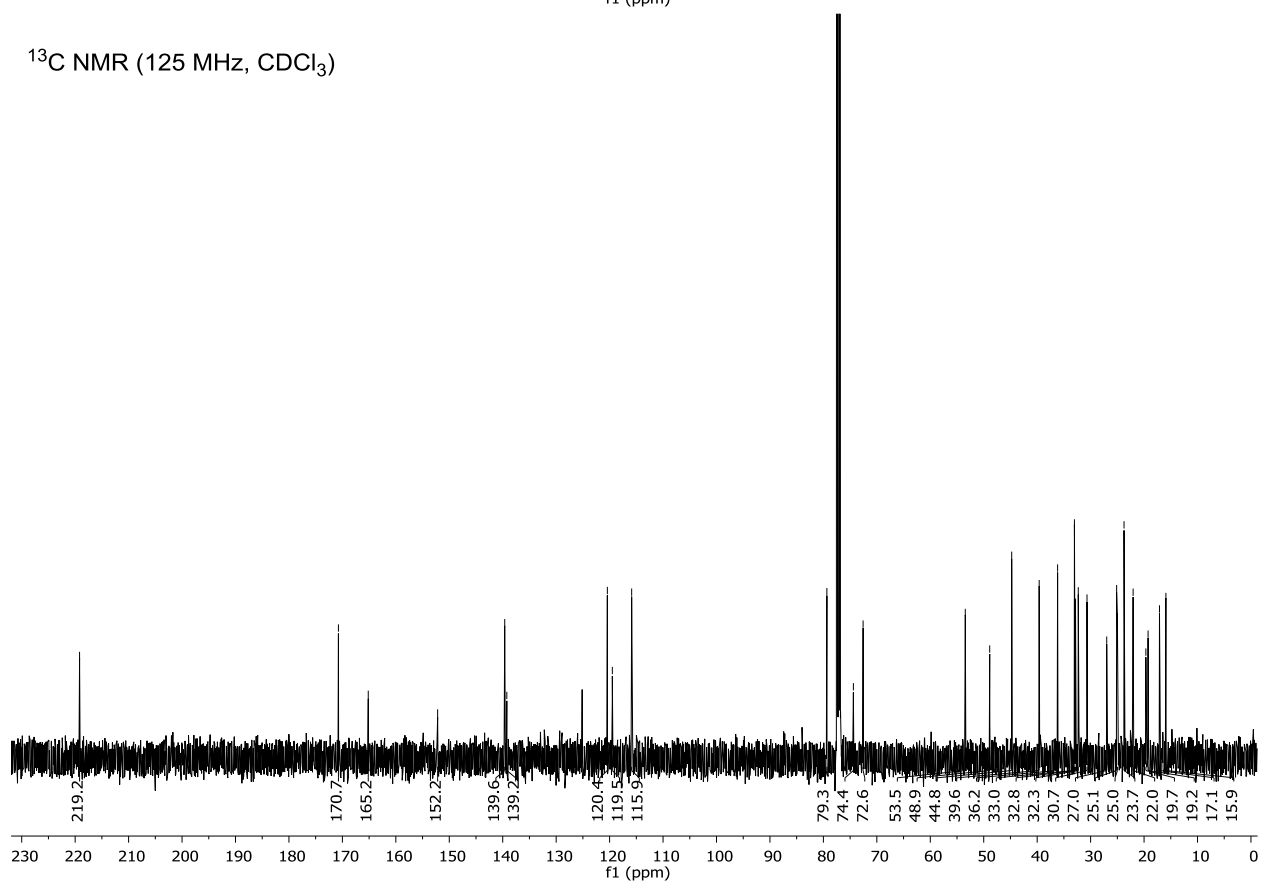


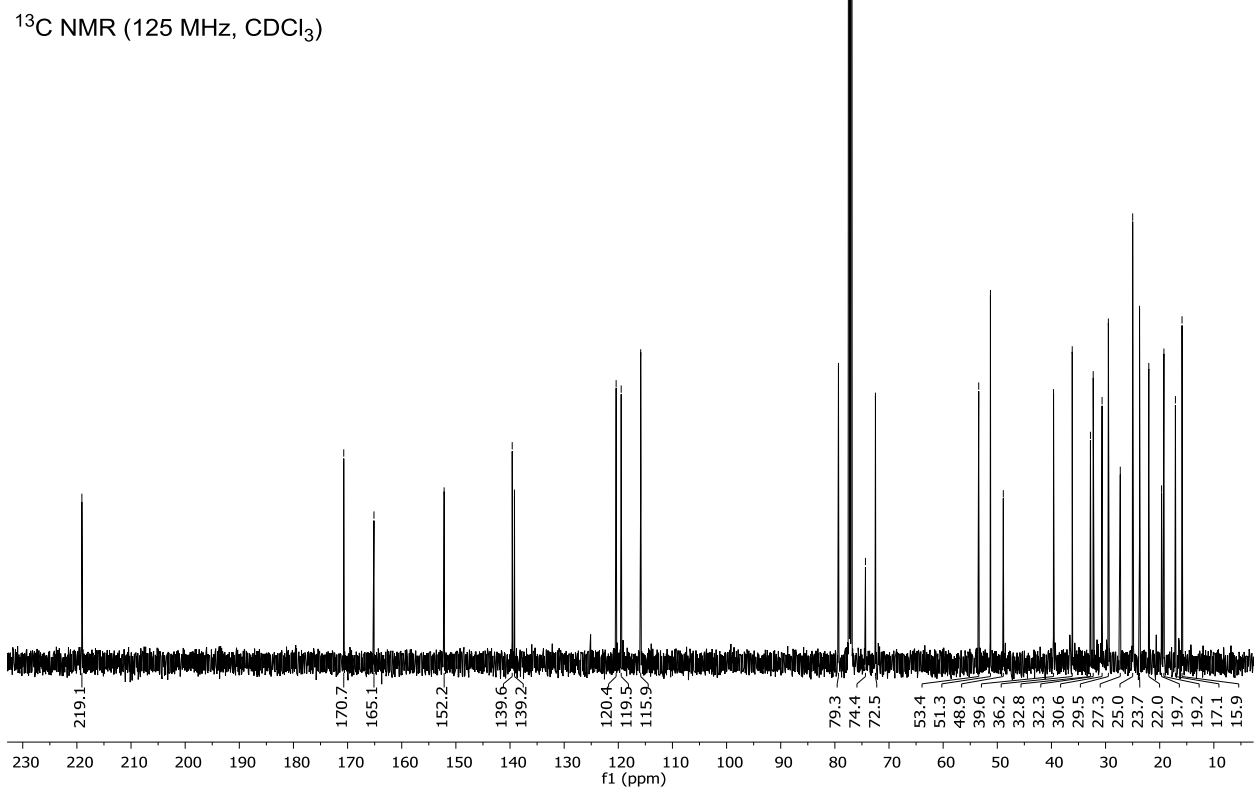
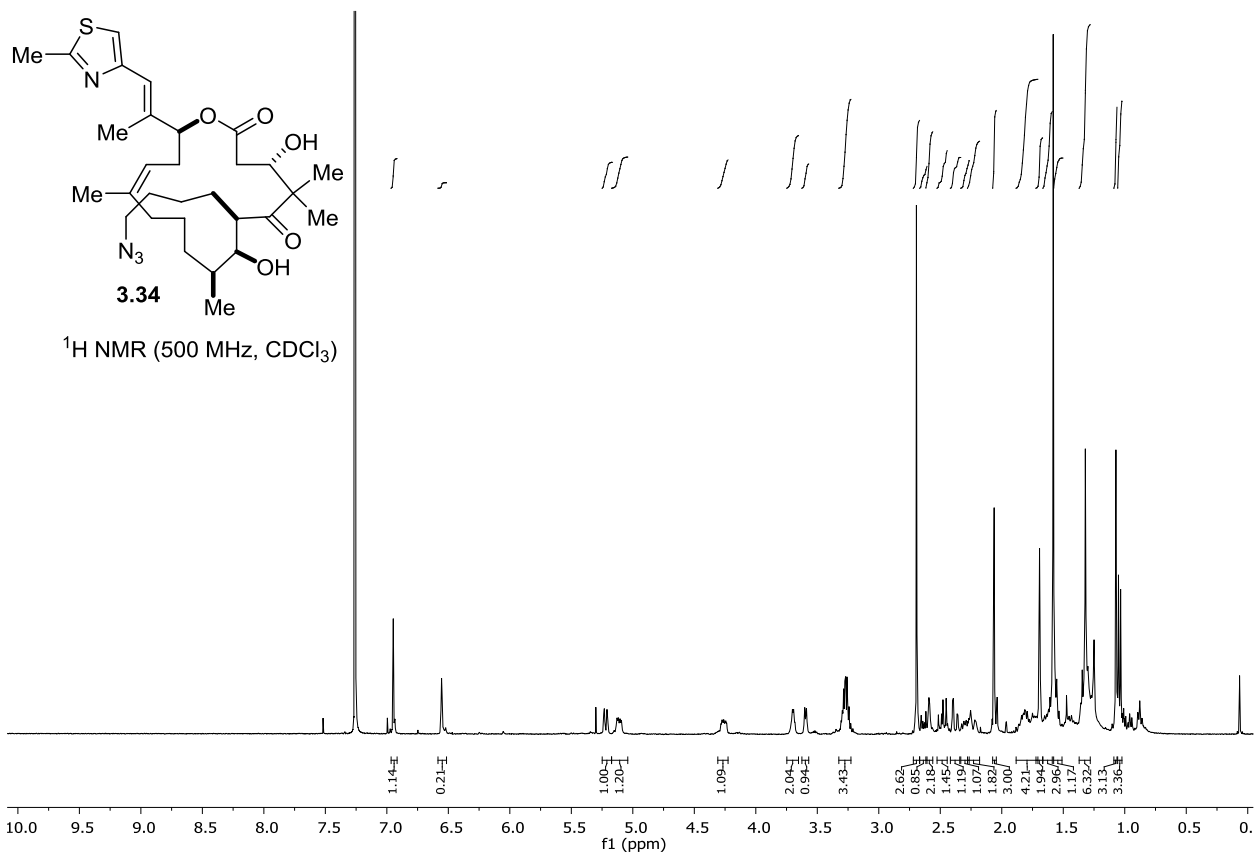


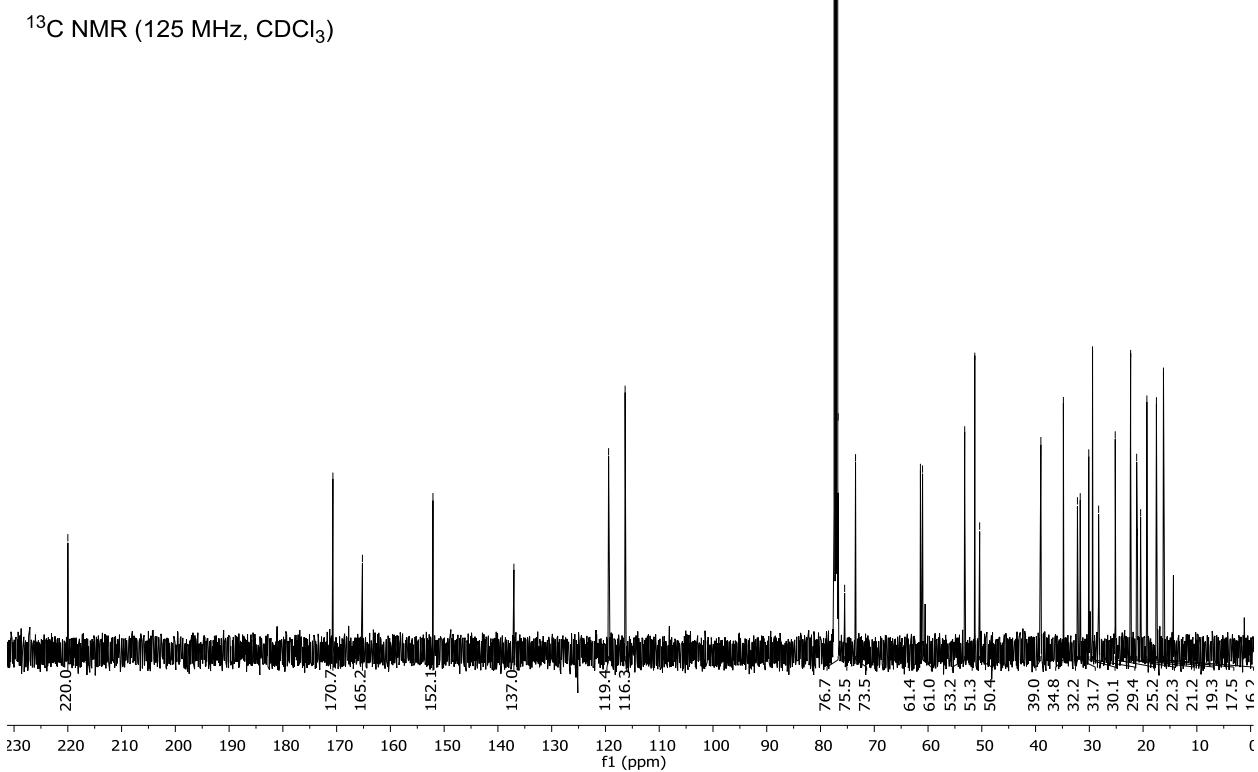
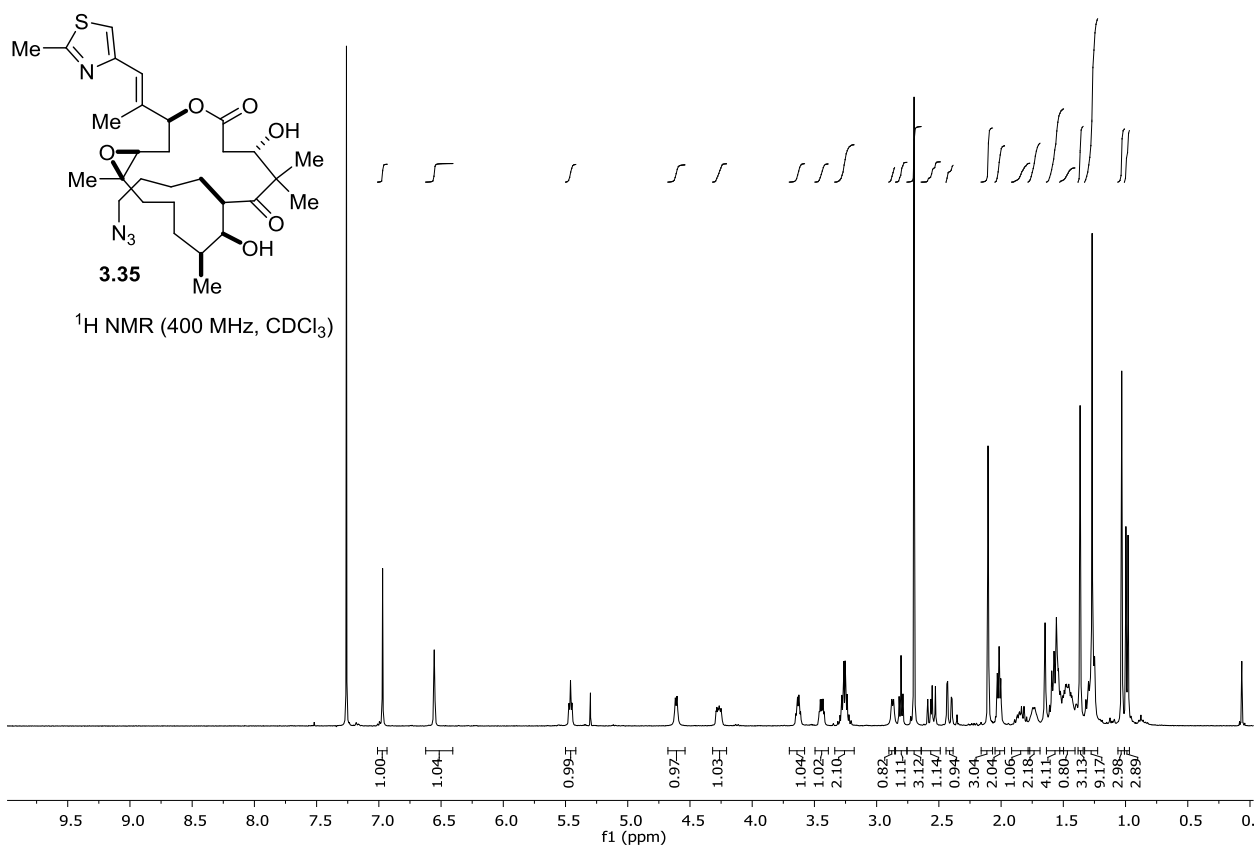
^1H NMR (500 MHz, CDCl_3)

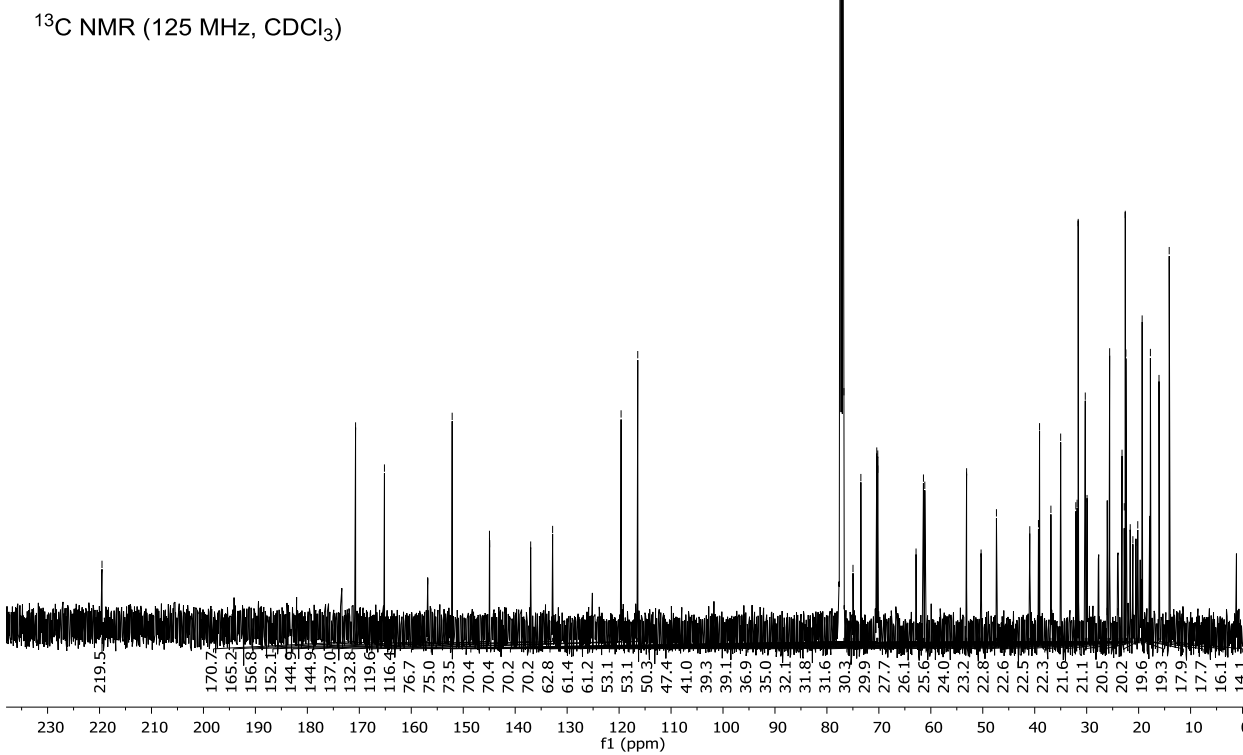
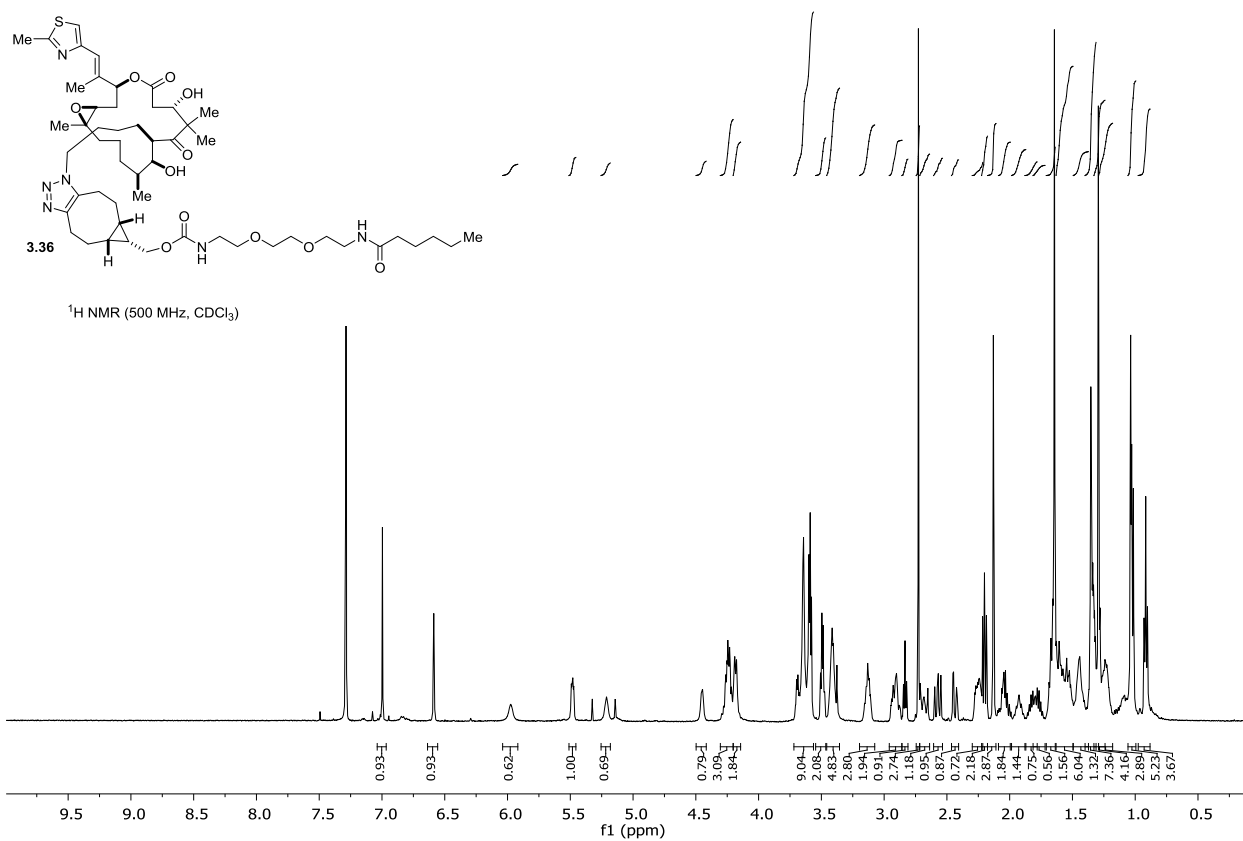


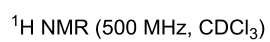
^{13}C NMR (125 MHz, CDCl_3)





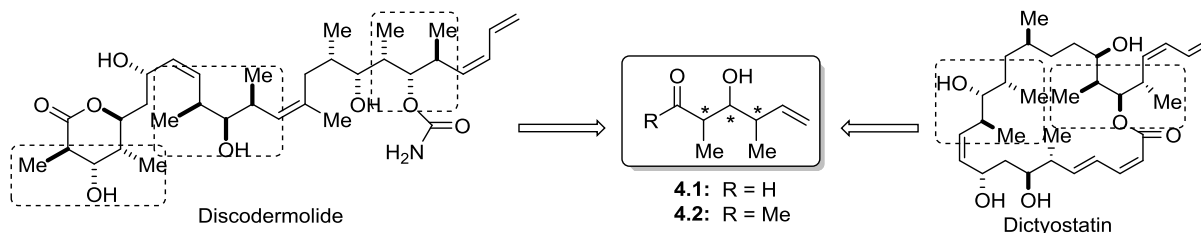






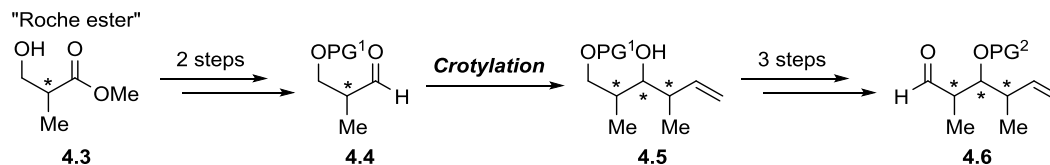
Chapter 4: A New Approach to the Rapid Synthesis of Polypropionate Stereotriad Building Blocks¹

4.1 Introduction



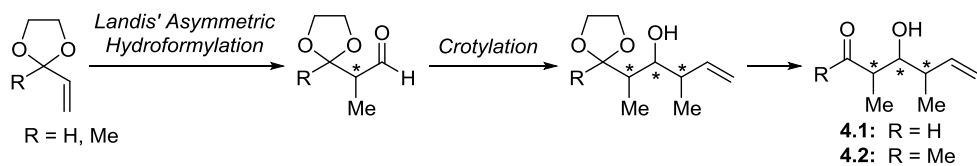
Scheme 4.1 Utility of Polypropionate Building Blocks for Natural Product Synthesis

Due to their synthetic versatility, stereotriad fragments such as **4.1** and **4.2** have commonly been utilized as building blocks in the construction of many nonaromatic polyketide natural products. Since its full development by Roush in 1987,^{2,3} total synthesis efforts that incorporate these stereotriad building blocks have relied heavily on the “Roche ester” approach for their formation.^{4–7} For example, most of the reported syntheses of related natural products discodermolide and dictyostatin (shown in Scheme 4.1) utilize the “Roche ester” approach,⁸ including the 60 gram production of discodermolide that has been reported by Novartis.⁹ In employing this approach, the hydroxyl group of the commercially available Roche ester **4.3** is first protected and then the ester moiety reduced to access the corresponding aldehyde **4.4**. Diastereoselective crotylation provides the stereotriad-containing product **4.5**, but further protecting group manipulations and redox adjustments are required to form useful building block **4.6** (Scheme 4.2). Of the six or seven steps required to obtain the stereotriad building block by this approach, only one is a carbon-carbon bond forming step that installs two stereocenters. The third stereocenter is purchased, and the rest of the steps are redox and protecting group manipulations that are required to access useful intermediates, as opposed to productive carbon-carbon bond-forming or stereocenter-setting steps.



Scheme 4.2 “Roche Ester” Approach to Stereotriad Synthesis

An alternative approach to these stereotriad building blocks has recently been reported by our group as part of a highly step-economical synthesis of dictyostatin.¹⁰ In this method, vinyl acetals can be converted into the functionalized building blocks through a three-step process utilizing Landis’ method for asymmetric hydroformylation¹¹ to set the α -stereocenter followed by crotylation to complete the stereotriad (Scheme 4.3). While this approach represents a much more direct synthesis of the building blocks, the regioselectivities of asymmetric hydroformylation reaction are only moderate to poor, and the required Landis ligand was very expensive and now no longer commercially available. Given these issues, we were interested in exploring another approach to the stereotriad building blocks **4.1** and **4.2**.

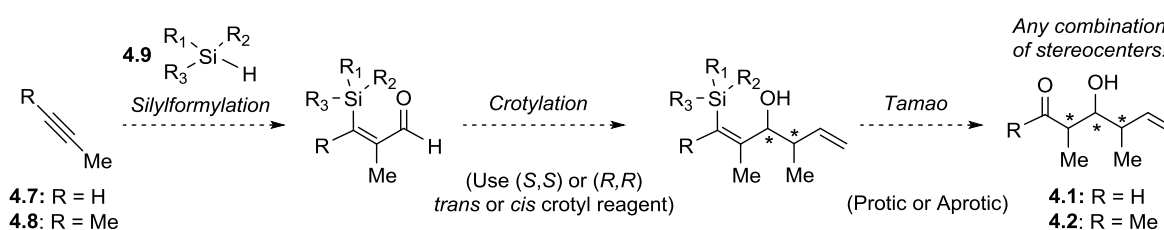


Scheme 4.3 Asymmetric Hydroformylation Approach to Stereotriad Building Blocks

After completing our synthesis of the C1-C9 fragment of the epothilones, we considered that our new intermolecular crotylation tactic may lend itself to a more general approach to stereotriad synthesis than the previous intramolecular tandem silylformylation-crotylsilylation approach could. The intramolecular approach required the use of a homopropargylic alcohol and was thus useful for access to 1,5-*anti*-diol moieties, though the level of selectivity was dependent on the substrate. It was also limited to an *anti* relationship for the stereocenters set by the crotylation reaction because access to the bis-*trans*-crotylsilane has not been possible. On the other hand, our new intermolecular crotylation approach utilizes our group’s highly enantioselective

crotylation reagent, which can provide access to any combination of the two new stereocenters, regardless of the existing stereochemistry in the molecule. The potential to apply the “aprotic” Tamao oxidation conditions to substrates other than the epothilone fragment is another advance, which has provided a switch in diastereoselectivity relative to the standard Tamao oxidation conditions for setting the third stereocenter. With all of these tools now at our disposal, it seemed that we could apply our strategy more generally, for potential access to any combination of stereotriad stereocenters.

We became interested in applying our new strategy towards a highly step-economical and scalable synthesis of stereotriad building blocks **4.1** and **4.2** due to their vast synthetic utility. Access to these products would also represent the most generalized example of such a strategy because the alkyne substrate would now have only a methyl group or hydrogen atom substituent, as opposed to a more elaborate system. For our approach we envisioned a three step sequence, starting with the intermolecular silylformylation of an alkyne **4.7** or **4.8** with a silane **4.9**, followed by crotylation with either (*S,S*)- or (*R,R*)- and *cis*- or *trans*-crotylation reagent, and finally oxidation using the standard (protic) or “aprotic” Tamao oxidation conditions to provide building block **4.1** or **4.2** with any combination of the three stereocenters (Scheme 4.4).



Scheme 4.4 Proposed Carbonylation-Crotylation Approach to Stereotriad Building Blocks

Since the α -stereocenter set during the Tamao oxidation would be induced by the existing stereochemistry of the neighboring hydroxyl group (β -stereocenter), this approach would be able to set all three stereocenters through the use of only one external source of chirality (the crotylation

reagent). Each step of this proposed synthesis involves either a carbon-carbon bond-forming step or sets a stereocenter (and installs the ketone moiety), so they can all be considered productive steps, without the need for oxidation adjustments or protecting group manipulations along the way.

4.2 Intermolecular Silylformylation-Crotylation of 2-Butyne

In approaching this synthesis, we knew that the choice of silane would be a key component for the success of our strategy. This silane would need to react efficiently in an intermolecular silylformylation reaction, provide stability for effective isolation of the crotylation product, and be activated enough towards oxidative cleavage in the Tamao oxidation. Since the oxidation step typically requires that the silicon have at least one heteroatom substituent, we decided to begin by investigating alkoxy silanes **4.10** (Table 4.1). Readily available dimethylethoxysilane **4.10a** did not undergo efficient silylformylation with 2-butyne, even over the course of 45 hours (entry 1). It is our working assumption that most, if not all, of the formation of product **4.12** occurs from hydrosilylation after the Parr bomb apparatus has been vented to release the CO pressure. Thus, the amount of **4.12** present can be used as a metric for the approximate amount of starting material remaining prior to venting. Based on this assumption, the conversion of starting materials to product **4.11a** was far from complete.

Given Matsuda's report that silylformylation of a given alkyne can proceed approximately 10 times faster with a silane that has a phenyl substituent than with a trialkyl silane,¹² we decided to try diphenylethoxysilane **4.10b**. While this change seemed to improve the rate of the reaction, it was still incomplete after 24 hours using 5 mol% of the rhodium catalyst (Table 4.1, entry 2). The use of acetonitrile instead of benzene as the solvent further increased the rate of the reaction. Unfortunately, along with this rate enhancement we also saw significant production of two new species: a silane-derived side product **4.14b**, which we were unable to isolate for full

characterization, and a hemiacetal side product **4.13b**, which is presumably formed via rearrangement of the silylformylation product and has been previously reported for alkoxy silane substrates.¹²

Table 4.1 Optimization of the Silylformylation of 2-Butyne

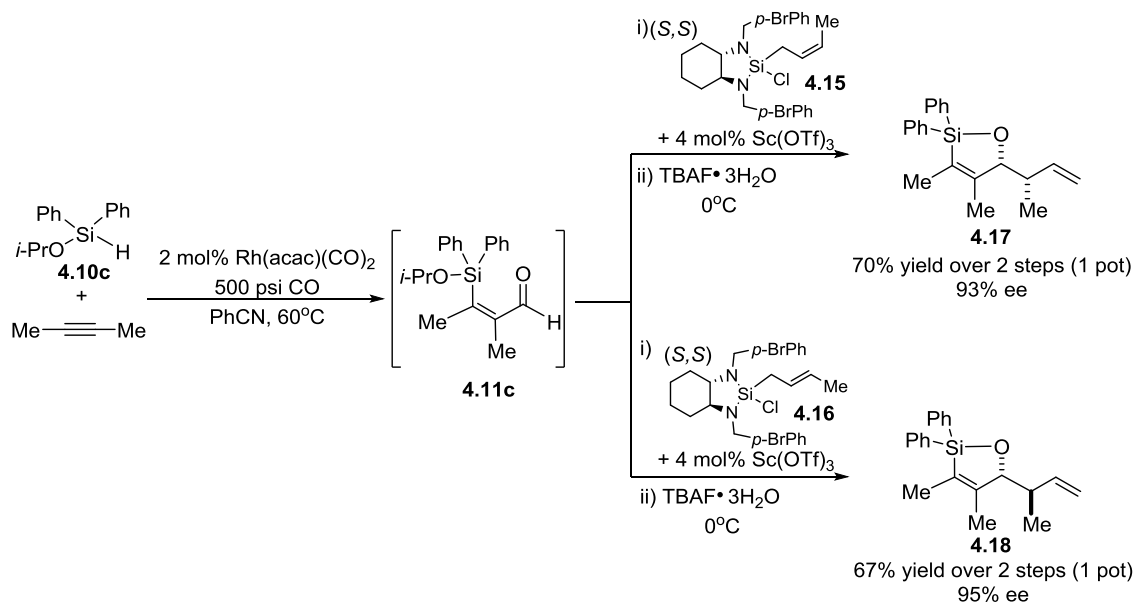
Entry	Silane			mol % Rh	Solvent	t (hours)	Products			
	R'	R''					4.11	4.12	4.13	4.14 ^a
1	4.10a	Me	Et	5.0	PhH	45	1	3.6	0	0
2	4.10b	Ph	Et	5.0	PhH	24	1	0.7	0	0
3	4.10b	Ph	Et	2.5	CH ₃ CN	14	1	0	0.5	0.3
4	4.10c	Ph	<i>i</i> -Pr	2.5	CH ₃ CN	20	1	0	0	0.7
5	4.10c	Ph	<i>i</i> -Pr	2.0	PhCN	24	1	0	0	0.2

^a**4.14** is a silane-derived side product

Utilizing a bulkier alkoxy group on the silane in the hopes of slowing down rearrangement of the product, we found that diphenylisopropoxysilane **4.10c** seemed to do just that, providing the desired product **4.11c** in the absence of **4.13c** within 20 hours (entry 4). This came with an increase in the silane-derived side product **4.14c**, however. After further optimization, we found we could minimize the production of this side product and lower the catalyst loading to 2 mol % of Rh(acac)(CO)₂ by using benzonitrile as the solvent (entry 5). It was these conditions that we chose to use in moving forward with our synthesis of stereotriad building blocks **4.2**.

In approaching the crotylation step, we hoped to use the unpurified product from the silylformylation as we had previously done in our synthesis of the C1-C9 epothilone fragment. We found that following silylformylation, we could directly dilute the benzonitrile solution with methylene chloride and then apply our *cis*- or *trans*-crotylation reagents **4.15** or **4.16** with catalytic

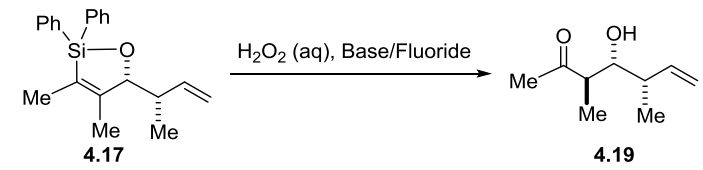
scandium(III) triflate¹³ as before, without a problem. Quenching this reaction with tetra-*n*-butylammonium fluoride trihydrate resulted in cyclization to form **4.17** or **4.18**, which we could isolate efficiently via chromatography. Final optimized conditions were able to provide *syn* crotylation product **4.17** in 70% yield over two steps with 93% ee and *anti* crotylation product **4.18** in 67% yield over 2 steps with 95% ee, both demonstrated on scale to provide more than 4.5 grams of each product (Scheme 4.5).



Scheme 4.5 Optimized Conditions for the 1-Pot Silylformylation-Crotylation of 2-Butyne

4.3 Optimization of the Standard and “Aprotic” Tamao Oxidation Conditions

With an efficient and highly enantioselective synthesis of **4.17** and **4.18** established, we were able to move forward to investigate the Tamao oxidation of these substrates using both the standard and “aprotic” conditions. It was our hope that the diastereochemical switch in the tautomerization selectivity that was established by the development of the *syn*-selective “aprotic” Tamao oxidation conditions for the C1-C9 epothilone fragment¹⁴ would extend to these new substrates to allow stereoselective access to both the *syn* and *anti* diastereomers.

Table 4.2 Optimization of the Standard (Protic) Tamao Oxidation Condition for **4.17**


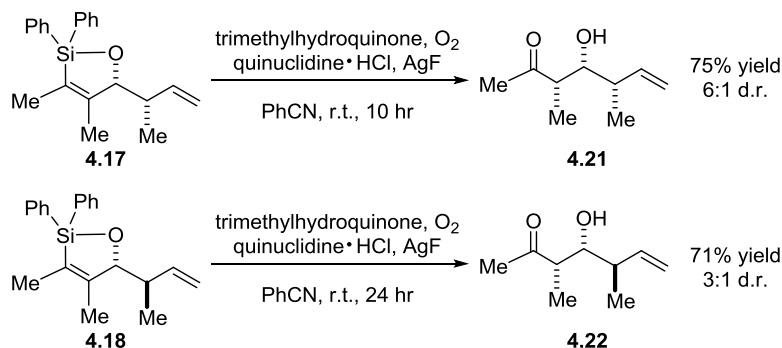
Entry	Base/Fluoride	Solvent	Temp (°C)	Time (hours)	Yield (%)	d.r. (<i>anti:syn</i>)
1	KHCO ₃	1:1 THF: <i>i</i> -PrOH	r.t.	3	55	>20:1
2	KF	1:1 THF: <i>i</i> -PrOH	r.t.	1.5	81	9:1
3	KF	3:1 THF: <i>i</i> -PrOH	r.t.	1	77	5:1
4	KF	1:3 THF: <i>i</i> -PrOH	r.t.	2.5	81	7:1
5	KF	1:1 THF: <i>i</i> -PrOH	0	4	84	18:1

Examining the standard (protic) Tamao oxidation conditions using the *syn* crotylation product **4.17**, we found that we were able to form the desired *anti* product **4.19** with high diastereoselectivity but moderate yields when utilizing potassium bicarbonate as the base (Table 4.2, entry 1). Alternatively, we obtained higher yields but lower selectivity using potassium fluoride as a fluoride source in place of base (entry 2). Modifying the fluoride conditions in the hopes of maintaining a good yield but improving the diastereoselectivity, we determined that modulation of the solvent ratio of tetrahydrofuran and isopropanol decreased the selectivity (entries 3 and 4), but lowering the temperature to 0°C was able to boost the selectivity to form **4.19** in 84% yield and 18:1 d.r. (entry 5). Applying these conditions to the *anti* crotylation product **4.18**, the selectivity was slightly eroded to provide the *anti, anti* stereotriad product **4.20** in 87% yield and 9:1 d.r. (Scheme 4.6).

**Scheme 4.6** Standard Tamao Oxidation of **4.18**

Turning next to the “aprotic” Tamao oxidation conditions, we found that our previously optimized conditions (Chapter 2) resulted in inefficient, sluggish reactions with poor

diastereoselectivity, providing the *syn, syn* stereotriad product **4.21** in 2.5:1 d.r. and the *syn, anti* stereotriad product **4.22** in 1.4:1 d.r. As observed previously while optimizing these conditions for the C1-C9 epothilone fragment synthesis, increasing the substitution of the hydroquinone by exchanging 2,3-dimethylhydroquinone for trimethylhydroquinone improved the efficiency. Again, we believe that this effect can be explained by the higher concentration of active oxidant present in our reaction due to the increased rate of its production.¹⁵ The increased efficiency of the reaction allowed us to reduce the temperature of the reaction (from 60°C to ambient temperature) and improve the diastereoselectivity to ultimately obtain the *syn-syn* product **4.21** in 75% yield and 6:1 d.r. and the *syn-anti* product **4.22** in 71% yield and 3:1 d.r. (Scheme 4.7). While these selectivities show that the “aprotic” Tamao oxidation conditions are not as general as we hoped, optimization provided a vast improvement over the initial results utilizing our previous conditions.

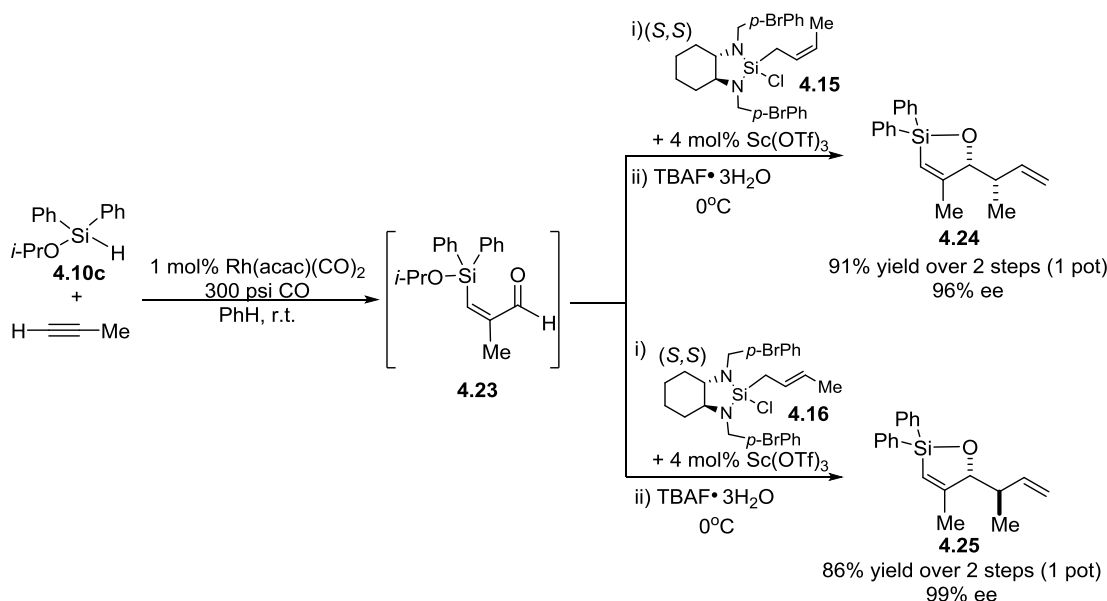


Scheme 4.7 Optimized Conditions for “Aprotic” Tamao Oxidation to Form **4.21** and **4.22**

4.4 Utilization of Propyne Substrate Towards the Synthesis of Aldehyde Building Blocks

As the corresponding aldehyde building blocks **4.1** might be even more generally useful for synthetic use, we aimed to extend our approach with propyne in the place of our previous 2-butyne substrate which could provide the corresponding aldehyde products. Since our desired regioselectivity was well-precedented and the reduced steric hindrance expected to require milder conditions,^{12,16} we were hopeful that the silylformylation reaction with propyne might provide a more efficient reaction. In practice, we were able to access **4.23** via the regio- and chemoselective

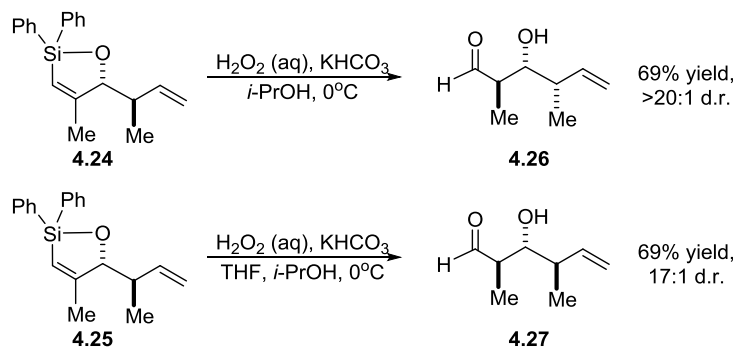
silylformylation of propyne with diphenylisopropoxysilane **4.10c** utilizing a lower catalyst loading and with decreased temperature, pressure, and reaction time relative to our optimized conditions for 2-butyne. In addition, we did not see any formation of the previously observed silane-derived side product **4.14c** (see Table 4.1). As before, we were able to directly dilute the silylformylation reaction mixture with methylene chloride and apply our *cis*- or *trans*- crotylation reagents **4.15** or **4.16** with catalytic scandium(III) triflate, followed by a tetra-*n*-butylammonium fluoride trihydrate quench to provide the cyclized products **4.24** and **4.25** in excellent overall yields and selectivities (Scheme 4.8). These reactions were demonstrated on gram scale in the indicated yields and selectivities.



Scheme 4.8 Optimized Silylformylation-Crotylation of Propyne

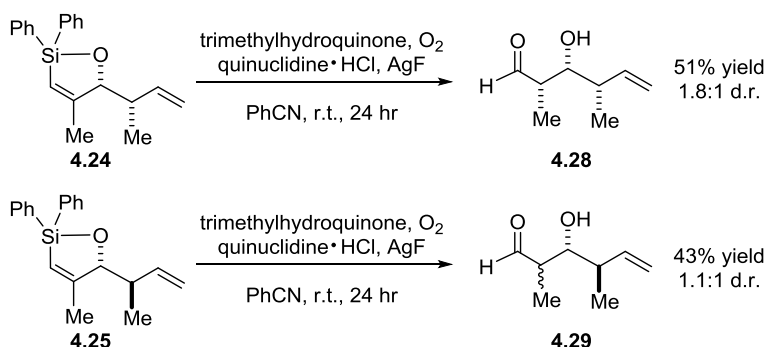
In applying our previously optimized conditions for the standard Tamao oxidation to these new substrates **4.24** and **4.25**, we found a decrease in selectivity and yield relative to the previous substrates **4.17** and **4.18**. Exploring alternative conditions, we found that the use of potassium bicarbonate provided higher diastereoselectivities but lower yields than the potassium fluoride conditions, as we had seen with the previous substrate (see table 4.2). In this case, however, the

yield was only slightly lower, so when taking into account both the selectivity and the yield, the potassium bicarbonate conditions seemed to give the better overall result for these substrates. With fully optimized conditions for the standard Tamao oxidation, **4.24** and **4.25** were each demonstrated on 500 mg scale to provide the *anti*, *syn* product **4.26** and *anti*, *anti* product **4.27**, respectively, in good yields and excellent diastereoselectivities (Scheme 4.9).



Scheme 4.9 Optimized Standard Tamao Oxidation Conditions for Aldehyde Stereotriads

Unfortunately, applying our optimized aprotic Tamao oxidation conditions to **4.24** gave the *syn*, *syn* product **4.28** in only moderate yield and poor diastereoselectivity, while the reaction of **4.25** was inefficient and nonselective (Scheme 4.10).

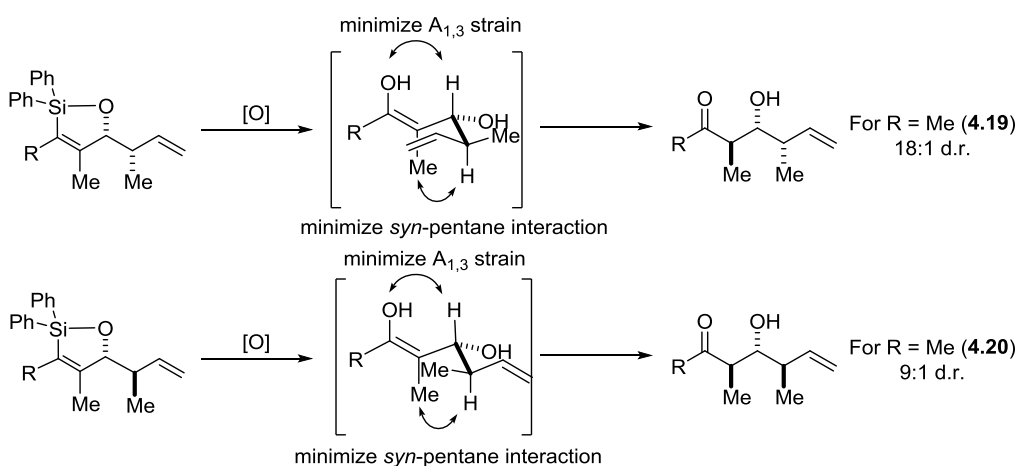


Scheme 4.10 "Aprotic" Tamao Oxidation Results

4.5 Observed Tamao Oxidation Selectivity Trends

Two interesting selectivity trends can be noted from our Tamao oxidation results. First, we found that for each substrate pair (i.e. **4.17/4.18** and **4.24/4.25**), the diastereoselectivity was consistently higher using the *syn* crotylation product **4.17** or **4.24** than for the *anti* crotylation

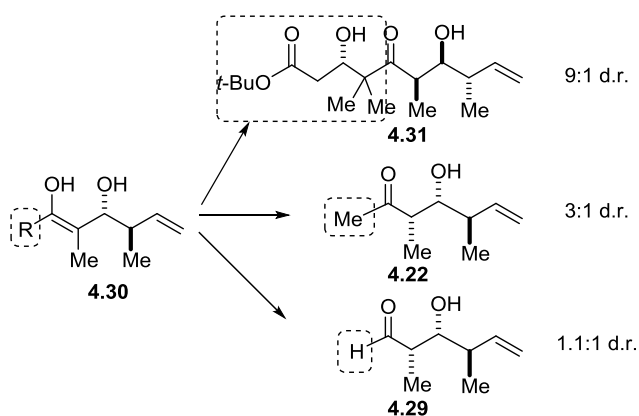
product **4.18** or **4.25** for both the standard and “aprotic” Tamao oxidation conditions (see Table 4.2 and Schemes 4.6, 4.7, 4.9, and 4.10). Under the standard Tamao oxidation conditions, this observation is consistent with the model that we have previously devised for the tautomerization selectivity.¹⁷ For the more selective *syn* crotylation product, the larger vinyl group would be hindering approach to the front side of the enol by this model, while the less selective *anti* crotylation product would result in the smaller methyl group in the corresponding blocking position (Scheme 4.11).



Scheme 4.11 Rationalized Model for Selectivity Trend Observed with Standard Tamao Oxidation Conditions

The corresponding effect for the “aprotic” Tamao is not as easily explained, since the origins of the observed *syn*-selectivity are not as clear. Indeed, in our attempts to expand the scope of these “aprotic” Tamao oxidation conditions from the substrate for which they were originally developed **4.31**, it has become clear that there is a trend in the selectivity which is highly dependent on the substrate used. When decreasing the steric bulk of the R group in going from a quaternary carbon center as in **4.31**, to R = Me for **4.22**, and finally to R = H in **4.29**, the selectivity drops significantly (Scheme 4.12), indicating that our current conditions are less general and more substrate-dependent. Reliable access to building blocks **4.22**, **4.28**, and **4.29** would require

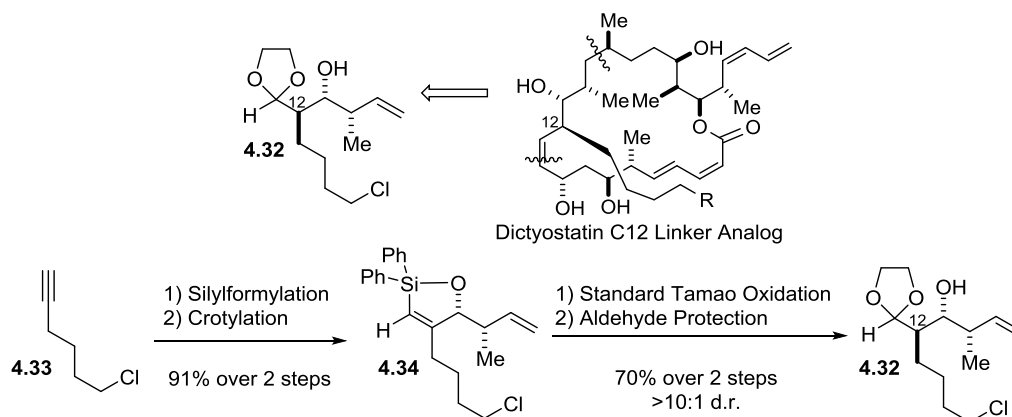
development of more general conditions for the *syn*-selective Tamao oxidation/diastereoselective tautomerization, which remains a long-term goal of the Leighton group.



Scheme 4.12 Selectivity Trend for “Aprotic” Tamao Oxidation (shown for *Syn*, *Anti* Stereotriads)

4.6 Demonstrated Application in Dictyostatin Analog Synthesis¹⁸

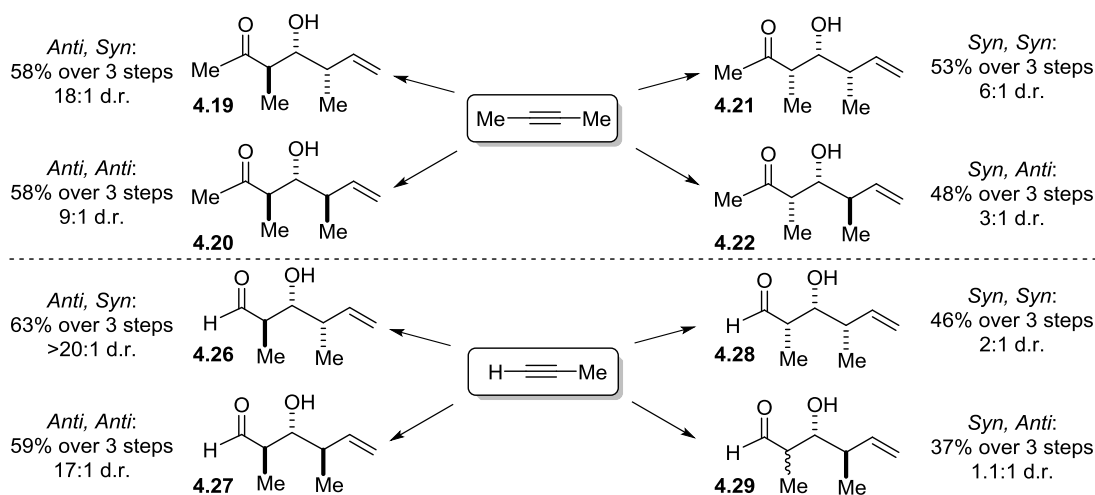
Soon after our new stereotriad synthesis strategy had been developed, it became useful for a fellow group member to employ it in efforts to obtain fragment **4.32**. This target fragment was simply the acetal-protected α -methyl linker analog of *anti*, *syn* aldehyde building block **4.26**, which was to be used in the synthesis of a dictyostatin C12 linker analog (Scheme 4.13). In applying our newly developed conditions to terminal alkyne **4.33**, the 1-pot silylformylation-crotylation sequence proceeded smoothly in 91% yield over the two steps to access intermediate **4.34**. Utilizing the standard Tamao oxidation conditions provided the desired *anti* diastereoselectivity in >10:1 d.r. and after direct acetal protection of the crude aldehyde, the desired fragment **4.32** was obtained in 70% over two steps. This route provided a direct and stereoselective synthesis of the desired fragment, which could then be used to access the desired dictyostatin C12 linker analog.



Scheme 4.13 Application of Our Route to Access Analog of *Anti*, *Syn* Stereotriad

4.7 Conclusion

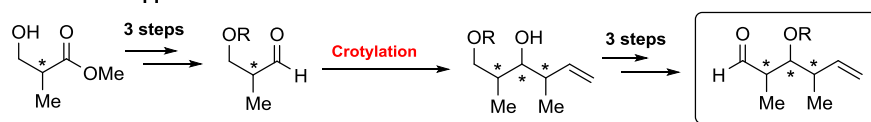
We have developed an efficient synthetic strategy for the synthesis of a number of widely useful polyketide building blocks, rapidly generating three contiguous stereocenters with moderately good to excellent levels of selectivity. Though not yet a comprehensive strategy, our efforts thus far have resulted in the development of highly efficient syntheses of building blocks **4.19**, **4.20**, **4.21**, **4.26**, and **4.27** which have been demonstrated on gram or multigram scale from 2-butyne or propyne, with yields in the range of 53-63% over 3 steps (average of 80-86% per step) (Scheme 4.14).



Scheme 4.14 Summary of the 2-Pot, 3-Step Synthesis of Stereotriad Building Blocks from 2-Butyne or Propyne

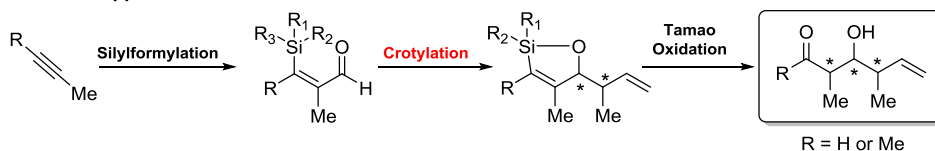
Further efforts to develop more generally useful conditions for *syn*-selective Tamao oxidation/diastereoselective tautomerization could allow improved access to the remaining building blocks **4.22**, **4.28**, and **4.29**. By eliminating a number of protecting group manipulations and redox reactions, we have developed a scalable and more direct way to access a number of these fragments relative to previous approaches, such as the widely employed “Roche ester” strategy (Scheme 4.15).

“Roche ester” approach:



- Purchase α stereocenter
- about 6-7 steps total, but only one is C-C bond forming

Our new approach:



- α stereocenter for “free”: internal diastereochemical control
- simple starting materials: CO, alkyne, silane
- 3 steps total (2 pots): 2 C-C bond forming steps

Scheme 4.15 Comparison of New Approach vs “Roche Ester” Approach

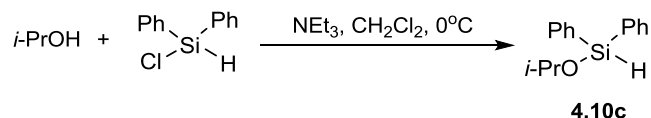
4.8 References

- (1) Foley, C. N.; Leighton, J. L. Beyond the Roche Ester: A New Approach to Polypropionate Stereotriad Synthesis. *Org. Lett.* **2014**, *16*, 1180–1183.
- (2) Roush, W. R.; Palkowitz, A. D.; Palmer, M. A. J. Reactions of Diisopropyl Tartrate Modified Allyl and (E)- and (Z)-Crotylboronates with Beta-Alkoxy-Alpha-Methylpropionaldehydes: A Reagent Based Solution to the Acyclic Dipropionate Problem. *J. Org. Chem.* **1987**, *52*, 316–318.
- (3) Roush, W. R.; Palkowitz, A. D.; Ando, K. Acyclic Diastereoselective Synthesis Using Tartrate Ester-Modified Crotylboronates. Double Asymmetric Reactions with .alpha.-Methyl Chiral Aldehydes and Synthesis of the C(19)-C(29) Segment of Rifamycin S. *J. Am. Chem. Soc.* **1990**, *112*, 6348–6359.
- (4) White, J. D.; Hanselmann, R.; Jackson, R. W.; Porter, W. J.; Ohba, Y.; Tiller, T.; Wang, S. Total Synthesis of Rutamycin B, a Macrolide Antibiotic from Streptomyces Aureofaciens. *J. Org. Chem.* **2001**, *66*, 5217–5231.
- (5) Barrett, A. G. M.; Edmunds, J. J.; Hendrix, J. A.; Horita, K.; Parkinson, C. J. Stereocontrolled Synthesis of Calyculin A: Construction of the C(1)-C(14) Tetraene Nitrile Unit. *J. Chem. Soc. Chem. Commun.* **1992**, *12*, 1238–1240.
- (6) Paterson, I.; Florence, G. J. The Development of a Practical Total Synthesis of Discodermolide, a Promising Microtubule-Stabilizing Anticancer Agent. *European J. Org. Chem.* **2003**, *2003*, 2193–2208.
- (7) Shin, Y.; Fournier, J.-H.; Fukui, Y.; Brückner, A. M.; Curran, D. P. Total Synthesis of (-)-Dictyostatin: Confirmation of Relative and Absolute Configurations. *Angew. Chem. Int. Ed. Engl.* **2004**, *43*, 4634–4637.
- (8) Smith, A. B.; Freeze, B. S. (+)-Discodermolide: Total Synthesis, Construction of Novel Analogues, and Biological Evaluation. *Tetrahedron* **2007**, *64*, 261–298.
- (9) Mickel, S. J.; Sedelmeier, G. H.; Niederer, D.; Daeffler, R.; Osmani, A.; Schreiner, K.; Seeger-weibel, M.; Berod, B.; Schaer, K.; Gamboni, R.; Chen, S.; Chen, W.; Jagoe, C. T.; Kinder, F. R.; Loo, M.; Prasad, K.; Repic, O.; Shieh, W.; Wang, R.; Waykole, L.; Xu, D. D.; Xue, S. Large-Scale Synthesis of the Anti-Cancer Marine Natural Product (+)-Discodermolide. Part 1: Synthetic Strategy and Preparation of a Common Precursor. *Org. Process Res. Dev.* **2004**, 92–100.
- (10) Ho, S.; Bucher, C.; Leighton, J. L. A Highly Step-Economical Synthesis of Dictyostatin. *Angew. Chem. Int. Ed.* **2013**, *52*, 6757–6761.
- (11) McDonald, R. I.; Wong, G. W.; Neupane, R. P.; Stahl, S. S.; Landis, C. R. Enantioselective Hydroformylation of N-Vinyl Carboxamides, Allyl Carbamates, and

- Allyl Ethers Using Chiral Diazaphospholane Ligands. *J. Am. Chem. Soc.* **2010**, *132*, 14027–14029.
- (12) Matsuda, I.; Fukuta, Y.; Tsuchihashi, T.; Nagashima, H.; Itoh, K. Rhodium-Catalyzed Silylformylation of Acetylenic Bonds: Its Scope and Mechanistic Considerations. *Organometallics* **1997**, *16*, 4327–4345.
- (13) Kim, H.; Ho, S.; Leighton, J. L. A More Comprehensive and Highly Practical Solution to Enantioselective Aldehyde Crotylation. *J. Am. Chem. Soc.* **2011**, *133*, 6517–6520.
- (14) Harrison, T. J.; Rabbat, P. M. A.; Leighton, J. L. An “Aprotic” Tamao Oxidation/Syn-Selective Tautomerization Reaction for the Efficient Synthesis of the C1-C9 Fragment of Fludelon. *Org. Lett.* **2012**, *14*, 4890–4893.
- (15) Tamao, K.; Hayashi, T.; Ito, Y. An Efficient Oxidative Cleavage of Carbon-Silicon Bonds by a Dioxygen/Hydroquinone System. *Tetrahedron Lett.* **1989**, *30*, 6533–6536.
- (16) Matsuda, I.; Ogiso, A.; Sato, S.; Izumi, Y. An Efficient Silylformylation of Alkynes Catalyzed by Rh₄(CO)₁₂. *J. Am. Chem. Soc.* **1989**, *111*, 2332–2333.
- (17) Spletstoser, J. T.; Zacuto, M. J.; Leighton, J. L. Tandem Silylformylation-crotylsilylation/Tamao Oxidation of Internal Alkynes: A Remarkable Example of Generating Complexity from Simplicity. *Org. Lett.* **2008**, *10*, 5593–5596.
- (18) Ho, S. *Unpublished results*.

4.9 Experimental Procedures and Characterization Data

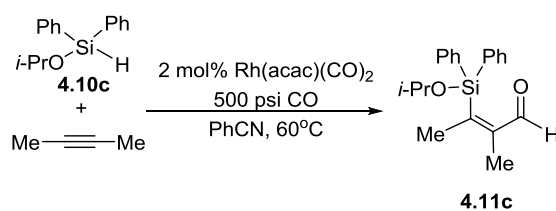
General Information. All reactions were carried out under an atmosphere of nitrogen in flame-dried glassware with magnetic stirring unless otherwise indicated. Degassed solvents were purified by passage through an activated alumina column. Thin-layer chromatography (TLC) was carried out on glass-backed silica gel XHL TLC plates (250 μ m) from Sorbent Technologies; visualization by UV light, *p*-anisaldehyde stain, phosphomolybdic acid stain, or potassium permanganate (KMnO₄) stain. Gas chromatographic analyses were performed on a Hewlett-Packard 6890 Series Gas Chromatograph equipped with a capillary split-splitless inlet and flame ionization detector with electronic pneumatics control using a Supelco β -Dex 325 (30 m x 0.25 mm) capillary GLC column. ¹H NMR spectra were recorded on a Bruker DPX-400 (400 MHz) or a Bruker Avance III 500 (500 MHz) spectrometer and are reported in ppm from CDCl₃ internal standard (7.26 ppm). Data are reported as follows: (bs= broad singlet, s = singlet, d = doublet, t = triplet, q = quartet, quin = quintet, sep = septet, m = multiplet, dd = doublet of doublets, ddd = doublet of doublet of doublets; coupling constant(s) in Hz; integration). Proton decoupled ¹³C NMR spectra were recorded on a Bruker Avance III 500 (125 MHz) spectrometer and are reported in ppm from CDCl₃ internal standard (77.16 ppm). Infrared spectra were recorded on a Perkin-Elmer Spectrum Two (Diamond ATR) IR spectrometer. Optical rotations were recorded on a Jasco DIP-1000 digital polarimeter.



Isopropoxydiphenylsilane **4.10c** was prepared using a modified literature procedure.¹ To a cooled (0°C) solution of diphenylchlorosilane (20.0 mL, 102 mmol) in CH₂Cl₂ (1000 mL) was

¹ Kim, H.; Ho, S.; Leighton, J. L. *J. Am. Chem. Soc.* **2011**, *133*, 6517-6520.

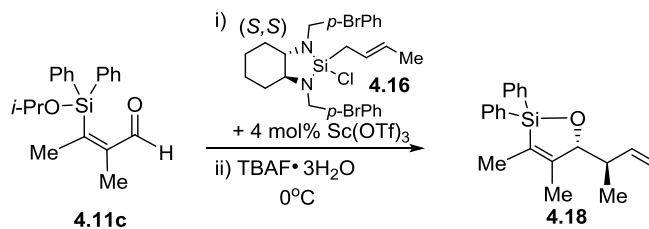
added Et₃N (21.3 mL, 153 mmol) followed by slow addition of *i*-PrOH (9.4 mL, 123 mmol). After 1 hour, the solvent was concentrated under reduced pressure. The residue was diluted with Et₂O (400 mL) and vigorously stirred for 10 minutes. The heterogeneous mixture was filtered, rinsing with Et₂O (200 mL). The filtrate was concentrated and the resulting oil vacuum distilled (bp ~100 °C @ ~0.5 mm Hg) to give isopropoxydiphenylsilane **4.10c** (22.0 g, 89%) as a colorless oil. The ¹H NMR spectroscopic data is in agreement with data reported in the literature.²



A glass liner for a Parr bomb was charged with isopropoxydiphenylsilane **4.10c** (5.25 g, 21.7 mmol). The bomb was assembled and pressurized with CO to approximately 500 psi and then vented. This procedure was repeated two more times then the bomb was pressurized again to 500 psi and stirred for approximately fifteen minutes at ambient temperature. The bomb was opened and Rh(acac)(CO)₂ (112 mg, 0.434 mmol) was added followed by 2-butyne (23.8 mmol, 5.5 mL of 4.3 M solution in PhCN). The bomb was reassembled and pressurized to 500 psi with CO, and then heated to 60°C (oil bath, external temperature). After 24 hours, the bomb was cooled, and then carefully vented and opened. ¹H NMR analysis of an aliquot indicated complete consumption of silane starting material and formation of product **4.11c** in a 5:1 ratio with an unidentified silane-related impurity. This reaction solution was used directly in the following crotylation reaction. For characterization purposes, an analytically pure sample of **4.11c** was obtained by flash chromatography (pH 7 buffered silica gel, 2% EtOAc/hexanes): ¹H NMR (500

² Horner, L.; Mathias, J. J. *Organometallic Chem.* **1985**, 282, 155-174.

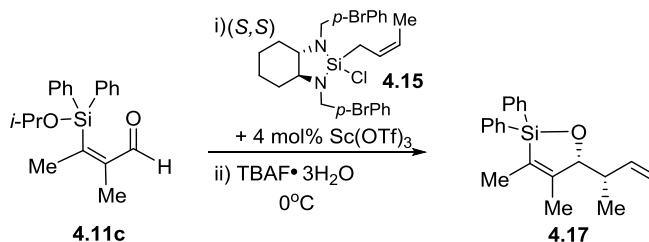
MHz, CDCl₃) δ 10.18 (s, 1H), 7.63 (d, J = 7.7 Hz, 4H), 7.45 – 7.48 (m, 2H), 7.40 – 7.43 (m, 4H), 4.17 – 3.99 (m, 1H), 2.01 (s, 3H), 1.93 (s, 3H), 1.12 (d, J = 6.1 Hz, 6H); ¹³C NMR (125 MHz, CDCl₃) δ 194.8, 157.1, 150.7, 135.2, 134.3, 130.4, 128.3, 67.1, 25.6, 20.6, 11.8; IR (neat): ν (cm⁻¹) 3399, 3069, 3049, 2971, 2916, 2072, 1675, 1589, 1428, 1370, 1256, 1113, 1017, 701, 540, 509; LRMS (FAB+) calcd C₂₀H₂₅O₂Si [M-H]⁻: 323.15, found 323.31.



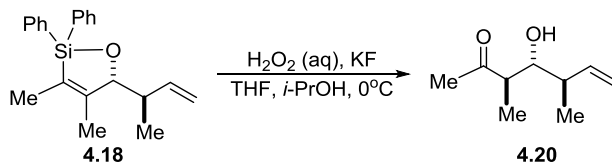
To a solution of the reaction mixture from aldehyde **4.11c** formation in CH₂Cl₂ (220 mL) was added (*S,S*)-*trans*-crotylsilane reagent **4.16** (11.11 g, 19.5 mmol) and Sc(OTf)₃ (428 mg, 0.868 mmol)^{1,3}. After 2 hours at ambient temperature, the reaction was cooled to 0°C and tetrabutylammonium fluoride (TBAF) trihydrate (6.14 g, 19.5 mmol) was added. After 1 hour, the mixture was concentrated and the residue purified via flash chromatography on silica gel (gradient of 100% hexanes to 2.5% EtOAc/hexanes) to afford **4.18** (4.63 g, 67% over 2 steps) as a colorless oil. ¹H NMR (500 MHz, CDCl₃) δ 7.63 (dd, J = 7.7, 1.2 Hz, 2H), 7.53 (dd, J = 7.7, 1.2 Hz, 2H), 7.39 (m, 6H), 5.67 – 5.50 (m, 1H), 4.97 (d, J = 17.3 Hz, 1H), 4.85 (d, J = 10.3 Hz, 1H), 4.70 (s, 1H), 2.62 (m, 1H), 1.84 (s, 3H), 1.76 (s, 3H), 1.22 (d, J = 6.9 Hz, 3H); ¹³C NMR (125 MHz, CDCl₃) δ 153.6, 139.3, 135.6, 135.3, 135.0, 134.6, 130.2, 130.1, 128.0, 127.9, 127.2, 114.9, 89.7, 41.6, 17.7, 13.4, 12.7; IR (neat): ν (cm⁻¹) 3067, 2966, 2919, 2856, 1614, 1428, 1374, 1114, 1008, 914, 840, 734, 704, 541, 514, 486; LRMS (APCI+) calcd C₂₁H₂₅OSi [M+H]⁺: 321.16, found 320.62; [α]_D²² -98.3 (*c* 0.22, CHCl₃). Chiral GC analysis of **4.20** (Supelco β -dex

³ Hackman, B. M.; Lombardi, P. J.; Leighton, J. L. Org. Lett. **2004**, 6, 4375.

325, Isothermal 100°C, 1 mL/min) revealed that **4.18** was produced in 95% enantiomeric excess (ee).

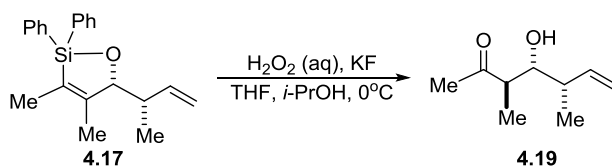


Utilizing the same procedure as above with (*S,S*)-*cis*-crotylsilane reagent **4.15**, product **4.17** (4.58 g, 70% over 2 steps) was isolated as a colorless oil. ^1H NMR (500 MHz, CDCl_3) δ 7.63 (dd, $J = 7.9, 1.4$ Hz, 2H), 7.52 (dd, $J = 7.9, 1.4$ Hz, 2H), 7.47 – 7.43 (m, 1H), 7.43 – 7.37 (m, 3H), 7.37 – 7.32 (m, 2H), 6.09 (ddd, $J = 17.4, 10.3, 7.1$ Hz, 1H), 5.13 – 5.08 (m, 1H), 5.08 – 5.04 (m, 1H), 4.80 (s, 1H), 2.66 – 2.52 (m, 1H), 1.88 (d, $J = 0.7$ Hz, 3H), 1.79 (s, 3H), 0.76 (d, $J = 6.9$ Hz, 3H); ^{13}C NMR (125 MHz, CDCl_3) δ 153.1, 142.9, 135.5, 135.1, 135.0, 134.6, 130.2, 130.2, 128.0, 127.9, 127.9, 113.8, 89.2, 40.9, 13.3, 12.8, 12.2; IR (neat): ν (cm^{-1}) 3067, 2969, 2912, 2854, 1613, 1428, 1374, 1332, 1113, 1004, 912, 863, 836, 798, 705, 514; LRMS (APCI+) calcd $\text{C}_{21}\text{H}_{25}\text{OSi}$ $[\text{M}+\text{H}]^+$: 321.16, found 320.61; $[\alpha]^{20}_{\text{D}} -26.7$ (c 1.38, CHCl_3). Chiral GC analysis of **4.19** (Supelco β -dex 325, Isothermal 100°C , 1 mL/min) revealed that **4.17** was produced in 93% enantiomeric excess (ee).

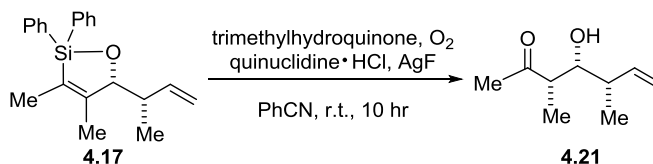


To a cooled (0°C) solution of **4.18** (4.63 g, 14.4 mmol) in THF (72 mL) and *i*-PrOH (72 mL) was added KF (3.35 g, 57.6 mmol) followed by 30% H_2O_2 aqueous solution (18.7 mL, 187 mmol). After 4 hours, the solution was diluted with distilled water (50 mL) and extracted with Et_2O (4 x 50 mL). The combined organic layers were washed with brine (30 mL), dried over

MgSO₄, filtered, and concentrated. Purification of the residue by flash chromatography on silica gel (20% EtOAc/hexanes) afforded the product **4.20** as a yellow oil (1.96 g, 87%) in 9:1 d.r. ¹H NMR (500 MHz, CDCl₃) δ 5.83 (ddd, *J* = 17.2, 10.4, 8.6 Hz, 1H), 5.10 (m, 1H), 5.09 – 5.05 (m, 1H), 3.60 (dd, *J* = 7.4, 3.5 Hz, 1H), 2.68 (m, 1H), 2.52 (s, 1H), 2.41 – 2.29 (m, 1H), 2.19 (s, 3H), 1.12 (d, *J* = 7.4 Hz, 3H), 1.11 (d, *J* = 7.0 Hz, 3H); ¹³C NMR (125 MHz, CDCl₃) δ 214.1, 139.0, 116.1, 77.0, 50.2, 41.0, 29.9, 17.8, 14.0; IR (neat): ν (cm⁻¹) 3446, 3073, 2970, 2931, 2876, 1704, 1641, 1456, 1421, 1356, 1239, 1121, 1001, 962, 915, 702, 582, 498; LRMS (APCI+) calcd C₉H₁₇O₂ [M+H]⁺: 157.12, found 156.93; [α]²¹_D +0.7 (*c* 1.27, CHCl₃).

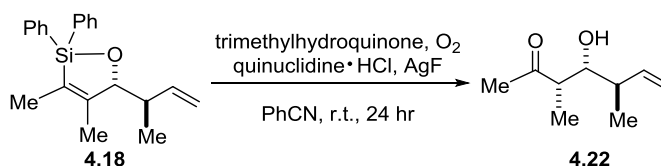


Utilizing the same procedure as above, product **4.19** was isolated (1.87 g, 84%) as a yellow oil in 18:1 d.r. ¹H NMR (500 MHz, CDCl₃) δ 5.85 – 5.70 (m, 1H), 5.07 (d, *J* = 0.7 Hz, 1H), 5.05 (m, 1H), 3.46 (q, *J* = 5.8 Hz, 1H), 2.80 (qd, *J* = 7.2, 5.6 Hz, 1H), 2.68 (d, *J* = 6.7 Hz, 1H), 2.33 (m, 1H), 2.19 (s, 3H), 1.18 (d, *J* = 7.3 Hz, 3H), 1.07 (d, *J* = 6.8 Hz, 3H); ¹³C NMR (125 MHz, CDCl₃) δ 214.9, 141.7, 115.3, 77.3, 48.4, 42.0, 30.3, 14.6, 14.6; IR (neat): ν (cm⁻¹) 3449, 3076, 2972, 2933, 2881, 1702, 1641, 1456, 1418, 1356, 1238, 1170, 1108, 1066, 998, 968, 915, 699, 496; LRMS (APCI+) calcd C₉H₁₇O₂ [M+H]⁺: 157.12, found 156.93; [α]²¹_D +18.8 (*c* 0.90, CHCl₃).



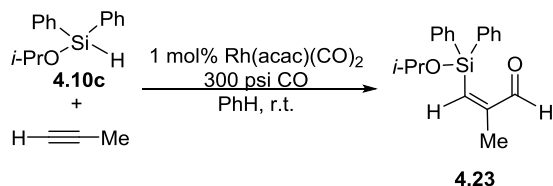
To a flask containing trimethylhydroquinone (473mg, 3.11 mmol), quinuclidine·HCl (367 mg, 2.49 mmol), and AgF (345 mg, 2.72 mmol) was added **4.17** (249 mg, 0.777 mmol) as a

solution in PhCN (15.5 mL). The solution was purged with O₂, and then the reaction was stirred under an atmosphere of O₂ (balloon). After 10 hours at room temperature, the reaction was diluted with CHCl₃ (15 mL). The solution was filtered through Celite then washed with distilled water (10 mL). The aqueous layer was extracted with CHCl₃ (3 x 15 mL). The combined organics were washed with brine, dried over MgSO₄, filtered, and concentrated. The residue was purified via flash chromatography on silica gel (gradient of 10% EtOAc/hexanes to 20% EtOAc/hexanes) to give **4.21** (90 mg, 75%) as an orange oil with 6:1 diastereomeric ratio (d.r.) with respect to the newly formed stereocenter. ¹H NMR (500 MHz, CDCl₃) δ 5.61 (ddd, *J* = 17.2, 10.2, 8.9 Hz, 1H), 5.09 (dd, *J* = 17.2, 0.8 Hz, 1H), 5.02 (dd, *J* = 10.3, 1.6 Hz, 1H), 3.72 (dd, *J* = 9.1, 2.6 Hz, 1H), 2.71 (qd, *J* = 7.3, 2.7 Hz, 1H), 2.28 (d, *J* = 8.9 Hz, 1H), 2.19 (s, 3H), 1.14 (d, *J* = 7.2 Hz, 3H), 1.12 (d, *J* = 6.6 Hz, 3H); ¹³C NMR (125 MHz, CDCl₃) δ 214.3, 140.7, 115.5, 73.9, 48.7, 41.7, 29.0, 17.2, 9.2; IR (neat): ν (cm⁻¹) 3444, 2923, 2853, 1701, 1641, 1456, 1420, 1358, 1260, 1087, 999, 981, 916, 796, 682, 505; LRMS (APCI+) calcd C₉H₁₇O₂ [M+H]⁺: 157.12, found 157.55; [α]_D²¹ -23.7 (*c* 0.32, CHCl₃).

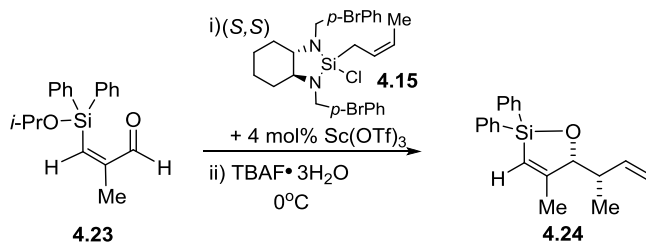


Utilizing the same procedure as above (24 hr reaction time), product **4.22** (57 mg, 71%) was isolated as an orange oil with 3:1 diastereomeric ratio (d.r.) with respect to the newly formed stereocenter. ¹H NMR (500 MHz, CDCl₃) δ 5.80 (ddd, *J* = 16.0, 11.4, 8.4 Hz, 1H), 5.14 (s, 1H), 5.13 – 5.09 (m, 1H), 3.73 (dd, *J* = 7.7, 3.9 Hz, 1H), 2.70 – 2.63 (m, 1H), 2.29 – 2.23 (m, 1H), 2.21 (s, 3H), 1.16 (d, *J* = 7.1 Hz, 3H), 1.01 (d, *J* = 6.8 Hz, 3H); ¹³C NMR (125 MHz, CDCl₃) δ 212.9, 140.8, 116.5, 74.5, 48.9, 41.8, 29.0, 16.8, 10.0; IR (neat): ν (cm⁻¹) 3451, 3082, 2970,

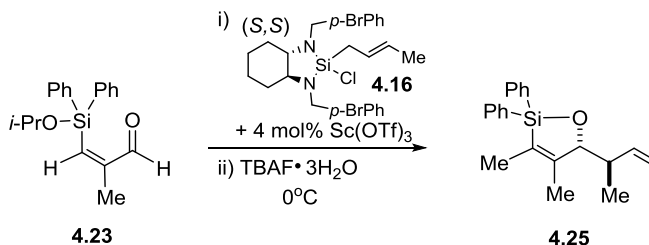
2926, 1704, 1644, 1456, 1430, 1357, 1267, 1133, 998, 916, 741, 698, 498; LRMS (APCI+) calcd C₉H₁₇O₂ [M+H]⁺: 157.12, found 157.60; [α]¹⁹_D -20.9 (c 0.11, CHCl₃).



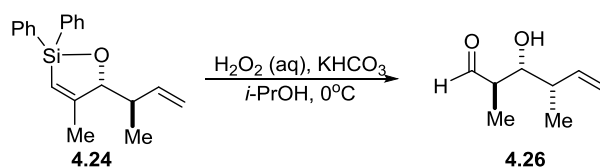
To a cooled (-78°C) glass liner for a Parr bomb charged with isopropoxydiphenylsilane **4.10c** (1.03 g, 4.25 mmol) was added propyne (~0.7 mL, ~13 mmol, condensed into a cooled (-78°C) pre-marked vial) via cannula, followed by benzene (4.2 mL). Once the solution was frozen, Rh(acac)(CO)₂ (11 mg, 0.0425 mmol) was added on top. The bomb was assembled and pressurized to 300 psi with CO, and then allowed to warm to ambient temperature and begin stirring. After 5 hours, the bomb was carefully vented and opened. ¹H NMR analysis of an aliquot indicated complete consumption of silane starting material and formation of product **4.23**. This reaction solution was used directly in the following crotylation reaction. For characterization purposes, an analytically pure sample of **4.23** was obtained by flash chromatography (pH 7 buffered silica gel, 2% EtOAc/hexanes): ¹H NMR (400 MHz, CDCl₃) δ 10.04 (s, 1H), 7.70 – 7.59 (m, 4H), 7.49 – 7.35 (m, 6H), 7.10 (s, 1H), 4.13 (hept, *J* = 6.0 Hz, 1H), 2.01 (d, *J* = 0.7 Hz, 3H), 1.16 (d, *J* = 6.1 Hz, 6H); ¹³C NMR (125 MHz, CDCl₃) δ 194.7, 155.1, 145.5, 134.9, 134.8, 130.4, 128.3, 66.9, 25.7, 19.0; IR (neat): ν (cm⁻¹) 2973, 1689, 1592, 1428, 1371, 1318, 1112, 1020, 879, 833, 733, 702, 511; LRMS (FAB+) calcd C₁₉H₂₂O₂SiNa [M+Na]⁺: 333.13, found 333.13.



To a solution of the reaction mixture from aldehyde **4.23** formation in CH_2Cl_2 (42.5 mL) was added (*S,S*)-*cis*-crotylsilane reagent **4.15** (2.66 g, 4.68 mmol) and Sc(OTf)_3 (84 mg, 0.170 mmol). After 1.5 hours at ambient temperature, the reaction was cooled to 0°C , and then tetrabutylammonium fluoride (TBAF) trihydrate (1.34 g, 4.25 mmol) was added. After 1 hour, the mixture was concentrated and the residue purified via flash chromatography on silica gel (gradient of 100% hexanes to 2% EtOAc/hexanes) to afford **4.24** (1.18 g, 91% over 2 steps) as a colorless oil. ^1H NMR (500 MHz, CDCl_3) δ 7.64 (d, $J = 6.8$ Hz, 2H), 7.52 (d, $J = 6.8$ Hz, 2H), 7.47 – 7.29 (m, 6H), 6.08 (ddd, $J = 17.4, 10.3, 7.1$ Hz, 1H), 5.98 (s, 1H), 5.10 (d, $J = 17.3$ Hz, 1H), 5.06 (d, $J = 10.3$ Hz, 1H), 4.81 (s, 1H), 2.56 (dq, $J = 7.1, 6.9$ Hz, 1H), 1.97 (s, 3H), 0.77 (d, $J = 6.9$ Hz, 3H); ^{13}C NMR (125 MHz, CDCl_3) δ 163.5, 142.6, 135.8, 135.1, 135.0, 134.8, 130.2, 128.5, 127.9, 127.9, 121.1, 114.0, 88.9, 40.7, 19.3, 12.2; IR (neat): ν (cm^{-1}) 3068, 2972, 2849, 1587, 1428, 1113, 1015, 973, 822, 738, 699, 528, 491; LRMS (APCI+) calcd $\text{C}_{20}\text{H}_{23}\text{OSi}$ $[\text{M}+\text{H}]^+$: 307.14, found 306.85; $[\alpha]^{19}_{\text{D}} -34.7$ (c 1.48, CHCl_3). Chiral GC analysis of **4.26** (Supelco β -dex 325, Isothermal 80°C , 1 mL/min) revealed that **4.24** was produced in 96% enantiomeric excess (ee).

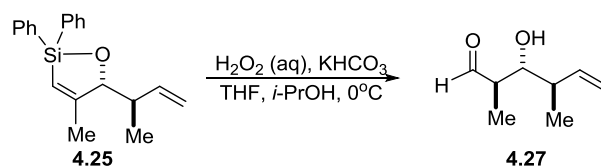


Utilizing the same procedure as above, product **4.25** (1.02 g, 86% over 2 steps) was isolated as a colorless oil. ^1H NMR (500 MHz, CDCl_3) δ 7.64 (dd, $J = 7.9, 1.4$ Hz, 2H), 7.54 (dd, $J = 7.9, 1.4$ Hz, 2H), 7.47 – 7.30 (m, 6H), 5.91 (s, 1H), 5.58 (ddd, $J = 17.4, 10.3, 8.0$ Hz, 1H), 4.99 (ddd, $J = 17.3, 1.8, 1.2$ Hz, 1H), 4.86 (dd, $J = 10.3, 1.2$ Hz, 1H), 4.71 (s, 1H), 2.60 (pd, $J = 8.0, 2.2$ Hz, 1H), 1.95 (s, 3H), 1.22 (d, $J = 6.9$ Hz, 3H); ^{13}C NMR (125 MHz, CDCl_3) δ 164.0, 138.9, 136.0, 135.3, 135.0, 130.2, 127.9, 127.8, 125.1, 120.4, 115.1, 89.3, 41.7, 19.3, 17.8; IR (neat): ν (cm^{-1}) 3068, 2974, 1747, 1587, 1428, 1116, 1016, 953, 809, 738, 699, 528, 492; LRMS (APCI+) calcd $\text{C}_{20}\text{H}_{23}\text{OSi}$ $[\text{M}+\text{H}]^+$: 307.14, found 306.83; $[\alpha]^{19}_{\text{D}} -95.9$ (c 1.56, CHCl_3). Chiral GC analysis of **4.27** (Supelco β -dex 325, Isothermal 90°C , 1 mL/min) revealed that **4.25** was produced in 99% enantiomeric excess (ee).



To a cooled (0°C) solution of **4.24** (519 mg, 1.69 mmol) in *i*-PrOH (16.9 mL) was added KHCO_3 (169 mg, 1.69 mmol) followed by 30% H_2O_2 aqueous solution (2.24 mL, 22.0 mmol). After 2 hours, the solution was diluted with distilled water (6 mL) and extracted with DCM (4 x 10 mL). The combined organic layers were washed with brine, dried over MgSO_4 , filtered, and concentrated. Purification of the residue by flash chromatography (pH 7 buffered silica gel, 15% EtOAc/hexanes) afforded the product **4.26** as a yellow oil (167 mg, 69%) in $>20:1$ d.r. ^1H NMR (400 MHz, CDCl_3) δ 9.78 (d, $J = 1.8$ Hz, 1H), 5.90 – 5.71 (m, 1H), 5.14 (d, $J = 1.1$ Hz, 1H), 5.12 – 5.10 (m, 1H), 3.71 – 3.59 (m, 1H), 2.67 – 2.59 (m, 1H), 2.52 – 2.40 (m, 1H), 2.11 (d, $J = 5.0$ Hz, 1H), 1.14 (d, $J = 7.3$ Hz, 3H), 1.07 (d, $J = 6.8$ Hz, 3H); ^{13}C NMR (125 MHz, CDCl_3) δ 205.5, 140.9, 116.0, 75.9, 49.1, 40.8, 13.4, 11.2; IR (neat): ν (cm^{-1}) 3448, 2974, 2880, 1717,

1640, 1456, 1376, 1232, 1078, 996, 917, 756, 679; LRMS (FAB+) calcd C₈H₁₄O₂ [M+H]⁺: 143.10, found 143.13; [α]¹⁹_D -7.9 (c 0.59, CHCl₃).



To a cooled (0°C) solution of **4.25** (501 mg, 1.63 mmol) in THF (8.2 mL) and *i*-PrOH (8.2 mL) was added KHCO₃ (171 mg, 1.71 mmol) followed by 30% H₂O₂ aqueous solution (2.1 mL, 21.2 mmol). After 4 hours, the solution was diluted with distilled water (6 mL) and extracted with DCM (4 x 10 mL). The combined organic layers were washed with brine, dried over MgSO₄, filtered, and concentrated. Purification of the residue by flash chromatography (pH 7 buffered silica gel, 15% EtOAc/hexanes) afforded the product **4.27** as a yellow oil (159 mg, 69%) in 17:1 d.r. ¹H NMR (400 MHz, CDCl₃) δ 9.77 (d, *J* = 2.0 Hz, 1H), 5.80 (ddd, *J* = 17.0, 10.5, 8.6 Hz, 1H), 5.17 – 5.15 (m, 1H), 5.15 – 5.10 (m, 1H), 3.65 – 3.62 (m, 1H), 2.55 – 2.51 (m, 1H), 2.43 – 2.37 (m, 1H), 2.31 (d, *J* = 3.1 Hz, 1H), 1.15 (d, *J* = 7.3 Hz, 3H), 1.11 (d, *J* = 6.9 Hz, 3H); ¹³C NMR (125 MHz, CDCl₃) δ 205.8, 138.9, 117.1, 76.0, 49.7, 41.3, 17.3, 11.0; IR (neat): ν (cm⁻¹) 3429, 2966, 2928, 2878, 1719, 1639, 1456, 1376, 1097, 997, 967, 915, 569; LRMS (FAB+) calcd C₈H₁₄O₂ [M+H]⁺: 143.10, found 143.10; [α]¹⁹_D +13.1 (c 0.72, CHCl₃).

Stereochemical Proofs.

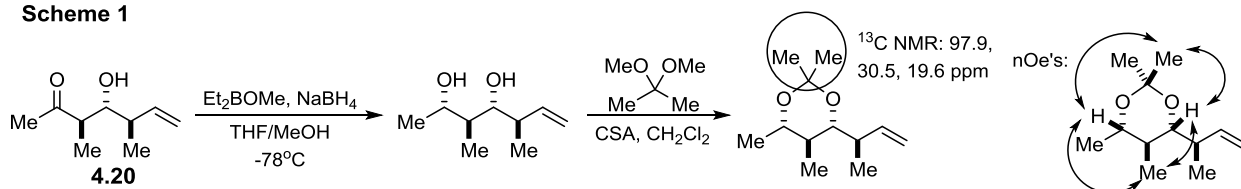
For β -hydroxyketone **4.20**, the proof was achieved by carrying out Narasaka's *syn*-selective reduction using Prasad's protocol⁴ followed by acetonide protection as shown in Scheme 1. Rychnovsky ¹³C NMR analysis⁵ confirmed that the acetonide possessed the 1,3-*syn* stereochemistry. Analysis of the acetonide by COSY and NOESY NMR established the relative stereochemistry of the methyl-bearing stereocenter set in the "standard" Tamao oxidation via the

⁴ Chen, K.-M.; Hardtmann, K.; Prasad, K.; Repič, O.; Shapiro, M.J. *Tetrahedron Lett.* **1987**, 28, 155-158.

⁵ Rychnovsky, S. D.; Rogers, B.; Yang, G. *J. Org. Chem.* **1993**, 58, 3511.

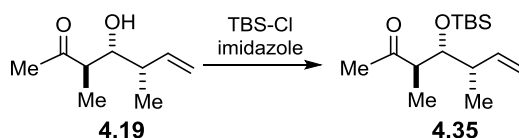
key nOe interactions indicated. Since **4.20** and **4.22** are derived from the same starting material **4.18** (with two of the stereocenters already established), the two compounds represent diastereomers at the α -methyl stereocenter and the stereochemistry of **4.22** must be as assigned.

Scheme 1

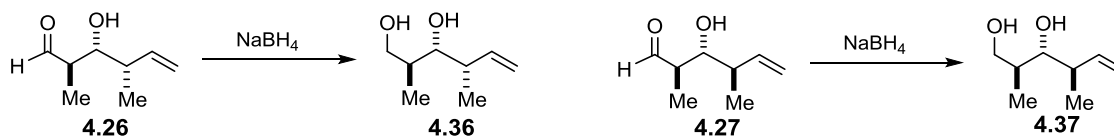


For β -hydroxyketone **4.19**, the proof was achieved by carrying out a TBS protection to intercept previously characterized compound **4.35**,⁶ verified by ^1H NMR. Since **4.19** and **4.21** are derived from the same starting material **4.17** (with two of the stereocenters already established), the two compounds represent diastereomers at the α -methyl stereocenter and the stereochemistry of **4.21** must be as assigned.

Scheme 2



For β -hydroxyaldehyde **4.26**, the proof was achieved by carrying out a sodium borohydride reduction to intercept previously characterized compound **4.36**,^{7,8} verified by ^1H and ^{13}C NMR. For β -hydroxyaldehyde **4.27**, the proof was achieved by carrying out a sodium borohydride reduction to intercept **4.37**, the enantiomer of a previously characterized compound,⁵ verified by ^1H and ^{13}C NMR with the opposite sign in the optical rotation.

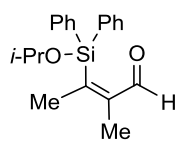


⁶ McGarvey, G. J.; Williams, J.M.; Hiner, R.N.; Matsubara, Y.; Oh, T. *J. Am. Chem. Soc.* **1986**, *108*, 4943-4952.

⁷ Mulzer, J.; Autenrieth-Ansorge, L.; Kirstein, H.; Matsuoka, T.; Münch, W. *J. Org. Chem.* **1987**, *52*, 3784-3789.

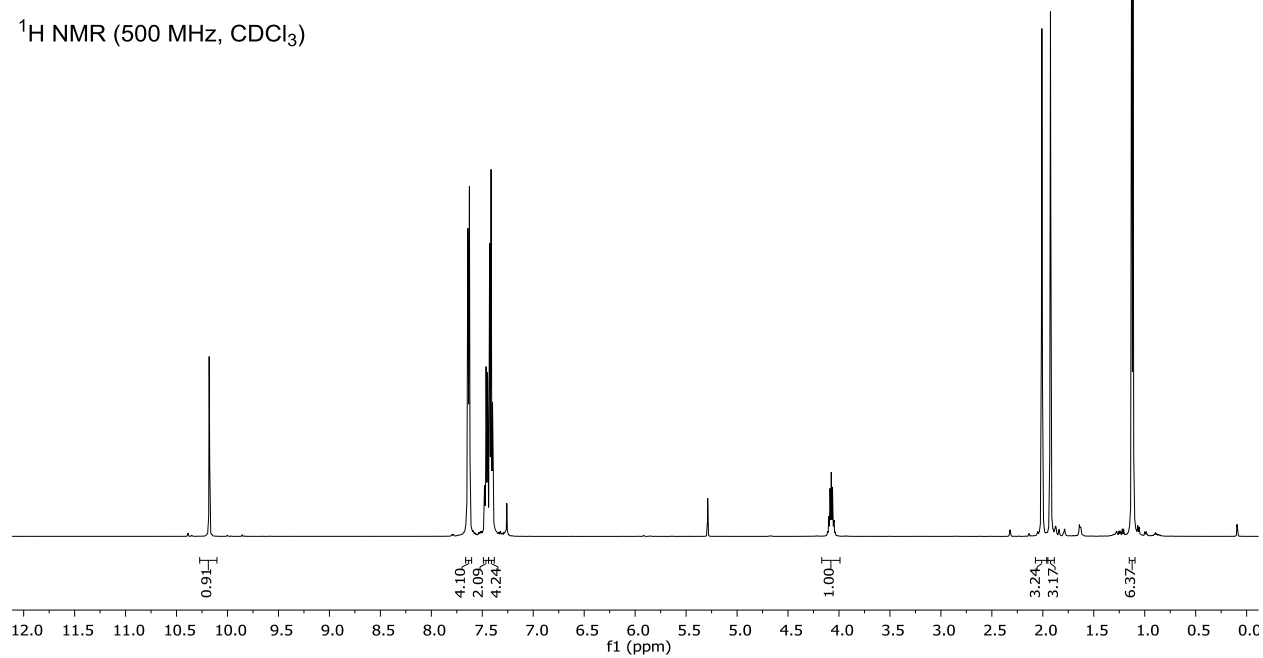
⁸ Marshall, J. A.; Palovich, M.R. *J. Org. Chem.* **1998**, *63*, 4381-4384.

4.10 ^1H and ^{13}C NMR Spectra

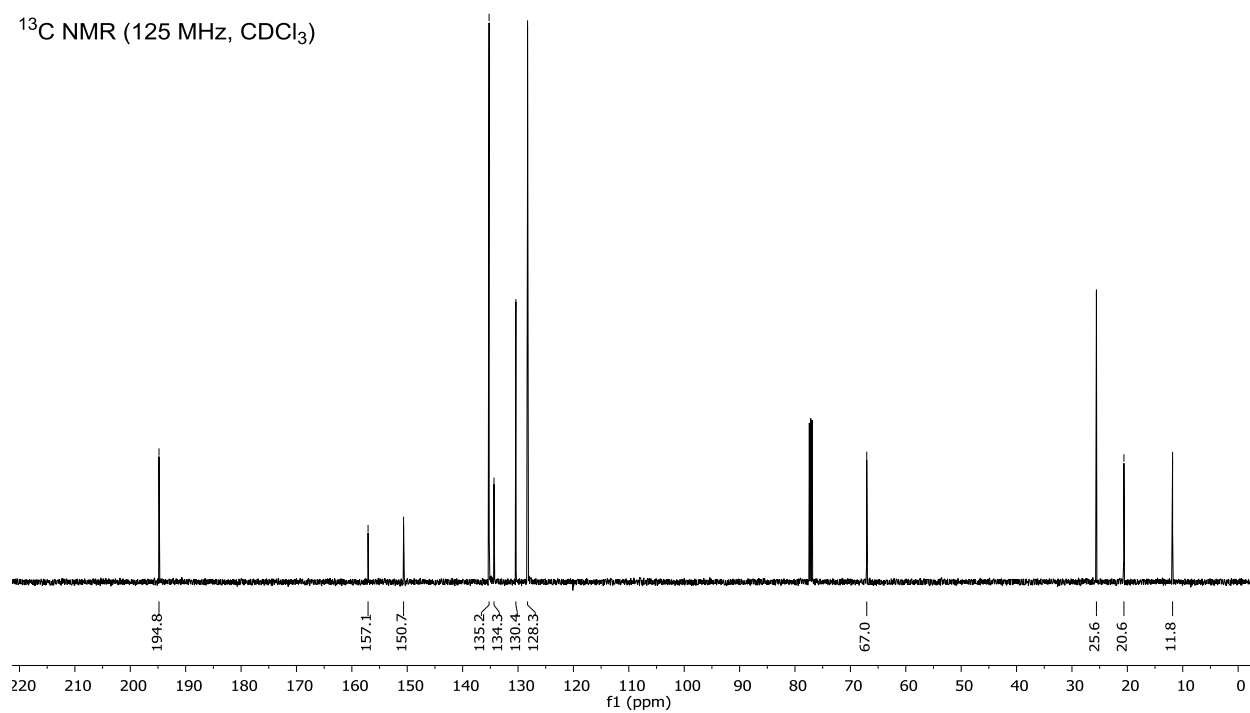


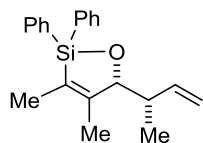
4.11c

^1H NMR (500 MHz, CDCl_3)



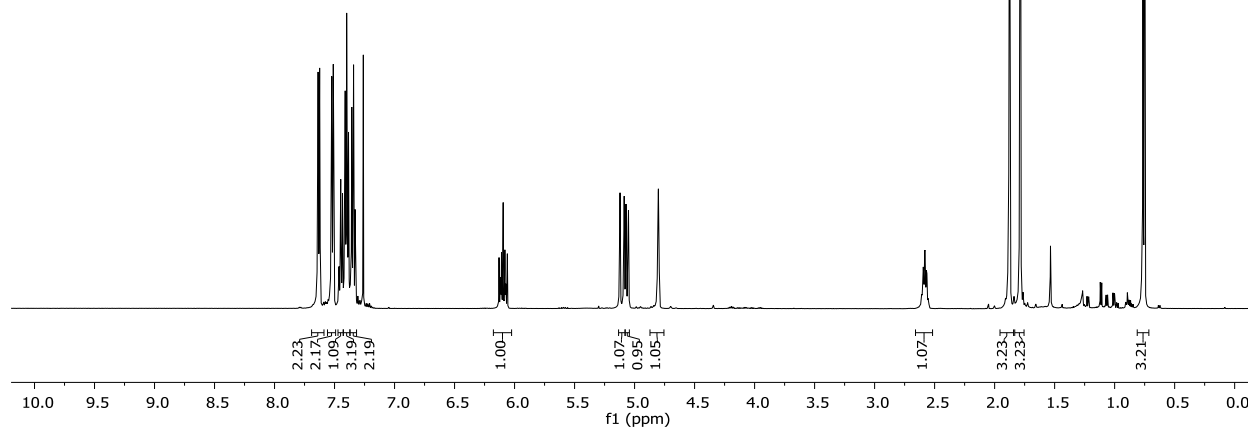
^{13}C NMR (125 MHz, CDCl_3)



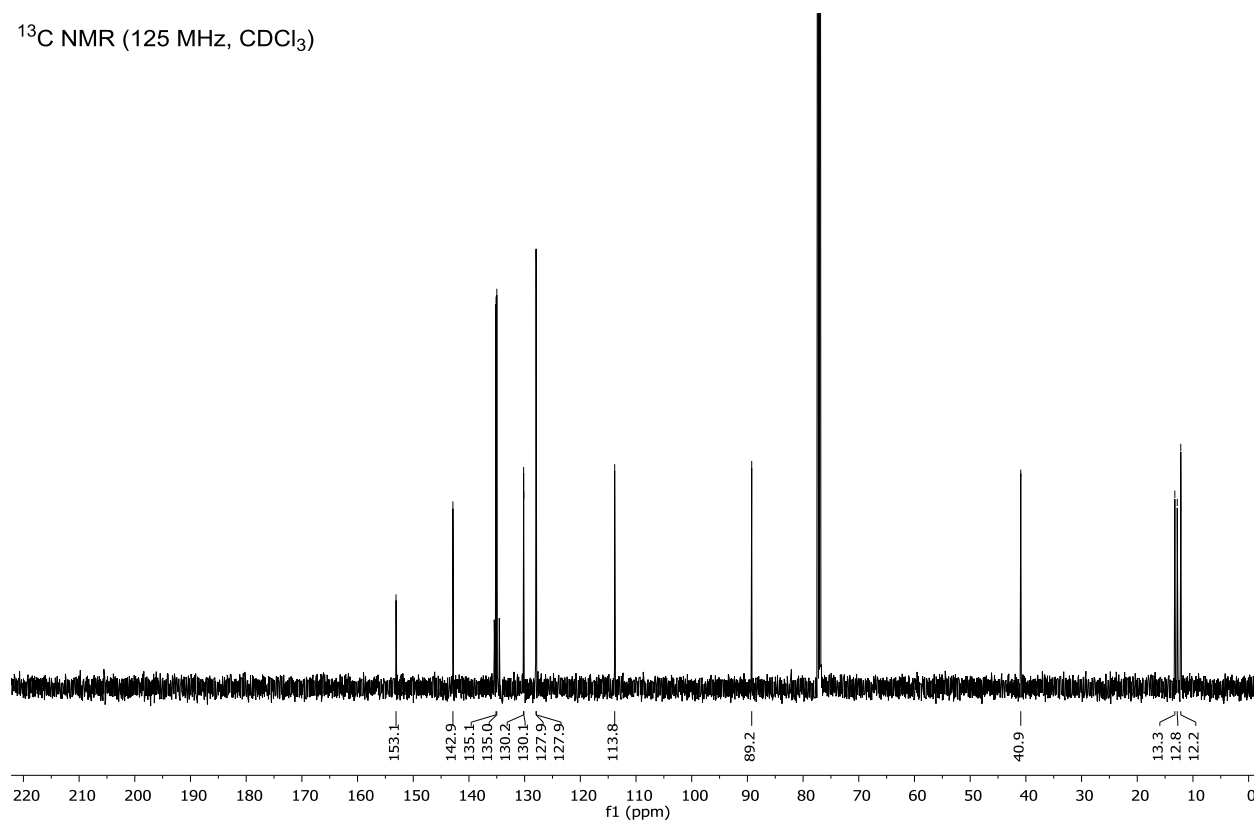


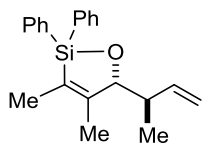
4.17

^1H NMR (500 MHz, CDCl_3)



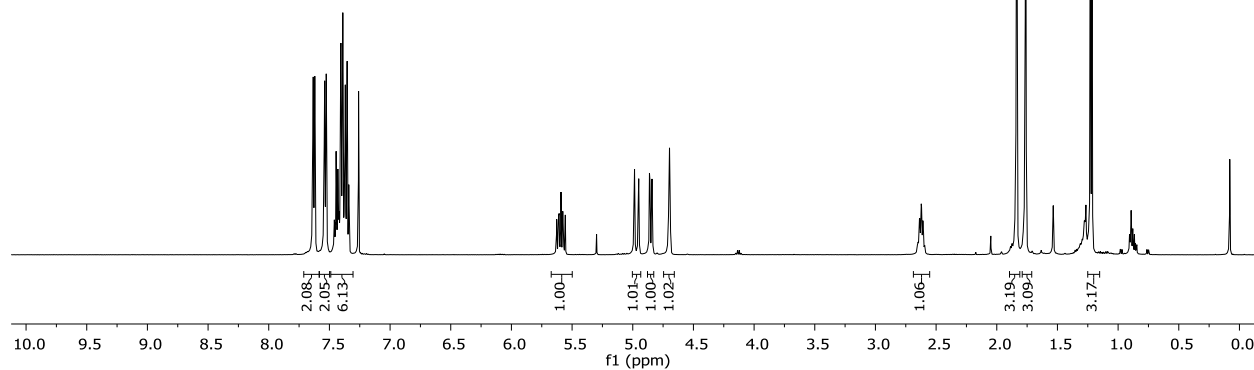
^{13}C NMR (125 MHz, CDCl_3)



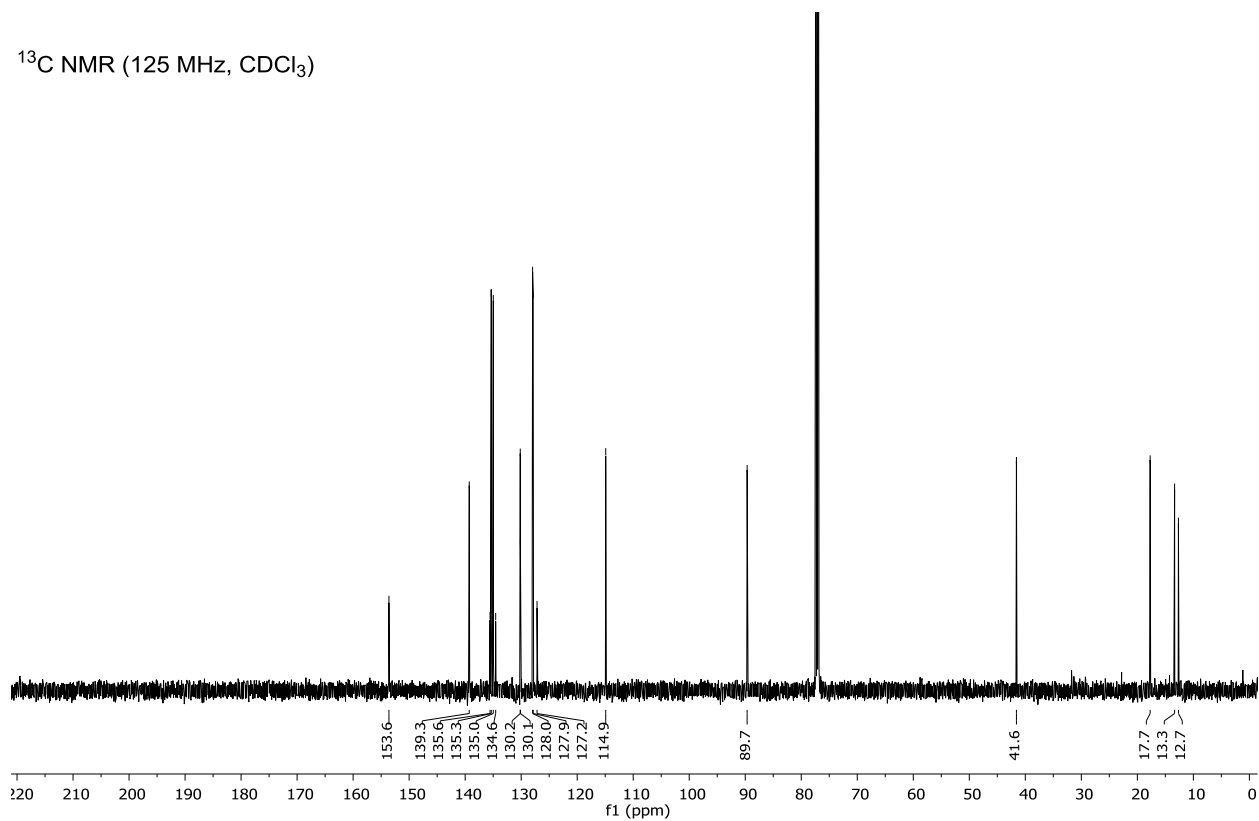


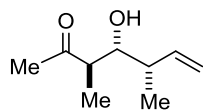
4.18

^1H NMR (500 MHz, CDCl_3)



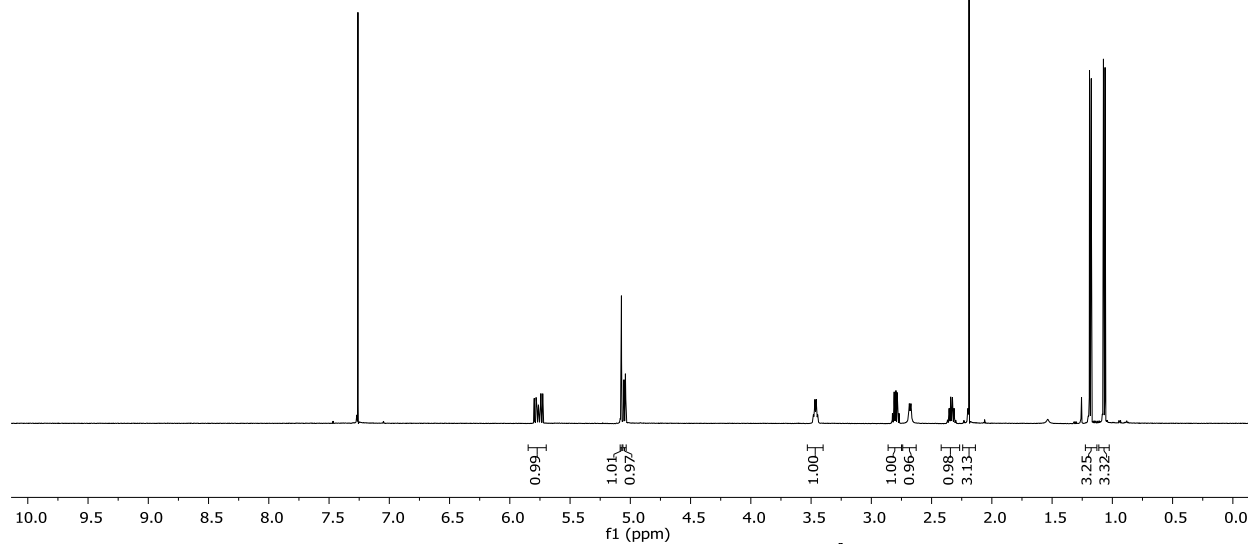
^{13}C NMR (125 MHz, CDCl_3)



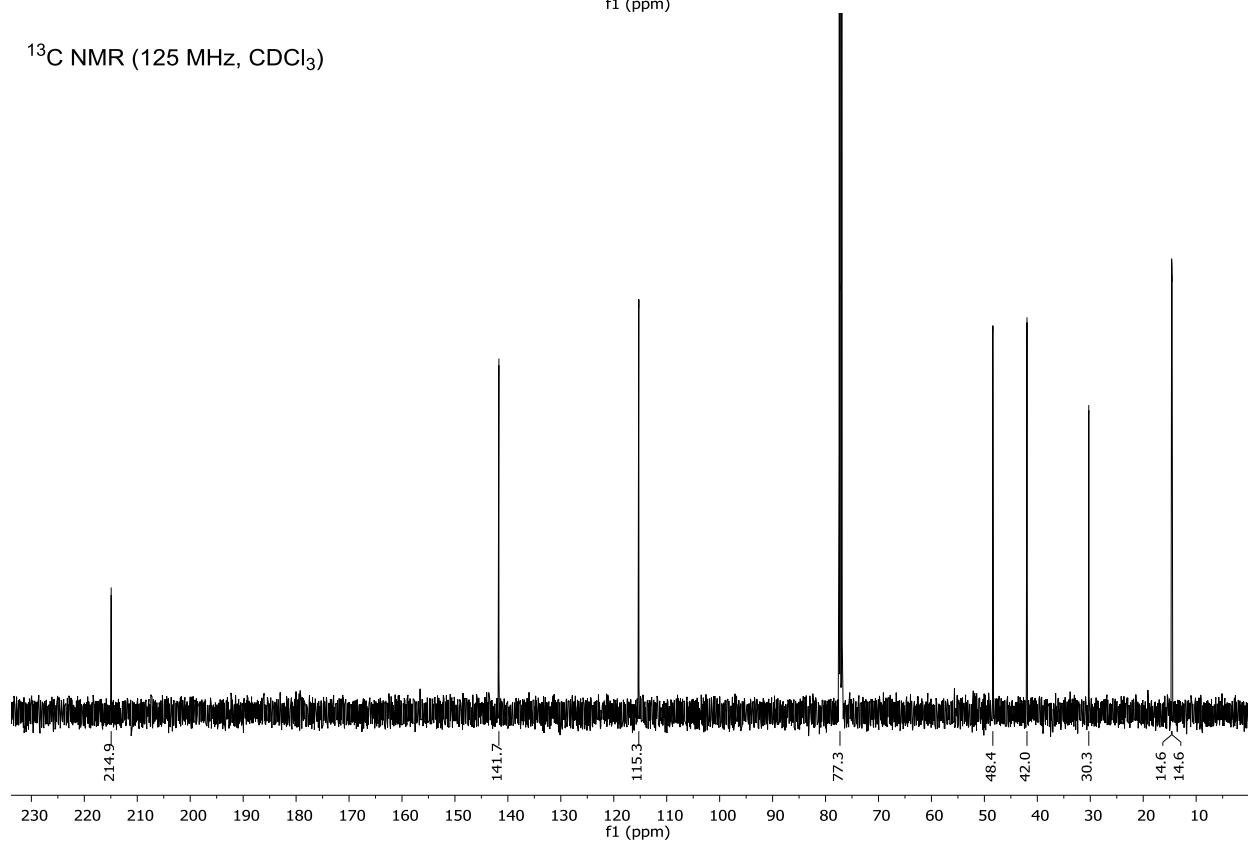


4.19

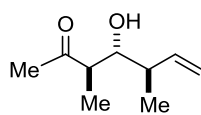
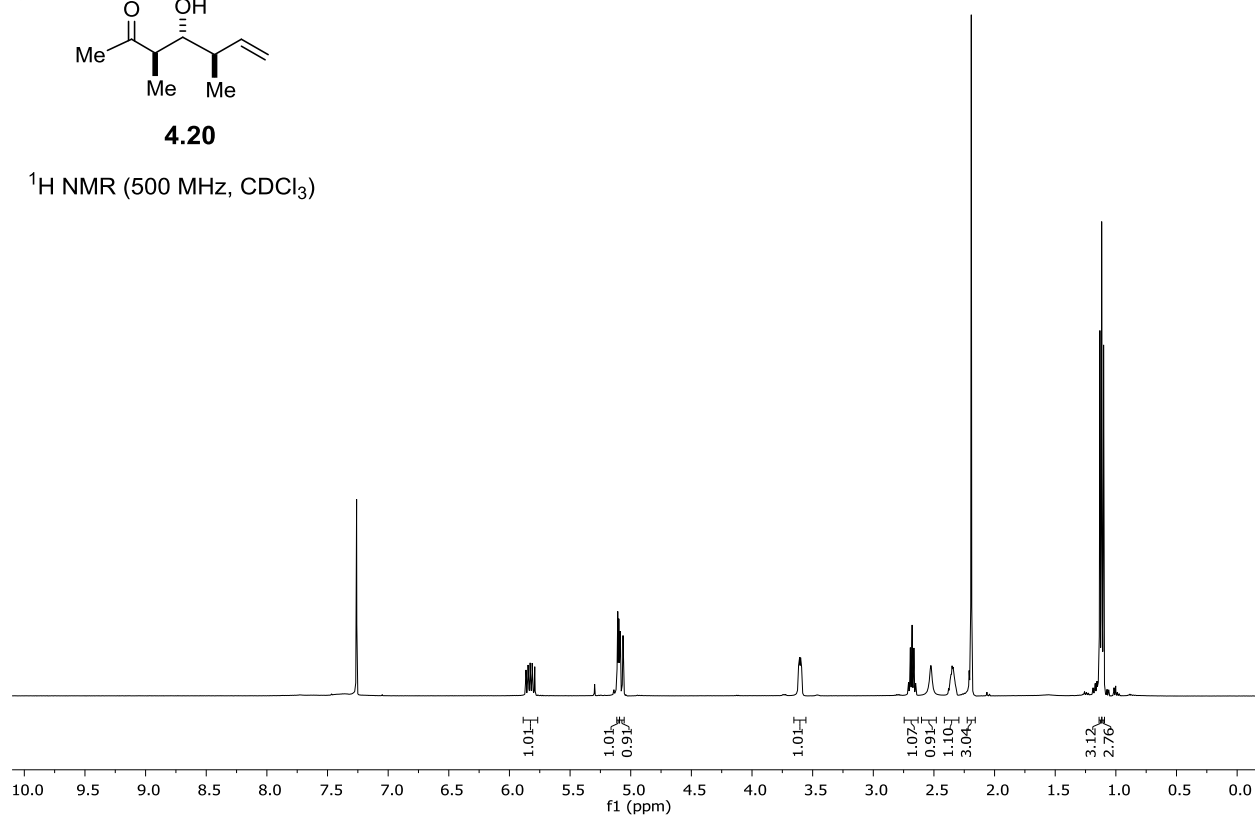
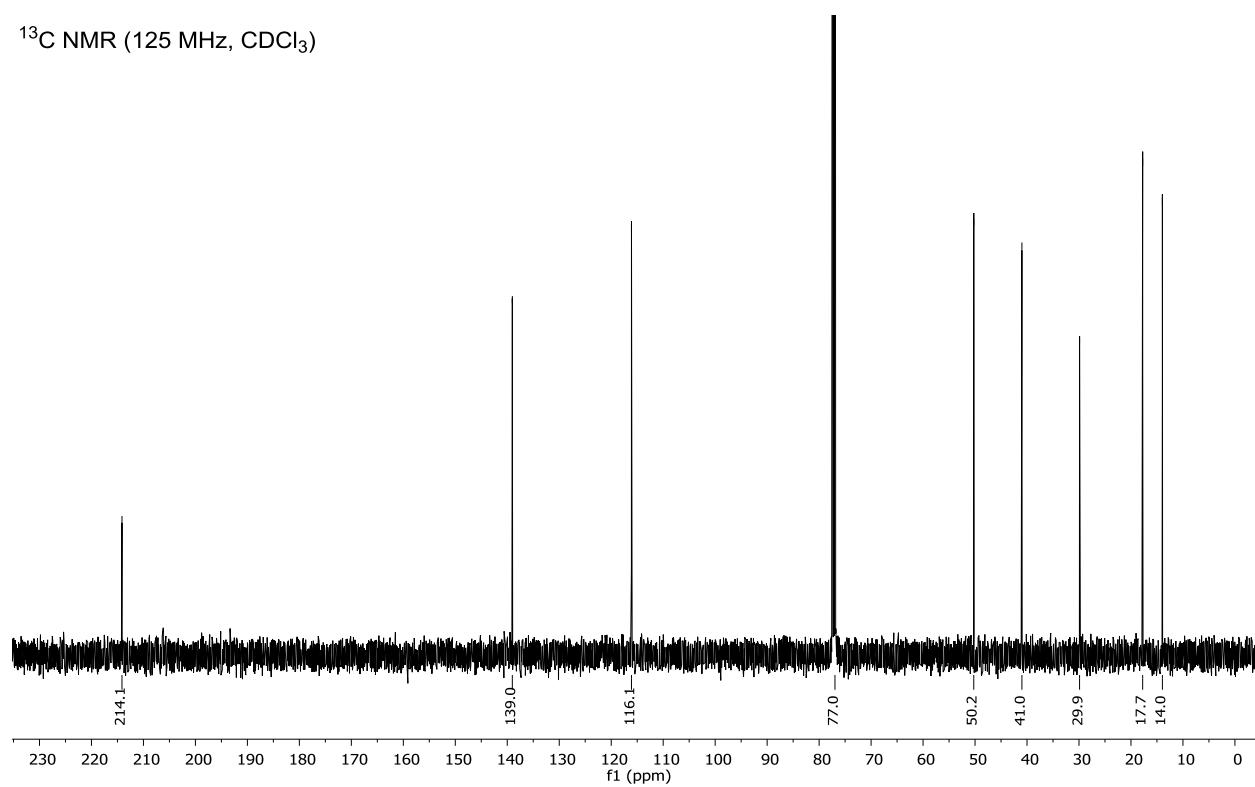
^1H NMR (500 MHz, CDCl_3)

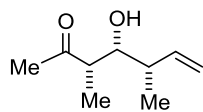


^{13}C NMR (125 MHz, CDCl_3)



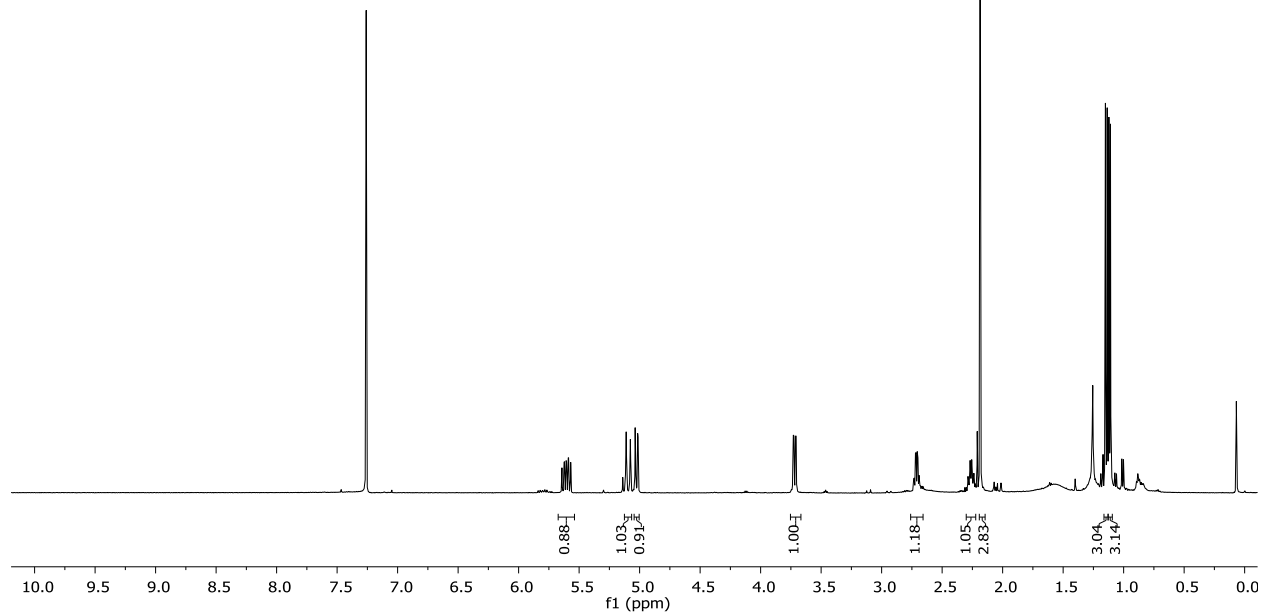
c

**4.20** ^1H NMR (500 MHz, CDCl_3) ^{13}C NMR (125 MHz, CDCl_3)

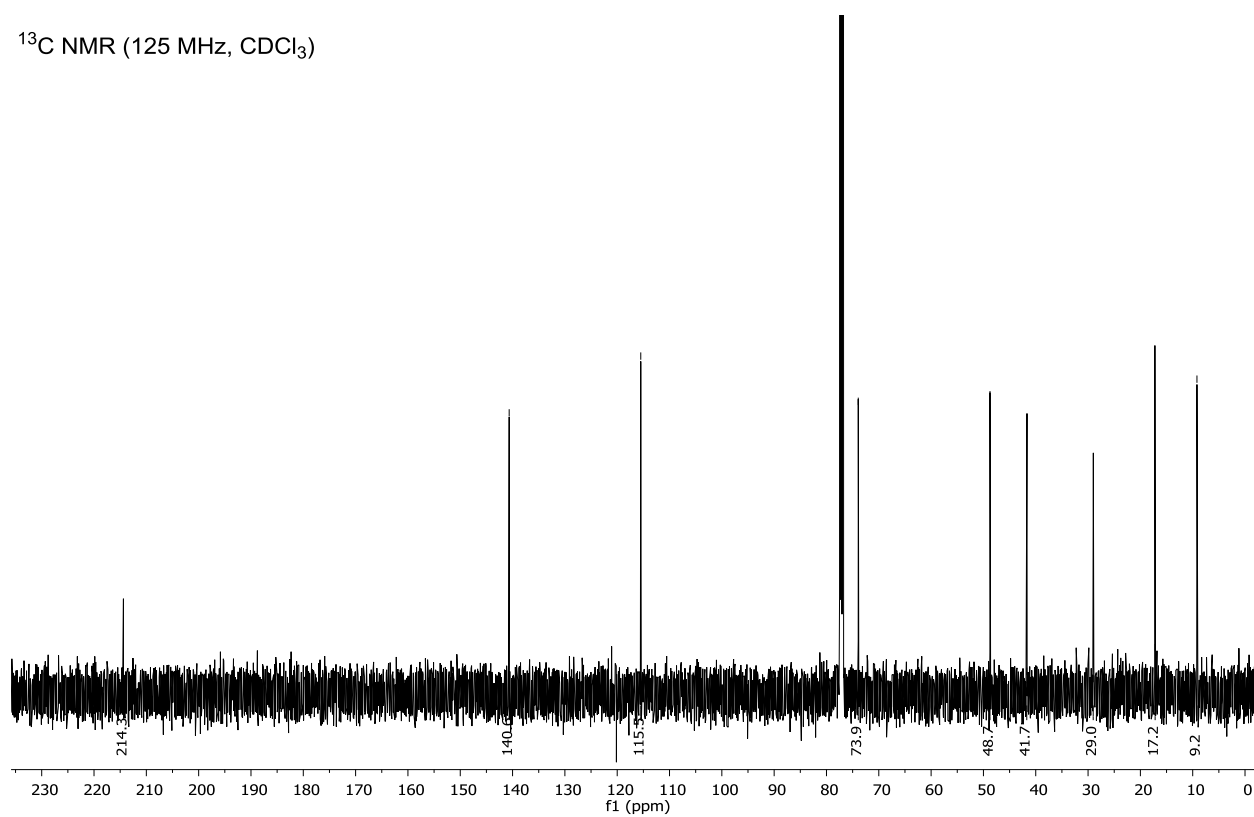


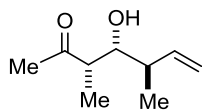
4.21

^1H NMR (500 MHz, CDCl_3)



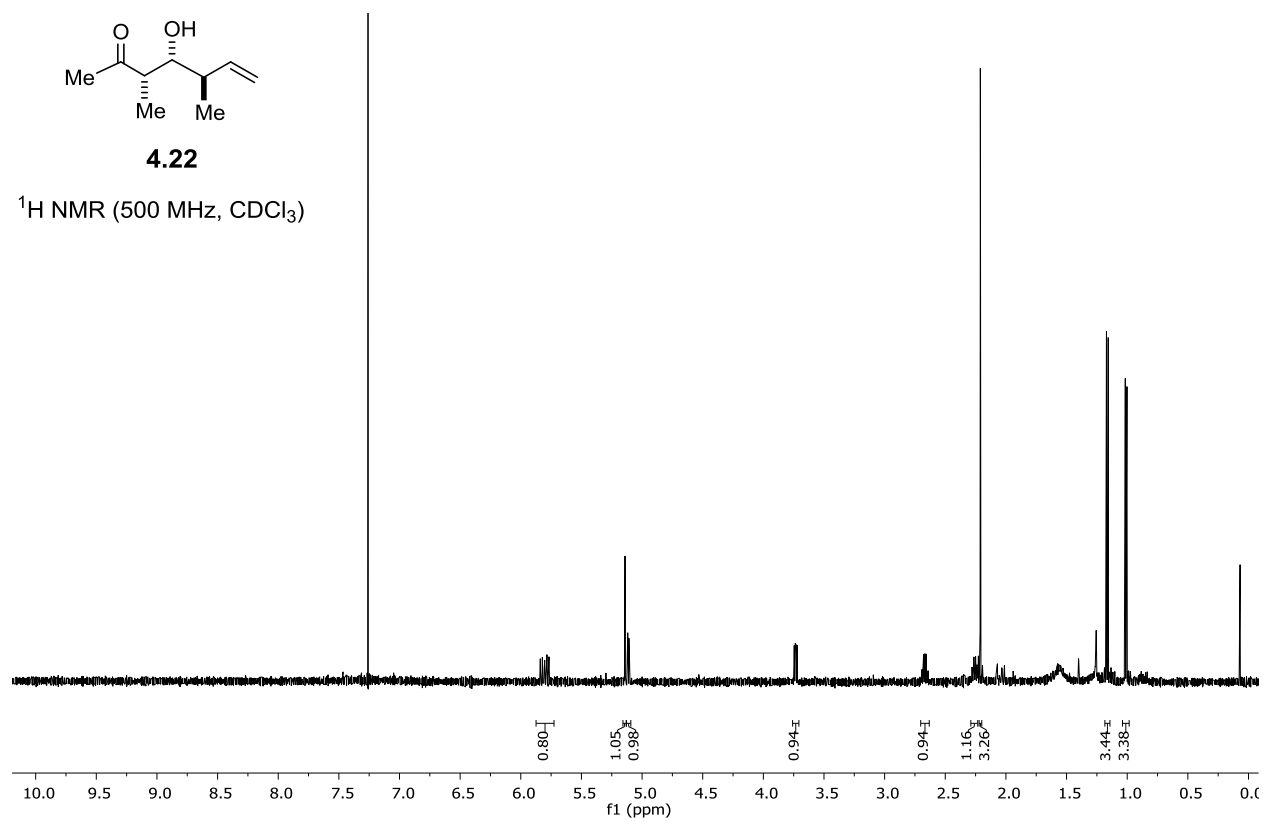
^{13}C NMR (125 MHz, CDCl_3)



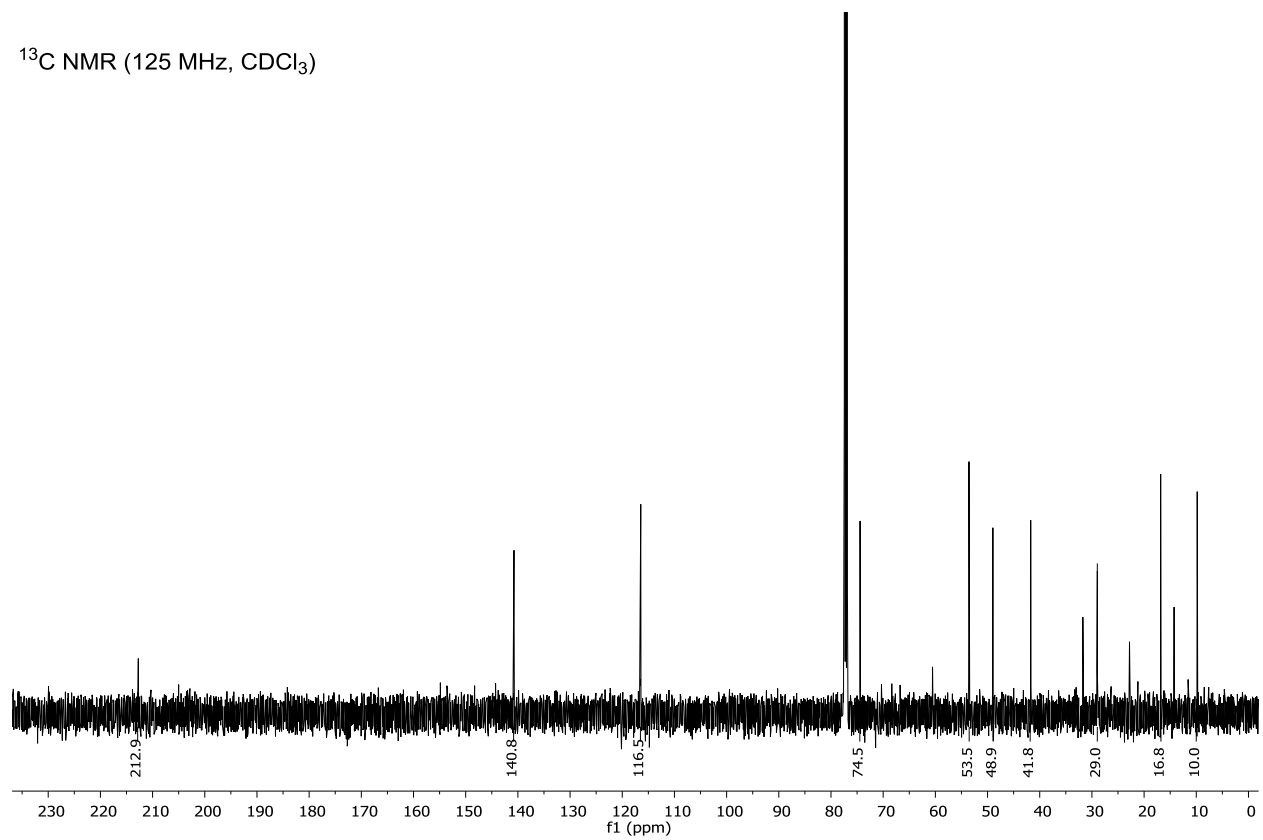


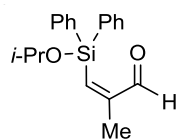
4.22

^1H NMR (500 MHz, CDCl_3)



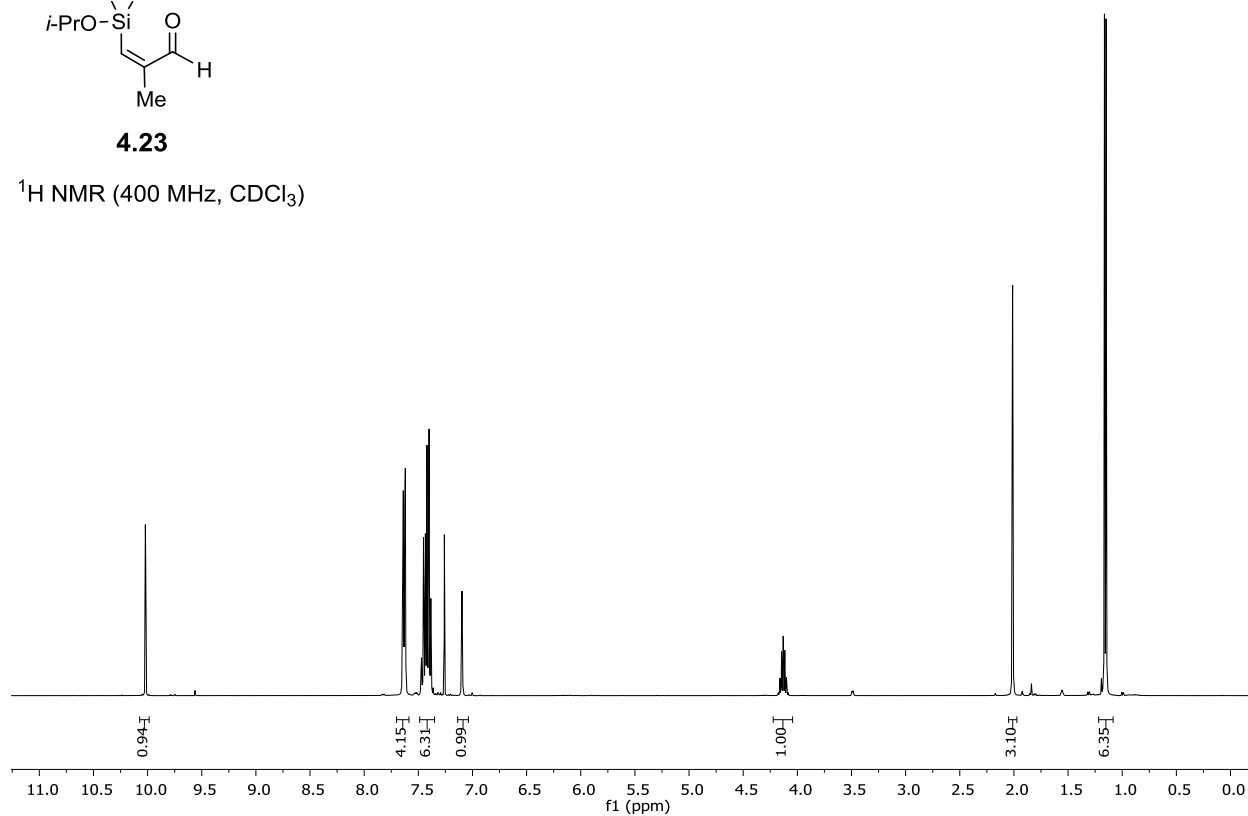
^{13}C NMR (125 MHz, CDCl_3)



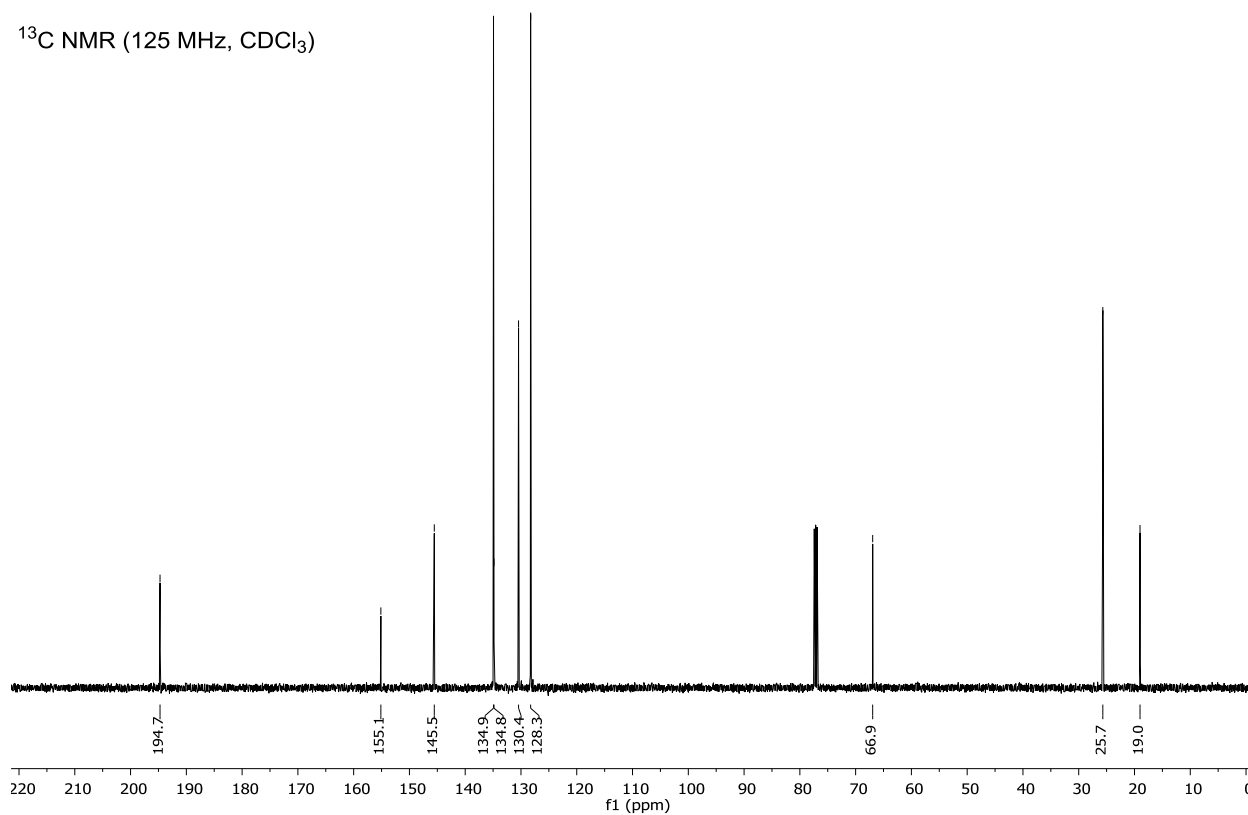


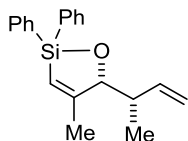
4.23

^1H NMR (400 MHz, CDCl_3)



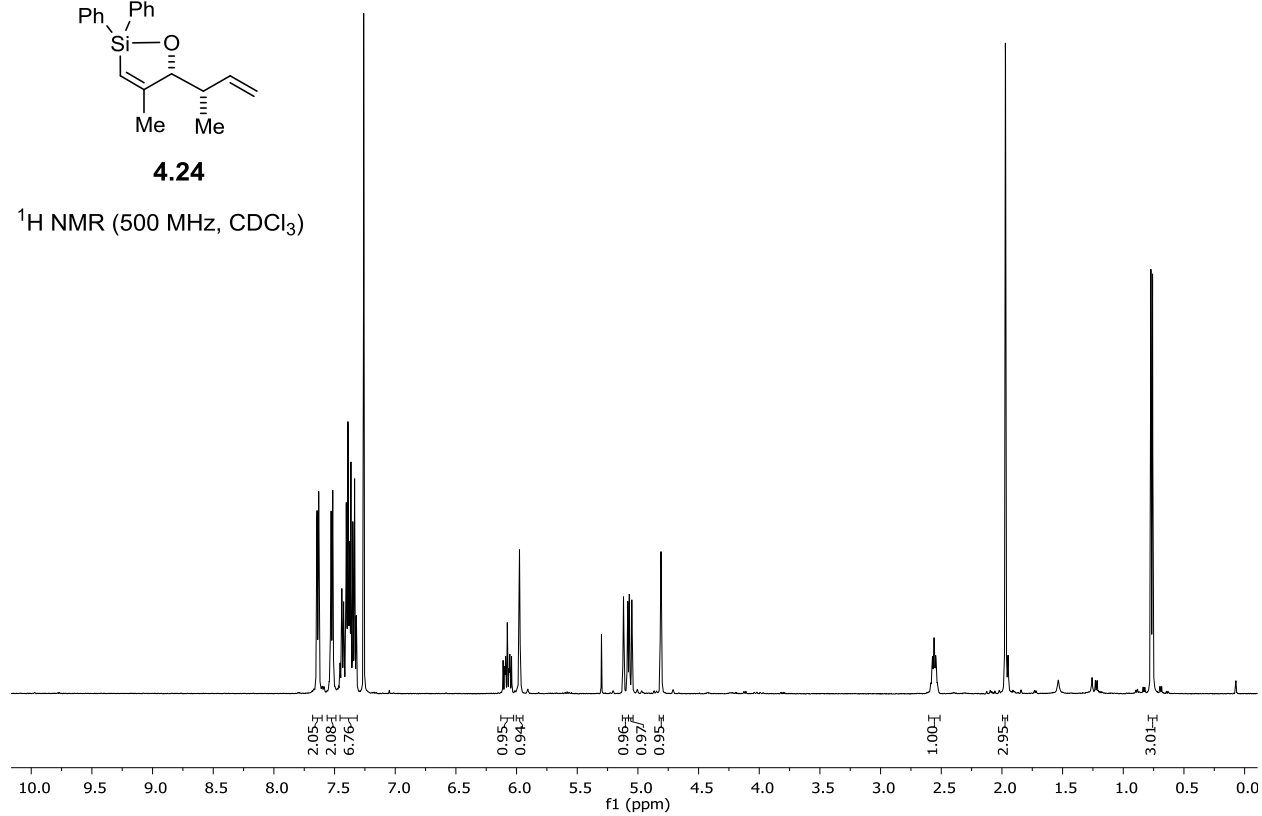
^{13}C NMR (125 MHz, CDCl_3)



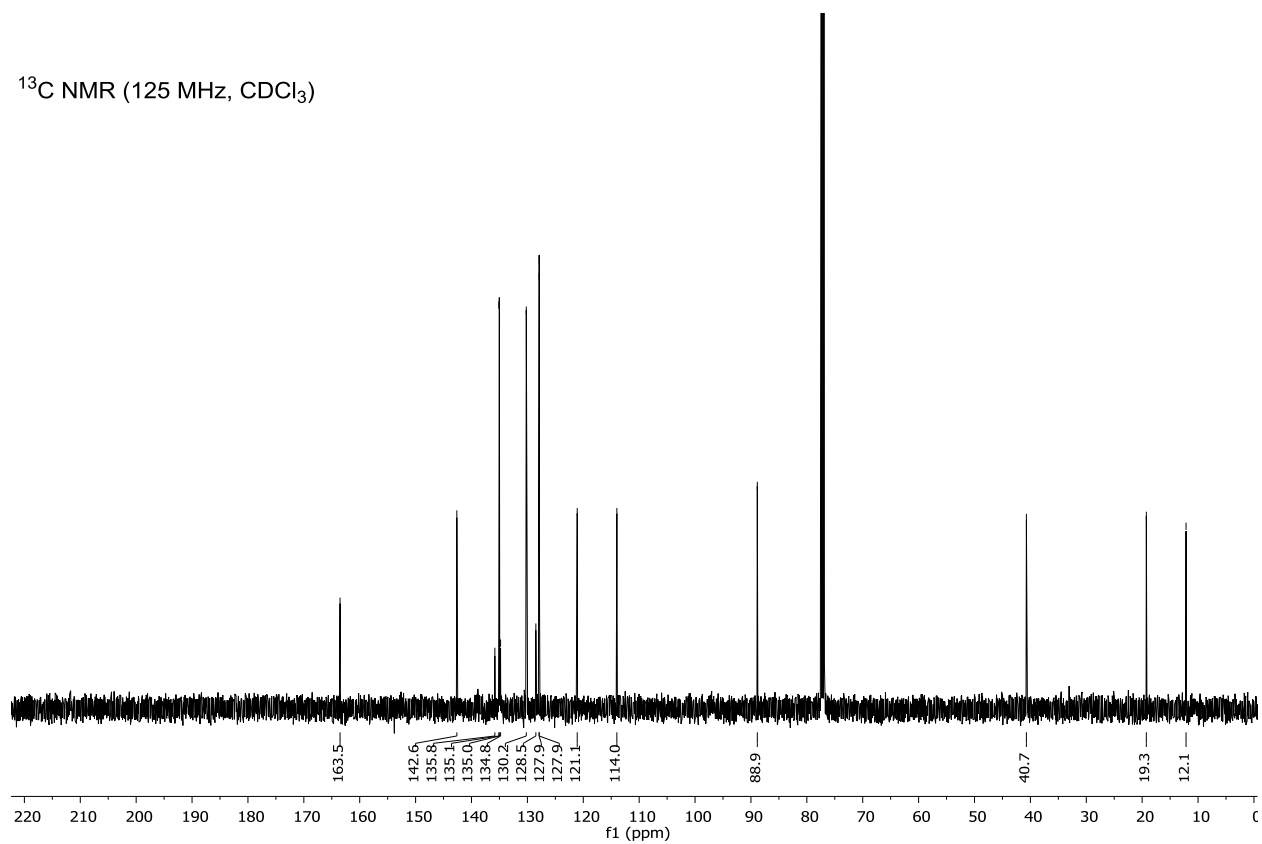


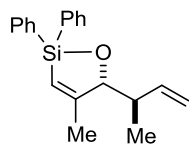
4.24

^1H NMR (500 MHz, CDCl_3)



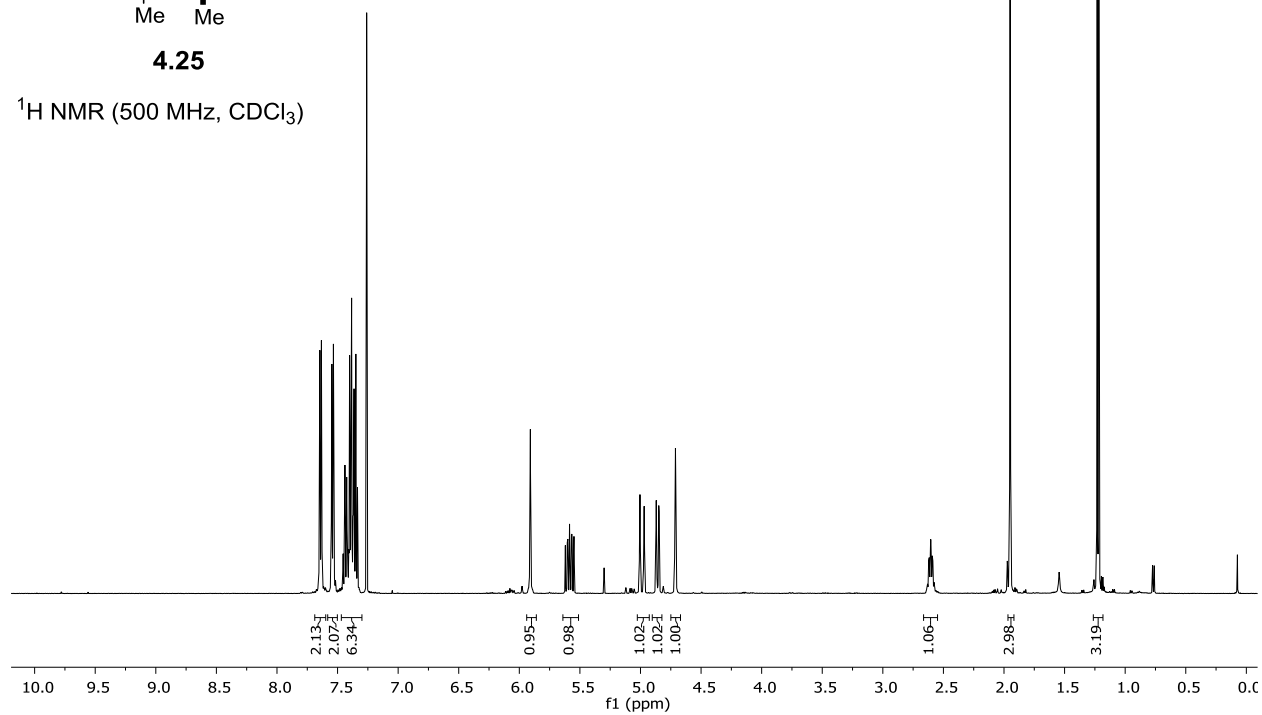
^{13}C NMR (125 MHz, CDCl_3)



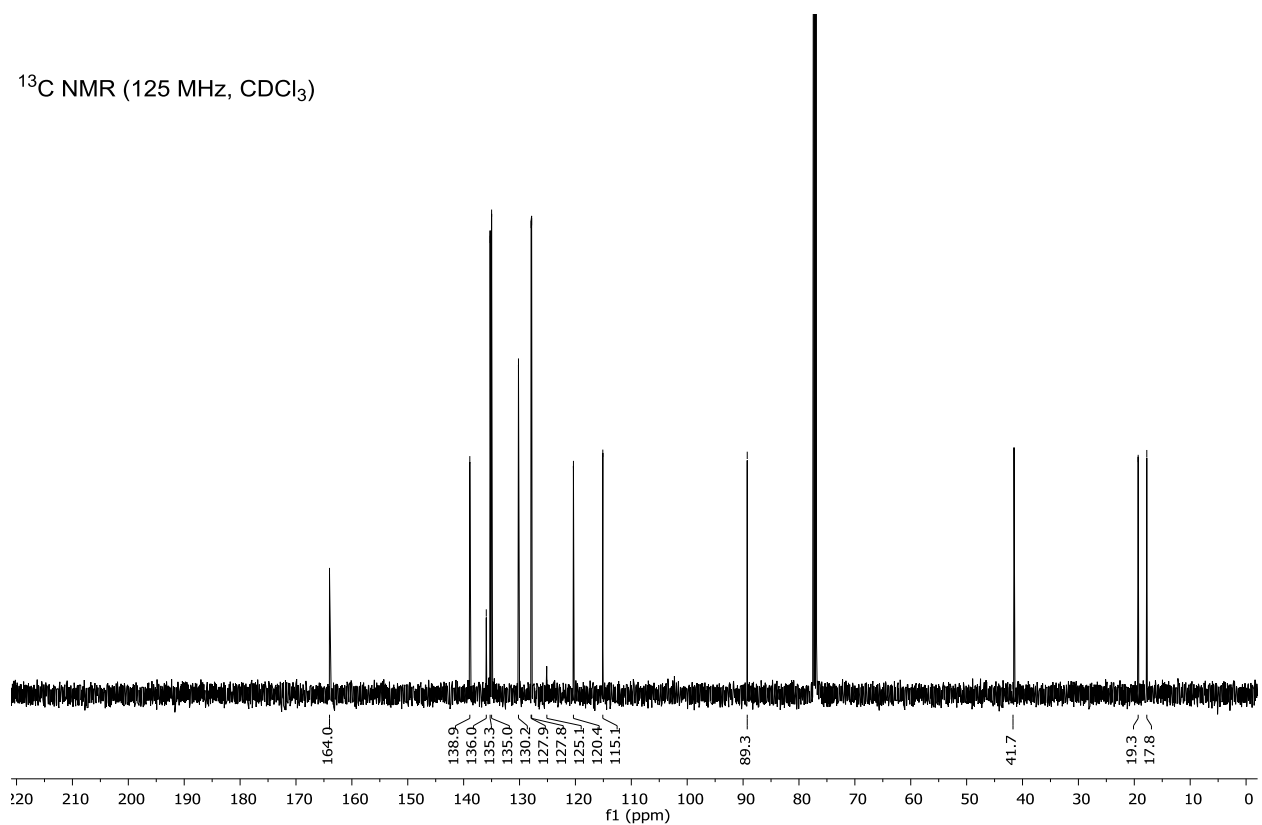


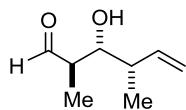
4.25

^1H NMR (500 MHz, CDCl_3)



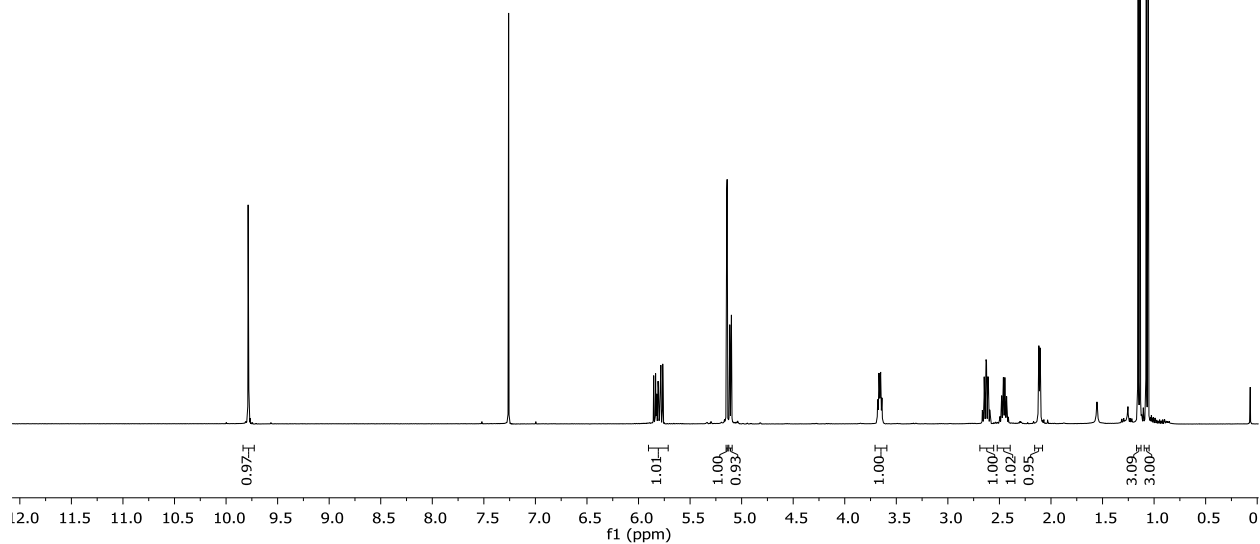
^{13}C NMR (125 MHz, CDCl_3)



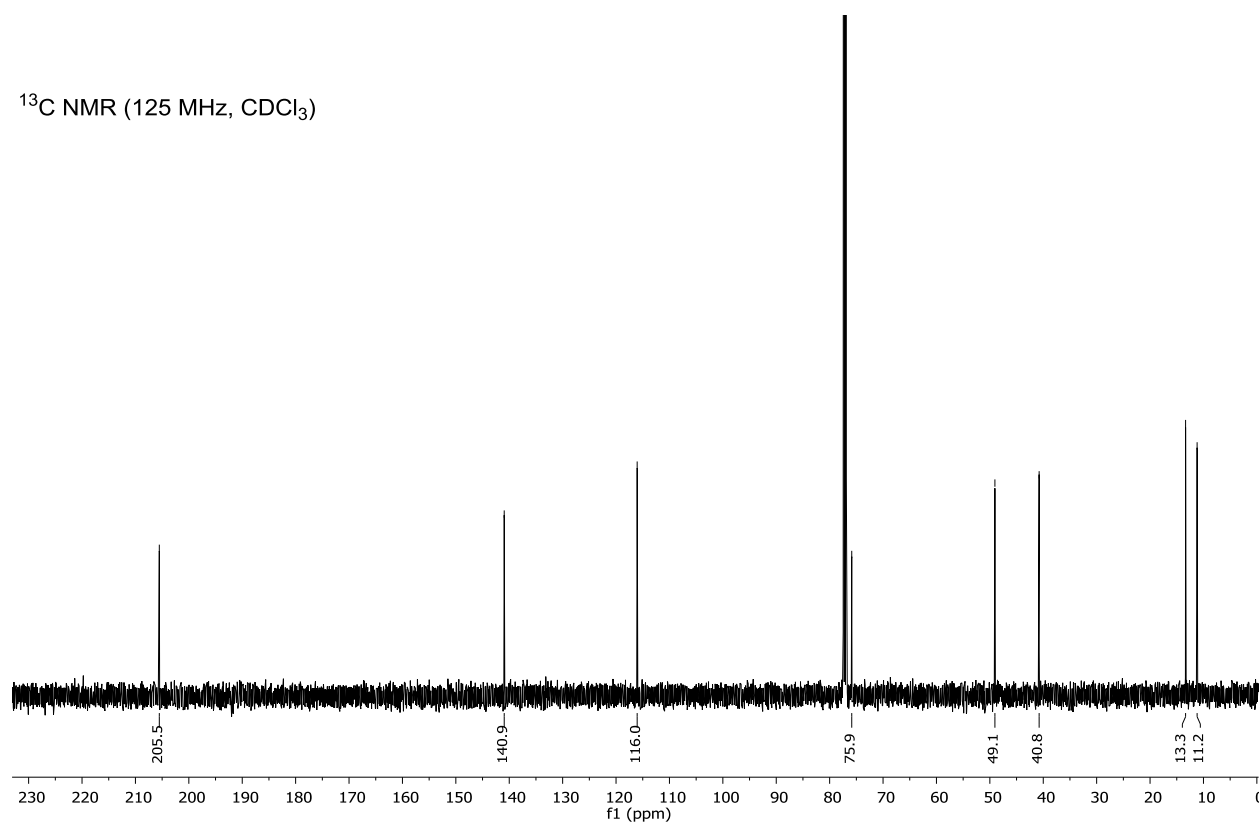


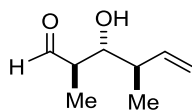
4.26

^1H NMR (400 MHz, CDCl_3)



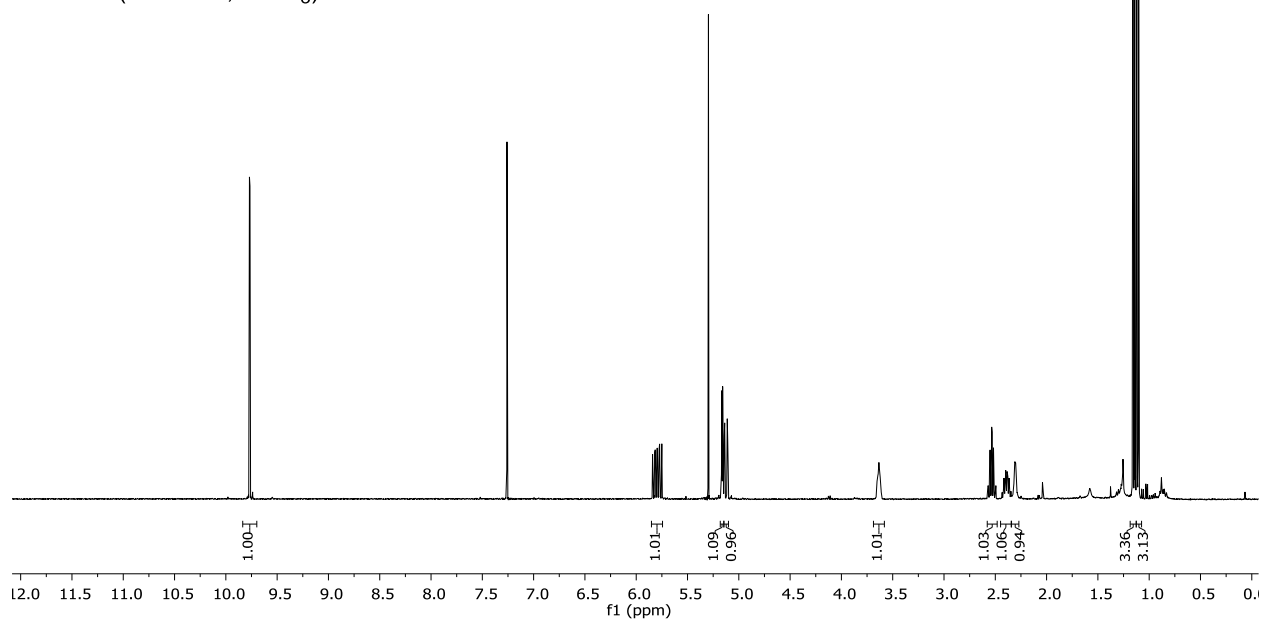
^{13}C NMR (125 MHz, CDCl_3)



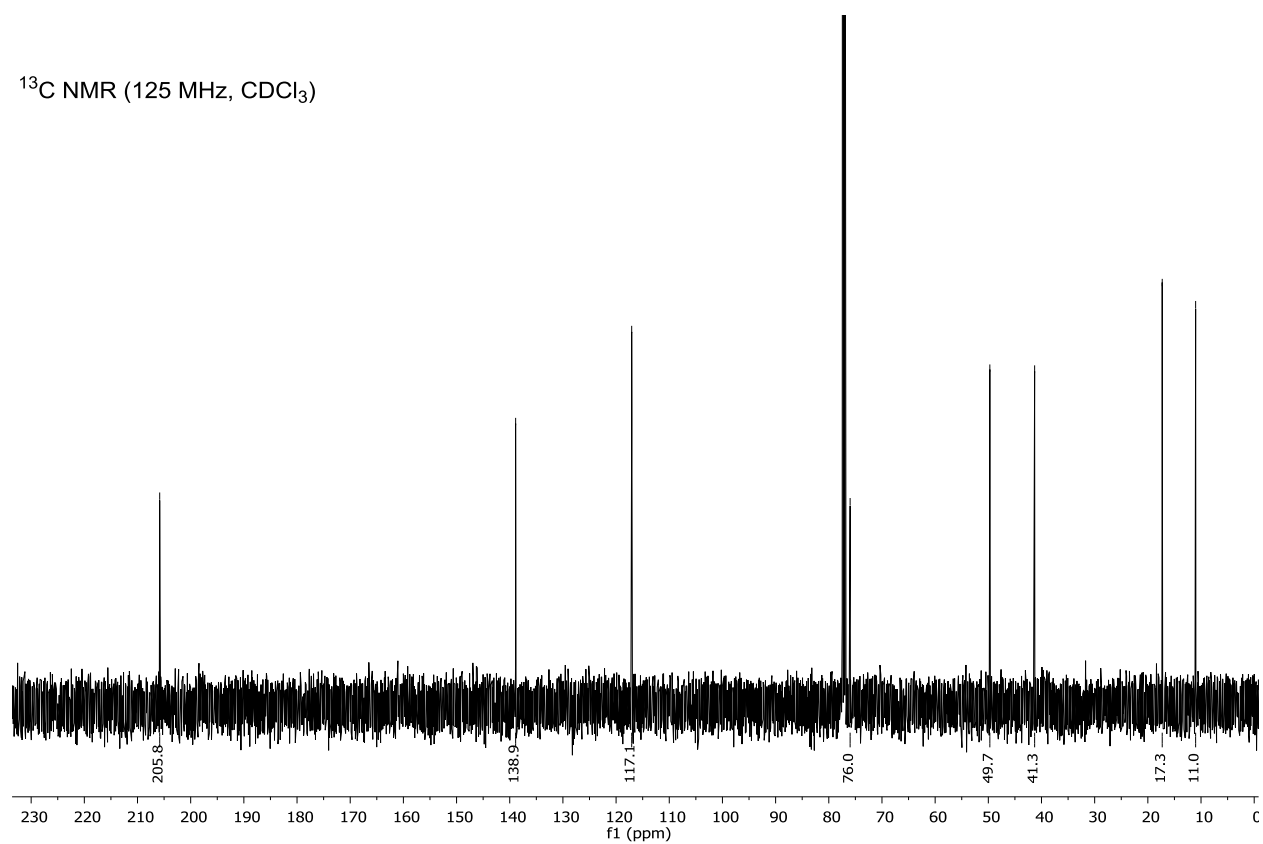


4.27

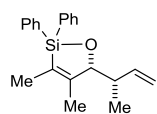
^1H NMR (400 MHz, CDCl_3)



^{13}C NMR (125 MHz, CDCl_3)



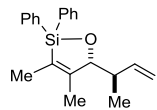
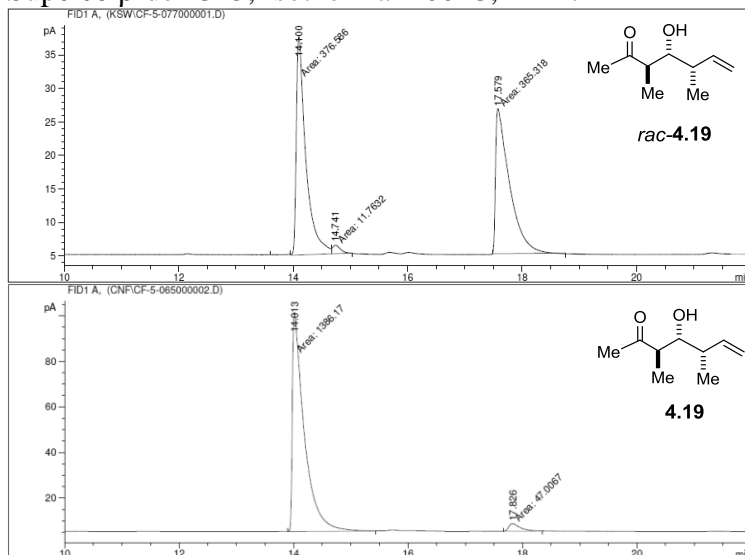
4.11 GC Traces



4.17

Chiral GC analysis of **4.19** (product of “standard” Tamao oxidation) revealed that **4.17** was produced in 93% enantiomeric excess (ee).

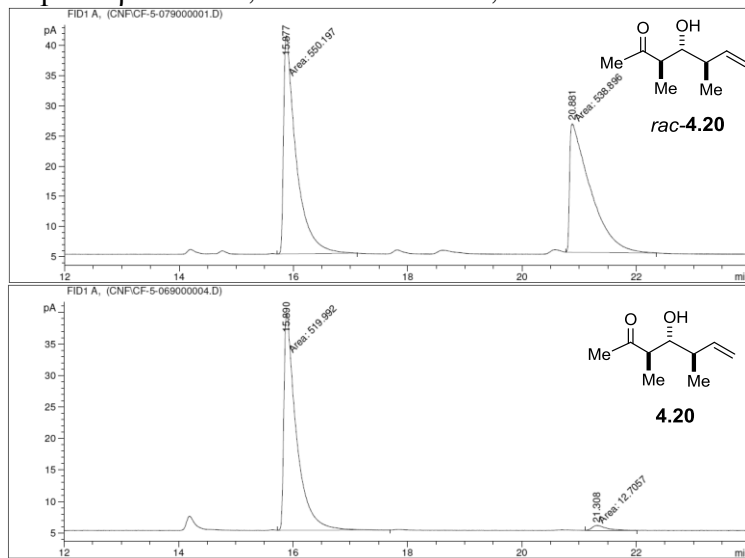
Supelco β -dex 325, Isothermal 100°C, 1 mL/min

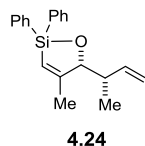


4.18

Chiral GC analysis of **4.20** (product of “standard” Tamao oxidation) revealed that **4.18** was produced in 95% enantiomeric excess (ee).

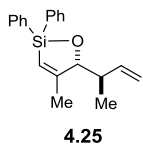
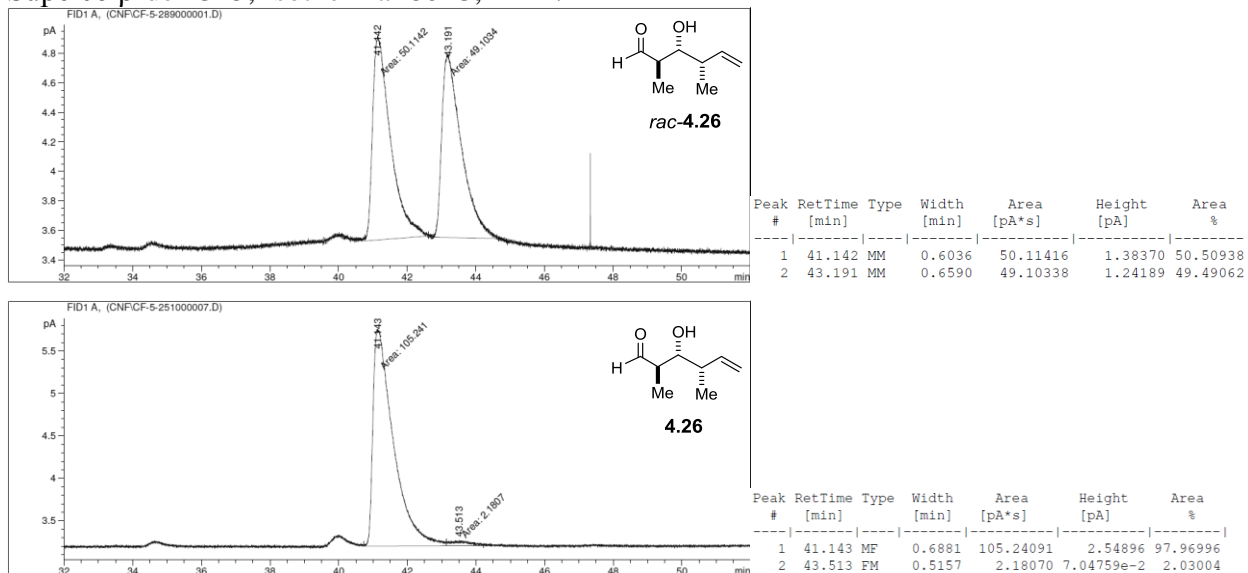
Supelco β -dex 325, Isothermal 100°C, 1 mL/min





Chiral GC analysis of **4.26** (product of “standard” Tamao oxidation) revealed that **4.24** was produced in 96% enantiomeric excess (ee).

Supelco β -dex 325, Isothermal 80°C, 1 mL/min



Chiral GC analysis of **4.27** (product of “standard” Tamao oxidation) revealed that **4.25** was produced in 99% enantiomeric excess (ee).

Supelco β -dex 325, Isothermal 90°C, 1 mL/min

